Greg H. Parlier
Federico Liberatore
Marc Demange (Eds.)

Communications in Computer and Information Science 884

Operations Research and Enterprise Systems

6th International Conference, ICORES 2017
Porto, Portugal, February 23–25, 2017
Revised Selected Papers

Springer

Communications in Computer and Information Science 884

Commenced Publication in 2007
Founding and Former Series Editors:
Alfredo Cuzzocrea, Xiaoyong Du, Orhun Kara, Ting Liu, Dominik Ślęzak, and Xiaokang Yang

Editorial Board

More information about this series at http://www.springer.com/series/7899

Greg H. Parlier · Federico Liberatore
Marc Demange (Eds.)

Operations Research and Enterprise Systems

6th International Conference, ICORES 2017
Porto, Portugal, February 23–25, 2017
Revised Selected Papers

Springer

Editors
Greg H. Parlier
INFORMS
Catonsville, MD
USA

Marc Demange
Royal Melbourne Institute of Technology
Melbourne, VIC
Australia

Federico Liberatore
Carlos III University of Madrid
Madrid
Spain

ISSN 1865-0929 ISSN 1865-0937 (electronic)
Communications in Computer and Information Science
ISBN 978-3-319-94766-2 ISBN 978-3-319-94767-9 (eBook)
https://doi.org/10.1007/978-3-319-94767-9

Library of Congress Control Number: 2018947444

Printed on acid-free paper

This Springer imprint is published by the registered company Springer International Publishing AG part of Springer Nature
The registered company address is: Gewerbestrasse 11, 6330 Cham, Switzerland

Preface

This book includes extended and revised versions of selected papers from the 6th International Conference on Operations Research and Enterprise Systems (ICORES 2017), held in Porto, Portugal, during February 23–25.

We received 90 paper submissions from 36 countries, of which 14% are included in this book. These papers were selected based on several criteria including reviews provided by Program Committee members, session chair assessments, and also program chair perspectives across all papers included in the technical program. The authors of these selected papers were then invited to submit revised and extended versions of their papers for formal publication.

The purpose of the annual ICORES conferences is to bring together researchers, engineers, and practitioners interested in both advances and applications in the field of operations research. Two simultaneous tracks are held, one covering domain-independent methodologies and technologies and the other practical work developed in specific application areas.

The papers selected for this book contribute to current research in operations research and toward a better understanding of complex enterprise systems. We commend each of the authors for their contributions, and gratefully thank our many reviewers who ensured the high quality of this publication.

February 2017

Greg H. Parlier
Federico Liberatore
Marc Demange

Organization

Conference Chair

Marc Demange	RMIT University, Australia

Program Co-chairs

Federico Liberatore	Universidad Complutense de Madrid, Spain
Greg H. Parlier	NCSU, USA

Program Committee

El-Houssaine Aghezzaf	Ghent University, Belgium
Maria Teresa Almeida	ISEG, Universidade de Lisboa, Portugal
Cláudio Alves	Universidade do Minho, Portugal
Annalisa Appice	Università degli Studi di Bari Aldo Moro, Italy
Necati Aras	Bogazici University, Turkey
Claudia Archetti	University of Brescia, Italy
Roberto Aringhieri	Università degli Studi di Torino, Italy
Ronald Askin	Arizona State University, USA
Patrizia Beraldi	University of Calabria, Italy
David Bergman	University of Connecticut, USA
Renato Bruni	University of Rome La Sapienza, Italy
Ahmed Bufardi	NA, Switzerland
Sujin Bureerat	KhonKaen University, Thailand
Alfonso Mateos Caballero	Universidad Politécnica de Madrid, Spain
Valentina Cacchiani	University of Bologna, Italy
Olivier Caelen	Atos Worldline, Belgium
Paola Cappanera	University of Firenze, Italy
Massimiliano Caramia	University of Rome Tor Vergata, Italy
José Manuel Vasconcelos Valério de Carvalho	Universidade do Minho, Portugal
Lorenzo Castelli	University of Trieste, Italy
Bo Chen	University of Warwick, UK
Weifeng Chen	University of Pennsylvania, USA
John Chinneck	Carleton University, Canada
Ta-Tao Chuang	Gonzaga University, USA
Andre Augusto Cire	University of Toronto, Canada
Roberto Cordone	University of Milan, Italy
Florbela Maria Cruz Domingues Correia	Instituto Politécnico de Viana do Castelo, Portugal
Alysson Costa	University of Melbourne, Australia

Lino Costa	Universidade do Minho, Portugal
Patrizia Daniele	University of Catania, Italy
Mirela Danubianu	Stefan cel Mare University of Suceava, Romania
Andrea D'Ariano	University of Rome TRE, Italy
Bernardo D'Auria	Universidad Carlos III de Madrid, Spain
Xavier Delorme	Ecole Nationale Supérieure des Mines de Saint-Etienne, France
Marc Demange	RMIT University, Australia
Paolo Detti	University of Siena, Italy
Clarisse Dhaenens	CRIStAL, France
Nikolai Dokuchaev	Curtin University, Australia
Christophe Duhamel	Université Blaise Pascal, Clermont-Ferrand, France
Khaled Elbassioni	Masdar Institute, Khalifa University of Science and Technology, UAE
Ali Emrouznejad	Aston University, UK
Nesim Erkip	Bilkent University, Turkey
Giovanni Fasano	University of Venice Ca' Foscari, Italy
Paola Festa	University of Naples, Italy
Carlo Filippi	University of Brescia, Italy
Ingrid Fischer	Universität Konstanz, Germany
Muhammad Marwan Muhammad Fuad	Technical University of Denmark, Denmark
Antonio Fuduli	University of Calabria, Italy
Heng-Soon Gan	The University of Melbourne, Australia
Claudio Gentile	CNR, Italy
Ronald Giachetti	Naval Postgraduate School, USA
Ilias Gialampoukidis	Information Technologies Institute, Greece
Stefano Giordani	University of Rome Tor Vergata, Italy
Alessandro Giuliani	University of Cagliari, Italy
Giorgio Gnecco	IMT, School for Advanced Studies, Lucca, Italy
Marc Goerigk	Lancaster University, UK
Boris Goldengorin	Ohio University, USA
Marta Castilho Gomes	CERIS-CESUR, Instituto Superior Técnico, Universidade de Lisboa, Portugal
Dries Goossens	Ghent University, Belgium
Stefano Gualandi	University of Pavia, Italy
Christelle Guéret	University of Angers, France
Francesca Guerriero	University of Calabria, Italy
Nalan Gulpinar	The University of Warwick, UK
Tias Guns	KU Leuven, Belgium
Gregory Z. Gutin	Royal Holloway University of London, UK
Jin-Kao Hao	University of Angers, France
Kenji Hatano	Doshisha University, Japan
Emmanuel Hebrard	LAAS-CNRS, France
Hanno Hildmann	Universidad Carlos III de Madrid, Spain

Chenyi Hu	The University of Central Arkansas, USA
Johann Hurink	University of Twente, The Netherlands
Josef Jablonsky	University of Economics, Czech Republic
Angel A. Juan	Open University of Catalonia, Spain
Itir Karaesmen	American University, USA
Daniel Karapetyan	University of Essex, UK
George Katsirelos	INRA, France
Ahmed Kheiri	Lancaster University, UK
Philip Kilby	NICTA and the Australian National University, Australia
Jesuk Ko	Gwangju University, South Korea
Leszek Koszalka	Wroclaw University of Technology, Poland
Sotiria Lampoudi	Droneseed, USA
Giuseppe Lancia	University of Udine, Italy
Dario Landa-Silva	University of Nottingham, UK
Pierre L'Ecuyer	Université de Montréal, Canada
Janny Leung	The Chinese University of Hong Kong (Shenzhen), China
Federico Liberatore	Universidad Complutense de Madrid, Spain
Michele Lombardi	DISI, University of Bologna, Italy
Pierre Lopez	LAAS-CNRS, Université de Toulouse, France
Helena Ramalhinho Lourenço	Universitat Pompeu Fabra, Spain
Guglielmo Lulli	Lancaster University, UK
Qiang Ma	Kyoto University, Japan
Prabhat K. Mahanti	University of New Brunswick, Canada
Viliam Makis	University of Toronto, Canada
Enrico Malaguti	University of Bologna, Italy
Arnaud Malapert	Université Côte d'Azur, CNRS, I3S, France
Federico Malucelli	Politecnico di Milano, Italy
Emanuele Manni	University of Salento, Italy
Patrice Marcotte	Université de Montréal, Canada
Concepción Maroto	Universidad Politécnica de Valencia, Spain
Pedro Coimbra Martins	Polytechnic Institute of Coimbra, Portugal
Nimrod Megiddo	IBM Almaden Research Center, USA
Carlo Meloni	Politecnico di Bari, Italy
Marta Mesquita	Universidade de Lisboa, Portugal
Rym MHallah	Kuwait University, Kuwait
Michele Monaci	Università degli Studi di Bologna, Italy
Jairo R. Montoya-Torres	Universidad de los Andes, Colombia
Young Moon	Syracuse University, USA
Gaia Nicosia	Università degli Studi Roma Tre, Italy
Inneke Van Nieuwenhuyse	KU Leuven, Belgium
José Oliveira	Universidade do Minho, Portugal
Pedro Nuno Ferreira Pinto Oliveira	Universidade do Porto, Portugal

Mohammad Oskoorouchi	California State University-San Marcos, USA
Selin Özpeynirci	Izmir University of Economics, Turkey
Massimo Paolucci	University of Genoa, Italy
Greg H. Parlier	NCSU, USA
Gabrielle Peko	The University of Auckland, New Zealand
Ana Isabel Pereira	Instituto Politécnico de Bragança, Portugal
Ulrich Pferschy	University of Graz, Austria
Diogo Pinheiro	Brooklyn College of the City University of New York, USA
Marco Pranzo	University of Siena, Italy
Steven Prestwich	University College Cork, Ireland
Caroline Prodhon	Charles Delaunay Institute, France
Luca Quadrifoglio	Texas A&M University, USA
Arash Rafiey	Indiana State University, USA
Günther Raidl	Vienna University of Technology, Austria
Celso Ribeiro	Universidade Federal Fluminense, Brazil
Michela Robba	University of Genoa, Italy
Ana Maria Alves Coutinho Rocha	Universidade do Minho, Portugal
Guzmán Santafé Rodrigo	Universidad Pública de Navarra, Spain
Helena Sofia Rodrigues	Instituto Politécnico de Viana do Castelo, Portugal
Andre Rossi	Université d'Angers, France
Lukas Ruf	Consecom AG, Switzerland
Stefan Ruzika	University of Kaiserslautern, Germany
Alessia Saggese	University of Salerno, Italy
Mohamed Saleh	Cairo University, Egypt
Flavio Sartoretto	Università Ca' Foscari di Venezia, Italy
Cem Saydam	University of North Carolina Charlotte, USA
Abdelkader Sbihi	EM Normandie, France
Pierre Schaus	UCLouvain, Belgium
Andrea Scozzari	Università degli Studi Niccolo' Cusano, Italy
Laura Scrimali	University of Catania, Italy
René Séguin	Defence Research Development Canada, Canada
Meinolf Sellmann	IBM, USA
Antonio Sforza	University of Naples Federico II, Italy
Fabio Stella	University of Milano-Bicocca, Italy
Claudio Sterle	University of Naples Federico II, Italy
Thomas Stützle	Université Libre de Bruxelles, Belgium
Wai Yuen Szeto	The University of Hong Kong, SAR China
Vadim Timkovski	South University, USA
Norbert Trautmann	University of Bern, Switzerland
Chefi Triki	University of Salento, Italy
Michael Tschuggnall	University of Innsbruck, Austria
Begoña Vitoriano	Complutense University, Spain
Maria Vlasiou	Eindhoven University of Technology, The Netherlands
Cameron Walker	University of Auckland, New Zealand

Qi Wang	Northwestern Polytechnical University, China
Dominique de Werra	École Polytechnique Fédérale de Lausanne (EPFL), Switzerland
Santoso Wibowo	Central Queensland University, Australia
Gerhard Woeginger	Eindhoven University of Technology, The Netherlands
Neil Yorke-Smith	TU Delft, The Netherlands
Hongzhong Zhang	Columbia University, USA
Yiqiang Zhao	Carleton University, Canada
Sanming Zhou	University of Melbourne, Australia
Jan Zizka	Mendel University in Brno, Czech Republic
Paola Zuddas	University of Cagliari, Italy

Additional Reviewers

Mikael Capelle	Thales Alenia Space, France
Yun He	CNRS, LAAS, Université de Toulouse, France
Markus Sinnl	University of Vienna, Austria
Dimitri Thomopulos	University of Bologna, Italy

Invited Speakers

Dries Goossens	Ghent University, Belgium
Olivier Hudry	Télécom ParisTech, France
José Oliveira	Universidade do Minho, Portugal

Contents

Methodologies and Technologies

Methodologies and Technologies

Optimization in Sports League Scheduling: Experiences from the Belgian Pro League Soccer

Dries Goossens(✉)

Faculty of Economics and Business Administration, Ghent University, Tweekerkenstraat 2, 9000 Ghent, Belgium
dries.goossens@ugent.be

Abstract. Every sports competition needs a schedule of play, stating who will play whom, when, and where. A good schedule is important given its impact on the competition's fairness and outcome, public attendance, commercial interests, and cost of policing. This paper discusses experiences with scheduling the Belgian Pro League soccer competition, for which we develop the official schedule since 2006. We present methods that have proven their value in real-life sports scheduling, and discuss how they benefited from continuous improvement, in order to accommodate changing requirements. We discuss fairness issues, as well as a discrete choice experiment we carried out to estimate the schedule's impact on stadium attendance and TV viewership.

Keywords: Sports scheduling · Belgian Pro League
Tv broadcasting · Soccer · Stadium attendance · Breaks
Canonical schedule

1 Introduction

It is safe to say that millions of people, all over the world, are enthralled by sports, be it actively participating or as a fan or spectator. Not surprisingly, sports has become big business. For instance, in 2014, the sports market in North America alone was worth 60.5 billion dollar and is expected to reach 73.5 billion dollar by 2019 according to a sports industry report by PricewaterhouseCoopers[1]. Apart from the purely economic impact, sports is also relevant for society because of its contribution to well-being in general. Indeed, according to Forrest and McHale [19], the impact of sports on happiness scores collected from nearly 28,000 adults in the UK turned out to be comparable with the impact of having a job.

Sports offer ample of opportunities for optimization on all kinds of levels. What strategy should a team or player apply (e.g. [28])? What players should a manager hire (e.g. [6])? How should referees be assigned to matches (e.g. [3])?

[1] See https://www.pwc.com/us/en/industry/entertainment-media/publications/assets/pwc-sports-outlook-north-america-2015.pdf.

G. H. Parlier et al. (Eds.): ICORES 2017, CCIS 884, pp. 3–19, 2018.
https://doi.org/10.1007/978-3-319-94767-9_1

How should the competition owner organize its league (e.g. [23])? How should public funds be allocated to sports (e.g. [4])? In this paper, we focus on the question how the schedule of play should be constructed. Not much more than a decade ago, most professional sports competitions were scheduled by unskilled personnel, equipped with little more than pen and paper. In some competitions, and certainly in amateur leagues, this is still the case. A good schedule is important though, because it affects the outcome and fairness of the competition, public attendance, commercial interests, as well as the cost of policing. As league owners manage to close astonishing broadcasting deals, and in light of the growing financial interests in the sports industry, the importance of a good schedule has become more and more apparent.

Sport scheduling is about determining a suitable date and venue for each match that is to be played (according to a given competition format). The complexity of this problem depends on what should be taken into account. Generating a schedule where each team plays against each other team an equal number of times, such that each team plays at most once on any given matchday is a simple task (see e.g. [12]). However, as more constraints and considerations have to be taken into account, sports scheduling can quickly become a huge challenge. Nurmi et al. [39] provide a framework for sports scheduling problems, modeled from the requirements of various professional sports leagues. This framework includes constraints related to venue availability, teams that should not have simultaneous home games, bounds on the number of consecutive matches against teams from a given strength group, and many more.

We discuss practical applications involving the scheduling of the Belgian Pro League soccer, for which we develop the official schedule since 2006 [21]. Our contract with the Belgian Pro League currently involves 2 professional and 1 amateur division, each playing a different league format and play-off competitions. Although there have been other papers that discuss the involvement of academics in real-life soccer scheduling (e.g. [5,14,41]), we believe that our collaboration with the Belgian Pro League is exceptional in its length. It allows us to discuss how our solution method needed continuous improvement, in order to accommodate changes in the competition format, as well as new requirements. Furthermore, we discuss how we gradually got involved in determining these requirements, e.g. by carrying out a discrete choice experiment in order to estimate the impact of the schedule on TV viewership and stadium attendance.

This paper is organized as follows. Section 2 presents an overview of the terminology and main results in sports scheduling. In Sect. 3, we discuss the competition format currently used in the Belgian Pro League. We also give an overview of the most important stakeholders, and their wishes and aspirations with respect to the schedule. Section 4 reports on our solution approach, and the changes it underwent over the years. We provide and a discussion and some directions for future research in Sect. 5.

2 Terminology and Fundamentals

Sports scheduling is a relatively young academic discipline: although the first substantial contributions were published in the early 80's, a considerable increase in sports scheduling articles appeared only in recent years, including publications in top journals in operations research. Simultaneously, several academics reached out to the sports scheduling practitioners, offering new methods to deal with the increasingly more complex problem of scheduling a league. Excellent overviews of sports scheduling have been written by Easton et al. [15] and Rasmussen and Trick [40]. An extensive bibliography can be found on a website maintained by Knust[2] and in an annotated bibliography by Kendall et al. [30]. In this section, we explain the most important concepts discussed in the sports scheduling literature.

In a sports tournament, n teams play against each other over a period of time according to a given schedule. The teams belong to a league, which organizes matches (or games) between the teams. Each match consists of an ordered pair of teams, denoted i-j, where team i plays a home match - that is, uses its own venue (stadium) for a game - and team j plays away. In a so-called *round robin tournament* each team plays against every other team an equal number of times. Most sports leagues play a double round robin tournament, where each team faces each other team twice, once at home and once away. Matches are typically grouped into so-called rounds, which are played on one or more consecutive days (usually a weekend). Teams play at most once per round; if a team does not play on some round, we say it has a bye on that round. A schedule is called *compact* or *temporally constrained* when its number of rounds is minimal. When the number of teams is even, this means that each team plays on every round. When more rounds are used than needed, we say the schedule is *temporally relaxed*.

Table 1. A compact double round robin schedule for 6 teams.

R1	R2	R3	R4	R5	R6	R7	R8	R9	R10
A-B	B-E	B-D	C-B	B-F	B-A	E-B	F-A	B-C	F-B
C-D	D-A	A-F	E-A	D-E	D-C	A-D	D-B	A-E	E-D
E-F	F-C	E-C	F-D	A-C	F-E	C-F	C-E	D-F	C-A

Table 1 presents an example of a compact schedule for a double round robin competition with 6 teams (A-F). If a team plays two home matches or two away matches in two consecutive rounds, it is said to have a *break*. For instance, team E in Table 1 has an away break in rounds 8–9. It is easy to see that any round robin schedule for an even number of teams will feature at most 2 teams that have a perfect alternation of home and away matches. Consequently, any

[2] See http://www.inf.uos.de/knust/sportssched/sportlit_class.

schedule for a single round robin tournament with an even number of teams will have at least $n-2$ breaks [12]. Goossens and Spieksma [22] introduced the so-called *generalized break*, which arises if a team has two home (away) games in a given pair of arbitrary (i.e. not necessarily consecutive) rounds, and present a number of theoretical results on this topic.

We can see a schedule as the combination of a timetable (e.g. Table 2 – left) and a set of home-away patterns (e.g. Table 2 – right). The timetable (sometimes also referred to as an opponent schedule) specifies for each round which opponent each team faces. The sequence of (H)ome and (A)way matches (and possibly also (B)yes) according to which a team plays is called the *home-away pattern* (HAP) of this team. A pair of home-away patterns is said to be complementary if the patterns never feature two home games (or two away games) on the same round. Clearly, a timetable and a home-away pattern set need to be compatible before a schedule can emerge: for each match in the timetable, the corresponding home-away patterns need to give one team the home advantage, and designate an away match for the other team. Seeing a schedule as a merging of a timetable and a pattern set, leads to two fundamental problems: the pattern set feasibility problem and the break minimization problem. The pattern set feasibility problem departs from a set of home away patterns and asks the question whether there exists a corresponding timetable (such that a given tournament format, e.g. single round robin, can be played), in which case we say the pattern set is feasible. It is still an open question whether this problem is NP-complete or not. Miyashiro et al. [36] present a necessary condition for HAP sets to be feasible. Moreover, for HAP sets having a minimum number of breaks, they show how this condition can be checked in polynomial time and conjecture it to be sufficient. In the break minimization problem, a timetable is given and the question is to determine the home assignment (i.e. the home away patterns) such that the number of breaks is minimized. To the best of our knowledge, the complexity status of this problem is also still unknown. However, Miyashiro and Matsui [37] proved a conjecture by Elf et al. [16], stating that deciding whether a feasible home-away pattern set with $n-2$ breaks exists for a given timetable, can be solved in polynomial time.

Table 2. The timetable (left) and home-away pattern set (right) corresponding to the schedule in Fig. 1.

Team	R1	R2	R3	R4	R5	R6	R7	R8	R9	R10
A	B	D	F	E	C	B	D	F	E	C
B	A	E	D	C	F	A	E	D	C	F
C	D	F	E	B	A	D	F	E	B	A
D	C	A	B	F	E	C	A	B	F	E
E	F	B	C	A	D	F	B	C	A	D
F	E	C	A	D	B	E	C	A	D	B

Team	R1	R2	R3	R4	R5	R6	R7	R8	R9	R10
A	H	A	H	A	H	A	H	A	H	A
B	A	H	H	A	H	H	A	A	H	A
C	H	A	A	H	A	A	H	H	A	H
D	A	H	A	A	H	H	A	H	H	A
E	H	A	H	H	A	A	H	A	A	H
F	A	H	A	H	A	H	A	H	A	H

There is a strong link between sports scheduling and graph theory (see e.g. [11,13,29]). For instance, a schedule for a single round robin tournament with an even number of teams can be seen as a one-factorization of K_n, the complete graph with n nodes. The nodes in this graph correspond to the teams, and each edge between two nodes represents a match between the two corresponding teams. A one-factorization of K_n is a partitioning into edge-disjoint one-factors [35]. A one-factor is a set of edges such that each node in the graph is incident to exactly one of these edges (i.e. a perfect matching), and corresponds to a round. One particular one-factorization, the so-called canonical one-factorization, can be traced back to a contribution by Kirkman in the 19th century [31], and has received special attention in sports scheduling. Indeed, when looking at the schedules used in practice, in particular for soccer (see e.g. [24]), the majority of the schedules are canonical schedules, i.e. based on the canonical one-factorization. Their success may be explained by the fact that there is an easy way to generate them (i.e. the circle method, also known as the clock method or the polygon method), and that they can be constructed using the minimum number of breaks [12]. Note however that apart from minimizing breaks, many other constraints typically play a role in sports scheduling, which may heavily complicate the problem. For instance, if costs corresponding to each possible combination of a match and a round are given and the objective is to minimize the sum of these costs for the scheduled matches, the resulting sports scheduling is NP-hard [7].

Of the many fairness issues that can arise when constructing a schedule, the carry-over effect as introduced by Russell [42] has probably been studied most intensively. Russell defines team A to receive a *carry-over effect* from team B if some team X plays against team B in one round, and against team A in the next round. The carry-over effect is perceived to be particularly relevant in physical sports. For instance, if team B is very strong, and tough-playing, one can imagine that its opponent, team X, is weakened by injuries, suspensions, fatigue or lowered morale, which could be an advantage for its next opponent, team A. The opposite may be true if team B is a weak team. As carry-over effects unavoidably are present in any schedule, one can only strive to spread these carry-over effects as evenly as possible over all teams to increase overall fairness. Let c_{ij} be the number of times team j receives a carry-over effect from team i in the previous round in a schedule. A schedule's degree of imbalance with respect to carry-over effects is given by the so-called carry-over effect value, which is defined as $\sum_{ij} c_{ij}^2$ [42]. A lower bound for the carry-over effect value of a single round robin tournament is $n(n-1)$; if this bound is attained, we say the schedule is *balanced*. Russell also presents an algorithm that results in a balanced schedule when n is a power of two. For other values of n, the best known results are by Anderson [2] and Guedes and Ribeiro [27]. Lambrechts et al. [33] have shown that the canonical schedule maximizes the carry-over effect value.

3 The Belgian Pro League Soccer

We first discuss the current league format used by the Belgian Pro League (Sect. 3.1), followed by an overview of the various stakeholders and their (often conflicting) wishes and interests with respect to the schedule (Sect. 3.2).

3.1 League Format

Since 2016–2017, the Belgian Pro League consists of 2 professional soccer divisions: a first division (1A) with 16 teams, which is also known as the Jupiler Pro League and a second division (1B) with 8 teams known as the Proximus League. Both division play a so-called regular stage, which involves a double round robin tournament for 1A and a quadruple round robin tournament for 1B, completed in 30 and 28 rounds respectively. The regular stage is followed by a post-competition, inaptly called *play-offs* by the Belgian Pro League. Indeed, in general, play-offs involve a direct knock-out competition, where teams are tied in pairs and the loser of each match is eliminated. This is not the case with the play-off stage in Belgian soccer: depending on their result in the regular season, the teams are divided into one of 4 play-off groups, each of which plays a double round robin tournament. The most awaited play-off group includes the six best teams of 1A: they keep half of the points they collected in the regular stage and play for the league title, as well as access to the (qualification stage of the) Champions League or the Europa League. Two other play-off competitions include 6 teams, collected from the other teams in 1A and the top half of 1B. These teams start with a clean sheet and play for the final ticket for the Europa League qualifiers. A final play-off competition includes the bottom half of 1B; these 4 teams retain half of the points from the regular stage and play to avoid being relegated to the amateur competition. An overview of the league format is given in Fig. 1.

Note that 2 teams do not take part in the play-off stage: the winner of the regular stage of 1B and the last team after the regular stage of 1A see an early end to their season. Certainly for the winner of 1B, this is peculiar, as this team does not get the opportunity to battle for access to the Europa League, as opposed to teams that performed worse in the regular stage of 1B. This competition format is quite rare in soccer; it bears resemblance to the format used in Cyprus, which also has a double round robin post-competition, after the teams have been split into two groups depending on their performance in the regular stage [24]. A similar format, including the rule that teams transfer half of their points from the regular stage to the post-competition stage has been in use in the Maltese Premier League, but it was recently abandoned in favor of a classic single stage, double round robin competition format. The main motivation for the Belgian Pro League competition format is the fact that it allows for more top matches, without drastically reducing the number of teams in the top division. This format should increase the level of the top teams, allowing them to perform better in the European competitions, and at the same time generate more revenue from TV broadcasting rights, ticketing, and sponsorship.

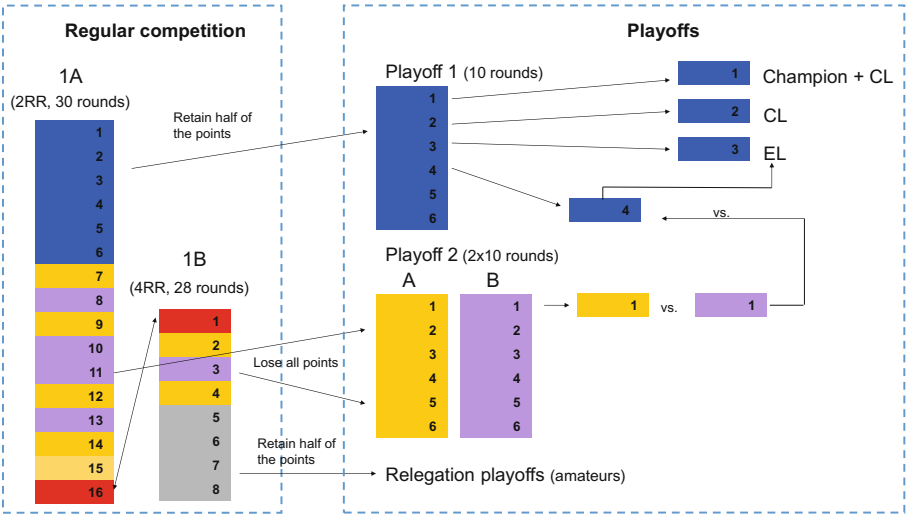

Fig. 1. The competition format for the Belgian Pro League.

3.2 Stakeholders and Their Requirements

The Belgian Pro League. Being the owner of the competition, the Belgian Pro League obviously has a large say in how the competition is organized and what the schedule should look like. The Pro League has appointed a so-called *schedule manager*, who gathers the various wishes and requirements from the other stakeholders and assesses the relative importance of the scheduling requests. The schedule manager is also responsible for rescheduling postponed matches and handling complaints.

The main concern of the Pro League is the fairness of the competition. Breaks play an important role in this. For instance, no team should start or end the season with two home games (or two away games), as it is assumed that this would give them an advantage (disadvantage, respectively). Similarly, as a succession of away games is seen as the path towards a performance slump, teams cannot have more than two consecutive away matches. In fact, breaks in general should be minimized.

Given the large number of rounds that come with the league format discussed in Sect. 3.1, midweek rounds are inevitable. However, teams generally do not appreciate a home game on a midweek round, as the revenue from ticketing and catering tends to be lower than on weekend days. Consequently, the Pro League prefers a balance between home and away matches on midweek rounds: if a team plays at home on one midweek round, they should not have a home game on the next midweek round. Note that, as midweek rounds need not be consecutive, we can see this as avoiding a generalized break.

Another fairness issue is the carry-over effect. At some point, carry-over effects have been suggested in the Belgian media as the cause of a team's

relegation (see e.g. [26]). Even though it was shown that there is no statistical evidence that carry-over effects have any meaningful impact on the outcome of soccer matches in the Belgian Pro League [25], the feeling still remains that unbalanced carry-over effects are to be avoided.

Finally, the Pro League strives for a balanced start of the season for all teams, avoiding that any team faces a disproportionate number of strong opponents in the first rounds. Exceptions are made for those teams that are involved in qualification rounds for Champions League or Europa League. In order to maximize their chances of success at the European stage, these teams are offered a start of the season without big domestic clashes.

The TV Broadcasters. TV broadcasters aim to maximize their revenue by attracting as many viewers as possible. Over the years, we have had many different scheduling requests from various TV broadcasters. In the beginning, each round needed to feature at least one (and preferably two) of four top teams playing an away match. The underlying motivation was that a top team's home matches are less attractive, as the top team tends to win these games without much opposition. Soon after that, we received a request to have at most one top match per round, and a balanced spread of top matches over the season. Later, the TV broadcaster wanted to have so-called Super Sundays, i.e. a Sunday with (at least) two top matches. Given this diverse set of requests, at some point we started to wonder whether the TV broadcasters actually knew what kind of schedule would maximize their viewing rates. The number of papers on the determinants for TV viewership of soccer matches is surprisingly limited. Most of them focus on the relation between viewer ratings and match outcome uncertainty (e.g. [1,8]); Forrest, Simmons, and Buraimo [17] apply their model to support the broadcasters' choice of which matches to televise in the English Premier League. However, none of these contributions show how the schedule should be constructed in order to maximize TV viewership.

On a typical weekend round in the regular stage of the competition, the following kick-off times are used for matches in 1A: Friday 20:30, Saturday 18:00, Saturday 20:00 (2 matches), Saturday 20:30, Sunday 14:30, Sunday 18:00, and Sunday 20:00. Essentially, the schedule determines which opponents will face each other in which part of the season and at what kickoff time. To obtain a better understanding of the impact of these match characteristics (month, kickoff time, and opponent strength) on TV viewership, we conducted a discrete choice experiment using an online survey questionnaire distributed to chart the preferences of Belgian soccer fans in watching the league matches [44]. Our results show that fans on average dislike matches scheduled for Wednesday 20:30, Saturday 18:00, Sunday 14:30, and Sunday 20:30. In particular, midweek matches are to be avoided, although there is quite some heterogeneity in the individual preferences for the Wednesday 20:30 kick-off time (probably due to the difference between employees who have to go to work the next morning and fans without a job). If midweek matches are inevitable, they are best planned in October or March to ensure a reasonably sized audience. We found that it does not

seem beneficial to start the season late in July or even early in August, as a considerable proportion of the fans take holidays in this period. Surprisingly, fans do not prefer to see their team play against a top team regardless of the month and kick-off time: matches against teams of average strength can attract more viewers than matches against top teams if carefully scheduled on attractive rounds and kick-off times. Our model can also be used to predict audience ratings for each (type of) match, depending on the planned month and kickoff time, which in turn can be used as input parameter for optimizing the schedule.

The Police and the Tax Payer. Soccer matches in the Belgian Pro League are events that can attract up to 30,000 fans. Moreover, some matches, labeled *risk matches*, are known to have an increased risk of hooliganism. Hence, it is clear that the police is an important stakeholder in professional soccer. Moreover, it is important to realize that a mayor has the right to forbid a match being played if he or she judges that public order and safety cannot be guaranteed.

Months before the start of the new season, various local police forces are queried about their concerns and requests with respect to the schedule. Most requests deal with risk matches, which should be avoided on dates when other events are scheduled in the city that require the attention of the local police (e.g. a festival, summit, or other sports event). Sometimes, the request only concerns the kick-off time, as some matches can be managed more easily during daylight. The impact on traffic of scheduling a match on a specific date and time is also regularly pointed out by the police. A few police zones contain the venues of two (or even more) teams, and in this case some coordination is needed: preferably, teams from the same police zone do not play a home game on the same weekend. For sure, no pair of teams from the same zone should host risk games simultaneously.

Ultimately, the tax payer bears the vast majority of the policing cost for soccer matches. Clearly, the schedule has an impact on the size of the policeforce needed, as well as the costs involved. For instance, scheduling a risk game in the beginning of the season will allow the police to deploy a smaller force compared to when this game is decisive for e.g. relegation. Furthermore, matches scheduled e.g. in the Christmas period result in a higher man-hour rate than midweek matches.

The Clubs and Their Fans. Clubs have a wide variety of wishes. Teams sharing a venue have a strong reason for not playing home games in the same round. Although Belgium currently does not have multi-purpose stadia (i.e. stadia designed to host multiple types of events, such as pop concerts and various types of sports contests), in some cases, the parking facilities are shared with a shopping mall or another sports club, resulting in a list of days on which home games are to be avoided. Most teams believe they can increase their chances of playing a good season by starting with a home game, ideally against an easy opponent. Champions League or Europa League contenders typically request a home game after their European match, as they believe a home game renders

them less vulnerable to the effects of fatigue resulting from this extra midweek match (and trip). Teams with cash flow problems prefer a steady number of home matches per month. Occasionally, a team requests to delay the first home game by starting the season with two consecutive away games, in order to have enough time to finish venue construction or renovation works.

In general, teams want to maximize the number of fans attending their home games, as this is closely related to their revenue. Various models have been developed to analyze the factors that determine stadium attendance (see e.g. [9,10,20,34,43]). Compared to TV broadcasting, more factors can influence a soccer fan's decision whether or not to travel to the stadium: distance from the stadium, weather, availability of car parking, availability of tickets, safety, service, catering, etc. Here, we limit ourselves to those factors that can be impacted by the schedule. Forrest and Simmons [18] show that consecutive home games negatively impact attendance. Hence, teams generally prefer a schedule in which breaks are minimized. Wang et al. [44] also studied the impact of month, kick-off time, and opponent strength on stadium attendance for Belgian soccer fans. They find that, contrary to the results with respect to TV viewership, January is not a popular month for attending a soccer match in the stadium (presumably because of the cold). Apparently, August's nice summer weather is neutralized by the fact that many people leave on holiday. Wednesday 20:30 and Sunday 20:30 are deplorable kick-off times with respect to stadium attendance, as the next day is a working day. In contrast, Saturday 18:00 and 20:00 and Sunday 14:30 and 18:00 all work very well.

4 Solution Approach

Before 2006, the Pro League's highest division consisted of 18 teams, playing a double round robin tournament without play-offs; the schedule was developed manually. The starting point was a so-called basic match schedule, i.e. a schedule that specifies the round and the home advantage for all matches, however using placeholders instead of real teams. For instance, the schedule in Table 3 shows the first 7 rounds of the basic match schedule that has been used by the Pro League for decades. Clearly, when each team is coupled with a placeholder (1–18), a schedule follows. Although the origin of this basic match schedule is not clear, it is a canonical schedule and it has many advantages. For instance, it consists of two halves, such that each team faces each other team exactly once in each half, and each half has the minimum number of breaks. Furthermore, no team plays three home games or away games in a row, and no team starts or ends the season with two home games or two away games. Moreover, it condenses the whole scheduling problem to a relatively easy question: which placeholder should be matched with which team? The way in which this should be done, however, was less transparent. The schedule manager did this assignment without the use of any optimization tool, till the point where he found no further improvement by manually swapping the placeholder assignment of a pair of teams. Not surprisingly, the resulting schedules typically satisfied merely a small fraction of

Table 3. A basic match schedule for a double round robin tournament with 18 teams, rounds 1–7.

R1	R2	R3	R4	R5	R6	R7
1–3	2–4	1–7	2–8	1–11	2–12	1–15
4–17	3–18	3–5	4–6	3–9	4–10	3–13
6–15	5–1	6–2	5–18	5–7	6–8	5–11
8–13	7–16	8–17	7–3	8–4	7–18	7–9
10–11	9–14	10–15	9–1	10–2	9–5	10–6
12–9	11–12	12–13	11–16	12–17	11–3	12–4
14–7	13–10	14–11	13–14	14–15	13–1	14–2
16–5	15–8	16–9	15–12	16–13	15–16	16–17
18–2	17–6	18–4	17–10	18–6	17–14	18–8

the constraints. As many teams found their wishes brushed aside without understanding how the schedule was constructed, this lead to several accusations of favoritism and lack of transparency in the media (see e.g. [32]).

When we got involved, our main challenge was to automate and optimize the assignment of teams to placeholders in the basic match schedule. This, however, could not be done without explicitly stating all requirements and their relative importance. The latter turned out problematic: a committee with representatives from some of the clubs, had to come to an agreement on the scheduling priorities, whereas they were used to deal with the schedule manager individually and informally. Eventually, we agreed to classify each requirement into one of 5 priority classes, where each class has a certain weight (it took some time to convince them that putting all requirements in the highest priority class is not the way to obtain the best schedule). The optimization model was based on the assignment model. We used a binary decision variable $x_{i,p}$ which is 1 if team i is assigned to placeholder p and 0 otherwise. Furthermore, y_c is 1 if constraint c is not satisfied, and 0 otherwise. We use parameters q_c for the weight associated with the class to which constraint c belongs, and $a_{i,p,c}$ and b_c as parameters to model the various requirements (M is a sufficiently large number). The problem formulation is then as follows:

$$\textbf{Min} \sum_c q_c \cdot y_c \tag{1}$$

subject to

$$\sum_p x_{i,p} = 1 \quad \forall i \tag{2}$$

$$\sum_i x_{i,p} = 1 \quad \forall p \tag{3}$$

$$\sum_i \sum_p a_{i,p,c} \cdot x_{i,p} \leqslant b_c + M \cdot y_c \quad \forall c \tag{4}$$

$$x_{i,p} \in \{0,1\} \quad \forall i,p \tag{5}$$

$$y_c \in \{0,1\} \quad \forall c. \tag{6}$$

The objective function minimizes the total weight of violated constraints. Constraints (2) and (3) ensure that each team is assigned to a placeholder and vice versa. The third set of constraints can be used to model all requirements stakeholders may have by selecting appropriate values for $a_{i,p}$ and b_c.

In the beginning of our collaboration, the Pro League insisted that we used their basic match schedule. The main reasons for this were that they were highly familiar with it, and that lower divisions – which to some extent tune their schedules based on the schedule of the highest division – also used it. However, we soon became the victim of our early success: as we were able to handle many more constraints than the manual approach, stakeholders gradually came up with more wishes and requirements and higher expectations in the next seasons. At some point, it became clear that no satisfactory solution existed, if we restricted the solution space to schedules resulting from the Pro League's basic match schedule. Hence, the next step was to use a phased approach, where we first assign each team to one of the home-away patterns from the basic match schedule, and subsequently decide on the opponents for each team in each round, given the home-away pattern assignment. We call this the two-phase approach; it is a so-called *first break, then schedule* approach, based on a decomposition introduced by Nemhauser and Trick [38].

The first phase can in fact also be modeled using formulation (1)–(6), however this time the binary decision variable $x_{i,p}$ is 1 if team i is assigned to home-away pattern p and 0 otherwise. Notice that constraints (4) now only include constraints that relate to the home advantage; no constraints involving specific opponents are included in this model. The second phase uses a binary decision variable $x_{i,j,k}$ which is 1 if team i plays a home game against team j on round k, and 0 otherwise. We use $a_{i,j,k,c}$ and b_c as parameters to model the various wishes from the stakeholders related to opponents. Note that we enforce that both halves of the schedule are mirrored, i.e. the second half of the schedule is identical to the first half, except the home advantage, which is inverted. Mirroring simplifies the model because we only need to schedule the first half of the season: constraints related to the second half can be modeled in terms of first-half constraints. The formulation is as follows:

$$\textbf{Min} \sum_c q_c \cdot y_c \tag{7}$$

subject to

$$\sum_j (x_{i,j,k} + x_{j,i,k}) = 1 \quad \forall i,k \tag{8}$$

$$\sum_k (x_{i,j,k} + x_{j,i,k}) = 1 \quad \forall i,j : i \neq j \tag{9}$$

$$\sum_i \sum_j \sum_k a_{i,j,k,c} \cdot x_{i,j,k} \leqslant b_c + M \cdot y_c \quad \forall c \tag{10}$$

$$x_{i,j,k} \in \{0,1\} \quad \forall i,j,k \text{ allowed by the HAPs of team } i \text{ and } j \tag{11}$$

$$y_c \in \{0,1\} \quad \forall c. \tag{12}$$

The objective function again minimizes the total weight of violated constraints. Constraints (8) ensure that each team plays exactly once on each round, and constraints (9) enforce that each team meets each other team once in the first half of the season. Constraints (10) are used to model all opponent-related stakeholder requirements. This approach keeps all properties of the basic match schedule related to home advantage and breaks, but drastically increases the search space, as the order of the opponents is no longer fixed. An important argument to abandon the basic match schedule was the carry-over effect. Indeed, since the basic match schedule, being a canonical schedule, has maximally unbalanced carry-over effects [33], any change results in a positive impact on the carry-over effect value.

Solving the two phases sequentially, however, does not guarantee an optimal solution and typically leaves a lot of room for improvement. Hence, we developed a tabu search algorithm around the first phase. This algorithm finds the best move in a neighborhood around some current solution; this neighborhood consists of all solutions that can be reached by swapping the home-away patterns of two teams in this solution. Computationally, computing the consequences of a swap with respect to the objective function in phase 1 is trivial. The evaluation of phase 2 can be more time-consuming, although it frequently happens that there is no need to solve phase 2, since the result after solving phase 1 is already worse than the best solution so far in this neighborhood. We maintain a tabu list to make sure that moves are not immediately reversed.

As new requirements kept coming, it did not take long before we again found no suitable solution in the solution space we considered. Hence we argued to drop the tradition of having the second half mirrored from the first half. Indeed, this created for each requirement connected to the first half of the season a counterpart in the second half, and vice versa, effectively doubling the number of constraints. It took quite some effort to convince the Pro League to allow non-mirrored schedules; in the end, the fact that a non-mirrored schedule had been played before in the Belgian Pro League, albeit a long time ago and for reasons no one could recollect, was a final nudge in the right direction. The fact that the home-away patterns where still mirrored resulted in a schedule that was still about 80% mirrored and at least did not preclude a mirrored schedule provided that this was feasible given the requirements.

The introduction of the play-offs in the season 2009–2010 entailed a number of changes with respect to the scheduling process. Until then, the exact kick-off times were not communicated in the beginning of the season: the broadcaster had the right to delay that decision until one month before the match. This allowed them to take into account more recent information on e.g. which teams qualify for what stages of other competitions (domestic cup, Europa League, Champions League) and which teams perform well in the domestic league. This is still the case for the regular stage of the season, however, for the play-off stage, all kick-off times are to be determined by the schedule manager before

the play-offs start. Furthermore, interdependencies between the various play-off competitions required a totally different scheduling approach, in which all play-off competitions are scheduled simultaneously. On the other hand, each play-off involves at most six teams, such that an IP model based on variables $x_{i,j,k,t} = 1$ if team i plays against team j on round k using kick-off time t (and 0 otherwise), and $y_{i,k} = 1$ if team i has a break on round k (and 0 otherwise) can be solved in a reasonable computation time with e.g. IBM Ilog Cplex.

Finally, we also moved away from the set of home-away patterns that follow from the basic match schedule. Interesting properties of these HA patterns are that (i) they don't begin or end with a break, (ii) they don't have consecutive breaks, (iii) they have at most 3 breaks, and (iv) they allow a mirrored schedule. It is easy to see that for e.g. a double round robin tournament with 16 teams, there are 26 such home-away patterns (13 complementary pairs), i.e. 10 more on top of the 16 HAPs implied by the basic match schedule. Hence, we found that among the 1287 possibilities to pick 8 pairs of complementary HAPs out of 13, 46 HAP sets lead to a feasible schedule. Again, this greatly increased the search space. Currently, we are also including HAPs with more than 3 breaks that do not allow a mirrored schedule, but have other properties that fit well with the requirements of that season.

5 Discussion

At the start of our collaboration with the Pro League in the season 2006–2007, the TV broadcasting rights for the highest division were sold for a price of 36 million euros per season. The current broadcasting contract has been marketed for 70 million euros per season, which is almost double as much (but still a trifle compared to the amounts paid in e.g. the English Premier League). In the seven seasons before our involvement, stadium attendance per season for the first division amounted to on average 2,954,311, which corresponds to an average of 9,654 fans per match. In the ten seasons for which we provided the schedule, stadium attendance equalled 3,451,945 per season (11,491 per match) on average, which corresponds to an increase of 17%. At the same time, the number of man-hours performed by the police decreased from 28,613 per season in the three seasons right before our involvement to 21,780 per season since we create the official schedule (i.e. a decrease of about 24%). This decrease is remarkable, because since the introduction of the play-offs more matches are played, and many of these additional matches are risk matches. Obviously, there are many factors that play a role in these changes, for instance the introduction of the play-offs has undoubtedly impacted the attractiveness of the competition, and the fanbase of the team that promotes to and the team that is relegated from the first division certainly plays a role. Nevertheless, we like to believe that our scheduling approach also has contributed considerably to these positive trends. Equally important, it has improved the transparency of the process. Although, obviously, the stakeholders do not have a real understanding of the optimization method itself, it is seen as neutral. Moreover, it is now clear to

everyone what the various requirements are, and what weight they get. Setting these weights is not an exact science. Therefore, we present the Pro League with several good schedules to choose from, instead of just the best. Occasionally, the Pro League eventually selects a schedule which is not optimal according to our approach, which is a motivation for us to reevaluate the weights that some of the requirements receive. Our method offers additional flexibility through what-if analyses, which can be used to assess the consequences of honoring certain wishes. As a result, the yearly tradition of stakeholders having a big fight in the media when the new schedule is announced has now disappeared.

Although we have made a lot of progress with the Pro League over the past 10 years, there are still a number of opportunities for further research. We believe that these opportunities not only apply to our case with the Belgian soccer league, but to the sports scheduling community in general. Phased approaches are very popular, and they perform well provided that the most important requirements can be solved in earlier phases. Nevertheless, there is still room for improvement with respect to solution methods. We are not able to solve highly-constrained sports scheduling problems optimally for league sizes larger than 12. We have little insight in what makes a HAPset feasible, particularly if the home-away patterns are not symmetrical and feature several breaks. Many practical sports scheduling problems require exactly these type of home-away patterns. Scheduling multiple leagues simultaneously is another major challenge for future research. Indeed, according to our experience, the focus is shifting from scheduling one important league to scheduling a multitude of leagues with interdependencies. This is even more apparent in amateur of youth sport leagues. Finally, we would like to point out the importance of sports analytics as a way to determine what is important in sports scheduling. We noticed that stakeholders often don't have a good view on the impact of the schedule on fairness, gate revenue, TV viewership, or other issues they care about. Hence, the sports scheduling community can contribute by clarifying these relationships, and assist practitioners with providing the right parameters for their sports scheduling problem.

References

1. Alavy, K., Gaskell, A., Leach, S., Szymanski, S.: On the edge of your seat: demand for football on television and the uncertainty of outcome hypothesis. Int. J. Sport Financ. **5**, 75–95 (2010)
2. Anderson, I.: Balancing carry-over effects in tournaments. In: Holroyd, F., Quinn, K., Rowley, C., Webb, B. (eds.) Combinatorial Designs and Their Applications, pp. 1–16 (1997)
3. Alarcón, F., Duran, G., Guajardo, M.: Referee assignment in the Chilean football league using integer programming and patterns. Int. Trans. Oper. Res. **21**, 415–438 (2014)
4. Angulo-Meza, L., Soares de Mello, J.C.C.B., Valério, R.P.: Assessing the efficiency of sports in using financial resources with DEA models? Procedia Comput. Sci. **55**, 1151–1159 (2015)

5. Bartsch, T., Drexl, A., Kröger, S.: Scheduling the professional soccer leagues of Austria and Germany. Comput. Oper. Res. **33**, 1907–1937 (2006)
6. Boon, B., Sierksma, G.: Team formation: matching quality supply and quality demand. Eur. J. Oper. Res. **148**(2), 277–292 (2003)
7. Briskorn, D., Drexl, A., Spieksma, F.C.R.: Round tobin tournaments and three index assignments. 4OR **8**, 365–374 (2010)
8. Buraimo, B.: Stadium attendance and television audience demand in English league football. Manag. Decis. Econ. **29**, 513–523 (2008)
9. Buraimo, B., Forrest, D., Simmons, R.: Insights for clubs from modeling match attendance in football. J. Oper. Res. Soc. **60**(2), 147–155 (2009)
10. de Carvalho, M., Boen, F., Sarmento, J., Scheerder, J.: What brings youngsters into the stadium? Sociopsychological predictors of soccer attendance among Belgian and Portuguese young fans. Portuguese J. Sports Sci. **1**, 21–40 (2015)
11. de Werra, D.: Geography, games and graphs. Discrete Appl. Math. **2**(4), 327–337 (1980)
12. de Werra, D.: Scheduling in sports. In: P. Hansen (ed.) Studies on Graphs and Discrete Programming, pp. 381–395 (1981)
13. Drexl, A., Knust, S.: Sports league scheduling: graph- and resource-based models. Omega **35**, 465–471 (2007)
14. Duran, G., Guajardo, M., Miranda, J., Saure, D., Souyris, S., Weintraub, A., Wolf, R.: Scheduling the Chilean soccer league by integer programming. Interfaces **37**, 539–552 (2007)
15. Easton, K., Nemhauser, G., Trick M.: Sports scheduling. In: Leung (ed.) Handbook of Scheduling, CRC Press, Florida, pp. 52.1–52.19 (2004)
16. Elf, M., Jünger, M., Rinaldi, G.: Minimizing breaks by maximizing cuts. Oper. Res. Lett. **31**, 343–349 (2003)
17. Forrest, D., Simmons, R., Buraimo, B.: Outcome uncertainty and the couch potato audience. Scott. J. Polit. Econ. **52**, 641–661 (2005)
18. Forrest, D., Simmons, R.: New issues in attendance demand: the case of the English football league. J. Sports Econ. **7**(3), 247–266 (2006)
19. Forrest, D., McHale, I.G.: Subjective well-being and engagement in sport: evidence from England. In: Rodríguez, P., Kesenne, S., Humphreys, B.R. (eds.) The Economics Of Sport, Health And Happiness: The Promotion of Well-Being Through Sporting Activities, pp. 184–199. Edward Elgar Publishing (2011)
20. Garcia, J., Rodriguez, P.: The determinants of football match attendance revisited: empirical evidence from the Spanish football league. J. Sports Econ. **3**, 18–38 (2002)
21. Goossens, D., Spieksma, F.C.R.: Scheduling the Belgian soccer league. Interfaces **39**(2), 109–118 (2009)
22. Goossens, D., Spieksma, F.C.R.: Breaks, cuts, and patterns. Oper. Res. Lett. **39**(6), 428–432 (2011)
23. Goossens, D., Belien, J., Spieksma, F.C.R.: Comparing league formats with respect to match importance in Belgian football. Ann. Oper. Res. **194**, 223–240 (2012)
24. Goossens, D., Spieksma, F.C.R.: Soccer schedules in Europe: an overview. J. Sched. **15**(5), 641–651 (2012)
25. Goossens, D., Spieksma, F.C.R.: The carryover effect does not influence football results. J. Sports Econ. **13**(3), 288–305 (2012)
26. Geril, J.: Ons budget voor transfers? Nul komma nul euro. Het Nieuwsblad (VUM), 2 February 2007. (in Dutch)
27. Guedes, A.C.B., Ribeiro, C.C.: A heuristic for minimizing weighted carry-over effects in round robin tournaments. J. Sched. **14**(6), 655–667 (2011)

28. Hirotsu, N., Wright, M.B.: Using a Markov process model of an association football match to determine the optimal timing of substitution and tactical decisions. J. Oper. Res. Soc. **53**(1), 88–96 (2002)
29. Januario, T., Urrutia, S., Ribeiro, C.C., de Werra, D.: Edge coloring: a natural model for sports scheduling. Eur. J. Oper. Res. **254**, 1–8 (2016)
30. Kendall, G., Knust, S., Ribeiro, C.C., Urrutia, S.: Scheduling in sports: an annotated bibliography. Comput. Oper. Res. **37**, 1–19 (2010)
31. Kirkman, T.: On a problem in combinations. Camb. Dublin Math. J. **2**, 191–204 (1847)
32. Reunes, M.: Club boos op Charleroi. Het Nieuwsblad (VUM), 29 September 2005. (in Dutch)
33. Lambrechts, E., Ficker, A.M.C., Goossens, D.R. Spieksma, F.C.R.: Round-robin tournaments generated by the circle method have maximum carry-over. Mathematical Programming (2018), in press. https://doi.org/10.1007/s10107-017-1115-x
34. Madalozzo, R., Villar, R.B.: Brazilian football: what brings fans to the game? J. Sports Econ. **10**, 639–650 (2009)
35. Mendelsohn, E., Rosa, A.: One-factorizations of the complete graph - a survey. J. Graph Theory **9**, 43–65 (1985)
36. Miyashiro, R., Iwasaki, H., Matsui, T.: Characterizing feasible pattern sets with a minimum number of breaks. In: Burke, E., De Causmaecker, P. (eds.) PATAT 2002. LNCS, vol. 2740, pp. 78–99. Springer, Heidelberg (2003). https://doi.org/10.1007/978-3-540-45157-0_5
37. Miyashiro, R., Matsui, T.: A polynomial-time algorithm to find an equitable home-away assignment. Oper. Res. Lett. **33**, 235–241 (2005)
38. Nemhauser, G.L., Trick, M.A.: Scheduling a major college basketball conference. Oper. Res. **46**, 1–8 (1998)
39. Nurmi, K., Goossens, D., Bartsch, T., Bonomo, F., Briskorn, D., Duran, G., Kyngäs, J., Marenco, J., Ribeiro, C.C., Spieksma, F., Urrutia, S., Wolf-Yadlin, R.: A Framework for Scheduling Professional Sports Leagues. In: Sio-Iong, A. (ed.) IAENG Transactions on Engineering Technologies, vol. 5, pp. 14–28 (2010)
40. Rasmussen, P., Trick, M.A.: Round robin scheduling - a survey. Eur. J. Oper. Res. **188**, 617–636 (2008)
41. Recalde, D., Torres, R., Vaca, P.: Scheduling the professional Ecuadorian football league by integer programming. Comput. Oper. Res. **40**, 2478–2484 (2013)
42. Russell, K.G.: Balancing carry-over effects in round robin tournaments. Biometrika **67**(1), 127–131 (1980)
43. Scarf, P.A., Shi, X.: The importance of a match in a tournament. Comput. Oper. Res. **35**(7), 2406–2418 (2008)
44. Wang, C., Goossens, D., Vandebroek, M.: The impact of the soccer schedule on T V viewership and stadium attendance: evidence from the Belgian Pro League. J. Sports Econ. (2017, to appear). https://doi.org/10.1177/1527002515612875

Operations Research and Voting Theory

Olivier Hudry(✉)

Télécom ParisTech, 46, rue Barrault, 75634 Paris Cedex 13, France
olivier.hudry@telecom-paristech.fr

Abstract. One main concern of voting theory is to determine a procedure for choosing a winner from among a set of candidates, based on the preferences of the voters or, more ambitiously, for ranking all the candidates or a part of them. In this presentation, we pay attention to some contributions of operations research to the design and the study of some voting procedures. First, we show through an easy example that the voting procedure plays an important role in the determination of the winner: for an election with four candidates, the choice of the voting procedure allows electing anyone of the four candidates with the same individual preferences of the voters. This provides also the opportunity to recall some main procedures, including Condorcet's procedure, and leads to the statement of Arrow's theorem. In a second step, more devoted to a mathematical approach, we detail a voting procedure based on the concept of Condorcet winner, namely the so-called median procedure. In this procedure, the aim is to rank the candidates in order to minimize the number of disagreements with respect to the voters' preferences. Thus we obtain a combinatorial optimization problem. We show how to state it as a linear programming problem with binary variables. We specify the complexity of this median procedure. Last, we show, once again through easy examples, that the lack of some desirable properties for the considered voting procedure may involve some "paradoxes".

Keywords: Voting theory · Combinatorial optimization · Condorcet winner
Median procedure · Voting paradoxes

1 Introduction

One main concern of voting theory is to determine a *procedure* (also called, according to the context or the authors, *rule*, *method*, *social choice function*, *social choice correspondence*, *system*, *scheme*, *count*, *rank aggregation*, *principle*, *solution* and so on) for choosing a winner from among a set of candidates or, more ambitiously, for ranking all the candidates or a part of them, based on the preferences of the voters (for the context and references, see for instance [1, 4, 5, 14, 15, 18, 27, 31, 37, 51, 55, 58]). In the sequel, we shall consider an election involving n candidates and v voters. The preferences of the voters are assumed to be *complete preorders* (i.e., binary relations which are reflexive, transitive and complete; as reflexivity is not important here, we shall not consider it in this contribution) defined on the set X of candidates. In other words, the voters are supposed to be able to rank all the candidates, possibly with ties, in a transitive manner: if the voter prefers a candidate x to another candidate y and y to a third candidate z, then he or she prefers also x to z. Most of the time, we shall assume

G. H. Parlier et al. (Eds.): ICORES 2017, CCIS 884, pp. 20–41, 2018.
https://doi.org/10.1007/978-3-319-94767-9_2

that there is no tie, which means that, for any pair $\{x, y\}$ of distinct candidates x and y, a voter strictly prefers x to y or y to x; in this case, the voters' preferences are in fact *linear orders* defined on X. For any voter V and for distinct candidates x and y, we shall write $x >_V y$ (or simply $x > y$ if V does not matter) to denote the fact that x is preferred to y by V. Then the preference $>_V$ of V is a complete preorder if we have simultaneously:

1. $\forall (x, y) \in X^2$ with $x \neq y$, $x >_V y$ or $y >_V x$ (completeness)
2. $\forall (x, y, z) \in X^3$ with $x \neq y \neq z \neq x$, $\{x >_V y \text{ and } y >_V z\} \Rightarrow x >_V z$ (transitivity).

It is a linear order if we have, in addition:

3. $\forall (x, y) \in X^2$ with $x \neq y$, $x >_V y \Rightarrow$ not $(y >_V x)$ (antisymmetry).

Thus a linear order is an antisymmetric complete preorder and conversely.

The aim of the election is to determine a winner of the election or to rank the candidates (or a part of them) into a collective preference, based on the individual preferences of the voters. Usually, it is considered that a voting procedure must fulfil some desirable properties to be satisfying. For example, it is usually wished that the preferences of all the voters are taken in consideration, which excludes any *dictator*, a dictator being a voter who imposes his or her preferences, without respect to the preferences of the other voters (in a variant, a dictator imposes only his or her strict preferences and leaves the choice to the other voters for the ties existing in the dictator's preferences). Or it is wished also that the voting method is *monotonous*, i.e. fulfils the following property: let x be the winner of an election; if the rank of x becomes better in the preferences of one voter while the preferences of the other voters remain the same, then x remains the winner of the election.

In fact, designing a voting procedure with satisfying properties is not always an easy task, depending on the required properties considered as "satisfying". The usual voting methods fail to respect simultaneously some basic properties, and *Arrow's theorem*, stated below (see Sect. 2.5) explains why, by showing that there does not exist any voting procedure fulfilling these basic properties. Anyway, since there does not exist an "ideal" voting method, how to elect the winner of the election or how to rank the candidates?

Section 2 recalls, through a small and easy example, the principles of four classic voting methods: *one-round procedure* (also known as *plurality rule*), *two-round procedure* (also known as *plurality rule with run-off*), *Borda's procedure*, *Condorcet's procedure*. This example outlines the role of the voting method in the choice of the winner: for the same given voters' preferences applied to an election with four candidates, we may elect any of these four candidates by selecting the appropriate voting procedure.

An important concept in voting theory is the one of *Condorcet winner*: a Condorcet winner is a candidate who is preferred to any other candidate by a majority of voters. In other words, a candidate C is a Condorcet winner if, for any other candidate x, the number of voters who prefer C to x is (strictly) greater than the number of voters who prefer x to C. Such a Condorcet winner does not necessarily exist; when he or she

exists, he or she is unique. When there is no Condorcet winner, several methods aim to recover a Condorcet winner by altering, though the least possible, the data (the voters' preferences) so that a Condorcet winner appears. In Sect. 3, we will focus on one of these methods: Condorcet-Kemeny's method. It leads to interesting, but hard (more precisely, NP-hard), combinatorial optimization problems.

The last part of this contribution will be devoted to some unexpected results, which we shall call *paradoxes*, related to the lack of some good properties, like *monotony*. For instance, we shall see that, for the two-round procedure, it can be better for a voter to vote for the candidate ranked last in his or her preferences rather than for the candidate that he or she prefers, in order to make his or her favourite candidate elected.

2 An Electoral Tale

2.1 Some Historical Milestones

It is usual to consider that the search for a "good" voting procedure goes back at least to the end of the eighteenth century, with the works by the chevalier de Borda (1733–1799) [11] and by the marquis de Condorcet (1743–1794) [16], and maybe before (for references upon the historical context, see [10, 27, 29, 40–45] and references below).

More precisely, in the 1770's, Borda [11], a member of the French Academy of Sciences, showed that the one-round procedure (see below) used at this time by this academy was not satisfactory. Indeed, with such a voting procedure, the winner can be contested by a majority of voters who would all agree to choose another candidate instead of the elected winner. (We shall see below that the two-round procedure used in many countries has the same defect.) Borda then suggested another procedure (see below). But, as pointed out by Condorcet in 1784 [16], the procedure advocated by Borda has the same defect as the one depicted by Borda himself for the one-round procedure: a majority of dissatisfied voters could agree to constitute a majority coalition against the candidate elected by Borda's procedure in favour of another candidate. Then Condorcet designed a method based on pairwise comparisons. By nature, this method cannot elect a winner who will give rise to a majority coalition against him or her. But, unfortunately, Condorcet's procedure does not always succeed in finding a winner (who is a *Condorcet winner* when he or she exists), as we are going to see below. By the way, notice that, according to McLean et al. [43], "both Ramon Llull (ca 1232–1316) and Nicolaus of Cusa (also known as Cusanus, 1401–1464) made contributions which have been believed to be centuries more recent. Llull promotes the method of pairwise comparison […]. Cusanus proposes the Borda rule, which should properly be renamed the Cusanus rule". Despite these historical discoveries, we shall keep the usual names here.

In order to illustrate Borda's and Condorcet's criticisms and procedures, consider the following example of an election (drown from [7]), with $n = 4$ candidates (noted x, y, z and t) and $v = 27$ voters. The voters' preferences are supposed to be the following linear orders:

- for 5 voters: $x > y > z > t$
- for 4 voters: $x > z > y > t$

- for 2 voters: $t > y > x > z$
- for 6 voters: $t > y > z > x$
- for 8 voters: $z > y > x > t$
- for 2 voters: $t > z > y > x$.

Then, the question is: who is the winner?

In fact, the answer depends strongly on the voting procedure adopted to determine the winner, as we are going to see now.

2.2 One-Round Procedure (Plurality Rule) and Two-Round Procedure (Plurality Rule with Run-off)

One of the easiest voting procedure in order to elect one candidate as the winner is the *one-round procedure* (also called *plurality rule* or *relative majority*, or sometimes *first-past-the-post*, or *winner-takes-all*, or also *majoritarian voting*…). In this procedure, each voter gives one point to his or her favourite candidate (so it is not necessary to know the preferences of the voters on the whole set of candidates). The candidate who gains the maximum number of points is the winner.

This procedure belongs to the family of *scoring procedures*. In such a procedure, a *score-vector* $(s_1, s_2,\ldots, s_n)$ is fixed independently of the voters, with $s_1 \geq s_2 \geq \ldots s_n$. For each voter, a candidate x receives s_i points if x is ranked at the i^{th} position by the considered voter. The *score* of x is the total number of points that x receives. The winner is any candidate with a maximum score. If the aim is to rank the candidates, we may also sort them according to the decreasing scores and then consider the linear extensions of the complete preorder provided by this sorting (another possibility would be to apply the procedure $n - 1$ times, after having removed the winner of the current iteration). For the one-round procedure, the score-vector is (1, 0, 0,…, 0).

Applied to our example, the one-round procedure provides the following scores:

$$9 \text{ for } x,\ 0 \text{ for } y,\ 8 \text{ for } z,\ 10 \text{ for } t.$$

Then the winner is t (we may also rank the four candidates thanks to these scores; we thus obtain the linear order $t > x > z > y$, that we may consider as the collective preference – according to the one-round procedure).

Anyway, following Borda's remarks, if a second-round is organized between the two candidates with the best scores after the first round, as in the two-round procedure, then t is no longer the winner. Indeed, t and x are the two candidates who are not eliminated by the first round. If we assume that the preferences of the voters remain the same between the two rounds, the eight voters who preferred z now vote for x (ranked third in their preferences while t is ranked fourth by them). After the second round, the scores are the following:

$$17 \text{ for } x,\ 10 \text{ for } t.$$

Now, t is defeated by x, and x is the winner according to the two-round procedure.

In other words, the election of t could give rise to a majority of dissatisfied voters who would agree to constitute a majority coalition against t in favour of another candidate, namely x.

So, is x better than t with this respect? Borda noticed that this drawback applies also to the two-round procedure. Indeed, for the example, if x is declared as the winner of the election, then another majority of dissatisfied voters could agree to constitute a majority coalition against x in favour of y: there are 18 voters who prefer y to x versus 9 who prefer x to y!

2.3 Borda's Procedure

The previous considerations led Borda to design his own method. In Borda's procedure, each voter gives points to the candidates according to their ranks in his or her preferences. More precisely, if there are n voters ($n = 4$ in the example), each voter gives n points to the candidate ranked first, then $n - 1$ to the second candidate, $n - 2$ to the third candidate, and so on, until the last candidate who receives only one point. Then, all these points are summed up for each candidate: this sum is the *Borda score* s_B of the candidate. The candidate with a maximum Borda score is the *Borda winner*. With this respect, Borda's procedure is also a scoring procedure, of which the score-vector is $(n, n-1,\ldots, 2, 1)$ (a variant consists in considering $(n-1, n-2,\ldots, 1, 0)$ or $(n+\alpha,\ n-1+\alpha,\ldots,\ 2+\alpha,\ 1+\alpha)$ as the score-vector, where α is any positive integer; the result is obviously the same).

For instance, the Borda score $s_B(x)$ of x in the example is equal to:

$$s_B(x) = 5 \times 4 + 4 \times 4 + 2 \times 2 + 6 \times 1 + 8 \times 2 + 2 \times 1 = 64.$$

Similarly, we obtain:

$$s_B(y) = 75, s_B(z) = 74, s_B(t) = 57.$$

With Borda's procedure, the winner is y. We may even rank all the candidates by sorting Borda scores decreasingly: we obtain the collective preference $y > z > x > t$ (which is the reverse order of the order provided by the one-round procedure!).

But Borda's procedure fails to avoid the previous criticism, since a majority of voters, more precisely 14 voters, would agree to constitute a majority coalition against y in favour of z! (In spite of this, Borda's procedure was adopted by the French Academy – and then by the Institut de France – until 1803…).

2.4 Condorcet's Procedure

In order to avoid the rise of a majority coalition of dissatisfied voters, Condorcet designed a method based on the *majority relation* in a *pairwise comparison method*. For each candidate x and each candidate y with $x \neq y$, we compute the number m_{xy}, that we will call the *pairwise comparison coefficients* below, of voters who prefer x to y. Then x is considered as better than y if a majority of voters prefers x to y, i.e. if we

have $m_{xy} > m_{yx}$. This defines the (*strict*) *majority relation* M: $xMy \Leftrightarrow m_{xy} > m_{yx}$. In some cases, there exists a Condorcet winner, i.e. a candidate C defeating any other candidate: $\forall\, x \neq C$, $m_{Cx} > m_{xC}$. As noticed above, if there exists a Condorcet winner, then he or she is unique. It may even happen that M is a linear order and allows to rank all the candidates. It is the case for our example. Indeed, for our example, the pairwise comparison coefficients are the following:

- $m_{xy} = 9$; $\boldsymbol{m_{yx} = 18}$;
- $m_{xz} = 11$; $\boldsymbol{m_{zx} = 16}$;
- $\boldsymbol{m_{xt} = 17}$; $m_{tx} = 10$;
- $m_{yz} = 13$; $\boldsymbol{m_{zy} = 14}$;
- $\boldsymbol{m_{yt} = 17}$; $m_{ty} = 10$;
- $\boldsymbol{m_{zt} = 17}$; $m_{tz} = 10$.

The bold values are the ones greater than the majority $v/2$ (= 13.5 in the example). These values show that the majority relation is here a linear order, $z > y > x > t$; here, z is the Condorcet winner and the winner of the election too. By the way, we may observe that, though the election admits a Condorcet winner, this one is not elected by the previous three procedures.

By construction, it is impossible to achieve a majority coalition of dissatisfied voters against a Condorcet winner. But the problem with this procedure, as noticed by Condorcet himself [16], relies in the fact that a Condorcet winner may not exist. The smallest example showing this is the following, with $n = 3$ candidates (x, y, z) and $v = 3$ voters as well (the preferences are still assumed to be linear orders):

- for 1 voter: $x > y > z$
- for 1 voter: $y > z > x$
- for 1 voter: $z > x > y$.

Then the pairwise comparison coefficients are:

- $\boldsymbol{m_{xy} = 2}$; $m_{yx} = 1$;
- $m_{xz} = 1$; $\boldsymbol{m_{zx} = 2}$;
- $\boldsymbol{m_{yz} = 2}$; $m_{zy} = 1$.

Here, we have a majority relation which is not transitive, but cyclic: x is preferred to y by a majority of voters, y is preferred to z by a(nother) majority of voters, and z is preferred to x by a (third) majority of voters. There is no Condorcet winner and so Condorcet's procedure cannot be applied here. It is the so-called "voting paradox" or also "Condorcet effect" [27]: the aggregation of linear orders does not necessarily provide a linear order. According to Guilbaud [27], the probability of the appearance of the Condorcet effect for three candidates varies from 5.56% (for three voters) to about 8.77% (for a number of voters that tends towards infinity). It grows with the number of candidates, and, for a given number of candidates, it grows when the number of voters increases. For example, according to Gehrlein [24] (see also [25]), it is about 52.5% for 25 candidates and 3 voters, reaching about 73% for 25 candidates and an infinite number of voters.

We can anyway distinguish between three cases:

- the Condorcet effect does not involve all the candidates and a Condorcet winner does exist; if the aim is only to elect one person, this situation is not problematic: the Condorcet winner is elected;
- candidates may be gathered into subsets in such a way that all candidates in one subset are preferred to all candidates in another subset; we may then focus our attention to the top subset and eliminate the candidates belonging to the other subsets; the problem is now to know how to rank candidates from the top subset;
- finally, the most embarrassing case is that in which the Condorcet effect involves all the candidates at once and does not allow any conclusion, even partial, for the collective preference.

In the case of 6 candidates and 21 voters, Mimiague and Rousseau [46] have experimentally estimated that the probability that the result of the procedure gives a "paradox" of the first type is about 35%, the second type is 20%, and of the third type 10%. According to these authors, when the numbers of candidates and voters increase, the last two cases (no Condorcet winner) become predominant and the first case disappears (however, there are significant differences between the values of these authors and those obtained by Gehrlein).

We can see from this example that the choice of the voting procedure is also a determining factor, while it is sometimes considered that the result of an election comes only and intrinsically from the voters' preferences: here, for a same set of preferences, four voting procedures, four different winners (the interested reader can find another example in [3], involving five voting methods applied to five candidates, with five different winners…). Borda was maybe the first to notice this explicitly (see [40]): "C'est une opinion généralement reçue, et contre laquelle je ne sache pas qu'on ait jamais fait d'objection, que dans une élection au scrutin, la pluralité des voix indique toujours le vœu des électeurs, c'est-à-dire que le candidat qui a obtenu cette pluralité est nécessairement celui que les électeurs préfèrent à ses concurrents. Mais […] cette opinion, qui est vraie dans le cas où l'élection se fait entre deux sujets seulement, peut induire en erreur dans tous les autres cas" ("It is a generally received opinion, and against which I do not know that anybody objected, that, in an election, the plurality of voices always indicates the wishes of voters, i.e. that the candidate who got this plurality is necessarily the one that voters prefer to its competitors. But […] this opinion, which is true when the election is between two candidates only, can be misleading in all other cases").

2.5 Arrow's Theorem

From the previous example, we may conclude that none of these four methods is utterly satisfactory when we consider the properties which are usually considered as desirable. In 1951, Arrow [1] shows that there does not exist a "good" voting procedure, with respect to some "reasonable" axiomatic properties; this is known as the famous "impossibility theorem". More precisely, assuming that the preferences of the voters are complete preorders (see above; as already noticed, the set of complete preorders

includes the one of linear orders, quite often considered to model the preferences of the voters) and that the result of the voting procedure should also be a complete preorder, Arrow considered the following properties:

- *unrestricted domain or universality*: the voting procedure must be able to provide a result whatever the preferences of the voters are;
- *independence of irrelevant candidates*: the collective preference between candidates x and y must depend only on the individual preferences between x and y; in other words, the collective preference between x and y must remain the same as long as the individual preferences between x and y do not change;
- *unanimity* (or *Pareto property*): if a candidate x is preferred to another candidate y by all the voters, then x must be preferred to y in the collective preference too.

Arrow showed that, if there are at least three candidates (things are much more comfortable with only two candidates!), the only procedure which satisfies these three conditions at once is the dictatorship, in which one voter (the dictator) imposes his or her preference. Though this impossibility theorem ruins the hope to design a voting procedure fulfilling the usual desirable properties, several procedures have been suggested since this date. Among the ways to escape Arrow's impossibility theorem, we find:

- the definition of other axiomatic systems leading to voting procedures which would not be the dictatorship;
- the restriction of the individual preferences to more constrained domains;
- adapting the result, when this one is not satisfactory with respect to the required axiomatic properties, into a result fulfilling these properties and fitting the genuine result as well as possible, for some criterion which must be defined.

The main questions associated with the first possibility are "given some axiomatic properties, what are the voting procedures satisfying these properties?" or, conversely, "given a voting procedure, what is the proper axiomatic system characterizing this procedure?"; we shall not consider this direction here.

The second possibility can be illustrated, for instance, by the restriction of the individual preferences to *single-peaked linear orders*. To define them, assume that we can order the candidates on a line, from the left to the right, and assume that this linear order Ω does not depend on the voters (from a practical point of view, Ω is not always easy to define, even for political elections). For any voter V, let $x(V)$ denote the candidate preferred by V. The preference of V is said to be Ω-*singled-peaked* if, for any candidates y and z with $x(V) \neq y \neq z \neq x(V)$ and located on the same side of Ω from $x(V)$, y is preferred to z by V if and only if y is closer to $x(V)$ than z with respect to Ω. Let L_Ω denote the set of Ω-single-peaked linear orders. Black [10] showed that, for any order Ω, the aggregation of Ω-single-peaked linear orders by Condorcet's procedure provides an Ω-single-peaked linear order (if we assume that there is no tie). So, if the individual preferences are assumed to be Ω-single-peaked linear orders, there is no "Condorcet effect" and Condorcet's procedure can be applied.

The third direction was followed by Kemeny in 1959 [39], when he studied the aggregation of complete preorders into a *median complete preorder* (see below). Notice that this approach is also attributed to Condorcet for the aggregation of linear orders

into a linear order; in the sequel, we will refer the search for a median linear order or of a median complete preorder as the Condorcet-Kemeny problem (as other people rediscovered this problem or some of its variants [48], the problem is also known under other names, see [17]). We detail such a possibility in the next section.

3 Condorcet-Kemeny's Problem

As seen in Sect. 2, Condorcet's procedure may fail in providing a Condorcet winner: the majority relation then contains cycles. The method depicted in this section, the Condorcet-Kemeny's procedure, selects the Condorcet winner as the winner of the election, when this Condorcet winner does exist; otherwise, we compute a linear order at minimum distance from the collection of voters' preferences: the candidate at the top of such an optimal linear order is considered as the winner of the election. We detail this method below.

3.1 Condorcet-Kemeny's Problem Stated as a 0–1 Linear Programming Problem

In Condorcet-Kemeny's method, the aim is to compute a complete preorder or a linear order fitting the majority relation M "as well as possible". To specify what "as well as possible" means, we use the *symmetric difference distance* δ defined, for two binary relations R and S defined on X, by:

$$\delta(R,S) \;=\; \left|\left\{(x,y)\in X^2 :\; (xRy \text{ and } x\bar{S}y) \text{ or } (x\bar{R}y \text{ and } xSy)\right\}\right|.$$

This quantity $\delta(R, S)$ measures the number of disagreements between R and S. Though it is possible to consider other distances, δ is used widely and is appropriate for many applications. Barthélemy [6] shows that δ satisfies a number of naturally desirable properties, and Barthélemy and Monjardet [8] recall that $\delta(R, S)$ is the Hamming distance between the characteristic matrices (see below) of R and S and point out the links between δ and the L_1-metric or the square of the Euclidean distance between these matrices (see also [47, 48]).

Then, let $\Pi = (R_1, R_2, \ldots, R_v)$ denote the collection, called *a profile*, of the preferences of the v voters (then, for $1 \leq i \leq v$, the R_i's are complete preorders or are linear orders according to the context). We then define a *remoteness* $\Delta(\Pi, R)$ between a binary relation R defined on X and the profile Π by:

$$\Delta(\Pi,\ R) = \sum_{i=1}^{v} \delta(R_i,\ R).$$

The remoteness $\Delta(\Pi, R)$ measures the total number of disagreements between Π and R (other remoteness functions are studied in [35]).

Our aggregation problem can be seen now as a combinatorial optimization problem: given the profile Π, determine a binary relation R^* minimizing Δ over the set of complete preorders or of linear orders defined on X. Such a relation R^* minimizing Δ is

called a *median relation* (more precisely a *median complete preorder* or a *median linear order*) of Π (see [8, 36]).

We may state $\Delta(\Pi, R)$ for any relation R thanks to variables describing R. Let $r = \left(r_{xy}\right)_{(x,y)\in X^2}$ be the *characteristic matrix* associated with R, i.e. the matrix defined by: $r_{xy} = 1$ if x is preferred to y by R and $r_{xy} = 0$ otherwise (as reflexivity does not matter, we may set $r_{xx} = 0$ if we wish…). Similarly, for $1 \leq i \leq v$, let r^i_{xy} be equal to 1 if x is preferred to y by R_i and to 0 otherwise (with $r^i_{xx} = 0$…); note the equalities $r^i_{xy} + r^i_{yx} = 1$ for any distinct x and y when the relations R_i are linear orders and the inequalities $r^i_{xy} + r^i_{yx} \geq 1$ when the relations R_i are complete preorders. Because the quantities r^i_{xy} and r_{xy} are equal to 1 or 0, we have:

$$\begin{aligned}\delta(R_i, R) &= \sum_{(x,y)\in X^2} \left| r^i_{xy} - r_{xy} \right| = \sum_{(x,y)\in X^2} \left(r^i_{xy} - r_{xy} \right)^2 \\ &= \sum_{(x,y)\in X^2} r^i_{xy} + \sum_{(x,y)\in X^2} (1 - 2r^i_{xy}) \cdot r_{xy}.\end{aligned}$$

From this, we obtain:

$$\Delta(\Pi,\ R) = \sum_{i=1}^{v} \delta(R_i,\ R) \ = \ \lambda \ - \sum_{(x,y)\in X^2} m_{xy} \cdot r_{xy}$$

where λ is a constant (depending only on the profile Π) and with, for $(x, y) \in X^2$, $m_{xy} = 2\sum_{i=1}^{v} r^i_{xy} - v$. The quantity m_{xy} may be interpreted as the difference between twice the number of the voters who prefer x to y and the total number v of voters. Moreover, when all the relations R_i for $1 \leq i \leq v$ are linear orders, then note the relation $m_{yx} = -m_{xy}$ and the equality $\lambda = vn(n - 1)/2$ (both relations coming from the equality $r^i_{xy} + r^i_{yx} = 1$, true for any distinct x and y, and from the equality $r^i_{xx} = 0$, true for any x); then m_{xy} can also be interpreted in this case as the difference between the number of voters who prefer y to x and the number of voters who prefer x to y: we recover the pairwise comparison coefficients of Condorcet's procedure (see above).

Thus the minimization of $\Delta(\Pi, R)$ is the same as the maximization of $\sum_{(x,y)\in X^2} m_{xy} \cdot r_{xy}$ over the set of complete preorders or of linear orders. The constraints defining the fact that R must be a complete preorder or a linear order are the following (except the reflexivity which, once again, does not matter here):

- completeness: $\forall\ (x, y) \in X^2$ with $x \neq y$, $r_{xy} + r_{yx} \geq 1$
- transitivity: $\forall\ (x, y, z) \in X^3$ with $x \neq y \neq z \neq x$, $r_{xy} + r_{yz} - r_{xz} \leq 1$
- and, for linear orders, antisymmetry: $\forall\ (x, y) \in X^2$ with $x \neq y$, $r_{xy} + r_{yx} \leq 1$, which, combined with completeness, gives: $\forall\ (x, y) \in X^2$ with $x \neq y$, $r_{xy} + r_{yx} = 1$.

We thus obtain a linear programming problem with binary variables:

- for the computation of a median complete preorder:

$$\text{Maximize} \sum_{(x,y)\in X^2} m_{xy} \cdot r_{xy}$$

with the following constraints:
$\forall\ (x, y) \in X^2$ with $x \neq y$, $r_{xy} + r_{yx} \geq 1$ (completeness),
$\forall\ x \in (x, y, z) \in X^3$ with $x \neq y \neq z \neq x$, $r_{xy} + r_{yz} - r_{xz} \leq 1$ (transitivity),
$\forall\ (x, y) \in X^2$, $r_{xy} \in \{0, 1\}$ (binarity);

- for the computation of a median linear order:

$$\text{Maximize} \sum_{(x,y)\in X^2} m_{xy} \cdot r_{xy}$$

with the following constraints:
$\forall\ (x, y) \in X^2$ with $x \neq y$, $r_{xy} + r_{yx} = 1$ (completeness and antisymmetry),
$\forall\ (x, y, z) \in X^3$ with $x \neq y \neq z \neq x$, $r_{xy} + r_{yz} - r_{xz} \leq 1$ (transitivity),
$\forall\ (x, y) \in X^2$, $r_{xy} \in \{0, 1\}$ (binarity).

3.2 Complexity of the Computation of Median Relations

The complexity of the computation of median relations has been studied by several researchers (for the theory of complexity of problems, see [23, 38] or [53]). To my knowledge, Yoshiko Wakabayashi was the first to publish results dealing with the complexity of the computation of median relations. In her PhD thesis ([59]; see also [60]), she pays attention to the computation of different kinds of median relations, including linear orders and complete preorders, but only for profiles of binary relations (i.e. relations without special structural properties). Some of her results deal with the case where the number v of voters is fixed. For the computation of median linear orders or of median complete preorders, her contribution is specified by the following theorem.

Theorem 1. The computation of a median complete preorder or a median linear order of a profile of binary relations is NP-hard. Moreover, for the computation of a median linear order, the problem remains NP-hard for any fixed value of v with $v \geq 1$.

This result has been improved and extended in three directions. First, it has been extended to a profile of v linear orders or to any profile of v relations extending the structure of linear order (which includes the case of complete preorders). Secondly, for the computation of median complete preorders, it has been extended to the case where the number of voters v is fixed. Thirdly, it has been extended to other kinds of medians. Some of these improvements or extensions are provided below.

Bartholdi et al. [9] studied in 1989 the computation of median orders, including the case where the preferences of the voters are linear orders. In their results, the number

v of voters is not fixed but depends on the number of candidates. The same is done, at the same time, in [28] (see also [30]). In 2001, Dwork et al. [20] showed that the computation of a median linear order of a profile of four linear orders is NP-hard (this result remains true for any even value greater than or equal to 4; the case of two voters can easily be shown to be polynomial). More recently (2016), Bachmeier et al. [2] showed that the problem also remains NP-hard for any odd value of v with $v \geq 7$. The cases $v = 3$ and $v = 5$ are still open to my knowledge. These results are summarized in the following theorem.

Theorem 2. The computation of a median linear order of a profile of linear orders is NP-hard and remains so even if the number v of voters is even with $v \geq 4$ or odd with $v \geq 7$. The problem is polynomial for $v = 2$.

The complexity of the computation of median complete preorders of a profile of linear orders is studied in [28, 30]. It is shown that this problem is also NP-hard if the number of voters is large enough with respect to the number of candidates. This result has been improved in [32] by dealing with the case where v is fixed: the problem remains NP-hard for any v with $v \geq 5$.

Theorem 3. The computation of a median complete preorder of a profile of linear orders is NP-hard and remains so even if the number v of voters is fixed with $v \geq 5$.

From the previous results, it is possible to prove (see [32]) that the computation of a median complete preorder of a profile of complete preorders (i.e. Kemeny's problem) is NP-hard. The next theorem is more specific:

Theorem 4. The computation of a median complete preorder of a profile of complete preorders (Kemeny's problem) is NP-hard and remains so even if the number v of voters is even with $v \geq 4$ or odd with $v \geq 7$.

For other results dealing with the complexity of voting procedures or of the computation of median relations, see [15, 31, 33–35].

4 "Paradoxes" in Voting Theory

Some of the "paradoxes" depicted in this section come from the lack of monotony (except if stated otherwise, the examples given below come from [29]; see also [52]). Monotony is the property saying that, if a candidate x is the winner of the election for some given voters' preferences, x must remain the winner if he or she is ranked better in the preferences of at least one voter. If such a property seems quite reasonable, it happens that many voting procedures are not monotonous. Which generates "paradoxes" or, at least, unexpected and usually undesirable effects.

The one-round procedure is obviously monotonous. Anyway, the situation depicted in the next section may appear as a "paradox".

4.1 "Paradox" for the One-Round Procedure

Let us imagine a country divided into constituencies and having a parliament whose members, belonging to political parties, are elected by means of a one-round procedure,

one member per constituency. Is it possible that a given party P has a majority in this parliament while being a minority compared to the voters? If so, what should be its minimum representativeness in the population so that it is so? Similarly, what is the maximum ratio of seats it can occupy in the parliament?

It is easy to see that, from a theoretical point of view, there is no minimum threshold to be respected for the representativeness of this party in the population so that it can obtain all the seats of the parliament, if we can involve as many parties as we want. Indeed, in order that all the members of the parliament belong to P, it is necessary and sufficient that P wins in each constituency. However, this can happen with a representativeness of P as low as we want: it is sufficient to assume that there is a large enough number of competitors and that each of them is ranked worse than the candidate of P. For example, P may represent less than 10% of the population and may win all the seats if we assume that at least eleven parties (including P) have candidates in each constituency and that each party other than P gets only 9.05% of the votes while P obtained 9.5%. This general result, however, is unrealistic because it assumes that the number of parties is unbounded (for the reasoning to be applicable, the number of parties increases when the required threshold decreases).

4.2 "Paradoxes" for the Two-Round Procedure

The result of the previous section remains valid for the two-round procedure if we assume that the transfer of votes between the first and second rounds occurs in favour of P. It is more interesting to know if a similar situation can occur in the second round (which amounts to asking the same question for a one-round vote, but limiting the number of parties to two).

In this case, in order to have all the seats in the parliament, P must win the second round in all constituencies, implying that it obtains an absolute majority in each constituency, which in turn implies that P is a majority in the population of voters. But, conversely, it is enough that P represents a little bit more than 50% of the voters of the second round to win all the seats of the parliament (which would not fail to provoke protests among the opponents of P!…), if the voters who vote at the second round for P are uniformly distributed in the constituencies.

What happens now if P does not seek to have all the seats necessarily, but only wants to be a majority in the parliament? Is it possible to control the parliament by being a minority in the country? The answer is "yes". It is enough that P wins the elections in half the constituencies plus one to have the absolute majority. However, since the constituencies do not necessarily have the same number of voters, P may represent a ratio of the population as low as we wish and still have more than half the seats.

This paradox becomes more interesting by assuming now that the constituencies have exactly the same number of voters. Then, split the constituencies into two categories: those for which P wins the second round and those for which P loses it. In order for P to have at least half the seats plus one in the parliament, the first type must gather at least half the constituencies plus one. In order to win a constituency, P must represent more than 50% of voters in the second round of that constituency. On the other hand, in the second case (constituency lost for P), the representativeness of P can be

zero. In such an extreme case (P represents just a little bit more than half the voters in the constituencies it wins and no one in those it loses), P represents about half of the voters in about half of the constituencies, that is approximately one quarter of the total number of voters (since it was assumed that the constituencies all have the same number of voters). Thus, even with constituencies of identical size, one can have half of the seats of the parliament while representing only about 25% of the voters. Of course, the distribution of voters in the constituencies plays a key role. To do this, they must be divided up so as to gather the opponents of P in "sacrificed" constituencies ("packing strategy", i.e. concentrating the opposing party's voting power in one district to reduce its voting power in other districts), and to distribute the voters favourable to P in the other constituencies to represent half of the voters ("cracking strategy", i.e. diluting the voting power of the opposing party's supporters across many districts). Anyway, this would lead to strange divisions of the constituencies, with bizarre shapes for the boundaries. Such a division is sometimes called "gerrymander", after the name of Governor Elbridge Gerry (1744–1814): in 1812, Gerry signed a bill that redistricted Massachusetts to benefit his Democratic-Republican Party; when mapped, one of the contorted districts in the Boston area was said to resemble the shape of a mythological salamander.

Let us now turn to the question of the monotony of the two-round procedure. For this, consider an election involving three candidates x, y, z and 17 voters whose preferences are given by the following profile of linear orders:

- for 6 voters: $x > y > z$
- for 5 voters: $z > x > y$
- for 4 voters: $y > z > x$
- for 2 voters: $y > x > z$.

Consequently, x and y remain for the second round, with 6 votes each against 5 for z. As the preferences are assumed to remain the same between the rounds, the 12 voters who voted for x or y in the first round keep their votes in the second round, while the 5 voters who voted for z vote now for their second choice, x. It is therefore x who is elected in the second round against y, with 11 votes against 6.

Imagine now that x, the winner, ignoring the outcome of the vote, campaigns against his rival y and succeeds in convincing the last two voters (whose preferences were given by $y > x > z$) to invert x and y in their choices. We thus obtain the following new preferences:

- for 8 voters: $x > y > z$
- for 5 voters: $z > x > y$
- for 4 voters: $y > z > x$.

It is now x and z who remain for the second round. The voters of y now vote for their second choice, z. This gives a total of $5 + 4 = 9$ votes for z in the second round, beating x who has only 8 votes: z is now the winner. And yet the ranks of x in the voters' preferences are better than in the initial situation. One could therefore expect that x remains the winner. This is at least what should happen if the two-round procedure was monotonous; but precisely, it is not! Here, x is still selected for the second

round (it could not be otherwise), but now y no longer collects enough votes to hold against x and is therefore eliminated in favour of z. It is this change of opponent that explains the defeat of x. Conclusion: although x progresses in the preferences of the voters, this progression is harmful to him or her and makes him or her pass from the state of winner to the one of loser. The two-round procedure is not monotonous.

A consequence of this lack of monotony concerns what has sometimes been called "the useful vote", related to "tactical voting" [21]. In voting methods, tactical voting (also called "strategic voting", "sophisticated voting" or "insincere voting") occurs, in elections with more than two candidates, when a voter supports another candidate more strongly than his or her *sincere preference* in order to prevent an undesirable outcome. In such a situation, a voter agrees not to vote for his or her preferred candidate, for example because he or she believes that the candidate is not sufficiently likely to be present in the second round, and transfers his or her vote to his or her second choice, who is considered to be more likely to win (but nevertheless threatened with elimination, so that this "useful vote" is justified in the eyes of the voter who is considering the manipulation of his or her vote). In fact, the previous example shows that this "useful vote" could harm those who believe in benefiting from it: the "useful vote" applied by the last two voters to x causes the latter to lose.

Another consequence, also paradoxical, is that a voter may have interest in voting for the candidate that he or she least likes to finally help his or her favourite candidate win. Consider the following example, again with three candidates x, y and z, and 17 voters:

- for 6 voters: $x > y > z$
- for 5 voters: $z > x > y$
- for 4 voters: $y > z > x$
- for 2 voters: $x > z > y$.

In the first round, y is eliminated; then z is the winner of the second round, thanks to the voters who voted for y. If now the two voters whose preferences are given by the linear order $x > z > y$ do not vote according to their preferences and decide to vote for the candidate they like least, i.e. for y, then z is eliminated from the first round (with 5 votes against 6 for x and 6 for y). Thanks to the contribution of the voters of z and independently of the behaviour of the two voters whose preferences were initially $x > z > y$, x then wins the second round against y. The Machiavellian behaviour of the two voters led them to vote for y, though y is ranked last, in fact in order to eliminate z and thus in order to make x be elected… Of course this strategy is risky and, if we assume, in our example, that all the voters of z prefer y to x, then the two voters who manipulated their votes would have failed in their aim, even contributing to the election of y instead of z, though they would have preferred z to y.

The next paradox is called "fishermen's paradox" by Bouyssou and Perny [12] (to whom I borrow the following example) and is in fact a paradox dealing with abstention, sometimes called "no-show paradox" [13]; no-show allows an unusual strategy of tactical voting: abstaining from an election can help a voter's preferred choice win. Consider an election with three candidates x, y and z, and eleven voters distributed as follows:

- for 4 voters: $x > y > z$
- for 4 voters: $z > y > x$
- for 3 voters: $y > z > x$.

If the eleven voters vote, the first round eliminates y and the second round elects z with seven votes against only four for x. But, guessing this result, two of the first four voters, discouraged by the expected victory of z, who is ranked last in their preferences, decide not to vote and go fishing instead. Then, x having only two voices left, x is eliminated in the first round; y and z compete in the second round, to the benefit of y, who benefits from the votes of the two (or of the four if we assume that the two abstentionists have returned from their fishing party and participate in the second round) first voters remaining: it is finally y who is elected. At the end of the second round, our two fishermen are thus satisfied to note that their abstention not only allowed them to spend a beautiful day in the countryside, but also helped to elect a candidate (y) whom they prefer rather than the one who would have been elected if they voted (z). And Bouyssou and Perny conclude that such a voting procedure does not encourage participation, since it may be worth abstaining instead of voting sincerely.

4.3 "Paradoxes" for Borda's Procedure

It is easy to see that Borda's procedure is monotonous: if a Borda winner is ranked better in the preferences of the voters, he or she obtains more points and thus remains the winner. But consider a variant of Borda's procedure sometimes used when there is more than one person to be elected and called the "iterated Borda's procedure". It consists of applying the usual Borda's procedure a first time to determine a first elected candidate; then this one is removed from the list of candidates and the same process is repeated, as many times as there are candidates to be elected. The following example shows that the iterated Borda's procedure is not monotonous, which in turn shows that monotony is not kept as easily as one might think, since repeating a monotonous procedure does not necessarily provide a monotonous procedure.

Consider twenty voters who want to choose two candidates out of three. Let us suppose that the preferences of the twenty voters over the three candidates x, y, and z are distributed as follows:

- for 4 voters: $x > y > z$
- for 4 voters: $y > z > x$
- for 5 voters: $y > x > z$
- for 7 voters: $z > x > y$.

Borda scores are:

$$s_B(x) = 40,\ s_B(y) = 42,\ s_B(z) = 38.$$

Thus y is the first elected candidate. We remove y, which gives 9 voters who prefer x to z, and therefore 11 who prefer z to x, i.e. Borda scores of 31 for z and 29 for x: z is elected second.

Suppose now that the five voters whose preferences are $y > x > z$ decide to invert x and z. Since x was not elected, one can expect that this regression does not improve his or her situation; and yet… The scores become:

$$s_B(x) = 35,\ s_B(y) = 42,\ s_B(z) = 43.$$

As expected, x's score decreases, while the one of z increases. This allows z to be elected first now. As a result, the second confrontation now opposes x and y. Now, after removing z from the candidates, we get 11 voters who prefer x to y and therefore 9 who prefer y to x (i.e. Borda scores of 31 for x and 29 for y): x is elected second. We are thus in a doubly paradoxical situation: not only x, less well ranked than before, is now elected, but in addition y, whose rank does not change for any voter and who was elected first before these modifications, is now eliminated from the elected candidates!

This example can easily be adapted to show how the progression of a candidate can lead to his or her elimination; just repeat the previous example and invert the two cases: we then pass from z and x elected to y and z elected after the progression of x in the opinion of the five voters (we shall then be surprised by the elimination of x and by the amazing progression of y, boosted to the first place instead of being eliminated).

Another paradox [19] of which Borda's procedure suffers is sometimes known as the *reverse order paradox*. It may happen when a candidate is removed from an election and that the effect of that removal is to reverse the order of the remaining candidates (of course without changing the preferences of the voters). To illustrate this paradox, let us consider the case of four candidates x, y, z and t and seven voters whose preferences are:

- for 2 voters: $x > t > z > y$
- for 2 voters: $y > x > t > z$
- for 3 voters: $t > z > y > x$.

Borda scores are:

$$s_B(x) = 17, s_B(y) = 16, s_B(z) = 15, s_B(t) = 22,$$

which provides the linear order $t > x > y > z$ as the collective preference.

But imagine that, for various reasons, t cannot assume the position he was running for. One could legitimately think that the voters would entrust the position to the one whom they had ranked second in the election, that is x here. And yet, what happens if we decide to re-elect the remaining three candidates (without changing the voters' preferences)? The restriction of the previous preferences to the three candidates x, y, z gives:

- for 2 voters: $x > z > y$
- for 2 voters: $y > x > z$
- for 3 voters: $z > y > x$

and Borda scores become:

$$s_B(x) = 13, s_B(y) = 14, s_B(z) = 15.$$

Now the collective preference is $z > y > x$, that is, maybe against all expectations, exactly the inverse order of the order obtained by suppressing t from the previous collective order!

A variant of this paradox (suggested by Plott and Ferejohn, according to Fishburn [22]; see also [54] for a complete analysis of the differences in rankings between scoring rules) consists in removing the loser from an election (i.e. a candidate with a smallest Borda score) and in observing that this removal may lead to a reversal of the ranking of the remaining candidates. It is easy to adapt the previous example to illustrate this variant: it is enough to reverse the order of the preferences of the voters. We then obtain:

- for 2 voters: $y > z > t > x$
- for 2 voters: $z > t > x > y$
- for 3 voters: $x > y > z > t$.

Borda scores are:

$$s_B(x) = 18, s_B(y) = 19, s_B(z) = 20, s_B(t) = 13,$$

which provides the linear order $z > y > x > t$ as the collective preference. Removing the loser, t, leads to the following Borda scores:

$$s_B(x) = 15, s_B(y) = 14, s_B(z) = 13.$$

Hence the collective order $x > y > z$: the suppression of the loser involves the reversing of the collective preference expressed on the other candidates. This will perhaps console the losers to know that, although they are the last ones, their presence may nevertheless be so important! Less anecdotally, it also shows that a candidate may have an interest in running for election, even if he or she is sure that he or she will lose, in order to prejudice some other candidates or exercise some form of blackmail. This is maybe not a surprise as political life offers such examples of blocking candidates…

The last paradox that we will consider in this paper concerns a variant of Borda's procedure. It consists in awarding points only to the candidates arriving among the first ones in the preferences expressed by the voters. More precisely, let k be an integer greater than or equal to 1; then, for each voter, k points are given to the candidate ranked at the top by the considered voter, $k - 1$ points to the candidate ranked at the second position, $k - 2$ to the candidate ranked in third, and so on, until the candidate ranked at the k^{th} position, which is awarded 1 point, after which no points are awarded to candidates ranked beyond. In other words, we consider the score-vector (k, $k - 1$,…, 1, 0,…, 0). When k is equal to the number of candidates, we recover Borda's procedure, and when k is equal to 1, we find the one-round procedure back.

What happens when k changes for a given profile? One might expect to see some stability in collective preferences, at least for the winners. The following example shows that this is not the case! Let x, y, z and t denote four candidates and let us consider the following preferences of seven voters:

- for 3 voters: $x > y > z > t$
- for 1 voter: $y > z > x > t$
- for 1 voter: $y > z > t > x$
- for 2 voters: $z > t > x > y$.

For $k = 1$ (one-round procedure), x is the winner (with 3 votes, against 2 for y, 2 also for z and 0 for t). For $k = 2$, y wins: the scores are 6 for x, 7 for y, 6 for z and 2 for t. For $k \geq 3$, it is z the winner (indeed, for $k = 3$, the scores are 12 for x, 12 for y, 13 for z, 5 for t; it is easy to see that, from $k = 3$, any increase in k has no effect on the ranking of the candidates with respect to the case $k = 3$; because of this, only $k - 1$ different winners can be obtained).

So, in this example, we obtain three different winners for three successive values of k. More generally, for n candidates, we may design profiles such that, when k varies from 1 to $n - 1$, $n - 1$ distinct winners are obtained (what Fishburn [22] proposes to call *the truncated point-total paradox*; as observed above, it is not possible to obtain n different winners).

5 Conclusion: "Impossibility Theorems"

The previous examples illustrate different kinds of paradoxes, for instance:

- it is possible that a candidate preferred to any other candidate by a majority of voters (i.e. a Condorcet winner) is not elected;
- the "useful vote" may prevent the expected beneficiary from being elected;
- it may be better for a voter to vote for the candidate that he or she likes least in order to make his or her favourite candidate be elected;
- there are voting procedures for which it may be better not to vote rather than voting for his or her favourite candidate;
- a party may have an absolute majority in the parliament while it represents only a minority, sometimes small, of the voters;
- it is possible to become elected by regressing in the preferences of the voters;
- and so on.

Arrow's theorem (see Sect. 2.5) provides an explanation to this multiplicity of paradoxes: there is no "perfect" voting procedure. Hence, any voting procedure will generate undesirable effects, which can be interpreted as "paradoxes".

There are other impossibility results. We have already encountered an illustration of Moulin's theorem [50] on abstention:

Theorem 5. When there are at least four candidates, any voting procedure choosing the Condorcet winner, when he or she exists, as the winner of the election is subject to the paradox of abstention.

Another impossibility theorem was independently established by Gibbard [26] and Satterthwaite [56, 57] (see also Moulin [49]). A voting procedure is said to be "manipulable" whenever it is more interesting for a voter V to misrepresent his or her preferences in order to secure an outcome preferred by V to the winner obtained when V votes

according to his or her true preferences (his or her vote is then called "strategic", or also "insincere" or "sophisticated"). The following result shows that the paradoxes related to manipulability and illustrated above are inevitable if we reject dictatorship:

Theorem 6. When there are at least three candidates, any voting procedure without dictators is manipulable.

However, the contribution of operations research to the study of voting procedures is not limited to these negative aspects and, though there does not exist an ideal procedure, operations research can also provide elements that can guide the choice of a voting procedure. By highlighting the difficulties encountered in designing a satisfying voting procedure, by combating prejudices, by separating what is possible from what is not possible and, more generally, by proposing standards, axiomatizations, methodologies for studying voting procedures, operations research applied to voting theory and social choice will have already achieved a positive goal: to help the citizens that we are to become more aware of the limitations intrinsic to any voting procedure and to enable us to act with a better knowledge of these limitations.

References

1. Arrow, K.J.: Social choice and individual values. Wiley, New York (1951, 1963)
2. Bachmeier, G., Brandt, F., Geist, C., Harrenstein, P., Kardel, K., Peters, D., Seedig, H. G.: k-majority digraphs and the hardness of voting with a constant number of voters. Working paper (2016)
3. Balinski, M.: Le Suffrage universel inachevé. Belin, Paris (2004)
4. Balinski, M., Laraki, R.: Majority Judgment: Measuring, Ranking, and Electing. MIT Press, Cambridge (2010)
5. Balinski, M., Young, P.: Fair Representation, Meeting the Ideal of One Man, One Vote. Yale University Press, New Haven and London (1982)
6. Barthélemy, J.-P.: Caractérisations axiomatiques de la distance de la différence symétrique entre des relations binaires. Mathématiques et Sciences Humaines **67**, 85–113 (1979)
7. Barthélemy, J.-P., Guénoche, A., Hudry, O.: Median linear orders: heuristics and a branch and bound algorithm. Eur. J. Oper. Res. **42**(3), 313–325 (1989)
8. Barthélemy, J.-P., Monjardet, B.: The median procedure in cluster analysis and social choice theory. Math. Soc. Sci. **1**, 235–267 (1981)
9. Bartholdi III, J.J., Tovey, C.A., Trick, M.A.: Voting schemes for which it can be difficult to tell who won the election. Soc. Choice Welfare **6**, 157–165 (1989)
10. Black, D.: The Theory of Committees and Elections. Cambridge University Press, Cambridge (1958)
11. Borda, J.-C.: Mémoire sur les élections au scrutin. Histoire de l'Académie royale des sciences pour 1781, Paris (1784)
12. Bouyssou, D., Perny, P.: Aide multicritère à la décision et théorie du choix social. Nouvelles de la Sci. et des Technol. **15**, 61–72 (1997)
13. Brams, S.J., Fishburn, P.C.: Paradoxes of preferential voting. Math. Mag. **56**, 207–214 (1983)
14. Brams, S.J., Fishburn, P.C.: Voting Procedures. In: Arrow, K., Sen, A., Suzumura, K. (eds.) Handbook of Social Choice and Welfare, vol. 1, pp. 175–236. Elsevier Science, Amsterdam (2002)

15. Brandt, F., Conitzer, V., Endriss, U., Lang, J., Procaccia, A. (eds.): Handbook of Computational Social Choice. Cambridge University Press, Cambridge (2016)
16. Caritat, M.J.A.N., marquis de Condorcet: Essai sur l'application de l'analyse à la probabilité des décisions rendues à la pluralité des voix. Imprimerie royale, Paris (1785). English translation in [45]
17. Charon, I., Hudry, O.: An updated survey on the linear ordering problem for weighted or unweighted tournaments. Ann. Oper. Res. **175**, 107–158 (2010)
18. Chevaleyre, Y., Endriss, U., Lang, J., Maudet, N.: A short introduction to computational social choice. In: van Leeuwen, J., Italiano, Giuseppe F., van der Hoek, W., Meinel, C., Sack, H., Plášil, F. (eds.) SOFSEM 2007. LNCS, vol. 4362, pp. 51–69. Springer, Heidelberg (2007). https://doi.org/10.1007/978-3-540-69507-3_4
19. Davidson, R.R., Odeh, R.E.: Some inconsistencies in judging problems. J. Comb. Theory (A) **13**, 162–169 (1972)
20. Dwork, C., Kumar, R., Naor, M., Sivakumar, D.: Rank aggregation methods for the Web. In: Proceedings of the 10th International Conference on World Wide Web (WWW10), Hong Kong, pp. 613–622 (2001)
21. Farquharson, R.: Theory of Voting. Yale University Press, New Haven (1969)
22. Fishburn, P.C.: Paradoxes of voting. Am. Polit. Sci. Rev. **68**, 537–546 (1974)
23. Garey, M.R., Johnson, D.S.: Computers and Intractability, a Guide to the Theory of NP-Completeness. Freeman, New York (1979)
24. Gehrlein, W.V.: Condorcet's paradox and the Condorcet efficiency of voting rules. Mathematica Japonica **45**(1), 173–199 (1997)
25. Gehrlein, W.V.: Condorcet's paradox and the likelihood of its occurrence: different perspectives on balanced preferences. Theor. Decis. **52**, 171–199 (2002)
26. Gibbard, A.F.: Manipulation of voting schemes: a general result. Econometrica **41**, 587–601 (1973)
27. Guilbaud, G.Th.: Les théories de l'intérêt général et le problème logique de l'agrégation. Économie appliquée **5**(4) (1952). Reedition in Éléments de la théorie des jeux. Dunod, Paris (1968)
28. Hudry, O.: Recherche d'ordres médians: complexité, algorithmique et problèmes combinatoires. Ph.D. thesis, Télécom ParisTech (1989)
29. Hudry, O.: Votes et paradoxes: les élections ne sont pas monotones! Mathématiques et Sciences Humaines **163**, 9–39 (2003)
30. Hudry, O.: NP-hardness results on the aggregation of linear orders into median orders. Ann. Oper. Res. **163**(1), 63–88 (2008)
31. Hudry, O.: Complexity of voting procedures. In: Meyers, R. (ed.) Encyclopedia of Complexity and Systems Science, pp. 9942–9965. Springer, New York (2009). New edns. Springer, New York (2013, 2015). https://doi.org/10.1007/978-0-387-30440-3_585
32. Hudry, O.: On the computation of median linear orders, of median complete preorders and of median weak orders. Math. Soc. Sci. **64**, 2–10 (2012)
33. Hudry, O.: NP-hardness of the computation of a median equivalence relation in classification (Régnier's problem). Mathematics and Social Sciences 197, 83–97 (2012)
34. Hudry, O.: Complexity of computing median linear orders and variants. Electron. Notes Discrete Math. **42**, 57–64 (2013)
35. Hudry, O.: Complexity results for extensions of median orders to different types of remoteness. Ann. Oper. Res. **225**, 111–123 (2015)
36. Hudry, O., Leclerc, B., Monjardet, B., Barthélemy, J.-P.: Metric and latticial medians. In: Bouyssou, D., Dubois, D., Pirlot, M., Prade, H. (eds.) Concepts and Methods of Decision-Making Process, pp. 771–812. Wiley (2009)

37. Hudry, O., Monjardet, B.: Consensus theories: an oriented survey. Math. Soc. Sci. **190**, 139–167 (2010)
38. Johnson, D.S.: A catalog of complexity classes. In van Leeuwen, J. (ed.) Handbook of Theoretical Computer Science Vol. A: Algorithms and Complexity, pp. 67–161. Elsevier, Amsterdam (1990)
39. Kemeny, J.G.: Mathematics without numbers. Daedalus **88**, 571–591 (1959)
40. Mascart, J.: La vie et les travaux du chevalier Jean-Charles de Borda (1733–1799). Annales de l'Université de Lyon, Lyon (1919). Reedition in Presses de l'Université de Paris-Sorbonne, Paris (2000)
41. McLean, I.: The Borda and Condorcet principles: three medieval applications. Soc. Choice Welfare **7**, 99–108 (1990)
42. McLean, I., Hewitt, F.: Condorcet: Foundations of Social Choice and Political Theory. Edward Elgar, Hants (1994)
43. McLean, I., Lorrey, H., Colomer, J.M.: Social choice in medieval Europe. In: Workshop Histoire des Mathématiques Sociales, Paris (2007)
44. McLean, I., McMillan, A., Monroe, B.L.: Duncan Black and Lewis Carroll. J. Theor. Polit. **7**, 107–124 (1995)
45. McLean, I., Urken, A. (eds.): Classics of Social Choice. The University of Michigan Press, Ann Arbor (1995)
46. Mimiague, F., Rousseau, J.-M.: Effet Condorcet: typologie et calculs de fréquences. Mathématiques et Sciences Humaines **43**, 7–27 (1973)
47. Monjardet, B.: Relations à éloignement minimum de relations binaires, note bibliographique. Mathématiques et Sciences Humaines **67**, 115–122 (1979)
48. Monjardet, B.: Sur diverses formes de la "règle de Condorcet" d'agrégation des préférences. Mathématiques Informatique et Sciences Humaines **111**, 61–71 (1990)
49. Moulin, H.: Fairness and strategy in voting. Fair Allocation 33, 109–142 (1985). Young, H. P. (ed.). American Mathematical Society, Proceedings of Symposia in Applied Mathematics (1985)
50. Moulin, H.: Condorcet's principle implies the no show paradox. J. Econ. Theory **45**, 53–64 (1988)
51. Nurmi, H.: Comparing Voting Systems. D. Reidel Publishing Company, Dordrecht (1987)
52. Nurmi, H.: Voting Paradoxes and How to Deal with Them. Springer, Heidelberg (1999). https://doi.org/10.1007/978-3-662-03782-9
53. Papadimitriou, C.H.: Computational Complexity. Addison-Wesley Publishing Company, Reading (1994)
54. Saari, D.: Millions of election outcomes from a single profile. Soc. Choice Welfare **9**, 227–306 (1992)
55. Saari, D.: Decisions and Elections, Explaining the Unexpected. Cambridge University Press, Cambridge (2001)
56. Satterthwaite, M.A.: The existence of a strategy proof voting procedure: a topic in social choice theory. Ph.D. thesis of the University of Wisconsin, Madison, USA (1973)
57. Satterthwaite, M.A.: Strategy-proofness and Arrow's conditions: existence and correspondences for voting procedures and social welfare functions. J. Econ. Theory **10**, 187–217 (1975)
58. Taylor, A.D.: Social Choice and the Mathematics of Manipulation. Cambridge University Press, Cambridge (2005)
59. Wakabayashi, Y.: Aggregation of binary relations: algorithmic and polyhedral investigations. Ph.D. thesis, Augsburg University (1986)
60. Wakabayashi, Y.: The complexity of computing medians of relations. Resenhas **3**(3), 323–349 (1998)

The Window Fill Rate with Nonzero Assembly Times: Application to a Battery Swapping Network

Michael Dreyfuss and Yahel Giat(✉)

Department of Industrial Engineering, Jerusalem College of Technology, HaVaad HaLeumi 21, Jerusalem, Israel
{dreyfuss,yahel}@jct.ac.il
http://www.jct.ac.il

Abstract. One suggestion to overcome the range anxiety of electrical vehicle owners is the use of a network of battery swapping stations. To improve the network's performance, managers can purchase spares and place them in the network's stations. The battery allocation problem, therefore, is finding the allocation that optimizes the network's performance. For the performance measure, we consider the window fill rate, that is, the probability that a customer that enters a swapping station will exit it within a certain time window. For the battery swapping network this time window is defined as the customer's tolerable wait. In our derivation of the window fill rate formulae, we differ from earlier research in that we assume that the time to remove and install a battery is not negligible. We numerically analyze the battery allocation problem for a hypothetical countrywide application in Israel and demonstrate the importance of estimating correctly customers' tolerable wait. We find that the window fill rate criterion leads to two classes of stations, those that are assigned spares and those that are not. Additionally, we show the savings attained by reducing the swapping time. Finally, we compare between a balanced and imbalanced system (in terms of customer arrival to the various stations) and show that the advantage of each system crucially depends on the length of the tolerable wait.

Keywords: Exchangeable-item Repair-system
Inventory optimization · $M/G/\infty$ · Tolerable wait · Electric vehicles

1 Introduction

As part of the grand global effort to reduce greenhouse gas emissions, governments around the world are pushing for the public to switch from regular, fuel burning cars to electric vehicles. However, despite many incentives offered by governments, the public is hesitant about adopting these vehicles. The reason to this hesitation is blamed on the batteries of these vehicles. These batteries need to be recharged frequently with inconveniently long recharging time. In 2007, the

G. H. Parlier et al. (Eds.): ICORES 2017, CCIS 884, pp. 42–62, 2018.
https://doi.org/10.1007/978-3-319-94767-9_3

US-based corporation Better Place suggested to overcome this problem by separating battery ownership from the vehicle's ownership. Customers will purchase the vehicle without its battery from the auto-maker and lease battery services from a third party ("the firm"), which will assume all the battery-associated risks. The firm will construct a network of battery swapping stations in which car owners replace their depleted batteries for charged ones from the station's stock. Separately, the depleted batteries are recharged and put back in the stock to be given to future customers. To expedite customer service, the firm will purchase spare batteries that will be placed each station. In the model presented in this paper we assume that the budget of spare batteries is given, and therefore the firm's problem is the 'spares allocation problem', namely, to decide how to allocate the spare batteries among the battery swapping stations with the goal of optimizing the network's service measure.

The service measure that we consider in this paper is a generalization of the fill rate. With the fill rate, the firm will allocate batteries to maximize the fraction of customers who are served upon arrival. In reality, however, the fill rate is rarely an accurate measure for the firm's costs. For example, if the battery provider advertises or is committed by contract to provide service within a certain period of time then it does not need to have a battery ready for the customers immediately when they arrive. From the customers' standpoint, too, there is a certain tolerable or acceptable period of wait, which may depend on their level of patience or their expectations about how time it is reasonable to wait. If we assume that a customer entering the station expects being served within the ten minutes it would take to fill a tank of a conventional car, then only if the customer waits more than ten minutes the firm will experience reputation and contractual losses. Thus, in lieu of optimizing the fill rate, the firm's objective should be to maximize the *window fill rate*, i.e., the probability that a customer is served *within* the tolerable wait.

To solve the spares allocation problem, we use related research in the field of exchangeable-item repair systems. Customers arrive to these systems with a failed item and exchange it for an operable item in a manner similar to the battery swapping scheme. Furthermore, since battery charging docks are relatively inexpensive, one may assume that there are sufficiently many ('ample server' assumption) in each location. Further, we assume Poisson arrival and therefore each location can be modelled as an $M/G/\infty$ queue. [1] develop an algorithm for finding a near-optimal solution in such multi-location systems assuming that the item's assembly and disassembly times are zero. This assumption, however, is unrealistic for the battery swapping problem since battery removal and installation times are significant compared to the customer's tolerable wait.

In the first part of this paper, which expands the research described in [2], we develop the window fill rate formula for the case of deterministic nonzero item assembly and disassembly times. The implication of our analysis is that as long as these times are less than the tolerable wait, a Δ *increase* in the assembly and disassembly time is equivalent to a Δ *decrease* in the tolerable wait. Using this finding we employ the [1] algorithm to find a solution to the battery swapping problem, i.e., how to allocate spare batteries in the network.

In the second part of this paper, we estimate the battery allocation problem of the Better Place corporation if it had succeeded going widespread in Israel and derive the optimal solution for different service criteria. This numerical example provides valuable insight into the critical importance of assessing correctly the tolerable wait time and the significant losses that the firm incurs if it neglects to do so. Second, we show how using the window fill rate as the optimization criterion creates two classes of battery exchange stations; high-traffic stations that receive spares and low-traffic stations that do not receive spares. As a practical consequence, managers should develop two different policies with respect to their service commitments to customers. Third, we conduct a sensitivity analysis and, in particular, we estimate the savings attained by reducing battery swapping time. Fourth, we demonstrate how a balanced network with the same total arrival rate differs from the imbalanced network and from a single location system. We find that the performance of each one of these systems may be higher or lower than the other systems depending on the size of the tolerable wait. Therefore, if managers wish to increase their customer base, the decision whether to target customers near high-traffic stations or near low-traffic stations crucially depends on customers' tolerable wait.

Although the Better Place endeavor has ended with its bankruptcy in 2013, the battery swapping idea is either applied or considered by other companies such as XJ Group Corporation in Qingdao and Gogoro in Taipei [3]. The model presented in this paper, therefore, may yet be applied in real-life large-scale situations.

2 Literature Review

Electric vehicles are considered an environmentally-friendly alternative to fuel-burning cars [4] and are projected to eventually replace them [5]. However, to date, drivers are wary of these vehicles and therefore, many governments provide substantial tax incentives to encourage their widespread adoption. Notable examples for countries with such policies are West European countries, the United States, China and Japan [6]. Despite these governmental efforts, customers' wariness persists and most governments' adoption goals have not been met [7]. The major customer concern is the 'range anxiety', namely, the fact that compared to internal combustion engines, batteries have a limited range and long recharging time. Range anxiety is discussed in numerous papers (e.g., [8]; [9]) and there seems to be a consensus among researchers that the electric vehicle industry must address customers' range anxiety for these vehicles to be widely adopted.

An innovative idea to overcome these battery-related concerns was introduced by the US-based company Better Place who proposed to separate the vehicle ownership from the battery ownership. Instead of owning the battery, vehicle owners will purchase battery services from a firm that will establish a network of battery swapping stations. There is a plethora of research that examines the many aspects of this proposition such as the station design, the battery removal

and installation times, the required number of spare batteries, the network layout and managing the loads on the power grid [10–12]. Better Place, which operated mainly in Israel and Denmark failed to sell more than 1500 cars [13] and filed for bankruptcy in 2013 (see, [9]'s explanation of its failure). Despite its failure, the ideas promoted by Better Place are still considered in different settings (e.g., scooters in Taipei [3]). We contribute to this stream of research by solving the spare battery allocation problem and demonstrating a large-scale application of this problem.

The assumption that customers will tolerate a certain wait is at the core of this paper, which lies at the intersection of inventory and customer service models. The concept of a tolerable wait is hardly ever considered in inventory model. In contrast, within the service industry this concept is more commonly assumed and is associated with numerous terms such as "expectation" [14], "reasonable duration" [15], "maximal tolerable wait" [16], and "wait acceptability" or "expected delay" of [17]. From a service-oriented approach, the customer's attitude to wait is mainly subjective and has cognitive and affective aspects [17]. Indeed, we propose manipulating the customer's expectations using behaviorial models originating from the service industry [18]. From a logistics point of view, however, the tolerable wait is more objective and usually stated in the service contract in clauses specifying within how much time service must be rendered. Unfortunately, only few inventory models consider the tolerable wait (e.g., [19,20]). Indeed, researchers have observed that most inventory models fail "to capture the time-based aspects of service agreements as they are actually written" [21, p. 744]. This study fills this void by incorporating the tolerable wait into the optimization criterion.

The battery swapping network may be modelled as an exchangeable-item repair system; see also [22] who take the same approach. These inventory systems have been investigated by researchers in different contexts; see [23] for a review of this literature. A common performance measure for such systems is the fill rate, which measures the fraction of customers who are served upon arrival [20,24]. These papers, however, do not develop explicit formulas for the window fill rate but use numerical techniques. In contrast, [25] develop an exact formula for the window fill rate in a single location and [1] find that the window fill rate is generally S-shaped with the number of spares in the location and exploit this property to develop an efficient near-optimal algorithm for finding the optimal spares allocation. Both papers, however, assume that item assembly and disassembly times are zero. We contribute to the exchangeable-item repair system literature by considering the window fill rate in the case of positive assembly and disassembly times.

3 The Model

Customers arrive with a depleted battery to a battery swapping network that comprises L stations and are served according to a first-come, first-serve policy. Upon arrival, the customer's battery is removed and placed in a charging dock

and once it is fully recharged it is added to the station's stock. To reduce customer waiting time, the network's managers purchase spare batteries and places them in the different locations, so that if there is a spare battery available on stock it is installed in the client's vehicle in exchange of the depleted battery that she has brought. Customers leave the swapping station once their replacement battery is installed.

For each station l, $l = 1, ..., L$, we assume that customer arrival rate follows an independent Poisson process with parameter λ_l. See [22] for a justification of this assumption and our discussion in Sect. 5. We assume that there are sufficiently many charging docks in each station ('ample server' assumption) and that charging time at each dock is i.i.d. The combination of these two assumptions is that once the battery is removed from the vehicle, it immediately begins recharging and that recharging times are independent. Let $R_l(t)$ denote the cumulative probability of a battery to be recharged by time t and let r_l denote the mean recharging time. Battery removal and battery installation times are t_1 and t_2, respectively. If the battery swapping time, $t_1 + t_2$, is greater than the tolerable wait, then the window fill rate is zero. Thus, in what follows it is assumed that $t_1 + t_2 \leq t$.

3.1 Single Station

Consider a random customer, Jane, that arrives at date s to station l that was allocated b spares. The non-stationary window fill rate, $F_l^{NS}(s, t, b)$ is the probability that Jane will exit the station by date $s + t$. Since installing a battery requires t_2 units of time, Jane exits the station by date $s + t$ if and only if by date $s + t - t_2$ she is at the head of the queue and there is at least one charged battery available at the station's stock. By "head of the queue" we mean that all the customers who arrived before Jane ("Pre-Jane customers") have either exited the station or are in the process of installing batteries in their vehicles. We can ensure this by verifying that the supply of recharged batteries is at least as large as the demand for these batteries. On the supply side, we consider the initial number of spare batteries in the station, b, plus all the batteries whose recharging was completed during the time segment $[0, s+t-t_2]$. On the demand side we consider the number of Pre-Jane customer plus Jane herself. Let:

- N_1 denote the number of batteries brought by Pre-Jane customers that were recharged before $s + t - t_2$.
- N_2 denote the number of batteries brought by Pre-Jane customers that were recharged after $s + t - t_2$.
- N_3 denote the number of batteries brought by customers who arrived after Jane ("Post-Jane customers") and that were recharged before $s + t - t_2$.
- Z denote a binary variable that is equal to one if Jane's battery were recharged before $s + t - t_2$ and zero if it were not.

The probability that Jane will exit the station by $s+t$ is the probability that the supply of recharged batteries is greater than the demand as follows

$$\begin{aligned} F_l^{NS}(s,t,b) &= Pr[Supply \geq Demand] \\ &= Pr[b + N_1 + Z + N_3 \geq N_1 + N_2 + 1] \\ &= Pr[b + Z + N_3 \geq N_2 + 1] \end{aligned} \tag{1}$$

Since removing the battery requires t_1 units of time, the battery brought by Jane begins recharging at $s + t_1$. Therefore, the probability for $Z = 1$ is the probability that a battery completes recharging during the interval $[s + t_1, s + t - t_2]$, which is equal to $R_l(t - t_1 - t_2)$. Therefore, we can condition on the value of Z and rewrite (1) as

$$\begin{aligned} F_l^{NS}(s,t,b) &= R_l(t - t_1 - t_2)Pr[b + 1 + N_3 \geq N_2 + 1] \\ &\quad + \big(1 - R_l(t - t_1 - t_2)\big)Pr[b + N_3 \geq N_2 + 1] \\ &= Pr[N_2 - N_3 \leq b - 1] + R_l(\hat{t})Pr[N_2 - N_3 = b], \end{aligned} \tag{2}$$

where $\hat{t} := t - t_1 - t_2$.

The ample server assumption and the assumption that batteries arrive according to a Poisson process guarantee that N_2 and N_3 are independent Poisson random variables that are also independent of Z. We now turn to derive the distribution of these variables.

The Distribution of N_2. Recall, N_2 is the number of batteries that arrived during $[0, s)$ and that were not repaired by $s + t - t_2$. Consider a customer that arrives during the time interval $[u, u + du]$ in $[0, s)$ and whose battery was not repaired by $s+t-t_2$. The probability for an arrival during $[u, u+du]$ is du/s [26, Chapter 5.3.5]. The customer's battery is removed and begins to be recharged at $u + t_1$, and the probability that recharging is completed later than $s + t - t_2$ is $1 - R_l\big(s + t - t_2 - (u + t_1)\big)$. Thus,

$$\begin{aligned} N_2 &\sim Poisson\Big(\lambda_l s \int_{u=0}^{s} \big(1 - R_l(s + t - t_2 - u - t_1)\big)\frac{du}{s}\Big) \\ &\sim Poisson\Big(\lambda_l \int_{u=\hat{t}}^{s+\hat{t}} \big(1 - R_l(u)\big)du\Big). \end{aligned} \tag{3}$$

The Distribution of N_3. To derive the distribution of N_3 we consider the customers that arrived during $(s, s + t - t_2]$ and whose batteries were recharged by date $s + t - t_2$. Of these customers, consider a customer that arrives during the time interval $[u, u + du]$. The probability for this arrival is $du/(t - t_2)$. This customer's battery is removed and begins to be recharged at $u+t_1$ and therefore, the probability that the battery's recharging is completed by $s+t-t_2$ is $R_l\big(s + t - t_2 - (u + t_1)\big)$. Thus,

$$N_3 \sim Poisson\Big(\lambda_l(t-t_2) \int_{u=s}^{s+t-t_2} R_l(s+t-t_2-u-t_1)\frac{du}{t-t_2}$$

$$\sim Poisson\Big(\lambda_l \int_{u=-t_1}^{\hat{t}} R_l(u)du = \lambda_l \int_{u=0}^{\hat{t}} R_l(u)du\Big). \quad (4)$$

The Stationary Window Fill Rate. We obtain the stationary window fill rate by taking the limit of s in (3) to infinity. This is summarized in the following proposition:

Proposition 1. *The stationary window fill rate for station l with b spares is given by*

$$F_l(t,b) = Pr[N \le b-1] + R_l(\hat{t})Pr[N=b]\ , \quad (5)$$

where $N := N_2 - N_3$ and where $N_2 \sim Poisson\big(\lambda_l \int_{u=\hat{t}}^{\infty}(1-R_l(u))du\big)$ and N_3 is defined in (4).

3.2 The Network

Let $\boldsymbol{b} = (b_1, ..., b_L)$ denote a network battery allocation and let $\lambda := \sum \lambda_l$ denote the (total) arrival rate to the network. The network's window fill rate, $F(t, \boldsymbol{b})$, is the weighted average of the local window fill rates. Thus, for a given a budget of B spare batteries, the battery allocation problem is:

$$\max_{\boldsymbol{b}\ge 0} F(t,\boldsymbol{b}) := \sum_{l=1}^{L} \frac{\lambda_l}{\lambda} F_l(t,b_l) \quad s.t. \quad \sum_{l=1}^{L} b_l = B. \quad (6)$$

The consequence of Proposition 1 is that the window fill rate depends only on $\hat{t} = t - t_1 - t_2$, and therefore we can instead assume that the battery removal and installment times are zero and use the adjusted tolerable wait, $\hat{t}$, in lieu of the true tolerable wait t. The implication of this observation is that all the result of [1] who assume zero swapping time are valid for our model as well. In the remainder of this section, we state the results of [1] that are necessary for understanding the battery allocation application.

Result 1: The Shape of the Window Fill Rate. The window fill rate of each location, $F_l(t,b)$ is strictly increasing in the number of spares in that location, b. If $t \ge r_l + t_1 + t_2$ then $F_l(t,b)$ is concave in b. Otherwise, $F_l(t,b)$ is either concave in b or initially convex and then concave (S-shaped) in b.

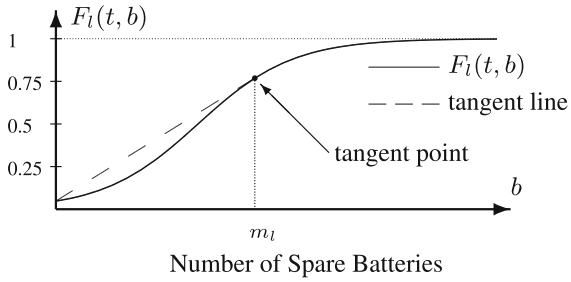

Fig. 1. The window fill rate for an S-shaped station (Source [2, p. 41]).

Result 2: The Optimization Algorithm. By (6) and Result 1, the window fill rate is a separable sum of either concave or S-shaped functions. For each S-shaped station we define the tangent point (see Fig. 1), m_l, as the first integer such that $\big(F_l(t,m_l) - F_l(t,0)\big)/m_l > \Delta F_l(t,m_l)$, where $\Delta F_l(t,b)$ is the first difference of $F_l(t,b)$ and is given by

$$\begin{aligned}\Delta F_l(t,b) &:= F_l(t,b+1) - F_l(t,b)\\ &= \big(1 - R_l(t)\big)Pr[N=b] + R_l(t)Pr[N=b+1]. \quad (7)\end{aligned}$$

The tangent point of concave stations is set to zero. The tangent point decreases with t and increases with t_1+t_2. For each station, let $H_l(t,b)$ denote the concave covering function of $F_l(t,b)$ in the following manner:

$$H_l(t,b) = \begin{cases} F_l(t,0) + \frac{F_l(t,m_l)-F_l(t,0)}{m_l} b & \text{if } 0 \le b \le m_l - 1 \\ F_l(t,b) & \text{if } \ b \ge m_l \ . \end{cases}$$

That is, for any b smaller than the tangent point, we replace $F_l(t,b)$ with the straight line connecting the point $\big(0, F_l(t,0)\big)$ and the point $\big(m_l, F_l(t,m_l)\big)$. By construction, for all $b \ge 0$, $H_l(t,b)$ is concave and $H_l(t,b) \ge F_l(t,b)$. Similarly to (6), we define $H(t,\boldsymbol{b})$ as the weighted average of all the stations' functions $H_l(t,b_l)$.

$H(t,\boldsymbol{b})$ is a separable sum of concave functions and therefore we can use a greedy algorithm to maximize it. This algorithm will choose the "best for the buck" station and since H_l is initially linear, it will stay with this station until it has reached the station's tangent point. The algorithm then continues with the next best station and so forth. Note that before switching to the next linear slope it is possible that stations that have reached their tangent will get additional spares (as long as their current slope is steeper than the next best linear slope). However, once a station begins receiving spares in its linear region, it will be the only one to receive spares until it has reached its tangent point. Consequently, the algorithm results with an allocation with properties stated in the following result.

Result 3: The Optimal Allocation. $\boldsymbol{b}^H$ satisfies one of the following two cases:

1. For every $l = 1 \ldots L$, either $b_l^H \geq m_l$ or $b_l^H = 0$ and the optimal solution to (6), $\boldsymbol{b}^F = \boldsymbol{b}^H$.
2. There exists a single station, denoted by $\hat{l}$ such that $0 < b_{\hat{l}}^H < m_{\hat{l}}$. For every other station $l \neq \hat{l}$, either $b_l^H \geq m_l$ or $b_l^H = 0$. In this case:
   (a) The optimal value of F is bounded above by $H(t, \boldsymbol{b}^H)$.
   (b) The distance from optimum is bounded by $\frac{\lambda_{\hat{l}}}{\lambda}\left(H_{\hat{l}}(t, b_{\hat{l}}^H) - F_{\hat{l}}(t, b_{\hat{l}}^H)\right)$.

4 Numerical Application

The US-based corporation Better Place was founded in 2007 by Shay Agassi with the ambitious goal of a large-scale adoption of fully electric vehicles. At the time, battery-related issues were considered to be the greatest obstacle to achieving this goal. Better Place developed a unique business model in which it retained battery ownership. Customers were to purchase the car absent the battery and Better Place was to provide battery swapping and recharging services and to assume all the battery-related risks [5].

Although Better Place has filed for bankruptcy in 2013, its innovative business model is still considered a promising solution to solving the battery problem in the electric car industry [22]. Most of the cars produced for Better Place's customers were sold in Israel, in which it even completed the construction of fifty battery swapping stations. The following numerical example is a hypothetical full scale application of the Better Place model in a country with geographical and demographical characteristics similar to Israel.

Each of the three largest fuel companies in Israel operate approximately two hundred fifty gasoline stations and accordingly we assume that the battery service firm ("the firm") operates a network of two hundred fifty battery swapping stations distributed throughout the country. The population density in Israel may be divided into three regions. The center region is the densest, followed by the northern region. The south of Israel, which constitutes more than half of Israel's land area, is sparsely populated. Consequently, the number of stations per customer in the south will be higher than the number of stations per customer in the center, reflecting the large geographical size that must be serviced. To model the differences between the different stations in Israel, as well as differences between small neighborhood stations and high-traffic major stations we assume that the arrival rates to the stations are equally spaced between 6.4 and 106 customers per hour.

An empty battery can be recharged to 50% of capacity within twenty minutes [27]. Recharging time, however, is random since the amount of recharging needed for each arriving battery is different, since customers may arrive to the station with partially depleted batteries. Hence, we assume that the recharging time is distributed normally with mean forty minutes and standard deviation ten minutes. Battery swapping time, i.e., the battery removal and battery installation,

is considerably shorter than recharging time and with state-of-the-art design, battery swapping can be done in less than two minutes [10]. Each station is assumed to have ample battery rechargers since recharging docks are relatively inexpensive. Anecdotal evidence suggests that car owners tolerate a ten minute stay in the station when they fuel their gasoline-fueled car. Since the electric vehicles are poised as an alternative to these cars, we assume that the tolerable wait for refueling is similar for both car types. Finally, we use a baseline budget of nine thousand spare batteries.

To summarize, the baseline parameters of the example are: $L = 250$ stations, $\lambda_l = 6 + 0.4 \cdot l$ customers per hour, $B = 9000$ spare batteries, $R_l \sim Normal(40, 10^2)$ min, $t_1 + t_2 = 2$ min, and the optimization criterion is the window fill rate for a tolerable wait $t = 10$ min $(F10)$.

4.1 The Baseline Scenario

In Fig. 2 we describe the near-optimal spares allocation for the baseline case, $\boldsymbol{b}^H$, and in Fig. 3 we display the window fill rate for the optimal allocation as a function of t, $F(\boldsymbol{b}^H, t)$. Recall, the optimization algorithm supplies spares to the station with the steepest slope until it reaches its tangent point and only then proceeds to the next steepest station. The tangent line's slope and the tangent point are increasing with the arrival rate and therefore the bigger the station's index, the greater the tangent point. The near-optimal allocation dictates that the 50 slowest-moving stations will have no spares, whereas each of the busier stations will receive at least its tangent point. Station 51 is the exception; although its tangent point is 19 it is allotted only 2 spare batteries (see case 1 of Result 3). This implies that the solution $F(\boldsymbol{b}^H, 10) = 88.5\%$ is a lower bound that it not necessarily optimal. However, the distance between the bounds is negligible as it is only 0.02% (see notes to Table 1).

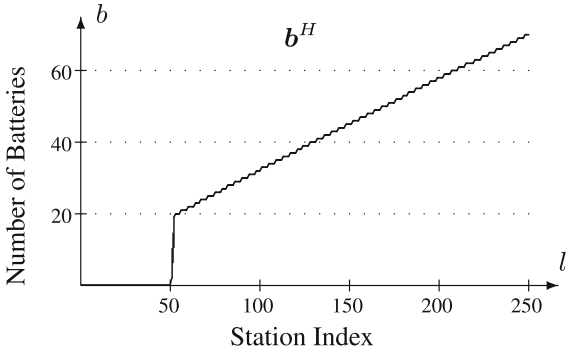

Fig. 2. The spare battery allocation for the baseline case (Source [2, p. 43]).

The implication of the baselines results is that from a service viewpoint, the network comprises two classes of locations. In Fig. 4, we describe the window fill

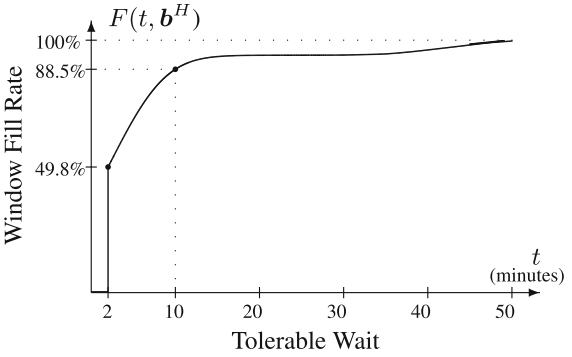

Fig. 3. The window fill rate as a function of t for the baseline optimal allocation (Source [2, p. 43]).

rate of each location. The low arrival rate stations are not given any spares and consequently, their window fill rate is almost zero. In contrast, locations 52–200 have a window fill rate of almost 100%. To compensate customers for the longer wait, the network's managers could offer customers, for example, discounted meals or drinks. Behavioral research about customer waiting experience may be used to incentivize customers to agree to longer than usual waiting times [18]. In Sect. 4.7 we discuss in more detail the trade-off between purchasing more batteries and the cost of compensating customers when they wait beyond their tolerable wait.

Since the low rate locations receive no spares, their local window fill rate is very low. For the specific parameter values of the baseline case, having zero spares results with $WFR_l(t = 10) \approx 0$ since now customers must surely wait for a battery to recharge and it is extremely rare for a battery to recharge within less than ten minutes (recall, recharge time is distributed $N(40, 10^2)$ min). In contrast, the higher rate locations achieve excellent results and if we consider these locations alone, then their average window fill rate is almost 92%. The peculiar shape of the graph is explained as follows. The number of spares is a step function with the locations' index (see Fig. 2). Therefore, a location that has a higher customer arrival rate than its neighbor but receives the same number of spares will have a lower window fill rate. The first next location that receives an additional spare will experience a jump in its window fill rate. The overall trend will be increasing since the higher rate locations have a stronger impact on the total fill rate and therefore at optimum their fill rate should be higher.

4.2 The Effect of the Tolerable Wait

To appreciate the effect of the tolerable wait we consider four optimization criteria; the baseline criterion, $F10$, and the window fill rate for tolerable waits of two ($F2$), five ($F5$) and fifteen ($F15$) minutes. Table 1 details the performance statistics for each of these criteria. The performance statistics that are detailed

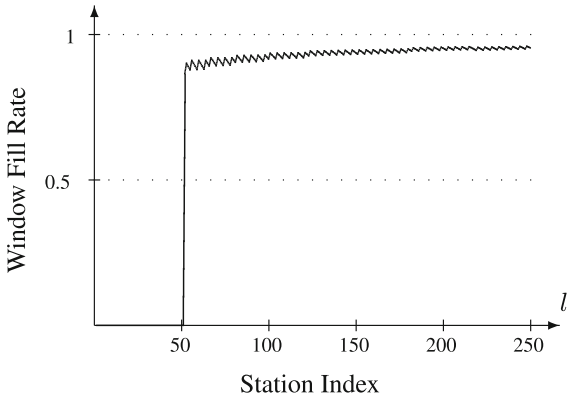

Fig. 4. The window fill rate of each location for the baseline case.

are the same measures that we use for the optimality criteria, i.e., the window fill rates for two, five, ten and fifteen minutes. We see that different criteria lead to significantly different optimal values of the objective function. As is discussed below, the near-optimal spares allocations also differ dramatically. These findings stress the importance of defining the criterion for optimality correctly. Consider, for example, the situation in which the firm mistakenly optimizes $F2$ instead of the "correct" criterion $F10$. As a result, the percentage of satisfied customers (i.e., customers who were serviced within ten minutes) is only 77.5% (instead of 88.5%). Similarly, if the firm errs to the other side and optimizes $F15$ then the percent of satisfied customers is only 84.9% instead of 88.5%.

Table 1. The network's performance for different optimization criteria (Source [2, p. 43]).

		Performance Statistic			
		$F2$	$F5$	$F10$	$F15$
Criterion	$F2$	73.5%[a]	76.5%	77.5%	77.6%
	$F5$	70.6%	78.6%[b]	82.8%	83.2%
	$F10$	49.8%	68.5%	88.5%[c]	93.5%
	$F15$	35.0%	54.2%	84.9%	97.9%[d]

Notes: a: Lower bound displayed. The distance between bounds is 0.12%.

b: Lower bound displayed. The distance between bounds is 0.05%.

c: Lower bound displayed. The distance between bounds is 0.02%.

d: Optimal value displayed.

In Fig. 5 we compare the near-optimal allocations for the criteria, $F2$, $F10$ and $F15$. When $t = 15$, the tangent points are appreciably less than the baseline case and therefore the 9000 batteries are more than the necessary to supply all the stations with their tangent points. Once all the stations are in their concave region the residual batteries are further distributed among all the stations. Conversely, when $t = 2$ the tangent points are higher than in the baseline case and the high-traffic stations demand more batteries to reach their tangent point. As a consequence, the budget is depleted after allocating spares to fewer stations compared to the baseline case.

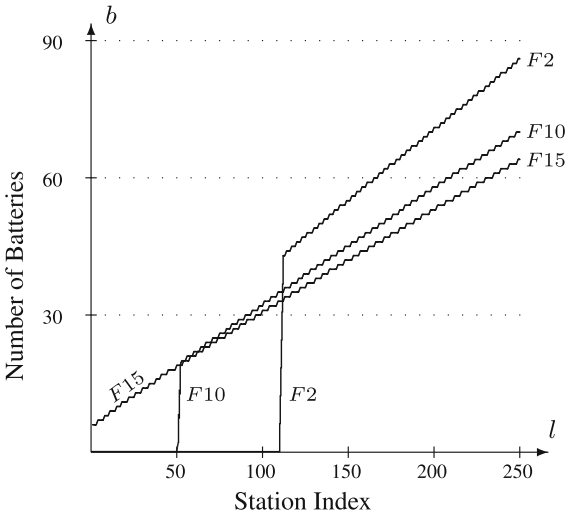

Fig. 5. The spare battery allocation for different optimization criteria (Source [2, p. 43]).

4.3 The Budget Effect

In Fig. 6 we describe the spares allocation for the baseline scenario (9000 spare batteries) and for budgets of 7000 and 11000 batteries. As result of increasing the budget beyond 9000 the low-rate stations start receiving batteries one by one according to their tangent point. Eventually, all the stations will reach their tangent point. From this point on, any additional batteries will be distributed among all the stations instead of given to only particular stations. In contrast, if the budget is decreased to below 9000, then some low-rate stations will forfeit all their batteries. The high-traffic stations, however, will lose at most the few (if any) batteries they received beyond their tangent point.

4.4 The Swapping-Time Effect

A corollary of Proposition 1 is that a Δ *increase* to the swapping time, $t_1 + t_2$ is equivalent to a Δ *decrease* to the tolerable wait, t. Figure 7 displays how the near-optimal allocation changes with the swapping time. As the swapping time increases, the tangent points increase too, and therefore the busiest stations require more spares. As a consequence, more and more low-traffic stations will be left with zero spares.

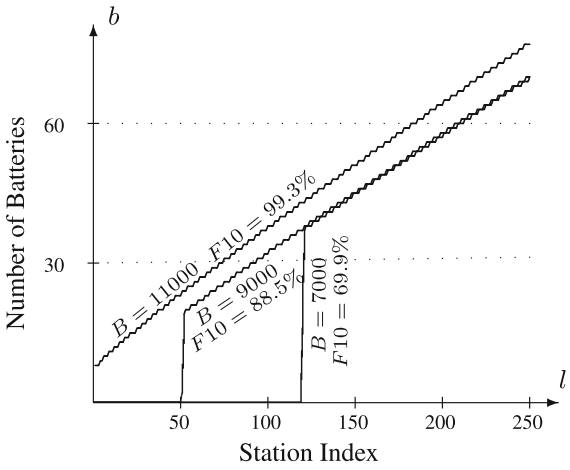

Fig. 6. The window fill rate and spare battery allocation for different values of B (Source [2, p. 44]).

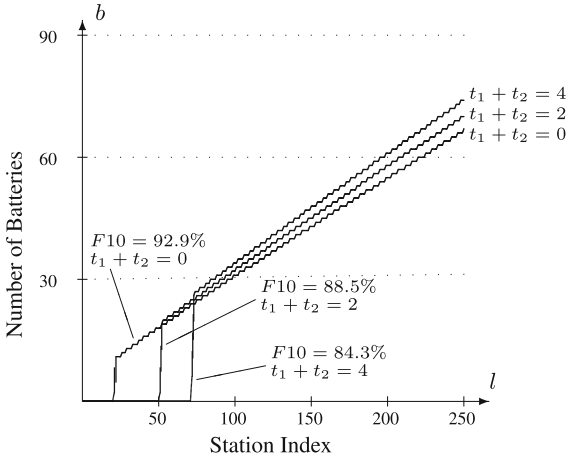

Fig. 7. The spare battery allocation for different battery swapping times (Source [2, p. 44]).

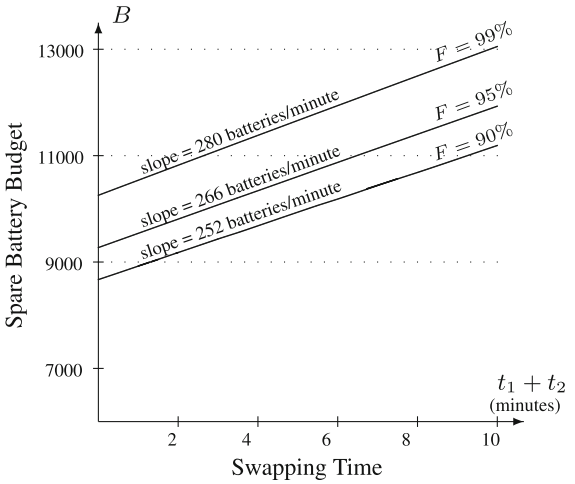

Fig. 8. The spares budget for different performance target levels (Source [2, p. 44]).

Thus far, we assume that the budget of spares is fixed. Consider, now the dual problem of (6).

$$\min_{\boldsymbol{b}\geq 0} \sum_{l=1}^{L} b_l \quad s.t. \quad F(t, \boldsymbol{b}) \geq \alpha \,. \tag{8}$$

where α is the network's target performance.

We can easily solve (8) using the optimization algorithm. The allocation of spares is done in an identical manner, but now the stopping condition is different. Previously, the algorithm stopped when all the batteries were assigned to stations. In contrast, now the algorithm stops once we have reached the required service level. Figure 8 displays the budget required to reach a 90%, 95% and 99% window fill rate for different swapping times. The graphs are near-linear and the slopes reveal the savings obtained by reducing swapping time. For the performance levels of 90%, 95% and 99% we find that a minute reduction in the swapping time saves the network approximately 252, 266 and 280 batteries, respectively.

4.5 Changing the Arrival Rate

We now consider changing the arrival rate to the network. In Fig. 9, we show the optimal allocation when the arrival rate to each location is 80%, 100% and 120% of the arrival rate in the baseline case.

If the network maintains a certain service level, then an increase in the customer base requires adding more spare batteries. In Fig. 10, we depict the number of batteries needed to maintain a 90%, 95% and 99% window fill rate for different levels of customer arrival rate. For example, if the arrival rate to each location is

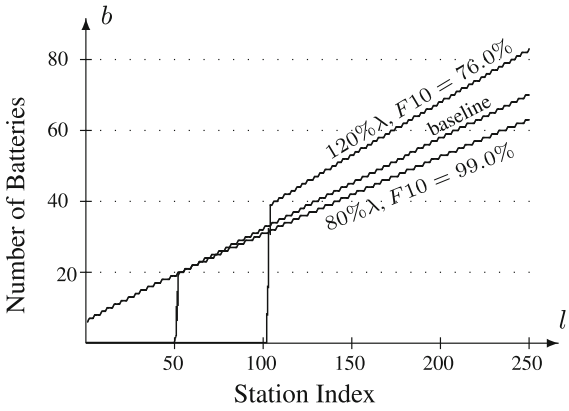

Fig. 9. The spare battery allocation for different arrival rates.

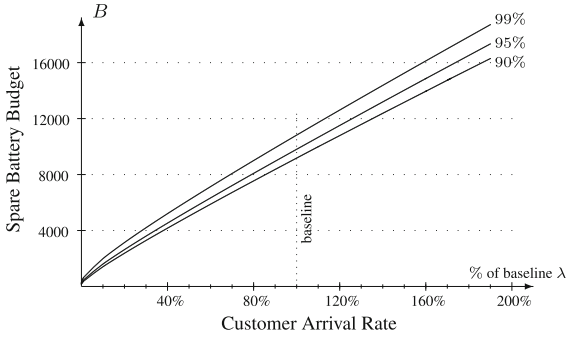

Fig. 10. The spare budget needed to meet performance targets as a function of the customer arrival rate for different performance targets.

only 80% compared to the baseline case, then 7544, 8084 and 9000 batteries are needed to maintain a window fill rate of 90%, 95% and 99%, respectively. The total arrival rate in the baseline case is 14,050 customers per hour and therefore a 10% increase in the arrival rate is an additional 1405 customers per hour. Using the slope of the graph around the baseline case we calculate that an additional 1000 customer per hour will require an additional 559, 588 and 619 batteries to maintain the 90%, 95% and 99% service levels, respectively.

4.6 Balanced Network

In the baseline scenario, we describe a network in which arrival to the locations varies along a linear slope. The total arrival to the network is $\lambda = \sum_{i=1}^{250} 6+0.4i = 14050$ customers per hour. We now consider a hypothetical example in which customer arrival is evenly distributed, namely for each station, $\lambda_l = \lambda/250 = 56.2$ customers per hour. In Fig. 11, we compare the optimal allocation under this

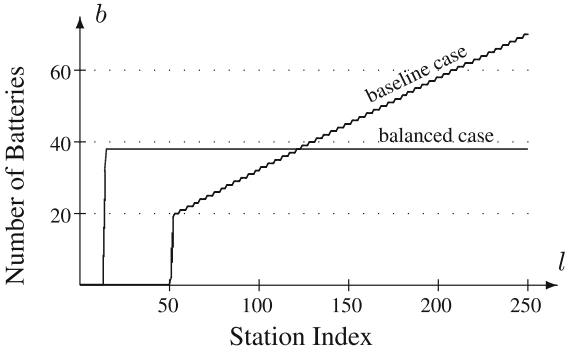

Fig. 11. The spare battery allocation for the baseline and balanced scenarios.

scenario with the optimal allocation in the baseline case. Note that since all the stations are identical, there are multiple optimal solutions (i.e., there are many ways in which we can choose which of the stations will receive spares and which will not). Therefore, in contrast to the baseline case in which the location index is significant (it describes the arrival rate to the station), in the balanced case locations are interchangeable. In Fig. 11 we see that in the balanced scenario 236 stations receive 38 spares each, and 13 stations receive no spares. There is one station that receives 32 spares.

From a managerial perspective it is extremely important to know whether a balanced network performs better or worse than the imbalanced network. For example, if managers wish to increase their customer base should they draw customers to the high-arrival locations (and create greater imbalance) or to the low-arrival locations (and create more balance). To address this question, we display in Fig. 12 the window fill rate as a function of the tolerable wait for the baseline and balanced scenarios. Figure 12 also depicts the window fill rate for the

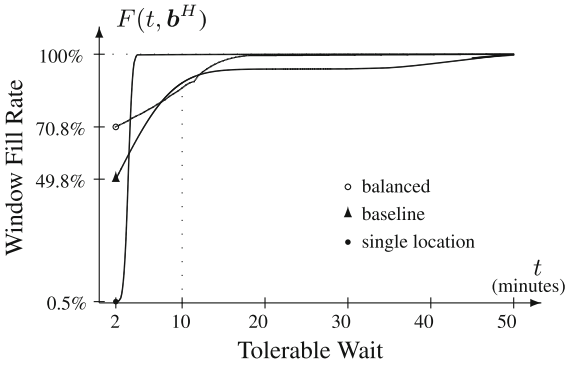

Fig. 12. The window fill rate as a function of t for the baseline, balanced and single location scenarios.

extreme case in which all the customers arrive to a single location that receives all the spare batteries. Interestingly, the answer to the question which system performs better heavily-depends on the tolerable wait. When $t = 2$, (i.e., the fill rate), then the balanced network performs better than the other networks. In contrast, when $t = 10$ then it is the worst performer.

If the network's managers wish to maintain a given service level, then as the assembly times increase we need more batteries. The results of the balanced network are similar to the baseline case, with each minute increase of installment time costing 257, 268 and 281 batteries for service levels of 90%, 95% and 99%, respectively. These prices are only slightly less than in the baseline case (see Fig. 8).

4.7 Optimizing Total Inventory Costs

Problems (6) and (8) assume that either the budget or the service level is predetermined. In what follows, we relax these constraints and consider the problem of minimizing the total inventory costs. Let c_p denote the penalty cost each time a customer is not served within the tolerable wait, and let c_B denote the cost of a battery. Since batteries have a limited lifetime, we assume a planning horizon of T. Therefore, the total number of customers arriving into the network during the planning horizon is λT, where, recall, $\lambda = 14,050$ customers per hour. The problem is now given by

$$\min_{\boldsymbol{b}\geq 0} TC(\boldsymbol{b}) := c_b \sum_{l=1}^{L} b_l \quad + \quad c_p \lambda T\big(1 - F(t, \boldsymbol{b})\big) \,. \tag{9}$$

The optimization algorithm can be easily adjusted to find the optimal solution to (9). Each time we consider adding a battery we measure its optimal contribution to the window fill rate, δ. As long as $\delta c_p \lambda T \geq c_b$ we increase the number of batteries in the network. Each time the additional battery is allocated to the location that maximally increases the window fill rate.

Batteries for family sized electric vehicles range between 20 kWH and 80 kWH with current prices reaching as low as US$200 per-kWh [12]. We therefore examine battery prices of up to US$25,000. We conservatively estimate battery life to be four years, and since we assume 12 daily hours of operation $T = 17520$ h [28].

Figure 13 depicts the near-optimal spares budget depending on battery prices for different penalty costs. We see that the budget may be very sensitive or very insensitive to battery prices. Consider, for example, the graph for the penalty cost of $1. In the battery price range of $3261 to $21378, the budget size is relatively flat and changes only between 11000 and 9000 batteries. In stark contrast, if the battery price increases from $21378 to only $25321, then the optimal budget dramatically decreases from 9000 to 0 batteries.

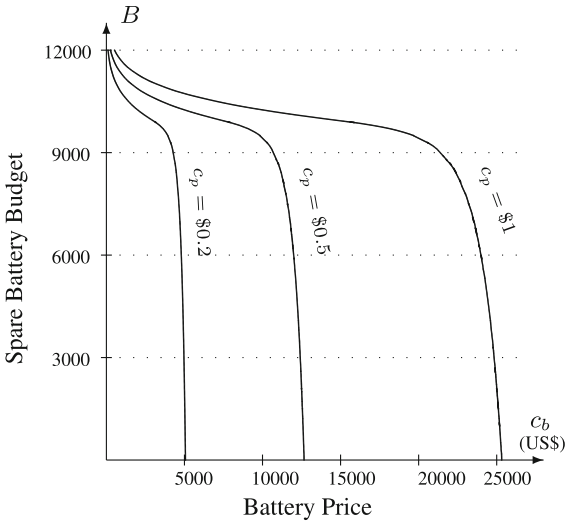

Fig. 13. Spares Budget for different penalty costs and battery price (Source [2, p. 45]).

5 Conclusions

In this paper, we develop and apply a model for solving the spare battery allocation problem. Since customers will tolerate a certain wait when they arrive at a battery-swapping stations, we argue that to minimize its penalty costs the network should maximize the fraction of customers who are served within the tolerable wait, the window fill rate. We show that one can set the removal and installment times to zero by adjusting the tolerable wait, that is by subtracting the total assembly times from the tolerable wait. Using this finding, we build on [1] to solve the spare battery allocation problem. To illustrate the application of the model we estimate a hypothetical application of a full-scale battery swapping network in Israel, similar to the network envisioned by the Better Place corporation. Our numerical analysis of the problem reveals interesting findings such as the value of better battery swapping design, the creation of different classes of stations and the critical importance of estimating the tolerable wait correctly.

Our model makes a number of assumptions that could be reconsidered. First, we assume that the battery swapping time is deterministic. This assumption may be reasonable in for the battery swapping problem since the cars and the swapping stations were designed to streamline the battery removal and installation operations. In other settings, this may be far from realistic. With stochastic assembly times the window fill rate formula will differ from (5). Moreover, managers may now depart from a strict FCFS policy. Consider for example a case in which a later customer's battery has been removed before an earlier customer. Will a spare battery on stock be given to the later customer, or must the later customer wait until the earlier customer's battery has been removed?

Our second assumption assumes that the customer arrival rate is constant over time. This assumption is clearly unrealistic. Our justification for this assumption is that we design the system for the high traffic hours and this solution is also applicable for the off-hours since in these hours the budget is more than necessary. A more careful analysis may reveal a better allocation due to the peak non-peak hours. These challenge are left for future research.

References

1. Dreyfuss, M., Giat, Y.: Optimal spares allocation in an exchangeable-item repair system with tolerable wait. Eur. J. Oper. Res. **261**, 584–594 (2017)
2. Dreyfuss, M., Giat, Y.: Optimizing spare battery allocation in an electric vehicle battery swapping system. In: Proceedings of the 6th International Conference on Operations Research and Enterprise Systems, pp. 38–46 (2017)
3. Davies, A.: The electric scooter scheme that could finally make battery-swapping work. Wired (2015)
4. Prata, J., Arsenio, E., Pontes, J.: Setting a city strategy for low carbon emissions: the role of electric vehicles, renewable energy and energy efficiency. Int. J. Sustain. Dev. Plann. **10**, 190–202 (2015)
5. Dijk, M., Orsato, R., Kemp, R.: The emergence of an electric mobility trajectory. Energy Policy **52**, 135–145 (2013)
6. Zhou, Y., Wang, M., Hao, H., Johnson, L., Wang, H.: Plug-in electric vehicle market penetration and incentives: a global review. Mitig. Adapt. Strat. Glob. Change **20**, 777–795 (2015)
7. Coffman, M., Bernstein, P., Wee, S.: Electric vehicles revisited: a review of factors that affect adoption. Transp. Rev. **37**, 79–93 (2017)
8. Neubauer, J., Wood, E.: The impact of range anxiety and home, workplace, and public charging infrastructure on simulated battery electric vehicle lifetime utility. J. Power Sources **257**, 12–20 (2014)
9. Noel, L., Sovacool, B.: Why did Better Place fail? Range anxiety, interpretive flexibility, and electric vehicle promotion in Denmark and Israel. Energy Policy **94**, 377–386 (2016)
10. Mak, H., Rong, Y., Shen, Z.: Infrastructure planning for electric vehicles with battery swapping. Manage. Sci. **59**, 1557–1575 (2013)
11. Yang, J., Sun, H.: Battery swap station location-routing problem with capacitated electric vehicles. Comput. Oper. Res. **55**, 217–232 (2015)
12. Sarker, M., Hrvoje, P., Ortega-Vazquez, M.: Optimal operation and services scheduling for an electric vehicle battery swapping station. IEEE Trans. Power Syst. **30**, 901–910 (2015)
13. Chafkin, M.: A broken place: the spectacular failure of the startup that was going to change the world. Fast Company (2014)
14. Durrande-Moreau, A.: Waiting for service: ten years of empirical research. Int. J. Serv. Ind. Manag. **10**, 171–194 (1990)
15. Katz, K., Larson, B., Larson, R.: Prescriptions for the waiting in line blues: entertain, enlighten and engage. Sloan Manage. Rev. Winter, 44–53 (1991)
16. Smidts, A., Pruyn, A.: How waiting affects customer satisfaction with service: the role of subjective variables. In: Proceedings of the 3rd International Research Seminar in Service Management, pp. 678–696. Université d'Aix-Marseille (1994)

17. Demoulin, N., Djelassi, S.: Customer responses to waits for online banking service delivery. Int. J. Retail Distrib. Manage. **41**, 442–460 (2013)
18. Maister, D.: The psychology of waiting lines. In: Czepiel, J., Solomon, M., Surprenant, C. (eds.) The Service Encounter: Managing Employee/Customer Interaction in Service Business. Lexington Books, Lexington, MA, pp. 113–123 (1985)
19. Song, J.: On the order fill rate in a multi-item, base-stock inventory system. Oper. Res. **46**, 831–845 (1998)
20. Caggiano, K., Jackson, L., Muckstadt, A., Rappold, A.: Optimizing service parts inventory in a multiechelon, multi-item supply chain with time-based customer service-level agreements. Oper. Res. **55**, 303–318 (2007)
21. Caggiano, K., Jackson, L., Muckstadt, A., Rappold, A.: Efficient computation of time-based customer service levels in a multi-item, multi-echelon supply chain: a practical approach for inventory optimization. Eur. J. Oper. Res. **199**, 744–749 (2009)
22. Avci, B., Girotra, K., Netessine, S.: Electric vehicles with a battery switching station: adoption and environmental impact. Manage. Sci. **61**, 772–794 (2014)
23. Basten, R., van Houtum, G.: System-oriented inventory models for spare parts. Surv. Oper. Res. Manage. Sci. **19**, 34–55 (2014)
24. Shtub, A., Simon, M.: Determination of reorder points for spare parts in a two-echelon inventory system: the case of non-identical maintenance facilities. Eur. J. Oper. Res. **73**, 458–464 (1994)
25. Berg, M., Posner, M.: Customer delay in M/G/∞ repair systems with spares. Oper. Res. **38**, 344–348 (1990)
26. Ross, S.: Introduction to Probability Models, 2nd edn. Academic Press, New York (1981)
27. Bullis, K.: Forget battery swapping: tesla aims to charge electric cars in five minutes. MIT Technol. Rev. (2013)
28. Arcus, C.: Battery lifetime: how long can electric vehicle batteries last? CleanTechnica (2016)

Solving the Integrated Production and Imperfect Preventive Maintenance Planning Problem

Phuoc Le Tam[1(✉)], El-Houssaine Aghezzaf[1,3], and Abdelhakim Khatab[2]

[1] Department of Industrial Systems Engineering and Product Design, Faculty of Engineering, Ghent University, Technologiepark 903, 9052 Zwijnaarde, Belgium
{Phuoc.LeTam,ElHoussaine.Aghezzaf}@UGent.be
[2] Industrial Engineering and Production Laboratory, Lorraine University, Metz, France
abdelhakim.khatab@univ-lorraine.fr
[3] Flanders Make, Graaf Karel de Goedelaan 5, 8500 Kortrijk, Belgium

Abstract. This paper considers the integrated production and imperfect preventive maintenance planning problem. The article provides more details on how Relax-and-Fix/Fix-and-Optimize as well as Dantzig-Wolfe Decomposition and Lagrangian Relaxation techniques were applied and implemented for solving the integrated production and imperfect preventive maintenance planning problem. More experiments were also carried out. The objective of this planning problem is to determine an optimal integrated production and preventive maintenance plan that concurrently minimizes production as well as preventive maintenance costs during a given finite planning horizon. Three solution approaches were investigated and applied to the reformulated version of the problem, and their performances are compared and discussed. The Relax-and-Fix/Fix-and-Optimize method (RFFO) determines first an initial feasible solution, generated by the relax-and-fix heuristic step, which is further improved in the fix-and-optimize step. Dantzig-Wolfe Decomposition (DWD) and Lagrangian Relaxation (LR) techniques are also applied to the same reformulation of the problem and the results of these three approaches are compared in terms of the solution quality as well as CPU time. The computational results obtained for different instances of the integrated production planning and imperfect preventive maintenance planning problem, show that the RFFO method is very efficient and is competitive in term of the solutions quality. It provides quite good solutions to the tested instances with a noticeable improvement in computational time. Dantzig-Wolfe Decomposition (DWD) and Lagrangian Relaxation (LR) methods, on the other hand, exhibit a good enhancement in terms of computational time especially for large instances, however, the quality of solution still requires some more improvements.

Keywords: Production planning · Imperfect preventive maintenance
Optimization · Integrated strategies

G. H. Parlier et al. (Eds.): ICORES 2017, CCIS 884, pp. 63–83, 2018.
https://doi.org/10.1007/978-3-319-94767-9_4

1 Introduction

Manufacturing systems are naturally subject to wear and breakdowns when they are operated. This deterioration affects in turn the quality of the system's output. Consequently, in order to enhance the system's actual utilization, to guarantee high quality of its output, and to meet the required market demand, maintenance must be regularly performed especially on critical components of the system. Preventive and corrective maintenance actions are performed, respectively, before and after the failure of the system or one of its critical components. A preventive maintenance action can be either perfect or imperfect. A perfect maintenance action restores the system's operating condition to an as good as new state. In contrast, an imperfect maintenance action restores the system's operating condition to state laying somewhere between the condition before maintenance and the as good as new state. The known results of replacements and maintenance policies were summarized and extensively discussed in the literature [4,10,11,20,27].

During the last two decades, the issue of integrating production and preventive maintenance, at the tactical planning level, attracted many researchers and several approaches are proposed to coordinate the production and maintenance functions and integrate their related planning decisions. The earliest work may be that of Wienstein and Chung [28] where they presented a three-parts hierarchical production planning and scheduling model taking into account the reliability of the production system. The first part in the model is an aggregated production planning model formulated as a linear program. The second part is a master production schedule with the objective of minimizing the weighted deviations with respect to the goals specified at the first part level. The third part focuses on simulating equipments' failures during the planning horizon. Several experiments are conducted to test the significant factors such as category, frequency and cost of maintenance activity, in addition to failure significance and aggregate production policy for maintenance policy selection.

Aghezzaf et al. [1] proposed an optimization model to generate optimal integrated production and preventive maintenance plans at the tactical level. Their approach assumes that the system is minimally repaired when it fails randomly during a production period. That is, the systems is returned to an operating state without altering its lifetime distribution. The system undergoes perfect periodic preventive maintenance after which it returns to an as good as new state, i.e., its failure rate is the same as the that of a new system. This approach also assumes that any maintenance action, minimal repair or preventive maintenance, reduces the available production capacity of the system.

The approach proposed in [1] has been extended under various assumptions' relaxations in several papers in the literature. In [3], the authors deal with simultaneous optimization of production and preventive maintenance in multiple-lines stochastic degrading manufacturing system. Najid et al. [19] extended the model in [3] and consider demand time windows and shortage cost. Nourelfath and Chatelet [21] discussed the same planning problem for a multi-component production system under economic dependence and common cause failures.

Zhao et al. [30] assume an order-dependent-failure (ODF) and proposed an iterative method to solve the problem on a single-machine system. Fitouhi and Nourelfath [8] extended the model [1] to multi-state systems [18]. The reliability of the production system is computed using the universal moment generating function (UMGF) [15]. The resulting integrated production and maintenance optimization model is solved with a genetic algorithm. To efficiently solve moderate to larger instances of the model developed in [3],Yalaoui et al. [29] proposed some useful exact and heuristic algorithms. The more recent extensions of the work in [1] have appeared in [2,6,22]. The resulting mathematical models are still naturally non-linear and hard to solve. In [2], the authors proposed a reformulation for the natural integrated production and imperfect preventive maintenance planning problem. The resulting optimization model is a mixed-integer linear programming problem which is solved using a MILP-based approximation method.

The model discussed in this paper is similar to the one proposed in [2]. It deals with the issue of integrating production and non-periodic imperfect preventive maintenance at the tactical planning level. Imperfect preventive maintenance is modeled according to the hybrid hazard model initially introduced in [17] and used in many research papers [5,12–14,16] among others. When an imperfect preventive maintenance action is performed it brings the system back to an operating state that is between the two extreme 'as bad as old' and the 'as good as new' operating states. Along the same lines as in [1,3], it is assumed that each imperfect preventive maintenance improves the available production capacity of the system and this according to the degree at which the maintenance is performed. However, the deterioration rate of the manufacturing system after each imperfect preventive maintenance increases and the production capacity decreases more rapidly due to more frequent minimal repair tasks. When the deterioration rate reaches an unacceptable level, the systems is overhauled and returns to an 'as good as new' state. The resulting optimization model is solved using Relax-and-Fix/Fix-and-Optimize approach. It is shown that such a solution approach provides quite good solutions, but it requires a large amount of computational time for medium and large problem instances. To obtain good quality solutions within a reasonable amount of the computational time, some heuristics based on the Dantzig-Wolfe decomposition techniques together with a new version of the Relax-and-Fix/Fix-and-Optimize method are developed.

A short version of the present work appeared in a conference proceeding [24]. The present extended version includes more references that enrich the literature review dealing with the problem of joint production and maintenance problem. It also provides more details on how Relax-and-Fix/Fix-and-Optimize as well as Dantzig-Wolfe Decomposition techniques were applied and implemented for solving the integrating production and imperfect preventive maintenance problem. Furthermore, Lagrangian Relaxation techniques are also investigated [7]. Finally, more detailed experiments are conducted to solve the optimization problem under each of the three solution approaches. The overall results obtained are then compared in terms of the solution quality as well as CPU time.

The remainder of this paper is organized as follows. Section 2 presents a slightly modified version of the mathematical model proposed in [2] for the integrated production and imperfect preventive maintenance planning. In Sect. 3, the Relax-and-Fix/Fix-and-Optimize (RFFO) solution technique is investigated and presented in details. Section 4 presents the Dantzig-Wolfe (DWD) decomposition to solve the MINLP reformulated production and maintenance planning model. Lagrange relaxation (LR) decomposition used to solve the reformulated problem is described in Sect. 5. Computational results of a set of benchmark test cases are presented and fully discussed in Sect. 6. Section 7 summarizes the main findings of this research work and provides some possible research directions.

2 Integrated Production and Imperfect Preventive Maintenance Planning Model

This section summarizes the mathematical optimization model for the integrated production and imperfect preventive maintenance problem as initially introduced in [2,24]. Its corresponding MILP reformulation proposed in [2,24] is also used as the underlying optimization model. In the present work, the imperfect preventive maintenance model is based on the hybrid failure rate model initially introduced in [17] and is also briefly described in the next subsection.

2.1 Modeling Imperfect Preventive Maintenance with Hybrid Failure Rates

In reliability engineering, failure rate is usually used as a measure which describes how a system improves or deteriorates with time. We consider a system whose lifetime is randomly distributed. Its corresponding initial hazard rate function, simply called the failure rate, is given by the function $r_0(t)$ as:

$$r_0(t) = \frac{g(t)}{1 - G(t)} \tag{1}$$

where $g(t)$ and $G(t)$ denote, respectively, the probability density and distribution functions of the system's lifetime.

If the k^{th} preventive maintenance takes place $T_k\tau$ units of time after an overhaul, that is in the beginning of period T_k having fixed length τ, the hazard rate function $r_k(t)$ of the system is then defined as:

$$r_k(t) = \beta_k r_0(t + \alpha_k T^k_{AOT}),\ t \in [0, (T_{k+1} - T_k)\tau[,\ \text{for all } k \in \{1, \ldots, k_{max}\} \tag{2}$$

where T^k_{AOT} is the actual operating time of the system since the beginning of the planning horizon until the beginning of period T_k, the period during which the k^{th} preventive maintenance is carried out. It is the timespan during which the system was in actually producing and not undergoing maintenance, neither preventive nor corrective. The parameters α_k and β_k stand, respectively, for the age reduction coefficient and the hazard rate increase coefficient (adjustment

factor) such that $0 = \alpha_1 < \alpha_2 < \cdots < \alpha_{k_{max}} = 1$ and $1 = \beta_1 \leq \beta_2 \leq \cdots \leq \beta_{k_{max}}$. Note again that for $t \in [0, T_1[$, $r_0(t)$ is the hazard rate of the system, which is initially assumed to be 'as good as new', that is after an overhauling. The baseline failure rate function $r_0(t)$ is assumed to be a monotonically increasing function throughout the text.

In the present work, if after the k^{th} preventive maintenance the failure rate function remains below some threshold function, $r_{k_{max}}(t)$, a preventive maintenance can be performed. However, if it reaches or exceeds this threshold level, the system is overhauled and then will return to an 'as good as new' state.

2.2 Modeling the Joint Production and Imperfect Prevetive Maintenance

We are given a production system which is subject to random failures. The system is capable of producing a set of products $j \in P = \{1, ...N\}$ during a planning horizon $H = \{1, ...T\}$ covering T production periods of the same length τ. For a given period $t \in H$, we denote by d_{jt}, f_{jt}, p_{jt} and h_{jt}, respectively, the demand for item j, the fixed cost of producing item j, the variable cost of producing item j, and the variable holding cost of item j. The quantity $d^j_{st} = \sum_{t'=s}^{t} d^j_{t'}$ is the cumulative demand of item $j \in P$ from s to t ($s \leq t$). The production system has a known maximum constant production capacity κ_{max} (given in time units) and the processing time of each unit of item j is given by ρ_j. The cost of carrying out a k^{th} preventive maintenance is denoted by c^k_{PM} and the cost of performing a corrective maintenance on the system, right after the k^{th} preventive maintenance, is denoted by c^k_{CM}. Finally, let δ^k_{PM} be the expected time required for the k^{th} preventive maintenance, and δ^k_{CM} the expected time required to perform a corrective maintenance, right after k^{th} preventive maintenance.

To define the variables of the model, let Q_{jt} be the quantity of item j produced during period t; I_{jt} be the inventory of item j at the end of period t; x_{jt} be a binary variable set to 1 if item j is produced during period t and 0 otherwise; y_t be a binary decision variable set to 1 if the machine is setup to production during period t and 0 otherwise. We also consider z^k_{st} defined as a binary variable set to 1 if the last preventive maintenance of the system before the time period t is the k^{th} one and has taken place during the time period s, and 0 otherwise. By convention we assume that the manufacturing system is preventively maintained in the beginning of period 1, that is $z^1_{11} = 1$.

The nonlinear mixed-integer optimization model corresponding to the Integrated Production and Imperfect Preventive Maintenance Planning Problem (IPImPMP) is given as follows [2]:

IPImPMP

$$\text{Minimize } Z^{IP}_{ImPMP} = \sum_{t=1}^{T}\sum_{j=1}^{N}(f_{jt}x_{jt} + p_{jt}Q_{jt} + h_{jt}I_{jt}) + \sum_{t=1}^{T}\sum_{k=1}^{t} c^k_{PM} z^k_{tt} + \sum_{t=1}^{T}\sum_{s=1}^{t}\sum_{k=1}^{s} c^k_{st}(\mathbf{y}) y_t z^k_{st}$$

Subject to:

$$Q_{jt} + I_{j,t-1} - I_{jt} = d_{jt}, \qquad \forall j \in P, \forall t \in H \tag{3}$$

$$Q_{jt} - \kappa_{max} x_{jt} \leq 0, \qquad \forall j \in P, \forall t \in H \tag{4}$$

$$x_{jt} - y_t \leq 0, \qquad \forall j \in P, \forall t \in H \tag{5}$$

$$\sum_{j=1}^{N} \rho_j Q_{jt} + \sum_{k=1}^{t} \delta^k_{PM} z^k_{tt} + \sum_{s=1}^{t}\sum_{k=1}^{s} \kappa^k_{st}(\mathbf{y}) y_t z^k_{st} \leq \kappa_{max}, \qquad \forall t \in H \tag{6}$$

$$\sum_{s=1}^{t}\sum_{k=1}^{s} z^k_{st} = 1, \qquad \forall t \in H \tag{7}$$

$$z^k_{st} - z^k_{s,t+1} \geq 0, \qquad \forall k, s, t \in H, k \leq s \leq t \leq T-1 \tag{8}$$

$$z^k_{tt} - \sum_{s=k-1}^{t-1} z^{k-1}_{s,t-1} \leq 0, \qquad \forall t, k \in H, 1 < k \leq t \tag{9}$$

$$\sum_{t=2}^{T}\sum_{s=2}^{t} z^1_{st} \leq (1 - z^1_{11}), \tag{10}$$

$$\sum_{k=1}^{t} z^k_{tt} - y_t \leq 0, \qquad \forall t \in H \tag{11}$$

$$Q_{jt}, I_{jt} \geq 0, \quad x_{jt}, y_t, z^k_{st} \in \{0,1\}, \qquad \forall j \in P, s, t \in H, k \leq s \leq t$$

Constraints (3) are the flow conservation constraints. They guarantee that the available inventory augmented with the quantity produced in period t is sufficient to satisfy the demand d_{jt} of item j in that period. The remainder is stocked for the subsequent periods. Constraints (4) make sure that, when the production of an item is scheduled in certain period, the system is setup accordingly to produce that item in that period. These constraints force also disbursement of the fixed costs. Constraints (5) indicate whether the system is operating or not in each period, in which case it is setup to produce some products. Constraints (6) are the capacity restrictions which are defined for each period $t \in H$. They guarantee that the quantity which is produced in a period t does not exceed the available capacity of the system, given its status in terms of the expected capacity loss during that period. Constraints (7) determine the periods during which the preventive maintenance activities take place. In order

to assure the consistency, constraints (8) are established to guarantee that if the last preventive maintenance action, before a time period $t+1$, takes place in a period $s < t$ and it is the k^{th} one, then this preventive maintenance action must also be the k^{th} and the last one before a period t. Again, for consistency, constraints (9) assure that the k^{th} preventive maintenance takes place in some period $t \geq k$, only if the $(k-1)^{th}$ preventive maintenance took place in some period before t. Constraint (10) enforces the convention $z_{11}^1 = 1$. Constraints (11) guarantee that the k^{th} preventive maintenance takes place only once and when the system is setup to production.

The two functions $\kappa_{ts}^k(y)$ and $c_{ts}^k(y)$ used in the above optimization model represent, respectively, the expected production capacity loss and the expected maintenance cost both evaluated during the time period t when the k^{th} and the last preventive maintenance action before time period t has taken place in the time period s, with $k \leq s \leq t$. These functions depend on the system's setup vector $\mathbf{y}$ and are computed as in [2]:

$$\kappa_{st}^k(y) = \begin{cases} \delta_{CM}^k \int_0^\tau \beta^k r_0 \left(u + \alpha^k \left[\sum_{t'=1}^{s-1} y_{t'} \right] \tau \right) du; & if\ t = s, k \leq s, \\ \delta_{CM}^k \int_0^\tau \beta^k r_0 \left(u + \alpha^k \left[\sum_{t'=1}^{s-1} y_{t'} \right] \tau + \left[\sum_{t'=s}^{t-1} y_{t'} \right] \tau \right) du; & if\ s \leq t \leq T. \end{cases} \tag{12}$$

$$c_{st}^k(y) = \begin{cases} c_{CM}^k \int_0^\tau \beta^k r_0 \left(u + \alpha^k \left[\sum_{t'=1}^{s-1} y_{t'} \right] \tau \right) du; & if\ t = s, k \leq s, \\ c_{CM}^k \int_0^\tau \beta^k r_0 \left(u + \alpha^k \left[\sum_{t'=1}^{s-1} y_{t'} \right] \tau + \left[\sum_{t'=s}^{t-1} y_{t'} \right] \tau \right) du & if\ s \leq t \leq T. \end{cases} \tag{13}$$

2.3 A Mixed-Integer Linear Reformulation of the IPImPMP

The optimization problem IPImPMPP, as given above, is a nonlinear mixed-integer optimization problem. Its non-linearity results both from the following component $\sum_{t=1}^{T} \sum_{s=1}^{t} \sum_{k=1}^{s} c_{st}^k(\boldsymbol{y}) y_t z_{st}^k$ in the objective function and from the component $\sum_{s=1}^{t} \sum_{k=1}^{s} \kappa_{st}^k(\boldsymbol{y}) y_t z_{st}^k$ in the constraints (6). It is worth noticing that when the periods during which the system is setup to production are fixed in advance, the expected maintenance cost components and the expected available production capacity of the system during each period can then directly be determined. In this case, the problem becomes a linear optimization problem integrating a multi-item capacitated lot-sizing problem with preventive maintenance. In the following subsection we propose a reformulation of this model as mixed-integer linear program which can be solved thanks to available MILP solvers such as CPLEX and Gurobi.

The proposed linearized formulation is adapted from that obtained in [2] by considering two new variables $v_{st}^k(p,q)$ and $w_{st}^k(p,q)$, with $p \leq s \leq t, k \leq s$ and $q \leq t-s+1$. The variable $v_{st}^k(p,q)$ is binary and assumes value 1 if the system is setup to production p times during the horizon $1,\ldots,s-1$ and q times during the period s,...,t, and the k^{th} maintenance takes place in period s. The variable $w_{st}^k(p,q)$ is also binary and assumes value 1 if the system is setup for production p times during the horizon $1,\ldots,s-1$ and q times during the period $s,\ldots,t$, the k^{th} maintenance takes place in period s, and the system is also operating at period t. As in [2], we alos consider the variable $u_{st}(p,q)$, with $p \leq s \leq t$ and $0 \leq q \leq t-s+1$, to be a binary variable assuming value 1 if the system is setup to production p times during the horizon 1,..., s − 1 and q times during the periods s,..., t-1. Here again, in line of the work in [2], we also consider the two functions $c_{st}^k(p,q)$ and $\kappa_{st}^k(p,q)$ be respectively the expected maintenance cost and expected loss in production capacity of the system during period t, when the last preventive maintenance action before time period t has taken place in the beginning of period s, $s \leq t$. The functions $c_{st}^k(p,q)$ and $\kappa_{st}^k(p,q)$ are formally computed as [2]:

$$c_{st}^k(p,q) = \begin{cases} c_{CM}^k \int_0^\tau \beta_k r_0(u+\alpha_k p\tau)du; & if \quad t=s, \\ c_{CM}^k \int_0^\tau \beta_k r_0(u+\alpha_k p\tau+q\tau)du; & if \quad s \leq t \leq T. \end{cases} \tag{14}$$

and

$$\kappa_{st}^k(p,q) = \begin{cases} \delta_{CM}^k \int_0^\tau \beta_k r_0(u+\alpha_k p\tau)du; & if \quad t=s, \\ \delta_{CM}^k \int_0^\tau \beta_k r_0(u+\alpha_k p\tau+q\tau)du; & if \quad s \leq t \leq T. \end{cases} \tag{15}$$

The proposed linear formulation (Re_IPImPMP) of the original problem (IPImPMPP) is then given as follows:

Re_IPImPMP

$$\text{Minimize } Z_{ImPMP}^{Re\_IP} = \sum_{t=1}^{T}\sum_{j=1}^{N}(f_{jt}x_{jt} + p_{jt}Q_{jt} + h_{jt}I_{jt}) + \sum_{t=1}^{T}\sum_{k=1}^{t} c_{PM}^k z_{tt}^k + \sum_{t=1}^{T}\sum_{s=1}^{t}\sum_{k=1}^{s}\sum_{p=0}^{s-1}\sum_{q=0}^{t-s} c_{st}^k(p,q)v_{st}^k(p,q)$$

Subject to: Eqs. (3)–(5) and (7)–(11),

$$\sum_{j=1}^{N}\rho_j Q_{jt} + \sum_{k=1}^{t}\delta_{PM}^k z_{tt}^k + \sum_{s=1}^{t}\sum_{k=1}^{s}\sum_{p=0}^{s-1}\sum_{q=0}^{t-s} c_{st}^k(p,q)v_{st}^k(p,q) \leq \kappa_{max}, \ \forall t \in H \tag{16}$$

$$\sum_{p=0}^{s-1}\sum_{q=0}^{t-s} p.u_{st}(p,q) - \begin{cases} \sum_{s'=1}^{s-1} y_{s'}\ , & if\ s>1 \\ 0, & if\ s=1 \end{cases} \leq 0, \quad \forall t,s \in H, 1 \leq s \leq t \tag{17}$$

$$\sum_{p=0}^{s-1}\sum_{q=0}^{t-s} q.u_{st}(p,q) - \begin{cases} \sum_{s'=s}^{t-1} y_{s'}\ , & if\ t>1 \\ 0, & if\ t=1 \end{cases} \leq 0, \quad \forall t,s \in H, 1 \leq s \leq t \tag{18}$$

$$\sum_{p=0}^{s-1}\sum_{q=0}^{t-s} u_{st}(p,q) = 1, \quad \forall t,s \in H, 1 \leq s \leq t \tag{19}$$

$$z_{st}^{k} + u_{st}(p,q) - v_{st}^{k}(p,q) \leq 1, \quad \forall k,s,t,p,q \in H, p \leq s-1, q \leq t-s \tag{20}$$

$$y_t + v_{st}^{k}(p,q) - w_{st}^{k}(p,q) \leq 1, \quad \forall k,s,t,p,q \in H, p \leq s-1, q \leq t-s \tag{21}$$

$$Q_{jt}, I_{jt} \geq 0, \quad x_{jt}, y_t, z_{st}^{k}, u_{st}\{p,q\}, v_{st}^{k}\{p,q\}, w_{st}^{k}\{p,q\} \in \{0,1\}, \forall j \in P,$$
$$s,t \in H, k \leq s \leq t, p \leq s-1, q \leq t-s$$

Constraints (3)–(5) and (7)–(11) are the same as those considered in the original problem. Constraints (16) are revisited versions of the constraints (6). Constraints (17), (18) and (19) determine the values of the variables u and v. Constraints (20) relate the variables z with u and v, meaning that if the k^{th} and last preventive maintenance before t takes place in period $s \leq t$ and if the system is setup to production p times during the horizon $\{1,\ldots,s-1\}$ and q times during the periods $\{s,\ldots,t-1\}$ then $v_{st}^{k}(p,q) = 1$. The constraints (21) relate the variables v with y and w, if both the k^{th} and last preventive maintenance before t takes places in period $s \leq t$ and if the system is setup to production p times during the horizon $\{1,\ldots,s-1\}$ and q times during the periods $\{s,\ldots,t-1\}$ and the system must operate at period t then $w_{st}^{k}(p,q) = 1$.

3 Relax-and-Fix/Fix-and-Optimize Heuristic (RFFO) to Solve the Re_IPImPMP Model

The Relax-and-Fix (RF) heuristic solves a mixed-integer problem (MIP) by sequentially resolving sub-problems in which some variables are fixed while the others are relaxed. Dealing with production planning problems, for example, the planning horizon is partitioned and the setup variables are fixed either backward or forward. The Fix-and-Optimize (FO) is a heuristic solution based on the decomposition of the original problem into multiple sub-problems with smaller number of binary variables. The RFFO method is a framework designed to combine the RF and FO heuristics. In [25], the authors propose an approach in which most binary variables are fixed or relaxed and only few of them are chosen and

forced to be integer and are optimized. The set of chosen variables is called a "window". Three window types are available [25]: (*i*) *row-wise*, in which the window moves along rows; (*ii*) *column-wise*, in which the window moves along columns; (*iii*) and *value-wise*, in which the window selects the variables with relaxed values closest to a half.

As in [25], to solve the Re_IPImPMP model with both RF and FO heuristics, we consider a matrix $\mathbf{Y}$ where each of its entries is the binary variable y_t. The pseudo codes corresponding to RF, FO, and RFFO heuristics are summarized in Algorithms 1, 2 and 3, respectively.

Algorithm 1. Relax-and-Fix heuristic.

Inputs: $sol.y$, $windowSize$, $overlap$, $timeLimit$
$window \leftarrow$ initWindow($sol.y, windowSize$)
$\bar{y}_{fixed} \leftarrow \emptyset$
$y_{MIP} \leftarrow window$
while fixed solution not reached **and** elapsedTime < timeLimit **do**
  Solve ($\bar{y}_{fixed}$, y_{MIP}, y_{LP})
  $window \leftarrow$ moveWindow($overlap, windowSize$)
  $\bar{y}_{fixed} \leftarrow \bar{y}_{fixed} \cup (y_{MIP} - window)$
  $y_{MIP} \leftarrow window$
  $y_{LP} \leftarrow y_{LP} - window$
end while
$sol.y \leftarrow \bar{y}_{fixed}$

Algorithm 2. FIX-and-Optimize heuristic.

Inputs:$sol.y, windowSize, overlap, timeLimit$
$window \leftarrow \emptyset$
while $elapsedTime \geq timeLimit$ **do**
  $window \leftarrow$ initWindow($windowSize, WindowType$)
  $y_{MIP} \leftarrow window$
  $\bar{y}_{fixed} \leftarrow sol.y - window$
  while window not reach end **do**
    Solve ($\bar{y}_{fixed}, y_{MIP}$)
    $window \leftarrow$ moveWindow($overlap, windowSize$)
    $y_{MIP} \leftarrow window$
    $\bar{y}_{fixed} \leftarrow (sol.y - window)$
    $sol.w \leftarrow \bar{y}_{fixed} \cup y_{MIP}$
  end while
end while

In Algorithm 1, the inputs of the RF heuristic are: the set of binary variables ($sol.y$), the number of binary variables ($windowSize$) to be chosen, the selection criteria to choose variables ($windowType$), the overlap rate of binary variables

Algorithm 3. Relax-and-Fix & FIX-and-Optimize heuristic.

1: Inputs: $rfSize, rfOverlap, foSize, foOverlap, timeLimit$
2: $sol \leftarrow$ RELAXANDFIX $(sol.y, rfSize, rfOverlap, timeLimit)$
3: $prevCost \leftarrow sol.cost$
4: **while** $timeElapsed < timeLimit$ **do**
5: FixAndOptimize $(sol.y, foSIZE, foOverlap, timeremaining)$
6: **end while**

to be re-optimized (*overlap*) and the execution time limit (*timeLimit*). Initially, all binary variables in the RF solution ($sol.y$) are relaxed, and a window is defined as a set that includes a fixed amount of (*windowSize*) variables. Then, those variables inside the window are enforced to be integer in the set y_{MIP}, while the others are kept in y_{LP}. We solve the problem to get the results of MIP. Next, a new set of variables (*window*) is defined by a subset of fixed integers (y_{fixed}), sets of optimized integer (y_{LP}) and relaxed variables (y_{MIP}). The *window* moves forward by the *step* parameter at each iteration on which each $step = round(|overlap * windowSize|)$, $overlap \in [0, 1]$. All variables that leave the window are fixed in the next iteration, and the same number of relaxed variables are enforced to be integer. The algorithm proceeds in this way until all variables are fixed. After completion of the RF phase, the FO heuristic is used to improve this initial solution until the time limit has been reached (see Algorithm 2). If the improvement achieved by a FO solution is not satisfactory, the size of the window is increased. As a result of this attempt to find a better solution, the MIP subproblems become then large.

4 Single Dantzig-Wolfe by Product Decomposition with Fix and Optimize to Solve the MINLP IPImPPMP Model

Implementing Dantzig-Wolfe decomposition (DWD) method to solve the multi-item capacitated lot sizing problem with setup times is discussed in [23] where the authors proposed three different approaches of the standard DWD implementation. In the first approach, the subproblems are defined for each item (PIDWD), in the second they are defined by periods (PJDWD), and in the third one the subproblems derived from the first two approaches are combined in the same model (MDWD). The three approaches were tested on the IPImPMP model developed in Sect. 2.2. Based on the results obtained, the suitable approach is found to be the item decomposition approach. Consequently, this decomposition approach is selected to be compared against the other solution methods. We consider the capacity constraints Eq. 6, linking the variables associated with different products, as the master problem for this decomposition.

4.1 The Master Problem

The master problem includes the collections of production plans of each item in addition to the maintenance planning. The decision variables are ϑ_j^m, corresponding to the item's production plans m generated by the subproblem for product j, together with the variables z_{st}^k corresponding to the maintenance plan developed at the master problem level. The linear programming relaxation of the master problem of the production decomposition is given as follows:

MPJ-PPM

$$\text{Minimize } Z_{IPImPPM}^{MPJ} = \sum_{j=1}^{N}\sum_{m=1}^{Mj}\left[\sum_{t=1}^{T}(f_{jt}\bar{x}_{jt}^m + p_{jt}\bar{Q}_{jt}^m + h_{jt}\bar{I}_{jt}^m)\right]\vartheta_j^m + \sum_{t=1}^{T}\sum_{k=1}^{t} c_{PM}^k z_{tt}^k + \sum_{t=1}^{T}\sum_{s=1}^{t}\sum_{k=1}^{s} c_{st}^k(\bar{y}).\bar{y}_t z_{st}^k$$

Subject to:
Equations (7)–(11),

$$\sum_{j=1}^{N}\sum_{m=1}^{Mj}\rho_j\bar{Q}_{jt}^m\vartheta_j^m + \sum_{t=1}^{T}\sum_{k=1}^{t}\delta_{PM}^k z_{tt}^k + \sum_{s=1}^{t}\sum_{k=1}^{s}\kappa_{st}^k(\bar{y})z_{st}^k \le \kappa_{max}, \forall t \in H \ (\mu_t) \tag{22}$$

$$\sum_{m=1}^{Mj}\vartheta_j^m = 1, \qquad \forall j \in N \qquad (\pi_j) \tag{23}$$

$$\sum_{m=1}^{Mj}\bar{x}_{jt}^m\vartheta_j^m \le \bar{y}_t, \qquad \forall j \in N; t \in H \qquad (\eta_{jt}) \tag{24}$$

$$\vartheta_j^m \ge 0, \qquad \forall j \in N \tag{25}$$

$$z_{st}^k \ge 0, \qquad \forall j \in N; t, s \in H \tag{26}$$

where $\bar{y}_t = \max_{j,m}\{\bar{x}_{jt}^m\}$ and the objective function minimizes the overall production and maintenance costs. The constraints (22) are capacity constraints. These require that the combination of the chosen production plans satisfies the available capacity in each period, while the maintenance plans are taken into account. Constraints (23) are the convexity constraints. The combination of the selected production plans is forced by constraints (24) to satisfy the production setup requirement. Constraints (25) and (26) force the decision variables to take nonnegative values. At the end of this process, the problem is solved again but with the variables ϑ_j^m and z_{st}^k for which the following conditions are satisfied:

$$\vartheta_j^m, z_{st}^k \in \{0,1\} \forall j \in N, s, t \in H, k \le s \le t, m \in Mj$$

To recover solution of the problem IPImPMP, in terms of the original variables, the values of Q_{jt} and x_{jt} variables are derived from the solution of the

master problem (MPJ_PPM) as follows:

$$Q_{jt} = \sum_{m=1}^{Mj} \bar{Q}_{jt}^{m} \vartheta_{j}^{m}, \qquad \forall j \in N, \quad \forall t \in T \tag{27}$$

$$x_{jt} = \sum_{m=1}^{Mj} \bar{x}_{jt}^{m} \vartheta_{j}^{m}, \qquad \forall j \in N, \quad \forall t \in T \tag{28}$$

4.2 The Subproblem

Assuming that μ_t is the dual variables associated with the constraints (22), indexed by t, that π_j is the dual variables associated with the set of convexity constraints (23) and that η_{jt} is the dual variables associated with constraints (24). Each subproblem is of following types for all $j \in N$:

SPJ-PPM

Minimize

$$Z_{IPImPMP}^{SPJ} = \sum_{t=1}^{T} (f_{jt} x_{jt} + p_{jt} Q_{jt} + h_{jt} I_{jt}) - \sum_{t=1}^{T} \rho_j Q_{jt} \mu_t - \pi_j - \sum_{t=1}^{T} \eta_{jt} x_{jt},$$

or

Minimize

$$Z_{IPImPMP}^{SPJ} = \sum_{t=1}^{T} [(f_{jt} - \eta_{jt}) x_{jt} + p_{jt} Q_{jt} + h_{jt} I_{jt}] - \sum_{t=1}^{T} \rho_j Q_{jt} \mu_t - \pi_j$$

Subject to:
Equations (3)–(4),

$$Q_{jt}, I_{jt} \geq 0,\ x_{jt}, y_t \in \{0,1\}, \forall j \in N,\ s,t \in H, k \leq s \leq t,\ p \leq s-1,\ q \leq t-s \tag{29}$$

The pseudo-code of the proposed DWD approach is summarized in Algorithm 4. This algorithm starts with two sets of initial plans that are generated. The first set of plans (one for each item), given by $\bar{Q}_{jt}^{1}, \bar{X}_{jt}^{1}$ and $\bar{I}_{jt}^{1}$, are obtained by assuming that the machine is operating in each period at its full capacity, i.e., by setting the value of $\kappa_{t,s}^{k}(\bar{y})$ and $c_{t,s}^{k}(\bar{y})$ to zero in each period and solving the original problem (IPImPMP) (assuming no preventive maintenance is undertaken). The second set of plans (again one for each item), given by ($\bar{Q}_{j,t}^{2} = demand_{jt}$ and $\bar{X}_{jt}^{2} = 1$ and $\bar{I}_{jt}^{2} = 0$, are obtained by assuming that the demand of each item in a period is produced in the that period (Lines 2 to 5). Then in lines 6 and 7, the values of $\bar{y}_t, \kappa_{t,s}^{k}(\bar{y})$ and $c_{t,s}^{k}(\bar{y})$ are recalculated.

The values resulting from the two mentioned initial sets of plans are handled by the master problem as input parameters. The master problem is solved to obtain the dual variables μ_t, π_j, η_{jt} associated with its constraints and are

Algorithm 4. Dantzig-Wolfe Product Decomposition heuristic.

1: Inputs: Q, I, X, Y, Z
2: $\kappa^k_{t,s}(\bar{y})$, $c^k_{t,s}(\bar{y}) \leftarrow 0$
3: Q_{jt}, X_{jt}, $I_{jt} \leftarrow$ solve IPImPMP(sol.IP)
4: $\bar{Q}^1_{jt}, \bar{X}^1_{jt}, \bar{I}^1_{jt} \leftarrow Q_{jt}, X_{jt}, I_{jt}$
5: $\bar{Q}^2_{jt}, \bar{X}^2_{jt}, \bar{I}^2_{jt} \leftarrow demand_{jt}, 1, 0$
6: $\bar{y}_t \leftarrow \max_j\{\bar{X}^2_{jt}\}$
7: $\kappa^k_{t,s}(\bar{y})$, $c^k_{t,s}(\bar{y}) \leftarrow$ formula (12) and (13)
8: solve Masterproblem($sol.LP, \vartheta^m_j, \mu_t, \pi_j, \eta_{jt}$)
9: $\mu_t, \pi_j, \eta_{jt} \leftarrow$ dual values of constraints (22), (23), (24)
10: solve SUBproblem($sol.IP, Q_{jt}, X_{jt}, I_{jt}$)
11: $m \leftarrow 3$
12: $\bar{Q}^m_{jt}, \bar{X}^m_{jt}, \bar{I}^m_{jt} \leftarrow Q_{jt}, X_{jt}, I_{jt}$
13: $\bar{y}_t \leftarrow \max_j\{\bar{X}^{kp}_{jt}\}$
14: $\kappa^k_{t,s}(\bar{y})$, $c^k_{t,s}(\bar{y}) \leftarrow$ formula formula (12) and (13)
15: **while** (min($sol.LP$) ≤ 0) **do**
16: solve Masterproblem($sol.LP, \vartheta^m_j, \mu_t, \pi_j, \eta_{jt}$)
17: $\mu_t, \pi_j, \eta_{jt} \leftarrow$ dual values of constraints (22), (23), (24)
18: solve SUBproblem($sol.IP, Q_{jt}, X_{jt}, I_{jt}$)
19: $m \leftarrow m + 1$
20: $\bar{Q}^m_{jt}, \bar{X}^m_{jt}, \bar{I}^m_{jt} \leftarrow Q_{jt}, X_{jt}, I_{jt}$
21: $\bar{y}_t \leftarrow \max_j\{\bar{X}^{kp}_{jt}\}$
22: $\kappa^k_{t,s}(\bar{y})$, $c^k_{t,s}(\bar{y}) \leftarrow$ formula formula (12) and (13)
23: **end while**
24: $\bar{y}_t \leftarrow 1$ if $\max_j(\sum_{m=1}^{Mj} \bar{X}^m_{jt} * \vartheta^m_j) \geq 0$, and 0 otherwise
25: $\kappa^k_{t,s}(\bar{y})$, $c^k_{t,s}(\bar{y}) \leftarrow$ formula formula (12) and (13)
26: solve IPImPMPP($sol.IP$)

communicated as input parameters to the subproblems (line 9–12). During the DWD generation process, subproblems are solved to generate new set of plans m_{th}. For a given product, if the subproblem's objective value is negative, i.e., if the m_{th} plan has a negative reduced cost, then this m_{th} plan is added to master problem in the next iteration. The process is repeated until the stopping criterion is reached. Here, the stopping criteria holds whenever all plans generated have positive reduced costs, or the limited number of iterations is reached (line 17–26). Finally, the variable $\bar{y}_t$ is set to 1 if $\max_j(\bar{X}^m_{jt} * \vartheta^m_j) > 0$ and to 0 otherwise. Then after, the values of $\kappa^k_{t,s}(\bar{y})$ and $c^k_{t,s}, (\bar{y})$ are calculated then a feasible final plan is obtained by solving the original IPImPMP problem as an integer linear problem.

5 Lagrange Relaxation Method

Lagrangian relaxation is a technique that is widely used to deal with combinatorial optimization problems. It generally provides better lower bounds than those obtained by the linear programming relaxation (see [7,9]). To generate

such lower bounds in case of the reformulation Re_IPImPMP of the problem, as presented in Sect. 2.3, we consider the relaxed problem in which the resource capacity constraints (16) (or (6)) is relaxed with the set of Lagrangian multipliers $\mu_t \geq 0$.

(CAP_Re_IPImPMP(μ):)

$$\begin{aligned}
&\text{Minimize } Z_{CAP}^{LR}(\mu) \\
&= \sum_{t=1}^{T}\sum_{j=1}^{N}\left(f_{jt}x_{jt} + p_{jt}Q_{jt} + h_{jt}I_{jt}\right) + \sum_{t=1}^{T}\sum_{k=1}^{t} C_{PM}^{k} z_{tt}^{k} \\
&+ \sum_{t=1}^{T}\sum_{s=1}^{t}\sum_{k=1}^{s}\sum_{p=0}^{s-1}\sum_{q=0}^{t-s} c_{st}^{k}(p,q) w_{st}^{k}(p,q) \\
&+ \sum_{t=1}^{T}\mu_t\left(\sum_{j=1}^{N}\rho Q_{jt} + \sum_{s=1}^{t}\sum_{k=1}^{s}\sum_{p=0}^{s-1}\sum_{q=0}^{t-s} c_{st}^{k}(p,q) v_{st}^{k}(p,q) - \kappa_{max}\right) \qquad (30)
\end{aligned}$$

Subject to:

Equations (3)–(5), (7)–(11), and (17)–(21).

The problem of finding the Lagrangian multipliers μ_t values that minimize the result of $CAP\_Re\_IPImPMP(\mu)$, which is a maximization problem, is called the Lagrangian dual problem. In general, this later is rather difficult to solve. There is however a fairly straightforward approach that begins with each multiplier μ_t set to 0. Next, the problem $CAP\_Re\_IPImPMP$ is solved to get current solution. The Lagrangean multipliers μ_t are then updated as shown below. The process is carried out until either a feasible solution (optimal) is found or until the quality of the lower bound is good enough. The Lagrangean multipliers μ_t^{k+1} are updated as follows:

$$\mu_t^{k+1} = max\left(0, \mu_t^k - \lambda \frac{(UB - LB)}{\sum_{t=1}^{T}(slack[t])^2} * slack[t]\right), \quad \forall t \in H \qquad (31)$$

where

$$slack[t] = \left(\kappa_{max} - \sum_{j=1}^{N}\rho Q_{jt} - \sum_{s=1}^{t}\sum_{k=1}^{s}\sum_{p=0}^{s-1}\sum_{q=0}^{t-s} c_{st}^{k}(p,q) v_{st}^{k}(p,q)\right) \qquad (32)$$

The Lagrangian relaxation pseudo code is given in Algorithm 5.

Algorithm 5. Lagrangian relaxation algorithm.

$\mu \leftarrow 0$
$LB \leftarrow -\infty$
$UB \leftarrow +\infty$
$X_{jt} \leftarrow 1$
$V_{ts}^{k}(p,q) \leftarrow \begin{cases} 1, & \text{if } t = s = k \text{ and } p = s - 1 \\ 0, & \text{otherwise} \end{cases}$
$W_{ts}^{k}(p,q) \leftarrow \begin{cases} 1, & \text{if } t = s = k \text{ and } p = s - 1 \\ 0, & \text{otherwise} \end{cases}$
$UB \leftarrow presolve(re\_PPImPMPP, sol.value)$
$k_{iter} \leftarrow 1$
while $LB \neq UB$ **do**
    solve$(sol.relaxed, Q, I, X, YS, Z, v, w, \mu)$
    $LB_{k_{iter}} \leftarrow sol.relaxed$
    $LB \leftarrow \max(LB, LB_{k_{iter}})$
    $recalculate(re\_PPImPMPP, sol.value)$
    $UB_k \leftarrow sol.value$
    $UB \leftarrow \min(UB, UB_{k_{iter}})$
    update$(\mu_{k_{iter}}, \lambda_{k_{iter}})$
    $k_{iter} \leftarrow k_{iter} + 1$
end while

6 Results and Discussions

To evaluate the effectiveness of the three different approaches described above, on the Re_IPImPMP model, this section presents the results of the computational experiments on some test instances, available in the literature. In particular, a collection of test instances from the LOTSIZELIB [26] is used for this experimental analysis. Of course, these instances from the LOTSIZELIB were extended and adapted to the integrate maintenance optimization aspect as done in [2,24].

6.1 The Test Instances

The algorithms presented above are coded in AMPL using the callable library CPLEX 12.6 to solve the MILP problems. The computation tests were carried out on an Intel(R) Core(TM) i7-3770 CPU @ 3.40 GHz, 3401 MHz, 4 Core(s), 8 Logical with 32 GB RAM operating under windows 7. CPU times are given in seconds. For the maintenance part, we assumed that the machine is subject to the random failures according to a Gamma distribution $\Gamma(m = 2, \nu = 2)$ with a shape parameter $m = 2$ and a scale parameter $\nu = 2$ as in [2], and that both preventive and corrective maintenance times are negligible. We also assume imperfect preventive maintenance with an age reduction coefficient $\alpha_k = k/(3k+7)$ and a failure rate adjustment coefficient $\beta_k = (12k+1)/(11k+1)$ for all k.

To evaluate the effect of *windowSize* and *overlap* for the RFFO heuristic method, we tested all the *windowSize* parameters from 1 to T, the last period of

the planning horizon, and we increased *overlap* by a *step* from 1 to $WindowSide$ for instances $A20007$ and $tr6\_15$ to get initial value of the problem as shown in Table 1.

Table 1. Initial value of $WindowSize$ and $Overlap$ chosen in RFFO Algorithm [24].

Instances	$WindowSize$	$Overlap$ %
A2007	5	60
tr6_15	8	60
tr6_30	12	60
tr12_15	8	60
tr12_30	12	60
tr24_15	8	60
tr24_30	12	60
set1ch	8	60

6.2 Analysis and Discussions About the Experiments

Table 2 summarizes the results of the experiments which were carried out to compare the Re_IPImPMP [2] and the RFFO heuristic solution method. The first column of the table identifies the instances solved. The second column reports the optimal value of each instance which was obtained from the Re_IPImPMP model and the third column reports the resulting CPU running time. The fourth column describes the value of each instance obtained by the proposed RFFO heuristic algorithm and the fifth column presents the obtained CPU running time. The last column shows the GAP between the RFFO heuristic value and the Re_IPImPMP value. When comparing the results of the proposed RFFO with the results of the Re_IPImPMP model, the RFFO algorithm provided the same optimal value with a considerable saving of the CPU time. This approaches is 4 to 10 times faster for the medium and/or large instance. However, in the small scale problems (A2007 and set1ch instances) the CPU time was larger for RFFO due to the inner loop of the algorithm.

Table 3 summarizes the results of the computational experiments carried out for the DWD decomposition method. The first column of the table identifies the instances solved. The second column presents the value of each instance obtained by the proposed DWD decomposition algorithm, and the third column reports the CPU time. The last column describes the GAP between the DWD decomposition value and the Re_IPImPMP value given by:

$$GAP\% = \frac{(valueDWD - valueRe\_IPImPMP)}{valueDWD} * 100$$

As shown in Table 3, the proposed DWD provides solutions which are not so far from the optimal Re_IPImPMP value, with the less CPU time and memory.

Table 2. A Summary of the experimental results for comparision between the Re_IPImPMP and RFFO Heuristic algorithm [24].

Instances	Re_PPImPMP	CPU time (sec)	RFFO	CPU time (sec)	GAP %
A2007	815.435	1.05	815.435	51.25	0.00
tr6_15	337,355.000	4,339.16	337,355.000	210.59	0.00
tr6_30	675,607.000	2,103,730.00	676,080.000	642,130.00	0.07
tr12_15	1,245,920.000	2,710.00	1,252,120.000	520.00	0.50
tr12_30	4,387,470.000	2,088,910.00	4,387,470.000	1,126,980.00	0.00
tr24_15	2,502,640.000	2,920.00	2,502,640.000	245.89	0.00
tr24_30	8,272,760.000	2,031,020.00	8,272,760.000	752,230.00	0.00
set1ch	107,532.000	130.00	107,532.000	244.69	0.00

Table 3. A summary of the experimental results of the DWD applied algorithm [24].

Instance	Value DWD	CPU time (sec)	Gap %
A2007	875.52	1.95	6.86
tr6_15	337,787.00	1.65	0.13
tr6_30	859,051.00	1.29	21.35
tr12_15	2,159,410.00	1.05	42.30
tr12_30	8,917,970.00	3.59	50.67
tr24_15	4,829,470.00	1.01	48.18
tr24_30	16,945,000.00	3.76	50.98
set1ch	172,504.00	1.72	37.66

However, the GAP defined as the ratio of the difference between the value of the DWD algorithm and the value of the Re_IPImPMP model, show that the approach is just suitable for small and medium scale instances.

Table 4 summarizes the results of the experiments carried out with Lagrange Relaxation method. The first column of the table identifies the instances solved. The second column shows the obtained Lower Bound (LB) value of each instance. The third column present the obtained Upper Bound (UP) value of each instance. The fourth column reports the CPU time. The last column describes the GAP between UB and valueRe_IPImPMP by:

$$GAP\% = \frac{(UB - valueRe\_IPImPMP)}{UB} * 100$$

In the Lagrange Relaxation decomposition method, the UB are also close to optimal value in case of small/medium scale problem and excessively large when the problems have more variables and constraints for large scale problems. The problem takes more memory, CPU solving time and rises up variables after each iteration which causes high CPU utilization and out of capacity of AMPL/CPLEX program. This returns back to feasible solution on inaccuracy

Table 4. Summary of the experimental results of Lagrange relaxation applied algorithm.

Instance	LB	UB	CPU time (sec)	GAP %
A2007	531.65	815.44	14.30	0.00
tr6_15	332,147.00	337,355.00	15,754.90	0.00
tr6_30	652,844.00	2,277,720.00	410.34	70.34
tr12_15	829,906.00	1,245,920.00	1,122.71	0.00
tr12_30	2,041,480.00	40,720,000.00	453.16	89.23
tr24_15	1,722,040.00	2,502,640.00	2,328.80	0.00
tr24_30	3,903,010.00	77,760,500.00	375.74	89.36
set1ch	84,751.80	107,532.00	365.88	0.00

valuable and no updated Lagrange multipliers. It means that GAP, computed by LB and UB, is huge when the problem becomes more complex.

7 Conclusions

This paper investigates the integrated production and imperfect preventive maintenance planning problem. The objective of this joint planning problem is to determine an optimal integrated production plan as well as a preventive maintenance plan that concurrently minimize production and preventive maintenance costs during a given finite planning horizon. Three approaches are used to solve the resulting reformulated models and compare the obtained results for a set of benchmark instances.

Thus, the Relax-and-Fix/Fix-and-Optimize (RFFO), Dantzig-Wolfe Decomposition (DWD) and Lagrangian Relaxation (LR) approaches were applied to the reformulated version of the problem, and their performances are compared and discussed. Eight difference instances ranging from small, medium to large-scale sized problems are considered.

The computational results show that the RFFO approach is quite efficient and competitive compared to the Dantzig-Wolfe Decomposition (DWD) and Lagrangian Relaxation (LR) techniques. It provides quite good solutions to the test problems with a noticeable improvement in computational time. DWD decomposition and Lagrangian Relaxation methods on the other hand exhibits a good enhancement in terms of computational time, however, the quality of solution still requires some more improvements.

Further studies are currently undertaken to investigate more in detail and improve the DWD decomposition and Lagrangian Relaxation methods to obtain better quality solutions and increase computational time savings, especially for large instances of this complex problem.

References

1. Aghezzaf, E.H., Jamali, M.A., Ait-Kadi, D.: An integrated production and preventive maintenance planning model. Euro. J. Oper. Res. **181**(2), 679–685 (2007)
2. Aghezzaf, E.-H., Khatab, A., Tam, P.L.: Optimizing production and imperfect preventive maintenance planning's integration in failure-prone manufacturing systems. Reliab. Eng. Syst. Saf. **145**, 190–198 (2016)
3. Aghezzaf, E.H., Najid, N.: Integrated production and preventive maintenance in deteriorating production systems. Inf. Sci. **178**, 3382–3392 (2008)
4. Barlow, R.E., Proschan, F.: Mathematical theory of reliability. Society for Industrial and Applied Mathematics, US (1996). reprint (31 December) edn
5. El-Ferik, S., Ben-Daya, M.: Age-based hybrid model for imperfect preventive maintenance. IIE Trans. **38**(4), 365–375 (2006)
6. Fakher, H.B., Nourelfath, M., Gendreau, M.: A cost minimisation model for joint production and maintenance planning under quality constraints. Int. J. Prod. Res. **55**, 2163–2176 (2016). https://doi.org/10.1080/00207543.2016.1201605
7. Fisher, M.L.: The lagrangian relaxation method for solving integer programming problems. Manag. Sci. **50**(12–supplement), 1861–1871 (2004)
8. Fitouhi, M.-C., Nourelfath, M.: Integrating noncyclical preventive maintenance scheduling and production planning for multi-state systems. Reliab. Eng. Syst. Saf. **121**, 175–186 (2014)
9. Geoffrion, A.M.: Lagrangean relaxation for integer programming. In: Balinski, M.L. (eds.) Approaches to Integer Programming. Mathematical Programming Studies, vol. 2, pp. 82–114. Springer, Heidelberg (1974). https://doi.org/10.1007/BFb0120690
10. Gertsbakh, I.: Reliability Theory with Applications to Preventive Maintenance. Springer, Heidelberg (2005). https://doi.org/10.1007/978-3-662-04236-6
11. Jardine, A.K.S., Tsang, A.H.C.: Maintenance, Replacement and Reliability, Theory and Applications. Taylor and Francis, Boca Raton (2006)
12. Khatab, A.: Hybrid hazard rate model for imperfect preventive maintenance of systems subject to random deterioration. J. Intell. Manufact. **26**(3), 601–608 (2015). https://doi.org/10.1007/s10845-013-0819-x
13. Khatab, A.: Maintenance optimization in failure-prone systems under imperfect preventive maintenance. J. Intell. Manufact. **29**, 707–717 (2018). https://doi.org/10.1007/s10845-013-0819-x
14. Khatab, A., Diallo, C., Sidibe, I.B.: Optimizing upgrade and imperfect preventive maintenance in failure-prone second-hand systems. J. Manufact. Syst. **43**(Part 1), 58–78 (2017)
15. Levitin, G.: Universal Generating Function in Reliability Analysis and Optimization. Springer, London (2005). https://doi.org/10.1007/1-84628-245-4
16. Lin, D., Zuo, M.J., Yam, R.C.M.: Sequential imperfect preventive maintenance models with two categories of failure modes. Naval Res. Logistics **48**, 172–183 (2001)
17. Lin, D., Zuo, M.J., Yam, R.C.M.: General sequential imperfect preventive maintenance models. Int. J. Reliab. Qual. Saf. Eng. **07**(03), 253–266 (2000)
18. Lisnianski, A., Levitin, G.: Multi-state Systems Reliability: Assesment, Optimization and Applications. World Scientific, Singapore (2003)
19. Najid, N.M., Alaoui-Selsouli, M., Mohafid, A.: An integrated production and maintenance planning model with time windows and shortage cost. Int. J. Prod. Res. **49**(8), 2265–2283 (2011)

20. Nakagawa, T.: Advanced Reliability Models and Maintenance Policies. Springer, London (2008)
21. Nourelfath, M., Châtelet, E.: Integrating production, inventory and maintenance planning for a parallel system with dependent components. Reliab. Eng. Syst. Saf. **101**, 59–66 (2012)
22. Nourelfath, M., Nahas, N., Ben-Daya, M.: Integrated preventive maintenance and production decisions for imperfect processes. Reliab. Eng. Syst. Saf. **148**, 21–31 (2016)
23. Pimentel, C.M.O., Pereira e Alvelos, F., de Carvalho, J.M.V.: Comparing dantzig-wolfe decompositions and branch-and-price algorithms for the multi-item capacitated lot sizing problem. Optim. Methods Softw. **25**(2), 299–319 (2010)
24. Le Tam, P., Aghezzaf, E.H., Khatab, A., Le, C.H.: Integrated production and imperfect preventive maintenance planning - an effective MILP-based relax-and-fix/fix-and-optimize method. In: Proceedings of the 6th International Conference on Operations Research and Enterprise Systems, ICORES, vol. 1, pp. 483–490 (2017)
25. Toledo, C.F.M., da Silva Arantes, M., Hossomi, M.Y.B., Frana, P.M., Akartunal, K.: A relax-and-fix with fix-and-optimize heuristic applied to multi-level lot-sizing problems. J. Heuristics **21**(5), 687–717 (2015)
26. Trigeiro, W.W.: A simple heuristic for lot sizing with setup times. Decis. Sci. **20**(2), 294–303 (1989)
27. Wang, H.Z., Pham, H.: Reliability and Optimal Maintenance. Springer, London (2006). https://doi.org/10.1007/b138077
28. Wienstein, L., Chung, C.H.: Integrated maintenance and production decisions in a hierarchical production planning environment. Comput. Oper. Res. **26**, 1059–1074 (1999)
29. Yalaoui, A., Chaabi, K., Yalaoui, F.: Integrated production planning and preventive maintenance in deteriorating production systems. Inf. Sci. **278**, 841–861 (2014)
30. Zhao, S., Wang, L., Zheng, Y.: Integrating production planning and maintenance: an iterative method. Indus. Manag. Data Syst. **114**(2), 162–182 (2014)

Markov Decision Processes Applied to the Payment of Dividends of a Reserve Process

Raúl Montes-de-Oca[1], Patricia Saavedra[1], Gabriel Zacarías-Espinoza[1], and Daniel Cruz-Suárez[2(✉)]

[1] Departamento de Matemáticas, Universidad Autónoma Metropolitana-Iztapalapa, Av. San Rafael Atlixco 186, Col. Vicentina, 09340 Mexico City, Mexico
{momr,psb,gzaces}@xanum.uam.mx

[2] División Académica de Ciencias Básicas, Universidad Juárez Autónoma de Tabasco, Km 1 Carr. Cunduacán-Jalpa, 86690 Cunduacán, Tabasco, Mexico
daniel.cruz@ujat.mx

Abstract. Markov decision theory is applied to study the distribution of dividends of a discrete reserve process with a fixed barrier. The non-payment of dividends is penalized through a cost function which implies solving an optimal control problem. Two objective functions are proposed: a discounted cost and an average one. In both cases, the same optimal strategy for the payment of dividends is obtained, which ensures a ruin probability that guarantees a sustainable reserve operation for claims distributed with light or heavy tails.

Keywords: Reserve processes
Discounted and average Markov Decision Processes · Ruin probability
Optimal premiums · Dividends

1 Introduction

Defining an optimal policy of dividends distribution of a reserve process of an insurance company that benefits the share-holders has been studied since De-Finetti proposed it for the first time in 1957 (see [9]). In this work we are interested in studying this problem through a discrete approach: dividends are distributed in fixed periods of time, for claims with light or heavy tails, when the reserve overpasses a fixed barrier. The payment of dividends is relevant because in the Lundberg-Cramér model, (see [7,22]), if the intensity of the premiums is higher than the average total amount of claims (the security loading is positive), then with probability 1, the paths of the reserve tend to infinity when the time t increases indefinitely. Therefore, dividends appear as a way to control an unlimited increment of the reserves. One possible policy is to determine the dividend strategy that maximizes the expected value of a utility function by means of control techniques. This approach has been studied in discrete time by [3,10,23,24,28,29] where the authors have applied the optimal control

G. H. Parlier et al. (Eds.): ICORES 2017, CCIS 884, pp. 84–104, 2018.
https://doi.org/10.1007/978-3-319-94767-9_5

theory in insurance companies. In particular, [24] introduced the control techniques for the first time by means of the theory of discounted Markov Decision Processes. There is also a wide variety of publications in continuous time, (see [5,11,12,15,16,26,29]).

Several criteria have been proposed to distribute dividends, (see [5,11,15, 23,29]). In this work, given an objective capital (barrier) $Z > 0$, if the reserve exceeds Z, then the dividends are distributed. A model with a fixed barrier reserve of an insurance company is proposed. The distribution of the total amount of claims, by time interval, represents a compound process which is supposed to be general, in the sense that it only requires for its density to be continuous almost everywhere, (see [25]).

The Markov Decision Processes (MDPs) at discrete time are those that are periodically observed under uncertainty, and can be influenced by application of controls [19]. The sequence of controls is called policy, and an optimal policy is obtained through the minimization of a cost function which penalizes the failure to pay dividends. The dynamic programming technique explicitly determines the optimal solution. In addition, a rate for the ruin probability for the reserve process is established when the optimal policy is applied.

In a previous work, see [25], we considered only the discounted cost function. In this work we extend the previous results, to consider the average cost function whose optimal policy results to be the same as in the discounted case, see Theorem 3 in Sect. 6. In order to prove Theorem 3, it was necessary to include a new subsection, see Sect. 2.3, in Sect. 2. We also add in Sect. 5 two new graphs to illustrate the behavior of the reserve process when the claims have light or heavy tails.

The paper is organized as follows: in the second section some main results from MDPs are presented, while in the third section the discrete time reserve process with a fixed barrier is introduced. In the fourth section the optimal premium for the discounted case is obtained. In the following section a rate for the ruin probability is given when the optimal strategy is applied to the reserve, and two illustrative examples are presented. In the sixth section the optimal premium is obtained for the average case. Finally, research conclusions are presented.

2 Markov Decision Processes

This section presents some results on the theory that will be used to solve the problem stated in the paper.

2.1 Preliminaries

Let X and Y be complete Borel spaces (recall that a Borel space is a Borel subset of a separable metric space). A **stochastic kernel** on X given Y is a function $P(\cdot|\cdot)$ such that $P(\cdot|y)$ is a probability measure on X for each fixed $y \in Y$, and

$P(B|\cdot)$ is a measurable function on Y for each fixed $B \in \mathcal{B}(X)$ (here, the Borel σ-algebra of X is denoted by $\mathcal{B}(X)$).

For a topological space Λ, $B(\Lambda)$ stands for the Banach space of real-valued, bounded, (Borel-) measurable functions h on Λ with the supremum norm $\| h \| := sup_x \mid h(x) \mid$. For a finite signed measure μ on Λ, $\| \mu \|$ denotes the **total variation norm**; in particular, if $\mu = Q_1 - Q_2$ is the difference between two probability measures Q_1 and Q_2, then

$$\| Q_1 - Q_2 \| = 2sup_D \mid Q_1(D) - Q_2(D) \mid, \tag{1}$$

where the sup is over all Borel sets $D \in \mathcal{B}(\Lambda)$. Besides, let us recall that for any finite signed measure μ and $h \in B(\Lambda)$,

$$\mid \int h d\mu \mid = \| h \| \| \mu \| . \tag{2}$$

Let W be a Borel space and suppose that W is complete and partially ordered. The partial order in W is denoted by $\prec$. Moreover a function $g : W \to \mathbb{R}$ is considered to be increasing if $x, y \in W$, $x \prec y$, imply that $g(x) \leq g(y)$, where $\leq$ is the usual order in $\mathbb{R}$.

Definition 1. *Let W be a complete Borel space and suppose that W is partially ordered. Let P and P' be probability measures on $(W, \mathcal{B}(W))$. It is said that P' **dominates** P **stochastically** if $\int g dP \leq \int g dP'$ for all $g : W \to \mathbb{R}$ measurable, bounded and increasing, so write $P \overset{st}{\leq} P'$ when this holds.*

Remark 1. Let P and P' be probability measures on $(\mathbb{R}, \mathcal{B}(\mathbb{R}))$. In this case, $P \overset{st}{\leq} P'$ if $F'(x) \leq F(x)$, for all $x \in R$, where F and F' are the distribution functions of P and P', respectively, (see [21] p. 127).

Lemma 1. *Let W be a complete Borel space, and suppose also that W is partially ordered. Let P and P' be probability measures on $(W, \mathcal{B}(W))$, such that, $P \overset{st}{\leq} P'$. Then $\int H_* dP \leq \int H_* dP'$, for $H_* :\to \mathbb{R}$ which is measurable, nonnegative, nondecreasing, and (possibly) unbounded.*

Proof [8] □

Let $(X, A, \{A(x) | x \in X\}, Q, c)$ be a discrete-time Markov control model (see [4] or [19] for notation and terminology). This model consists of the state space X, the control set A, the transition law Q, and the cost-per-stage c. For each $x \in X$, there is a nonempty measurable set $A(x) \subset A$ whose elements are the feasible actions when the state of the system is x. Define $\mathbb{K} := \{(x, a) : x \in X, a \in A(x)\}$.The cost-per-stage c is assumed to be a measurable function on $\mathbb{K}$.

The transition law Q is often induced by an equation of the form

$$x_{n+1} = G(x_n, a_n, \xi_n), \tag{3}$$

$n = 0, 1, \cdots$, with $x_0 \in X$ given, where $\{x_n\}$ and $\{a_n\}$ are the sequences of the states and controls, respectively, and $\{\xi_n\}$ is a sequence of random variables independent and identically distributed (i.i.d.), with values in some space S, common density function Δ, and independent of the initial state x_0; $G : \mathbb{K} \times S \to X$ is a measurable function.

2.2 Infinite-Horizon Discounted-Cost Problems

The control problem of interest in this subsection is the minimization of the infinite-horizon expected total discounted cost. For this, let $(X, A, \{A(x)|x \in X\}, Q, c)$ be a discrete-time Markov control model and consider the following assumption.

Assumption 1. **(a)** *$A(x)$ is compact for all $x \in X$;*
(b) *c is lower semicontinuous and nonnegative;*
(c) *The transition law Q is strongly continuous, that is, the function h', defined on $\mathbb{K}$ by:*

$$h'(x, a) := \int h(y)Q(dy|x, a), \tag{4}$$

is continuous and bounded for every measurable bounded function h on X.

Using the standard notation and definitions in [19], Π denotes the set of all policies and $\mathbb{F}$ is the subset of stationary policies. Each stationary policy $f \in \mathbb{F}$ is identified with the measurable function $f : X \to A$ such that $f(x) \in A(x)$ for every $x \in X$.

Remark 2. Given an initial state $x \in X$ and a stationary policy $f \in \mathbb{F}$, the process determined by (3) is a homogeneous Markov process with transition kernel $Q(\cdot|x, f)$ (see [19] Proposition 2.3.5 p. 19).

Let $(X, A, \{A(x)|x \in X\}, Q, c)$ be a discrete-time Markov Control Model; the **expected total discounted cost** is defined as

$$v_\alpha(\pi, x) := E_x^\pi \left[\sum_{n=0}^{+\infty} \alpha^n c(x_n, a_n) \right], \tag{5}$$

when using the policy $\pi \in \Pi$, given the initial state $x_0 = x \in X$. In this case, $\alpha \in (0, 1)$ is a given discount factor (note that α is fixed), and E_x^π denotes the expectation with respect to the probability measure P_x^π induced by π and x (see [19]).

A policy π^* is said to be **optimal** if

$$v_\alpha(\pi^*, x) = V_\alpha^*(x), \tag{6}$$

for each $x \in X$, where

$$V_\alpha^*(\cdot) := \inf_{\pi \in \Pi} v_\alpha(\pi, \cdot) \tag{7}$$

is the so-called **optimal value function**.

Remark 3. Assumptions 1(a) and (b) imply that c is inf-compact on $\mathbb{F}$, that is, for every $x \in X$ and $r \in \mathbb{R}$, the set

$$A_r(x) := \{a \in A(x) | c(x,a) \leq r\} \tag{8}$$

is compact. Therefore, Assumption 1 implies Assumptions 1(a) and (b) in [19]. Consequently, the validity of the next lemma is guaranteed.

Lemma 2. *Under Assumption 1,*

(a) The optimal value function V_α^* satisfies the optimality equation

$$V_\alpha^*(x) = \min_{a \in A(x)} \left\{ c(x,a) + \alpha \int V_\alpha^*(y) Q(dy|x,a) \right\}, \tag{9}$$

for each $x \in X$.

(b) There exists an optimal stationary policy $f^* \in \mathbb{F}$ such that

$$V_\alpha^*(x) = c(x, f^*(x)) + \alpha \int V_\alpha^*(y) Q(dy|x, f^*(x)), \tag{10}$$

for each $x \in X$.

(c) $V_{\alpha,n}(x) \to V_\alpha^*(x)$ when $n \to \infty$, where $V_{\alpha,n}$ is defined by

$$V_{\alpha,n}(x) = \min_{a \in A(x)} \left\{ c(x,a) + \alpha \int V_{\alpha,n-1}(y) Q(dy|x,a) \right\}, \tag{11}$$

for each $x \in X$, with $V_{\alpha,0}(\cdot) = 0$.

Proof. [19], pp. 46–51. □

2.3 Long-Run Average-Cost Problems

In this subsection a class of infinite horizon control problems in which the objective function depends only on the asymptotic behavior of the process will be taken into account. So, let $(X, A, \{A(X) : x \in X\}, Q, c)$, be a Markov control model as it has been previously described. The **long-run expected average cost (AC)** when using the policy π, given the initial state $x_0 = x$, is

$$J(\pi, x) := \limsup_{k \to \infty} k^{-1} E_x^\pi \left[\sum_{n=0}^{k-1} c(x_n, a_n) \right], \tag{12}$$

and the **AC-problem** is to find a policy π^* such that

$$J(\pi^*, x) = \inf_{\Pi} J(\pi, x) =: J^*(x) \text{ for all } x \in X. \tag{13}$$

A policy π^* that satisfies (13) is said to be **AC-optimal** and $J^*(\cdot)$ is the **AC-value function**.

In order to characterize AC-optimal policies, now the connection between the discounted case and the average case will be presented. This connection is known as the **vanishing discount factor approach** (see [19]) which consider α varying and, in fact, α tending to one. For $\alpha \in (0,1)$, let $V_\alpha^*(\cdot)$ be the corresponding optimal value function defined in (7).

Assumption 2. *There exist a state $y \in X$ and numbers $\overline{\beta} \in (0,1)$ and $\overline{M} \geq 0$ such that*

(a) $(1-\alpha)V_\alpha^*(y) \leq \overline{M}$, *for all* $\alpha \in [\overline{\beta}, 1]$. *Moreover, there is a constant* $\overline{N} > 0$ *and a nonnegative (not necessarily measurable) function* $b(\cdot)$ *such that, with* $h_\alpha(x) := V_\alpha^*(x) - V_\alpha^*(y)$, $x \in X$,

(b) $-\overline{N} \leq h_\alpha(x) \leq b(x)$, *for all* $x \in X$ *and* $\alpha \in [\overline{\beta}, 1)$.

Remark 4. By Remark 3, the validity of the next lemma is guaranteed.

Lemma 3. *Suppose that Assumption 1 holds. Then*

(i) *Under Assumption 2 there exist a constant* $\rho^* \geq 0$, *a measurable function* $\overline{h} : X \to \mathbb{R}$ *with* $-\overline{N} \leq \overline{h}(x) \leq b(x)$, *for all* $x \in X$, *and* $\overline{h}(y) = 0$, *and a selector* $g \in \mathbb{F}$ *such that*

(a)

$$\rho^* + \overline{h}(x) \geq \min_{a \in A(x)} \left[c(x,a) + \int \overline{h}(y) Q(dy|x,a) \right],$$

for all $x \in X$,

(b)

$$\rho^* + \overline{h}(x) \geq c(x, g(x)) + \int \overline{h}(y) Q(dy|x, g(x)),$$

$x \in X$, *and, moreover,*

(c) g *is AC-optimal and* ρ^* *is the AC-value function, i.e.*

$$J^*(x) = J(g,x) = \rho^*, \text{ for all } x \in X, \tag{14}$$

so that $\rho^* = \inf_X J^*(x) = \inf_X \inf_\Pi J(\pi, x)$; *in fact, any selector* $g \in \mathbb{F}$ *that satisfies (b) also satisfies (14).*

(ii) *Conversely, if* $g \in \mathbb{F}$ *is AC-optimal and satisfies (14), then there exists a measurable (possibly extended real-valued) function* $\widehat{h} \geq 0$ *on* X *such that* $(\rho^*, \widehat{h}, g)$ *satisfies (b) and hence (a) as well.*

Proof. [19], pp. 88–91. □

From definition (12) of the AC as a limit of "time averages" it is clear that the AC problems are related to certain ergodic properties of the controlled process, which will appear in the following two assumptions (see [18]).

Assumption 3. *There exists a state $y \in X$ and a positive α_0 such that*

$$Q(\{y\}|x,a) \geq \alpha_0,$$

for all $(x,a) \in \mathbb{K}$.

Assumption 4. *There exists a number $\lambda_0 \in (0,1)$ such that*

$$\sup_{k,k'} \|Q(\cdot|k) - Q(\cdot|k')\| \leq 2\lambda_0, \tag{15}$$

where the sup *is over all k, $k' \in \mathbb{K}$.*

Lemma 4. *Assumption 3 implies Assumption 4.*

Proof. [18], pp. 56–59. □

For $f \in \mathbb{F}$, the **n-step transient probability** $Q^n(\cdot|x,f(x))$, $x \in X$, is given recursively by

$$Q^n(D|x,f(x)) = \int Q^{n-1}(D|y,f(y))Q(dy|x,f(x)), \tag{16}$$

for all $D \in \mathcal{B}(X)$ and $n \geq 1$, where $Q^0(\cdot|x,f(x)) := p_x(\cdot)$ is the probability measure concentrated at the point $x \in X$.

Lemma 5. *Suppose that Assumptions 1 and 3 hold. Moreover, assume that the cost function $c \in B(\mathbb{K})$.*

Then,

$$|V_\alpha^*(x) - V_\alpha^*(y)| \leq \frac{2\|c\|}{1-\lambda_0}, \tag{17}$$

for all $x \in X$, where λ_0 is the constant in Assumption 4 (recall that by Lemma 4, Assumption 4 also holds) and y is a fixed state.

Proof. Firstly, under Assumption 3, by [14], for all $x,z \in X$, $f \in \mathbb{F}$ and $n \geq 1$,

$$\|Q^n(\cdot|x,f(x)) - Q^n(\cdot|z,f(z))\| \leq 2^{-n+1} \sup_{x,z} \|Q(\cdot|x,f(x)) - Q(\cdot|z,f(z))\|^n \tag{18}$$

holds (see also (16)). Hence, from (2), Assumption 4, (18), and considering the optimal policy for the discounted case f^*, it results that, for all $x \in X$,

$$
\begin{aligned}
|V_\alpha^*(x) - V_\alpha^*(y)| &\leq \sum_{n=0}^{+\infty} \alpha^n \left| \int c(z, f^*(z)) \left[Q^n(dz|x, f^*(x)) - Q^n(dz|y, f^*(y)) \right] \right| \\
&\leq \|c\| \sum_{n=0}^{+\infty} 2^{-n+1} (2\lambda_0)^n \alpha^n \\
&= 2\|c\| \sum_{n=0}^{+\infty} (\lambda_0 \alpha)^n \\
&= \frac{2\|c\|}{1 - \lambda_0 \alpha} \\
&\leq \frac{2\|c\|}{1 - \lambda_0}.
\end{aligned}
$$

This is the end of the proof of Lemma 5. □

3 Reserve Process

The process $\{R_t\}_{t \geq 0}$ is called **Reserve Process**. R_t represents the reserve of the company at time t and is given by

$$R_t = R_0 + P_t - S_t, \tag{19}$$

where $R_0 = u > 0$ is the initial reserve of the company, P_t are the premiums earned and S_t the total amount of claims until time t.

Definition 2. *The ruin probability $\psi(u)$, with initial reserve $u > 0$, is defined by*

$$\psi(u) := Pr[\tau(u) < +\infty] \tag{20}$$

where $\tau(u) := inf\{t > 0 | R_t < 0\}$ with $\tau(u) = +\infty$ if $R_t > 0$ for all $t \geq 0$.

As in the classical model of Lundberg and Cramér, the premiums are determined continuously and deterministically, i.e., $P_t = Ct$ where $C > 0$ and $t \geq 0$. In addition, the total amount of claims S_t may depend on two process: a homogeneous Poisson process $\{N(t)\}_{t \geq 0}$, with intensity $\lambda > 0$, and a claims amounts process $\{Y_i : i = 1, 2, \cdots\}$, where Y_i are independent and identically distributed random variables. Thus, the total amount of claims until time t is given by

$$S_t = \sum_{i=1}^{N(t)} Y_i, \tag{21}$$

where $S_t = 0$ if $t = 0$.

Thus, the reserve process is described by

$$R_t = u + Ct - S_t.$$

Choosing $C > \lambda E[Y_1]$, known as the safety loading condition, it is concluded that the average reserves of the company grow indefinitely. In other words, the reserve R_t tends to infinity when t does so with probability $1 - \psi(u)$. Different methods have been proposed to determine the premium value for the safety loading condition to hold (see [11,29]). In this work the expectation principle will be used.

In order to avoid the accumulation of earnings, we propose to establish an upper limit (barrier) Z for the reserve, when $R_t > Z$, the surplus $R_t - Z$ is paid as dividends, (see [5,9,11,12,29]). Dividends can be understood as payments made by a company to its shareholders, either in cash or in shares. Formally, the cash dividends, d_t, are defined as $d_t = [R_t - Z]^+$, where $[z]^+ = \max\{0, z\}$.

Remark 5. It is important to mention that in a more general setting, some of the assumptions may be relaxed, e.g., $\{N(t)\}$ could be a non-homogeneous Poisson process or a more general renewal process. Hence it is possible to assume that the claim size cumulative distribution function is of a particular parametric form, eg., gamma, Weibull, etc. (see Assumption 5 and Examples 5.1 and 5.2, below).

3.1 Discrete-Time Reserve Process

Now, a discrete-time reserve model will be developed assuming that the insurance company defines its operational policy at fixed points of time (see [3,10,20,29]).

Let $\{R_t\}$ be a reserve process with initial reserve $R_0 = u > 0$, and $\{t_n\}$ be an increasing sequence of positive real numbers with $t_0 = 0$. Then, (19) implies that

$$R_{t_{n+1}} - R_{t_n} = (P_{t_{n+1}} - P_{t_n}) - (S_{t_{n+1}} - S_{t_n}), \tag{22}$$

for $n = 0, 1, \cdots$, where $(P_{t_{n+1}} - P_{t_n})$ and $(S_{t_{n+1}} - S_{t_n})$ are the premiums earned and the total amount of claims during the period $(t_n, t_{n+1}]$, respectively.

Let $x_{t_n} := R_{t_n}$, $a_{t_n} := (P_{t_{n+1}} - P_{t_n})$ and $\xi_{t_n} := (S_{t_{n+1}} - S_{t_n})$. Then, without loss of generality, it is possible to assume that $t_n = n$ for $n > 0$. Then, the discrete-time reserve model is as follows:

$$x_{n+1} = x_n + a_n - \xi_n, \tag{23}$$

with $x_0 = u > 0$.

In this case, x_{n+1} represents the reserve at time $t = n + 1$. Moreover, the discrete-time ruin probability is determined by

$$\psi_d(u) := Pr[\tau_d(u) < +\infty] \tag{24}$$

where $\tau_d(u) := \inf\{n \geq 1 | x_n \leq 0\}$ with $\tau_d(u) = +\infty$ if $x_n > 0$ for all $n > 0$.

According to the ruin probability defined above, the ruin of the company is attained when $x_n + a_n - \xi_n \leq 0$ for some $n > 0$.

If the following dynamics is considered:

$$x_{n+1} = [x_n + a_n - \xi_n]^+, \tag{25}$$

for $n = 1, 2, \cdots$, with $x_0 = u > 0$, then the ruin is attained when $x_n = 0$ for some $n = 1, 2, \cdots$. However, just as in the continuous case model, if the safety loading condition holds, $E[x_n] \to +\infty$ when $n \to +\infty$.

The dynamics described in (25) is known as the Lindley random walk (see [2]) which has various applications, for example, in storage processes, waiting time model, queue size models, to name a few [2].

We will extend our model to incorporate the fixed barrier Z which defines the payments of dividends (see [5,9,11,23]). Let Z be a fixed barrier such that, if at time t_n, $x_n > Z$, the surplus $x_n - Z$ is used to pay dividends. This is described by the following dynamics:

$$x_{n+1} = \min\{[x_n + a_n - \xi_n]^+, Z\} \tag{26}$$

with $x_0 = u > 0$. In this case, x_n, a_n and ξ_n denotes respectively: reserve, premium and the total amount of claims of the company at the beginning of the period $(n, n+1]$.

The dynamics given in (26) has been used to describe storage processes with finite capacity such as: dams, inventory, waiting time model and queue sizes, to name a few (see [13,17]).

Assumption 5. *Suppose that $\{\xi_n\}$ is a sequence of i.i.d. random variables with values on $[0, \infty)$, and a common distribution F whose density Δ is continuous almost everywhere (a.e.), with $E[\xi] < +\infty$ (ξ is a generic element of the sequence $\{\xi_n\}$).*

Remark 6. In the rest of this paper Assumption 5 will not be mentioned in each result, but it is supposed to hold.

Using the expectation principle for premiums calculation, it is ensured that the safety loading condition for the process described in (26) holds. Define

$$K := (1 + \epsilon)E[\xi] \tag{27}$$

and

$$M := (1 + \beta)E[\xi], \tag{28}$$

where $0 < \varepsilon < \beta$. Then, by [11,29] $K < M$, therefore, the admissible premiums set is the compact subset $[K, M]$. (Note that for all premium $a \in A(x) = [K, M]$, the safety loading condition is satisfied, and β is fixed in order to be competitive in the insurance market).

Every time that the reserve is below the barrier Z, the non-payments of dividends is penalized. Therefore, the following cost function is proposed:

$$c(x, a) := [Z - x]^+, \tag{29}$$

for each $x \in [0, +\infty)$ and $a \in [K, M]$.

Remark 7. This model defines an MDP: take $X = [0, +\infty)$ as the state space (it is important to note that the state space may also be a compact set of the form $X = [0, \Theta]$ for some $\Theta \geq Z$) ; $A = [K, M]$ as the action space; $A(x) = [K, M]$ as admissible actions for each $x \in X$; the transition law Q is induced by the function $G(x, a, s) := \min\{[x + a - s]^+, Z\}$ for each $(x, a) \in \mathbb{K}$ and $s \in [0, +\infty)$ (see (3)). Finally, the cost function is defined in (29).

According to Remark 7, there is a problem (an OCP) to determine the sequence of premiums $\pi = \{a_n\}$ which optimizes

$$\nu_\alpha(\pi, x) := E_x^\pi \left[\sum_{n=0}^{+\infty} \alpha^n [Z - x_n]^+ \right], \tag{30}$$

where $x \geq 0$ is the initial reserve, and α is a given discount factor.

4 Discounted Optimal Premiums

In this section the research results are presented using discounted MDPs theory. (Note that α is considered to be fixed).

By the definition of the cost function in (29) it is concluded that it is non-negative and continuous. Moreover, for each $x \in X$, $A(x) = [K, M]$ is a compact set. So, now it is only necessary to show Assumption 1(c) which is presented in the following lemma.

Lemma 6. *The transition law Q, induced by (26), is strongly continuous.*

Proof. Let $h : X \to \mathbb{R}$ be a measurable function bounded by the constant γ. Using the Variable Change Theorem ([1] p. 52), it follows that

$$\int h(y)Q(dy|x, a) = \int_0^\infty h(min\{[x + a - s]^+, Z\})\Delta(s)ds, \tag{31}$$

$(x, a) \in K$.

Furthermore,

$$\int_0^\infty h(min\{[x + a - s]^+, Z\})\Delta(s)ds = \quad h(0)(1 - F(x + a))$$

$$+ h(Z)F(x + a - Z) + \textstyle\int_{x+a-Z}^{x+a} h(x + a - s)\Delta(s)ds,$$

$(x, a) \in \mathbb{K}$, where F is the common distribution function of ξ.

Since density Δ is a continuous function a.e. (see Assumption 5), F is also continuous (see [1], p. 175).

Given the above, it suffices to prove that

$$\int_{x+a-Z}^{x+a} h(x + a - s)\Delta(s)ds \tag{32}$$

is a continuous function on $(x, a) \in \mathbb{K}$.

For this purpose, let $\{(x_k, a_k)\}$ be a sequence in $\mathbb{K}$ converging to $(x, a) \in \mathbb{K}$. By the Variable Change Theorem ([1] p. 52),

$$\int_{x+a-Z}^{x+a} h(x+a-s)\Delta(s)ds = \int_0^Z h(y)\Delta(x+a-y)dy. \tag{33}$$

Consider the following functions defined by

$$h_k(y) := h(y)\Delta(x_k + a_k - y)I_{[0,Z]}(y), \tag{34}$$
$$g_k(y) := \gamma\Delta(x_k + a_k - y)I_{[0,Z]}(y), \tag{35}$$

for $k = 1, 2, \cdots$, $y \in [0, +\infty)$, where $I_B(\cdot)$ denotes the indicator function on the set B.

Note that $|h_k| \leq g_k$ for all $k \geq 1$. Furthermore, $\{g_k\}$ converges a.e. to the function g which is defined by

$$g(y) := \gamma\Delta(x + a - y)I_{[0,Z]}(y), \tag{36}$$

$y \in [0, +\infty)$.

Furthermore,

$$\begin{aligned}\int g_k(y)dy &= \gamma \int_0^Z \Delta(x_k + a_k - y)dy, \\ &= \gamma Pr[x_k + a_k - Z \leq \xi \leq x_k + a_k], \\ &= \gamma(F(x_k + a_k) - F(x_k + a_k - Z)),\end{aligned}$$

and, as the distribution F is continuous, then

$$\lim_{k\to\infty} \int g_k(y)dy = \int g(y)dy. \tag{37}$$

Finally, by the Dominated Convergence Theorem ([27] p. 92)

$$\begin{aligned}\lim_{k\to\infty} \int_{x_k+a_k-Z}^{x_k+a_k} h(x_k + a_k - s)\Delta(s)ds &= \lim_{k\to\infty} \int h_k(y)dy \\ &= \int \lim_{k\to\infty} h_k(y)dy \\ &= \int_0^Z h(y)\Delta(x + a - y)dy \\ &= \int_{x+a-Z}^{x+a} h(x + a - s)\Delta(s)ds\end{aligned}$$

and therefore the result holds. □

Remark 8. By Lemma 6, Assumption 1 holds, and therefore Lemma 2 guarantees the existence of the optimal policy, $f^* \in \mathbb{F}$, which, in the context of the reserve process, describes the sequence of optimum premiums that minimizes the performance index given in (30) for the model established in Remark 7.

Lemma 7. *(a) The transition law Q, induced by (26), is stochastically ordered, i.e.,*

$$Q(\cdot|x,a) \overset{st}{\leq} Q(\cdot|w,b) \tag{38}$$

for each (x,a), $(w,b) \in \mathbb{K}$ with $x \leq w$ and $a \leq b$.

(b) The optimal value function $V_\alpha^*(\cdot)$, and the value iteration functions $V_{\alpha,n}(\cdot)$, defined in (11), are decreasing on X.

Proof. (a) Let $(x,a),(w,b) \in \mathbb{K}$ with $x \leq w$ and $a \leq b$. Observe that

$$[x+a-s]^+ \leq [w+b-s]^+, \tag{39}$$

$s \in [0,+\infty)$.

On the other hand, if $\min\{[w+b-s]^+, Z\} = Z$, then $\min\{[x+a-s]^+, Z\} \leq \min\{[w+b-s]^+, Z\}$, and if $\min\{[w+b-s]^+, Z\} = [w+b-s]^+$, by (39) $\min\{[x+a-s]^+, Z\} \leq \min\{[w+b-s]^+, Z\}$. Therefore

$$\min\{[x+a-s]^+, Z\} \leq \min\{[w+b-s]^+, Z\}, \tag{40}$$

$s \in [0,+\infty)$. Thus, by (40) if $\min\{[w+b-\xi]^+, Z\} \leq \varsigma$, then $\min\{[x+a-\xi]^+, Z\} \leq \varsigma$, and therefore

$$Q(\min\{[w+b-\xi]^+, Z\} \leq \varsigma|w,b) \leq Q(\min\{[x+a-\xi]^+, Z\} \leq \varsigma|x,a). \tag{41}$$

Finally, by Remark 1, the result holds.

(b) First it will be shown that V_n is decreasing on X. The proof is made by mathematical induction.

Let $x, w \in X$ with $x \leq w$. By definition of $V_{\alpha,n}$, for $n = 1$,

$$V_{\alpha,1}(x) = \min_{a \in A(x)} \left\{[Z-x]^+\right\}; \tag{42}$$

this implies that $V_{\alpha,1}(x) = [Z-x]^+$, therefore $V_{\alpha,1}$ is decreasing on X. Now, for $n = 2$,

$$\begin{aligned}
V_{\alpha,2}(x) &= \min_{a \in A(x)} \left\{ c(x,a) + \alpha \int V_{\alpha,1}(\min\{[x+a-s]^+, Z\}) \Delta(s) ds \right\} \\
&= \min_{a \in A(x)} \left\{ c(x,a) + \alpha \int [Z - \min\{[x+a-s]^+, Z\}]^+ \Delta(s) ds \right\} \\
&= \min_{a \in A(x)} \left\{ c(x,a) + \alpha \int (Z - \min\{[x+a-s]^+, Z\}) \Delta(s) ds \right\} \\
&= \min_{a \in A(x)} \left\{ [Z-x]^+ + \alpha Z - \alpha \int \min\{[x+a-s]^+, Z\} \Delta(s) ds \right\} \\
&= \min_{a \in A(x)} \left\{ [Z-x]^+ + \alpha Z - \alpha \int y Q(dy|x,a) \right\}.
\end{aligned}$$

Hence, by part (a) of this lemma and using Lemma 1 with $H_*(y) = y$, $y \in X$, the function g_*, defined by

$$g_*(a) := -\alpha \int yQ(dy|x,a), \tag{43}$$

$a \in [K, M]$ is decreasing, and so its minimum is M. This implies that

$$V_{\alpha,2}(x) = [Z - x]^+ + \alpha Z - \alpha \int yQ(dy|x, M). \tag{44}$$

Since $x \leq w$ and after some calculations, it is obtained that $V_2(w) \leq V_2(x)$. As x and w are arbitrary, then V_2 is a decreasing function on X. Suppose that V_n is decreasing on X for some $n > 2$. Again, take $x, w \in X$ with $x \leq w$. Then

$$\begin{aligned} V_{\alpha,n+1}(x) &= \min_{a \in A(x)} \left\{ c(x,a) + \alpha \int V_{\alpha,n}(\min\{[x + a - s]^+, Z\}) \Delta(s) ds \right\} \\ &= \min_{a \in A(x)} \left\{ [Z - x]^+ + \alpha \int V_{\alpha,n}(y) Q(dy|x,a) \right\}. \end{aligned} \tag{45}$$

Let $a \in [K, M]$. By induction hypothesis and by the stochastic order of Q, it yields that

$$[Z - w]^+ + \alpha \int V_{\alpha,n}(y) Q(dy|w,a) \leq [Z - x]^+ + \alpha \int V_{\alpha,n}(y) Q(dy|x,a), \tag{46}$$

then taking minimum on $a \in [K, M]$ on both sides of the inequality, it is obtained that $V_{\alpha,n+1}(w) \leq V_{\alpha,n+1}(x)$. Therefore, $V_{\alpha,n+1}$ is decreasing. By Lemma 2(c), $V_{\alpha,n}(x) \to V_\alpha^*(x)$, $x \in X$, which implies that V_α^* is a decreasing function on X.

□

Theorem 1. *The optimal policy for the reserve process with dividends, induced by (26), is $f^*(\cdot) \equiv M$.*

Proof. Let $x \in X$ be fixed. By Lemma 2, V_α^* satisfies the optimality equation (9), that is,

$$V_\alpha^*(x) = \min_{a \in A(x)} \left\{ [Z - x]^+ + \alpha \int V_\alpha^*(y) Q(dy|x,a) \right\}. \tag{47}$$

Also, by Lemma 7, V_α^* is decreasing and Q is stochastically ordered. Then, if $a, b \in [K, M]$, with $a \leq b$, it is obtained that

$$\alpha \int V_\alpha^*(y) Q(dy|x,b) \leq \alpha \int V_\alpha^*(y) Q(dy|x,a). \tag{48}$$

Adding $[Z - x]^+$ on both sides of the inequality above, it is concluded that, for $a \in [K, M]$,

$$H(a) := [Z - x]^+ + \alpha \int V_\alpha^*(y) Q(dy|x,a) \tag{49}$$

is a decreasing function and its minimum is reached in M. Since x is arbitrary, the result follows. □

Finally, in this section, by Theorem 1 it is obtained that the optimal value function is of the form

$$V_\alpha^*(x) = \nu_\alpha(M, x) = E_x^M \left[\sum_{n=0}^{+\infty} \alpha^n [Z - x_n]^+ \right], \tag{50}$$

for each $x \in X$. That is, the expected total discounted cost of the penalties for not reaching the barrier Z, and therefore not paying the dividends to shareholders is brought to present value, given the discount factor α.

5 Sustainability of the Optimal Reserve Process

This section presents a rate for ruin probability which permits to determine a period of sustainability for the company under the optimum reserve process, that is, the process under the optimal policy (premium) $f^*(\cdot) \equiv M$,

$$x_{n+1}^M = \min\{[x_n^M + M - \xi_n]^+, Z\}, \tag{51}$$

with $x_0^M = u > 0$.

To this end,

$$\psi_d^N(u) := Pr[x_0^M = u, x_1^M \neq 0, \cdots, x_{N-1}^M \neq 0, x_N^M = 0] \tag{52}$$

is defined for $u > 0$ and $N > 2$.

Observe that $\psi_d^N(u)$ is the ruin probability when $\tau_d(u) = N$, where τ_d is the stopping time for the state zero (see (24)).

Theorem 2. *Let $\{x_n^M\}$ be the optimal reserve process generated for the optimal policy $f^* \equiv M$, with $x_0^M = u > 0$ and $N > 2$. Then*

$$\psi_d^N(u) \leq (Pr[\xi < Z + M])^{N-2} \cdot Pr[\xi < u + M]. \tag{53}$$

Proof. The optimal process $\{x_n^M\}$ is a homogeneous Markov process with transition law Q (see Remark 2).

Consider the following sets: $B_0 = \{x_0^M = u\}$, $B_N = \{x_N^M = 0\}$ and $B_i = \{x_i^M \neq 0\}$, for $i = 1, 2, \cdots, N-1$, and observe that $B_i \in \mathcal{B}(X)$ for $i = 1, 2, \cdots, N$.

Then, by Proposition 7.3 p. 130 in [6],

$$\begin{aligned}\psi_d^N(u) &= Pr[x_0^M = u, x_1^M \neq 0, \cdots, x_{N-1}^M \neq 0, x_N^M = 0] \\ &= \int_{B_{N-1}} \cdots \int_{B_0} Q(B_N | w_{N-1}, M) Q(dw_{N-1} | w_{N-2}, M) \cdots Q(dw_1 | w_0, M) \rho(dw_0),\end{aligned}$$

where the initial distribution ρ is the Dirac measure concentrated on u.

On the other hand, observe that

$$Q(B_N|w_{N-1}, M) \leq 1. \tag{54}$$

Therefore

$$\psi_d^N(u) \leq \int_{B_{N-1}} \cdots \int_{B_0} Q(dw_{N-1}|w_{N-2}, M) \cdots Q(dw_1|w_0, M)\rho(dw_0). \tag{55}$$

furthermore, for each $i = 1, 2, \cdots, N-1$, $B_i \subseteq \{\xi_{i-1} < x_{i-1}^M + M\} \subseteq \{\xi < Z + M\}$; this implies that

$$Q(B_i|w_{i-1}, M) \leq Pr[\xi_{i-1} < x_{i-1}^M + M] \leq Pr[\xi < Z + M]. \tag{56}$$

So

$$\psi_d^N(u) \leq \int_{B_{N-2}} \cdots \int_{B_0} Pr[\xi < Z + M]Q(dw_{N-2}|w_{N-3}, M) \cdots Q(dw_1|w_0, M)\rho(dw_0). \tag{57}$$

Finally, iterating this way $N-3$ times and since ρ is concentrated in B_0, it is obtained that

$$\psi_d^N(u) \leq (Pr[\xi < Z + M])^{N-2} Q(B_1|u, M), \tag{58}$$

where $Q(B_1|u, M) = Q(x_1^M \neq 0|u, M) = Pr[\xi < u + M]$. □

The examples that follow illustrate the application of Theorem 2. To do this, the ruin probability $\psi_d^N(u) = 0.001$ and $\nu := 1 - \psi_d^N(u)$. $N = 1$ day and the period of sustainability is given in years (360 days). Z is chosen in such a way that $Pr[\xi < Z + M] = \nu$.

Table 1. Gamma distribution.

u	$\kappa = 1$	Years	$\kappa = 3$	Years
1	Z = 5	19.04	Z = 5.22	19.10
2	M = 2	19.13	M = 6	19.14
3		19.17		19.16
4		19.18		19.17

5.1 Example 1

Suppose that ξ has a Gamma distribution with parameters (λ, κ) whose density is of the form

$$\Delta(s) = \frac{\lambda}{\Gamma(\kappa)}(\frac{s}{\lambda})^{\kappa-1} e^{-(s/\lambda)}, s > 0, \tag{59}$$

where $\Gamma(k) = \int_0^{+\infty} s^{k-1}e^{-s}ds$ is the Gamma function.

It is known that the Gamma distribution is not analytically integrable, so it is necessary to resort to tables for this distribution given in [30] Appendix B Table B.2.

In this case, the optimal premium is

$$M = (1+\beta)\kappa\lambda, \tag{60}$$

where β is the loading factor.

Given $\lambda = \beta = 1$, and different values of u, Z, and M, their respective period of sustainability (in years) are calculated for $\kappa = 1, 3$. These values are shown in Table 1. In Fig. 1 a possible realization of the reserve is shown when the reserve is ruined at the eight year.

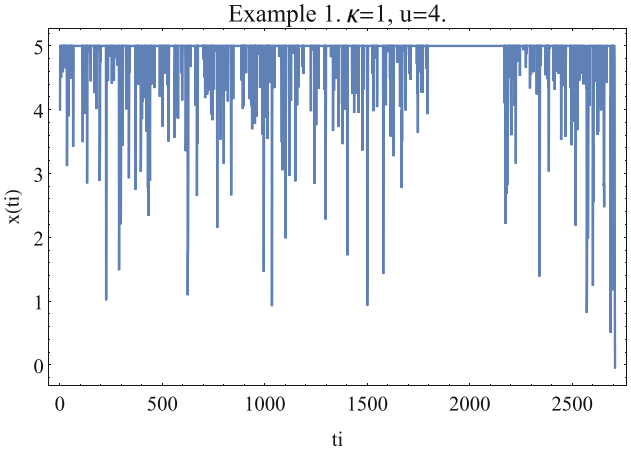

Fig. 1. A possible realization of the reserve process of example 1 in the case of $\kappa = 1$.

5.2 Example 2

Suppose that ξ has a Weibull distribution with parameters (λ, κ). It is known that the distribution function is as follows:

$$F(s) = 1 - e^{-(s/\lambda)^{\kappa}}, s > 0. \tag{61}$$

Since $F(M+Z) = \nu$, it follows that

$$Z = \lambda(ln(1-\nu)^{-1})^{1/\kappa} - M. \tag{62}$$

In this case, the optimal premium is

$$M = (1+\beta)\lambda\Gamma(1+\frac{1}{\kappa}), \tag{63}$$

where β is the loading factor.

Table 2. Weibull distribution.

u	$\kappa = 0.8$	Years	$\kappa = 0.6$	Years
1	Z = 8.94	18.96	Z = 22.06	18.88
2	M = 2.26	19.06	M = 2.99	18.97
3		19.11		19.03
4		19.14		19.06

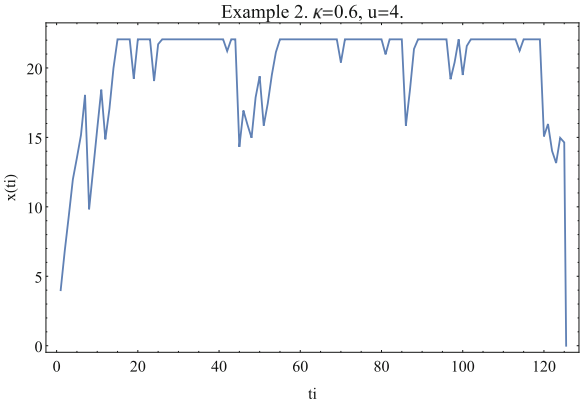

Fig. 2. A possible realization of the reserve process of example 2 in the case of $\kappa = .6$.

Given $\lambda = \beta = 1$, and different values of u, Z, and M, their respective period of sustainability are calculated for $\kappa = 0.8, 0.6$. These values are shown in Table 2. In Fig. 2 a possible realization of the reserve, for the case $\kappa = 0.6$ is shown when the reserve is ruined before the end of the first year.

6 Average Optimality of $f^*(\cdot) = M$

Remark 9. Take into account the MDP described in Remark 7 with the difference that in this section the state space is the compact set $X = [0, \Theta]$, with $\Theta \geq Z$.

Assumption 6. $P[\xi \geq \Theta + M] := \alpha_0 > 0$ *(recall that ξ is a generic element of the sequence $\{\xi_t\}$).*

Remark 10. The corresponding $\xi's$ proposed in Examples 5.1 and 5.2 of previous section trivially satisfy Assumption 6. This assumption can be verified in some inventory-production systems and in some control of water reservoirs problems [31].

Theorem 3. *Consider the MDP described in Remark 9. Suppose that Assumption 6 holds. Then $f^*(x) = M$, $x \in X$ is AC-optimal.*

Proof. Firstly, note that in Lemma 6 it has been proved that Assumption 1 holds. Secondly, observe that from Assumption 6 and the fact that, for all $x \in X$ and $a \in [K, M]$, $[\xi \geq \Theta + M] \subseteq [\xi \geq x + a]$, it follows that

$$\begin{aligned} Q(\{0\}|x, a) &= P[x_{t+1} = 0|x_t = x, a_t = a] \\ &= P[\xi \geq x + a] \\ &\geqslant P[\xi \geqslant \Theta + M] = \alpha_0 \ > 0. \end{aligned}$$

Hence, Assumption 3 holds, and from Lemma 4, Assumption 4 holds as well.

Thirdly, from Lemma 5, taking $y = 0$, it results that

$$| V_\alpha^*(x) - V_\alpha^*(0)| \leq \frac{2Z}{1 - \lambda_0}, \tag{64}$$

for all $x \in X$ and $\alpha \in (0, 1)$ (it is easy to verify that Z is a bound of c).

Now, fix $\overline{\beta} \in (0, 1)$. With this $\overline{\beta}$ and from the boundedness of the cost function c and (64), it follows that Assumption 2 holds. Consequently, from Lemma 3, there exists $g \in \mathbb{F}$ which is AC-optimal for the MDP described in Remark 9. Besides, this optimal policy g satisfies (a) and (b) in Lemma 3 for

$$\overline{h}(x) = lim_{n\to\infty}(V_{\alpha_n}^*(x) - V_{\alpha_n}^*(0)), \tag{65}$$

$x \in X$ and for certain sequence $\{\alpha_n\} \uparrow 1$ (see the proof of Theorem 5.4.3 in [19]). Hence, as $V_{\alpha_n}^*(\cdot)$ is decreasing, for each $n = 1, 2, ...$ (see Lemma 7), it results $\overline{h}(\cdot)$ is decreasing as well. Therefore, it is easy to see, from Lemmas 3 and 7, that

$$\min_{a\in A(x)} \left\{ c(x, a) + \int \overline{h}(y) Q(dy|x, a) \right\} = \min_{a\in A(x)} \left\{ [Z - x]^+ + \int \overline{h}(y) Q(dy|x, a) \right\}, \tag{66}$$

$x \in X$, is attained for $g(x) = M$, $x \in X$, that is, $g(x) = f^*(x) = M$, $x \in X$ is AC-optimal. This finalizes the proof of Theorem 3. □

7 Conclusions

We study the behavior of a reserve with a fixed barrier when it is modelled as a Markov Decision Process. The dynamics presented in (26) describes the reserve when it is below the barrier. This allows us to set a penalty to take into account non-payments of dividends. Two objective functions are proposed: a discounted cost and an average one. In both cases, by controlling the process generated by premiums, it is found that the optimal policy is M.

Given a ruin probability and an initial value of the reserve, the rate presented in Theorem 2 permits to determine the periods of sustainability of the company when optimal policy is applied. This bound depends on the distribution of the total amount of claims per time interval which are only assumed to have a density that is continuous almost everywhere, with finite first and second moments. This condition is satisfied by a wide range of distributions. Two examples illustrate how to apply the rate in the case of distributions with light or heavy tails, and how to choose the fixed barrier.

Acknowledgements. R. Montes-de-Oca, P. Saavedra, and D. Cruz-Suárez dedicate this article to the memory of their co-worker and co-author of the present work, Gabriel Zacarías-Espinoza, whose sensible death occured on November, 10, 2015.

This work was partially supported by CONACYT (México) and ASCR (Czech Republic) under Grant No. 171396.

References

1. Ash, R.B., Doléans-Dade, C.A.: Probability and Measure Theory. Elsevier, London (2000)
2. Asmussen, S.: Ruin Probability. World Scientific, Singapore (2010)
3. Bulinskaya, Y.G., Muromskaya, A.: Discrete-time insurance model with capital injections and reinsurance. Methodol. Comput. Appl. Probab. **17**, 899–914 (2014)
4. Bäuerle, N., Rieder, U.: Markov Decision Processes with Applications to Finance. Springer, Berlin (2011)
5. Azcue, P., Muler, N.: Stochastic Optimization in Insurance a Dynamic Programming Approach. Springer, London (2014)
6. Breiman, L.: Probability. SIAM, Berkeley (1992)
7. Cramér, H.: On the Mathematical Theory of Risk. Skandia Jubillee, Stockholm (1930)
8. Cruz-Suárez, D., Montes-de-Oca, R., Salem-Silva, F.: Conditions for the uniqueness of optimal policies of discounted Markov decision processes. Math. Methods Oper. Res. **60**, 415–436 (2004)
9. De-Finetti, B.: Su un'impostaziones alternativa della teoria collectiva del rischio. Trans. XV. Int. Congr. Act. **2**, 433–443 (1957)
10. Diasparra, M.A., Romera, R.: Bounds for the ruin probability of a discrete-time risk process. J. Appl. Probab. **46**, 99–112 (2009)
11. Dickson, D.C.M.: Insurance Risk and Ruin. Cambridge University Press, Cambridge (2005)
12. Dickson, D.C.M., Waters, H.R.: Some optimal dividend problems. ASTIN Bull. **34**, 49–74 (2004)
13. Finch, P.D.: Deterministic costumer impatience in the queueing system GI/M/1. Biometrika **47**, 45–52 (1960)
14. Georgin, J.P.: Contrôle des chaînes de Markov sur des espaces arbitraires. Ann. Inst. H. Poincaré **14**, Sect. B, 255–277 (1978)
15. Gerber, H.U.: On the probability of ruin in the presence of a linear dividend barrier. Scand. Actuarial J. **1981**(2), 105–115 (1981). https://doi.org/10.1080/03461238.1981.10413735
16. Gerber, H.U., Shiu, E.S.W., Smith, N.: Maximizing dividends without bankruptcy. ASTIN Bull. **36**, 5–23 (2006)
17. Ghosal, A.: Some Aspects on Queueing and Storage System. Springer, New York (1970). https://doi.org/10.1007/978-3-642-88208-1
18. Hernández-Lerma, O.: Adaptive Markov Control Processes. Springer, New York (1989). https://doi.org/10.1007/978-1-4419-8714-3
19. Hernández-Lerma, O., Lasserre, J.B.: Discrete-time Markov Control Processes: Basic Optimality Criteria. Springer, New York (1996). https://doi.org/10.1007/978-1-4612-0729-0
20. Li, S., Lu, Y., Garrido, J.A.: A review of discrete-time risk models. Rev. R. Acad. Cien. Ser. A Mat. **103**(2), 321–337 (2009)

21. Lindvall, T.: Lectures on the Coupling Method. Wiley, New York (1992)
22. Lundberg, F.: Über die theorie der ruckversicherung. Trans. VIth Int. Congr. Act. **1**, 877–948 (1909)
23. Martínez-Morales, M.: Adaptive Premium in an Insurance Risk Process. Doctoral thesis, Texas Tech University, Texas (1991)
24. Martin-Löf, A.: Lectures on the use of control theory in insurance. Scand. Actuarial J. **1994**, 1–25 (1994)
25. Montes-de-Oca, R., Saavedra, P., Zacarías-Espinoza, Cruz-Suárez, D.: Optimal policies for payment of dividends through a fixed barrier at discrete time. In: Proceedings of the 6th International Conference on Operations Research and Enterprise Systems (ICORES 2017), pp. 140–149 (2017). https://doi.org/10.5220/0006193701400149
26. Rolski, T., Schmidli, H., Schmidt, V., Teugels, J.L.: Stochastic Processes for Insurance and Finance. Wiley, Chichester (1999)
27. Royden, H.L.: Real Analysis. Macmillan, New York (1988)
28. Schäl, M.: On discrete-time dynamic programming in insurance: exponential utility and minimizing the ruin probability. Scand. Actuarial J. **2004**, 189–210 (2004)
29. Schmidli, H.: Stochastic Control in Insurance. Springer, London (2009)
30. Wilks, D.S.: Statistical Methods in the Atmospheric Sciences. Academic Press, Burlington (2011)
31. Yushkevich, A.A.: Blackwell optimality in Borelian continuous-in-action Markov decision processes. SIAM J. Control Optim. **35**, 2157–2182 (1997)

Impact of Collaborative External Truck Scheduling on Yard Efficiency in Container Terminals

Ahmed Azab[1(✉)], Ahmed Karam[2], and Amr Eltawil[1]

[1] Department of Industrial Engineering and Systems Management, Egypt-Japan University of Science and Technology, PO Box 179, New Borg El Arab 21934, Alexandria, Egypt
Ahmed.azab@ejust.edu.eg
[2] Mechanical Engineering Department, Faculty of Engineering at Shoubra, Benha University, Cairo, Egypt

Abstract. In Container Terminals, managing the external truck arrivals is one of the essential managerial activities that, typically, the terminal operators conduct continuously on the short term using a Truck Appointment System (TAS). However, the trucking companies are influenced by the developed appointments and schedules which affect their operations and resources. This paper introduces a collaborative TAS to enable the trucking companies and container terminals to share making the decisions on scheduling the external truck appointments. This paper proposes a Dynamic Collaborative Truck Appointment System (DCTAS) which adopts a simulation optimization approach which integrates a discrete event simulation model with a mixed integer programming model. The DCTAS considers some realistic parameters that enhance the development of reliable appointments that fit the dynamic and stochastic circumstances of container terminals environment. The performance of the developed DCTAS is investigated by solving a numerical instance. The results show that both the container terminals and trucking companies can gain benefits from using the DCTAS. Yard efficiency performance indicators such as the maximum queue lengths, average waiting times, maximum waiting times and average truck turn times are improved using the developed appointment system.

Keywords: Collaborative scheduling · Dynamic · Container terminals
Simulation optimization · Truck appointment system

1 Introduction

Container Terminals (CTs) are essential nodes in the global supply chain. The tremendous growth of the containerized cargo trade around the world is resulting in increased congestion in many container terminals. This, in turn, leads to more dissatisfaction implications for many stakeholders in the maritime supply chain such as the trucking companies and shipping companies. The negative consequences of congestion inside the CTs make the external transportation modes like trucks, trains and vessels to

G. H. Parlier et al. (Eds.): ICORES 2017, CCIS 884, pp. 105–128, 2018.
https://doi.org/10.1007/978-3-319-94767-9_6

spend more time to be served. On the contrary, stakeholders need to deliver and receive their containers to/from the CTs in a flexible way with low costs and short time. As a result, container terminals confront considerable challenges to achieve higher levels of satisfaction for their stakeholders with maintaining their productivity as high as possible. Therefore, recent literatures are paying increasing interest to reduce congestion in CTs.

Typically, CTs comprises three main areas: the seaside, yard area, and land-side (see Fig. 1). The seaside is the area where the vessels are berthed, loaded and/or unloaded with the desired containers using quay cranes. Containers are transported by internal transport means like trucks or Automated Guided Vehicles (AGVs) to be temporarily stored in the yard blocks through the quay-yard transport area. At the yard, handling operations are performed using yard equipment like yard cranes and straddle carriers. The operations in each yard block depend on the vessels' operations and hinterland operations. On the other side of the terminal, the landside comprises the terminal gates. The gates are equipped with X-Ray scanners where import containers are allowed to leave the terminal, and export containers are allowed to enter the yard area. Transport areas between the main CT areas are used to link these areas together.

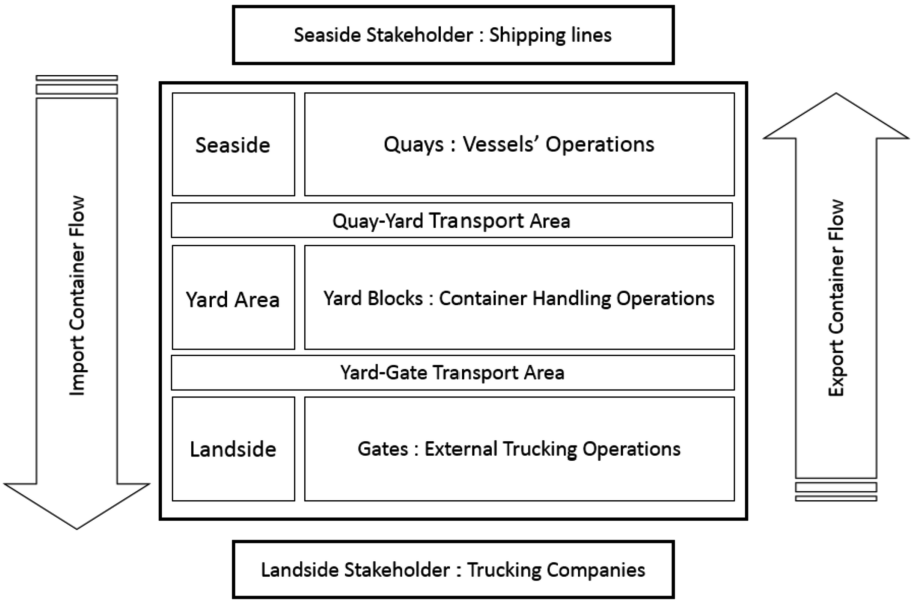

Fig. 1. Container terminal areas and corresponding operations

Container terminal problems are classified according to the decision level into operational, tactical and strategic decision problems [1]. The operational problems are related to the scheduling of operations and assignment of the resources. These kinds of problems are solved simultaneously in the short term with updating solutions and schedules daily. For instance, berth allocation and quay crane assignment are

considered the main operational decisions at the seaside [2, 3]. Also, at the yard area, container handling problems and scheduling the stacking and reshuffling of container affect the yard efficiency [4, 5]. In this paper, more discussion about landside operational problems will be introduced focusing on managing the arrival of external trucks to CTs.

Generally, at the operational level, export/import containers are delivered/picked up from the terminal by external transport means such as trucks and trains. The trucks are operated by trucking companies. The essential target of these companies is to perform the delivery/pick-up operations in minimum time and cost. On the other hand, terminal operators adopt the suitable rules and approaches to develop schedules which achieve the performance metrics of the terminal such as minimum truck turn time or shortest queue lengths at the gates or in the yard. In most of terminals around the world, the trucking operations have the dominant part of CT's external services rather than the rail operations due to the high flexibility of the trucking operations. To organize the transaction between CTs and the trucking companies, some CTs implement a Truck Appointment System (TAS) to manage external truck arrivals, while other terminals do not follow an appointment system. The appointment systems can be used to increase the service quality in CTs for all transshipment means; trucks, train, barges and vessels [6]. Many terminals have adopted TASs to make a balance in truck arrivals in order to alleviate the terminal rush hours. This paper introduces a dynamic and collaborative appointment management solution to support the collaborative decision making between the CTs and trucking companies to schedule the arrivals of external trucks.

The remaining of the paper is organized as follows. The literature review is introduced in Sect. 2. Section 3 explains the proposed appointment management system. In Sect. 4, numerical experiments are presented. Finally, results and conclusions are introduced in Sects. 5 and 6 respectively.

2 Literature Review

Using truck appointment systems in managing external truck arrivals received a wide interest in the literature. The developed models and approaches for appointment systems addressed various objectives that can be summarized as follows:

- Increasing the CT efficiency.
- Reducing truck turn time.
- Reducing the terminal congestion.
- Reducing environmental emissions.
- Reducing transportation costs.

This section reviews existing literature with a special focus on the used methodology and important results. At the end of this section, the use of the collaboration decision making in managing the external truck arrivals in container terminals is addressed.

2.1 Increasing CT Efficiency

In container terminals, the main objectives of the terminal managers are to increase the operational efficiency and service quality which directly impact the terminal competitiveness. Consequently, improving the operations provides more opportunities for the terminals to receive higher demand and gain more shipping lines and trucking companies to serve. In this context, many researchers studied the use of truck appointment management systems to increase the efficiency inside the CTs. [7] studied the impact of using the arrival information of external trucks on the yard operations. They concluded that prior knowledge about the arrival time of external trucks reduces the queue lengths at gates and re-handling frequency at the yard. Based on a previous work, [8] used a Discrete Event Simulation (DES) model to investigate the effect of truck announcement system on the yard operations performance. Significant reduction in yard crane moves is obtained using the proposed algorithms.

To study the yard crane performance, [9] used a hybrid approach of simulation and queuing models to examine the impact of the TAS on the performance of yard crane operations. The results showed a significant improvement in system performance and efficiency after using the TAS. A mixed integer programming model is formulated by [6] to find the optimum number of appointments to offer with regard to the overall workload and the available handling capacity of the terminal. Results are validated using the DES to ensure the improvements of service quality for both the trucks and also for all terminal resources.

2.2 Reducing Truck Turn Time

The terminal customers in the maritime supply chain are represented mainly in the trucking and shipping companies. Providing a faster service for these two important stakeholders leads to higher satisfaction. Trucking companies are in need to be served with high service rates in order to maximize the utilization of their resources (trucks and drivers). One way to achieve this, is to reduce the total time that an external truck spends within the terminal or what is called the Truck Turnaround Time (TTT).

To reduce the TTT, [10, 11] investigated limiting the arrivals and individual appointments versus using block appointments via a combined DES and mathematical models. TAS is one of the most viable strategies to avoid the terminal congestion, improve the system efficiency, and reduce the truck turn time [12]. To achieve that, authors formulated a nonlinear optimization model and applied a multi-server queuing model.

A stationary time-dependent queueing model providing a supporting tool to improve demand management at CTs is introduced by [13]. A convex nonlinear programming model is developed to obtain the optimum arrival pattern that minimizes the turnaround time of the external trucks and reduces the discomfort of shifting the arrivals. The effect various external truck arrival patterns on truck turn times in CTs is studied [14]. Based on a simulation study, results showed that arrival patterns affect significantly the terminal performance. Moreover, understanding the arrival patterns impacts on terminal operations contributes to establishing a robust and reliable truck appointment system.

2.3 Reducing CT Congestion

Due to the increase of the global containerized cargo trade, many CTs confront the problem of high demand that their capacity cannot afford. This typical situation results in high congestion levels at the terminal gates, yard blocks, and quay side. One of the earliest case studies was conducted by [15] at Hong Kong International Terminal (HIT) to investigate and solve the congestion problems using a truck appointment system. Authors developed a decision support system based on an information system to help in making the terminal operational decisions efficiently. A comprehensive study by [16] was developed to review the appointment system implemented in terminals across North America. They adopted various strategies to reduce the idling of trucks, congestion at gates and emissions related to CT drayage operations. To achieve a steady arrival of external trucks at container terminals, [17] developed an agent-based simulation model. The results showed that the congestion at CTs can be minimized by using gate congestion information and estimating the truck idling times. A comprehensive study investigate the congestions and related emissions is conducted by [18]. The authors a used a dynamic traffic simulation model to investigate the emissions with congestion levels. They concluded that extending the gate working hours increases the terminal productivity and reduces the emissions, especially at peak hours.

To reduce the heavy truck congestions in CTs, [19] developed an optimization approach for truck appointments. A method based on Genetic Algorithms (GA) and Point Wise Stationary Fluid Flow Approximation (PSFFA) was designed to solve the problem resulting in reducing truck turn times. Concepts such as the chassis exchange were introduced by [20] to reduce the CT congestion using simulation as a calculation tool. The main goal of the chassis exchange concept is to reduce the extra YC handling needs by putting containers on a chassis and applying a chassis pool. They concluded that the proposed method required more land space but the congestion and related greenhouse emissions were reduced. To control the external truck arrival based on truck-vessel service relationship, some strategies are developed by [21] to reduce the terminal congestion. The authors developed a comparison study for the proposed strategies, and the results showed that the quality planning coordination between the landside and seaside operations in very essential.

2.4 Reducing Environmental Emissions

The global warming problem motivated many researchers to study how to reduce greenhouse gases from service and industry sectors. In container terminals, environmental emissions result from the unutilized resources that consume fuel or are operated by electric power coming from power stations. In this concern, reducing environmental emissions in container terminals received considerable interests. a bi-objective function is developed by [22] to reduce the truck turn time and the resulted emissions. The authors developed a genetic algorithm to solve this optimization problem. The results showed that shifting the arrivals of external trucks reduced the emissions, particularly at terminal gates. Form a collaborative management perspective, [23] developed a collaborative TAS to reduce the emissions related to the empty trips to and from the terminal by coordinating the appointments among truck drivers. To assess the

coordinated appointments generated from the appointment matching procedure, a DES model was developed and the port-related truck emissions were reported. Results illustrated that, although there was a significant reduction in truck emissions, sometimes terminal experienced higher congestion. [24] proposed some response strategies that help in solving the problem of truck arrivals' deviation from its appointments. Results showed that the greenness of operations is significantly affected by the use of truck appointments.

2.5 Reducing Transportation Costs

From an economical perspective, reducing transportation costs is essential for trucking companies and terminal authorities. To reduce the transportation costs, [25] used a planning strategy for pickup and delivery operations in CTs based on an integer programming heuristic. The sequence of the drayage operations is determined by minimizing the transportation cost. An improvement in productivity and capacity utilization is obtained with some sensitivity to poor selection of the appointment time. [26] Studied the export container's drayage operations in Chinese CT. They proposed an integer programming model to reduce the transportation cost through time window management. They indicated that the peak arrivals are smoothed by solving the problem using a genetic algorithm (GA).

2.6 Collaborative Management in Container Terminals

There is an increasing attention paid to the TAS in literature. However, only two studies for [27, 28] investigated the TAS considering the collaboration among trucking companies and the container terminal. In these two papers, an iterative approach is used to model the collaboration among trucking companies and the terminal operator. The iterative approach consists of two levels which are interconnected by a feedback loop. The first level is a mathematical model which includes a sub-problem for each trucking company to minimize the total waiting cost of trucks at the yard. On the other hand, the second level is a procedure to estimate the expected times the trucks spend at the yard based on the solution of first level. This iterative approach enables the collaboration process.

In this paper, some-real world aspects are considered to improve the collaborative appointments approaches found in the literature. The first aspect is reducing the solution number of iterations by developing a straightforward scheduling approach instead of the existing iterative approaches. From a practical point of view, the large number of iterations may cause some of the trucking companies not to submit their appointment applications for some reasons such as not having time to reschedule their truck operation or forgetting to resubmit their applications. In this case, the quality of the solution may be impaired. The second aspect is that the developed approach considers the randomness of the terminal operation which is not considered in existing collaborative systems. The third aspect is a dynamic scheduling procedure that adopted in the proposed appointment system. In reality, CTs can receive arrivals at any time during the day, which makes it is important to use an appointment system that

considers the dynamic change in the arrival demand to the terminal and enables trucking companies to book for the delivery or pick-up tasks flexibly.

To consider the previously mentioned aspects in one appointment systems, we propose a TAS that considers dynamic, collaborative and stochastic nature of the realistic truck scheduling problem requirements. The proposed approach integrates a discrete event simulation (DES) model with mixed integer programming model. This paper contributes to the literature by developing a Dynamic Collaborative Truck Appointment System (DCTAS) through introducing the mentioned aspects with a comprehensive numerical analysis.

3 The Dynamic Collaborative Truck Appointment System (DCTAS)

The Proposed Dynamic Collaborative Truck Appointment System (DCTAS) is developed based on a collaboration decision making concept where the stakeholders cooperate in scheduling the appointments considering a degree of convenience. In this section, an integrated simulation optimization approach is introduced considering two main aspects in appointment scheduling problems: the dynamic and stochastic nature of the problem [29]. Figure 2 illustrates the operational steps of using the proposed DCTAS. The proposed simulation optimization approach integrates the MIP model with the DES model in a pre-processing way [31] in which the problem under particular circumstances is solved to produce the input data for the other problem. The DES model provide the input to the MIP model. After solving the MIP model, the optimum truck appointment schedules are evaluated using the simulation model to get the turn time of trucks after optimization.

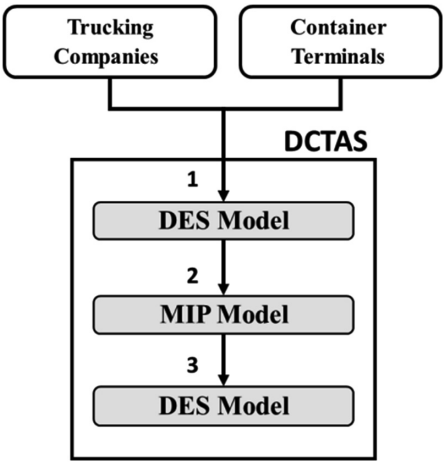

Fig. 2. The operational steps of the DCTAS.

The DCTAS operational steps are as follows:

1. Both trucking companies and CTs submit their scheduling parameters and requirements to the appointment system using an information system for example. The trucking companies send their preferred arrival schedules and CTs submit the terminal workload and needed scheduling parameters. These parameters will be the inputs to the first DCTAS stage which is the simulation model. The DES model is used as the first stage to determine the average truck turn time for each trucking company considering the terminal workload and the randomness of the terminal operations.
   DES Model Inputs:
   From trucking company: the preferable number of trucks per each Time Window (TW).
   From container terminal inputs: container location – yard carne serve rate/handling speed- gate service rat- vessels operations - yard and gate operations.
2. The second stage inside the DCTAS is to use the MIP model to solve a scheduling problem to minimize the congestion cost that is calculated based on the average truck turn time that results from the simulation. In this step, the MIP solution is considered the optimum schedules that reduce both congestion of the CT and inconvenience of the trucking companies.
   MIP Model Inputs:
   From simulation results: the average truck turn time per each time interval for each trucking company.
   From trucking companies: preferable/proposed arrival schedules - available number on trucks that a trucking company have per each time window.
   From container terminal: container location.
3. Finally, the developed appointments are evaluated and the performance measures are calculated for the DES model for the newly developed schedules.
   DES Model Inputs:
   From MIP model: optimum appointments (number of trucks to be dispatched to the terminal per each time window for each trucking company).

The DCTAS Outputs are optimum appointments and key performance indicators such as the truck turn time, waiting time, and queue lengths.As illustrated, the DCTAS provides an interactive management strategy between the stakeholders to cope with the dynamic nature of the appointment process in CTs. Interacting communication among stakeholders can be implemented easily using an online collaboration platform. The online collaboration platform is designed and synthesized using a design thinking strategy [30]. Whenever a trucking company is ready to submit its preferable arrival times, the system receives the requests and deals with the workload updates and changes on an hourly basis. Moreover, using the DES model is expected to enhance the solution and to accommodate the system's actual variability and randomness. This randomness results from the stochastic operations and events such as the gate service rate, inter-terminal traveling times, yard crane handling rates, quay crane handling rate, and the failure of equipment.

3.1 The Discrete Event Simulation (DES) Model

"Flexsim CT®" package was used to develop the DES model. "Flexsim CT®" is a special simulation package for simulating CT operations. The developed DES model includes the following objects: four gates processors, five yard blocks, five yard cranes, and a single shared gate queue (see Fig. 3). When the external truck arrives at the gate according to the predetermined schedule (Tables 2 and 3), in case of busy gate server, the truck joins the gate queue then leaves to the first gate that becomes available. At the gate, the arriving truck will be served according to an Erlang distribution (0.65, 4) [12]. After that, the served trucks are routed to the destination where the container is to be dropped or picked up from a yard block. At the yard area, one yard crane is used at each yard block to move the container to/from the external truck and restack it to the appropriate block position. After finishing the pickup/drop off process, the external truck is directed to the terminal gate exit which is represented by a gate sink in the developed DES model. At the seaside, the arriving vessel receives export containers form the yard or delivers import containers to the yard. A group of four external trucks (truck gang) are used to transport containers between the vessel and yard blocks. A quay crane is assigned to the arriving vessel to load/unload containers. At the yard block, a higher priority is given to internal truck operations rather than the external trucking operations to reduce the vessel turnaround time.

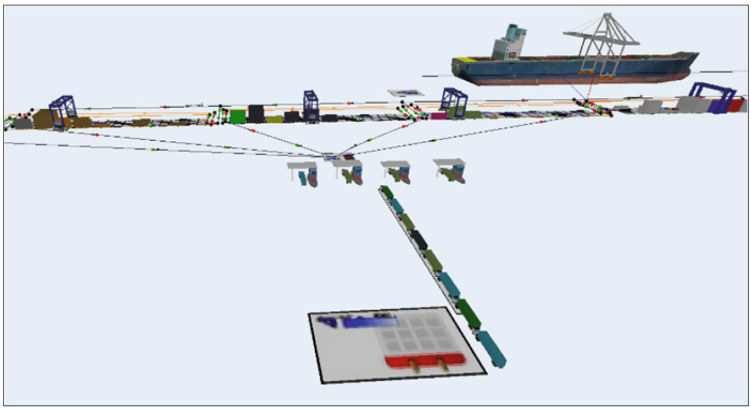

a. FleXsim discrete event simulation model of the study terminal

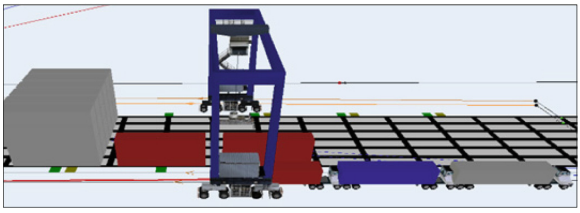

b. The yard area

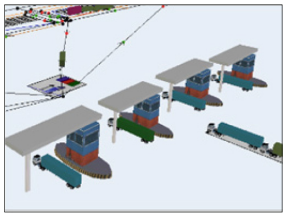

c. The gate severs

Fig. 3. Container terminal discrete event simulation model.

There are some assumptions that were considered in developing this simulation model. For the landside, it is assumed that all arriving trucks will share the same queue before going to the first available gate. Moreover, the distance that an external truck travels inside the terminal is neglected. As a result, the truck turn time will be calculated as the sum of the following times: waiting time at the gate queue, service time at the gate processor, waiting time at the yard block, and finally service time at the yard block. To obtain more accurate results, each time window is divided into four time intervals which means that each time interval is equal to 15 min, and the average truck turn time is calculated per each time interval to be used in the MIP model. Another assumption is that the collision of trucks traveling through the internal transportation network of the terminal is not considered.

This scheduling problem is regarded as a design problem for a new collaborative appointment system. Therefore, the input parameters are driven from a case study existing in literature and some parameters are based on some practical experience. Table 1 illustrates the input parameters to the DES model.

Table 1. The DES model input parameters [29].

General parameters	
Working hours (Tws)	8:00 am–12 pm
Truck speed (max)	300 m/min (18 km/h)
Container dwell time	Exponential (0.3) [days]
Gate parameters	
Process time (min)	Erlang (0.65, 4)
Gate capacity	1 truck/one gate
Yard parameters	
Crane speed (max)	90 m/min (empty/loaded)
Block capacity (max)	24 containers
Crane net moves	27.7 move/h (average)
Quayside parameters	
Crane speed (max)	120 m/min (empty/loaded)
Crane net moves	12.3 move/h (average)

3.2 The Proposed Mathematical Model

In most container Terminals, the arrival of external trucks from the hinterland is a random process that is affected by the preferable arrival times of trucking companies. These preferable arrival times are not known by the terminal operators to be considered in planning and scheduling operations. As a result, a truck may arrive during a congestion time where the waiting time is costly and the emissions are high. On the other hand, if these trucks are forced to come at certain times that are specified by the terminal operators, it may be inconvenient for some trucking companies due to the trucks availability and other operations outside the terminal. To tackle this problem, the following mathematical model considers both, the convenience of trucking companies to arrive at their preferable times and the total time spent in the terminal which is influenced by the terminal congestion.

Based on the mathematical models formulated by [27], the model is modified to consider the truck turn time of trucks which is produced by the DES model. The proposed DCTAS assumes that each trucking company develops its preferable schedule considering the available number of trucks at each time window. The trucking company's operator defines all tasks to be performed, which represent a pick up or a delivery operation for one container using one truck. Tasks that are assigned in the same preferable arrival hour (time window) are grouped together in one task group. For a certain task group, containers can be delivered or picked up from the same yard block or from several yard blocks (Table 2). The used parameters and indices in MIP model are defined as follows:

Indices

i index for a task group.
j index for a yard block.
k index for a trucking company.
τ index of a time window.
t Index of a time interval. Note that multiple time intervals exist in a time window.

Table 2. Validating the DCTAS vs DDM [29].

DDM model					DCTAS			
Task group	Yard block	Time window	$Xij\tau$	Truck co.	Task group	Yard block	Time window	$Xij\tau$
1	1	2	5	TC1	1	1	1	3
							3	1
							4	1
2	2	2	1	TC2	2	2	2	1
	2	3	1			2	3	1
	2	4	2			2	4	2
3	1	2	1	TC3	3	1	3	2
	1	4	3			1	4	2
	3	3	2			3	4	2
4	4	2	3	TC4	4	4	3	3
5	2	4	3	TC1	5	2	4	3
6	3	1	4	TC2	6	3	1	4
7	2	1	2	TC3	7	2	1	2
	4	1	3			4	1	3
8	3	3	1	TC4	8	3	4	1
	5	3	2			5	2	4
	5	4	3			5	4	1
9	1	4	1	TC1	9	1	3	1
	2	3	2			2	3	2
10	4	4	3	TC2	10	4	4	3
Objective function value = $ 116					Objective function value = $ 180			

b_i^l earliest possible (lower) bound of the time window for task group *i.*
b_i^u latest possible (upper) bound of the time window for task group *i.*
d_i number of tasks to be done for task group *i.*
$S_{k\tau}$ number of available trucks of company k during time window τ.
p_i most preferable time window at which containers of task group *i* to be stored or retrieved.
σ number of time intervals per each time window.
a_{ij} maximum number of containers of task i that can be allocated to yard block *j.*
w_i^+ cost of late arrival by a unit time compared with the preferable time window of task *i.*
w_i^- cost of early arrival by a unit time compared with the preferable time window of task *i.*
w_k truck waiting cost in the terminal of truck company *k* per time interval.
P Congestion penalty in $, a strategic parameter determined by the terminal manager.
TT_{jt} average truck turn time for a truck arriving at yard block *j* at time interval *t* derived variables from the DES model.

Sets

I set of task groups
K set of trucking companies
T set of time intervals
J set of yard blocks *j*
W set of time windows.

Decision Variables

$X_{ij\tau}$ number of trucks for task group *i* which are deployed to yard block *j* at time window τ.

Derived Variables From the MIP Model

λ_{ijt} average arrival rate of trucks for task group *i* at yard block *j* at time interval *t.*

The objective function is to Minimize:

$$\sum_{i\in I}\sum_{j\in J}\left[w_i^+\sum_{\tau\in W}X_{ij\tau}(\tau-p_i)^+ + w_i^-\sum_{\tau\in W}X_{ij\tau}(p_i-\tau)^+ + \sum_{t\in T}(w_k+p)TT_{jt}\lambda i_{jt}\right] \tag{1}$$

Subjected to:

$$\sum_{j\in J}\sum_{\tau\in W}X_{ij\tau}\geq d_i \quad \forall i\in \mathrm{I} \tag{2}$$

$$\sum_{i\in I}\sum_{j\in J} X_{ij\tau} \le S_{k\tau} \quad \forall k \in \mathrm{K},\ \tau \in \mathrm{W} \tag{3}$$

$$\sum_{\tau\in W} X_{ij\tau} \le a_{ij} \quad \forall i \in \mathrm{I},\ j \in \mathrm{J} \tag{4}$$

$$b_i^l \sum_j X_{ij\tau} \le \tau \sum_j X_{ij\tau} \le b_i^u \sum_j X_{ij\tau} \quad \forall i \in \mathrm{I},\ \tau \in \mathrm{W} \tag{5}$$

$$\lambda_{ijt} = \frac{X_{ij\tau}}{\sigma} \quad \forall i \in \mathrm{I},\ j \in \mathrm{J},\ \tau \in \mathrm{W} \tag{6}$$

$$\lambda_{ijt} \ge 0,\ X_{ij\tau}\ integer \quad \forall i \in \mathrm{I},\ j \in \mathrm{J},\ \tau \in \mathrm{W},\ t \in T \tag{7}$$

The objective function (1) is to minimize the cost of shifting (delaying or advancing) the appointment and the truck turn time (TT_{jt}) cost within the terminal. The total number of scheduled trucks must satisfy the number of containers to be delivered or picked up (2). Constraint (3) states that the number of trucks to be assigned to task i cannot be larger than the resource level of the trucking company. The capacity constraint of each yard block is described in (4) to ensure that the number of containers for each task group have to be smaller than or equal to the available spaces in yard blocks. There is an earliest and latest feasible time window for each container (5). To calculate the arrival rate for each task group, constraint (6) is used. Constraint (7) illustrates the domain of each variable in the problem.

3.3 Model Validation

To validate the proposed DCTAS, the system is used to solve an instance from literature solved by M. Phan and K. Kim (2015). In their work, they developed a Decentralized Decision Making (DDM) model to provide a negotiation process for scheduling the external trucks' appointments between CTs and Trucking companies. The same input parameters are used and fitted to the developed simulation optimization approach in this paper. After solving the given instance, the results show that 70% of the resulted schedules are identical, while 30% are not the same. In other words, the optimum appointments resulting from the DCTAS for seven task groups out of ten are the same result of the DDM model as illustrated in [27]. The 7 task groups are equal in the number of tasks and the size of each task. For the remaining three task groups (1, 8, 3), two of them have the same number of tasks but different in the task sizes. This experiment illustrates the validity of the proposed system in this paper.

4 Numerical Experiments

In this section, a numerical example is solved to illustrate the operational scenario and performance of the proposed DCTAS. Table 3 shows a proposed appointment application for 4 trucking companies. Each trucking company is assumed to have a specific number of containers (d_i) in the terminal. The task group is a set of tasks that will be submitted by the same trucking company at the same preferred arrival time (p_i). It is

also assumed that each trucking company knows which yard block (j) holds its containers. To create a workload in the terminal, the externally confirmed applications and inter-terminal tasks are developed in order to investigate the response of the proposed system to the heavy-loaded time windows. The proposed system (DCTAS) is expected to shift the proposed arrival appointments to the time windows where the cost of truck turn time will be minimized with consideration of the preferred arrival times. Table 4 illustrates the tasks that are assumed to be already reserved and confirmed.

Table 3. Proposed appointment applications for four trucking companies [29].

Truck. company	Task group	*di*	*pi*	*j*
TC1	1	5	2	1
	2	3	4	2
	3	1	3	1
		2		2
TC2	4	3	4	4
	5	4	3	2
	6	4	1	3
TC3	7	4	2	1
		2		3
	8	2	1	2
		3		4
TC4	9	3	2	4
	10	1	3	3
		5		5

Table 4. The reserved tasks in the CT [29].

Confirmed tasks	*Di*	*TW*	*j*
11	30	2	1
12	30	3	2
13	30	2	3
14	30	2	4
15	30	3	5
16	10 (to ship)	3–4	1

To start working with the DCTAS, all tasks are input to the simulation model. Each task has a corresponding arrival time, the number of containers, and yard block location. By running the DES model, the external trucks arrive to the terminal model according to the predetermined scheduled times and released out of the system as the task is completed. The average truck turn times at each yard block are recorded for each time window to be used in the MIP model input. Other performance measures can be derived from the simulation model such as the queue length at gates, waiting times at gates and yard, service rate at gates and yard, cranes' utilization, etc.

To get statistically reliable results, the simulation model is run for 35 replications which are used to determine the 95% confidence intervals of the targeted mean performance measures. After obtaining the results from the simulation model, the derived variables are sent to the MIP model. The MIP model is solved using a personal computer with Intel® Core i7 CPU and 4 GB RAM. IBM Ilog CPLEX Optimization Studio version 12.2 is used to code the MIP model and get the optimum solution. The cost parameters in the objective function are assumed to be \$1, \$4, \$5, and \$2 per each time for $wi+$, $wi-$, wk, and P respectively. Table 5 shows the available number of trucks ($sk\tau$) for each trucking company per each time window. In Constraint 3, the number of available trucks is used to guarantee that the new assigned tasks do not exceed the trucking company's available trucks per each time window.

Table 5. The available number ($S_{k\tau}$) of trucks for each trucking company per each time widow [29].

Truck. company	*TW*1	*TW*2	*TW*3	*TW*4
TC1	3	5	6	4
TC2	7	4	1	5
TC3	6	1	2	4
TC4	3	4	3	4

5 Results

After solving the MIP model, the optimum schedules obtained from the MIP model are shown in Table 6. For Example, trucking company 1 prefers to send 11 (di) trucks in tree task groups of 5, 3, and 3 trucks per time windows 2,4, and 3 respectively (see Table 3). After using the DCTAS, the 11 trucks are rescheduled ($Xijt$) i.e. the first task group of 5 trucks is scheduled as 2 trucks in *TW*1 and 3 truck in *TW*4. By carefully investigating the solutions of the proposed approach, there are three possibilities noticed from the results to occur. In the first possibility, there will be no change in the schedule such as task group 8. The second possibility, the task group preferred time window will be advanced or delayed resulting in an advancing and/or delaying cost without any change in the number of containers per task. For example, the arrival time of task group 5 is shifted from *TW*3 to *TW*2. This seems reasonable because, at yard block 2, the workload in *TW*3 was the highest among the other three time windows in the same block before the solution. For the third possibility, the system will decompose the task group into smaller mini-task groups. It is evident that the second and third possibility may occur together like in task groups 1, 2, 7, and 10.

To investigate the solution performance, the simulation model is used to test the performance of the resulting schedule from the MIP model and compare it with simulation results before solving the MIP model. In other words, it is needed to see how the proposed schedule differs from the optimum schedule after applying the DCTAS. Some performance measures of yard operations are studied such as truck turn time, external truck queue length, waiting time, and yard crane utilization. To investigate the

Table 6. The DCTAS solution [29].

Truck. company	Obj. value ($)	Task group	Task group size *(di)*	Scheduled trucks *(Xijt)*	Time widow *(τ)*	Yard block *(j)*
TC1	137.8	1	5	2	1	1
				3	4	
		2	3	1	1	2
				2	2	
		3	1	1	4	1
			2	2	2	2
TC2	114.7	4	3	3	4	4
		5	4	4	2	2
		6	4	4	1	3
TC3	101.75	7	4	4	4	1
			2	1	2	3
				1	3	
		8	2	2	1	2
			3	3	1	4
TC4	130.31	9	3	3	4	4
		10	1	1	4	3
			5	4	2	5
				1	3	

significance of difference for the performance measure before and after using the DCTAS, t-tests are conducted with a 95% confidence interval using Minitab 17 statistical software to test the 35 samples (replications).

5.1 The Impact of Using DCTAS on Truck Turn Time

The truck turn time is used in many container terminals to measure the productivity of the terminal [32]. Short truck turn times mean that the terminal can serve the external trucks faster. Therefore a larger number of trucks can be served, and more containers can be delivered with less dwell time at the yard blocks. In this experiment, the average truck turn times at each block j per each time window τ ($TTj\tau$) are recorded for the proposed (preferred) appointments and the optimum appointments. Figures 4, 5, 6, 7 and 8 show a comparison between the $TTj\tau$ values for the proposed (preferred) appointments by the trucking companies versus the optimum appointments after applying the DCTAS. Results show that there is a difference between the $TTj\tau$ values before and after applying the proposed appointment management system. The statistical results show that there is a significant difference between the average $TTj\tau$ values before and after solution for most points such as *TW*3 at *YB*1, *TW*4 at *YB*2, *TW*4 at *YB*3, *TW*3 at *YB*4, and *TW*4 at *YB*. While, some points did not show significant differences in average $TTj\tau$ such as *TW*1 at *YB*2, *TW*2 at *YB*3, *TW*2 at *YB*4, *TW*4 at *YB*4.

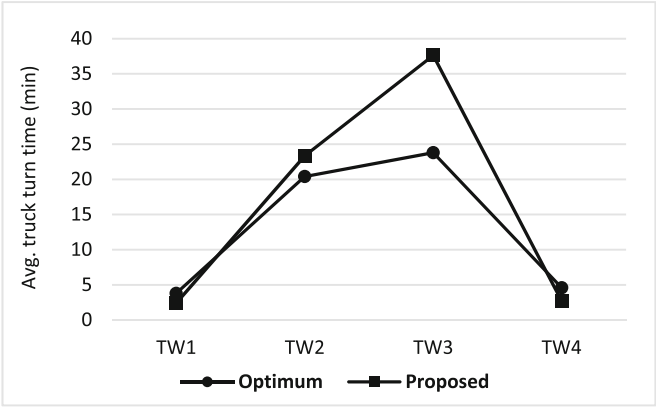

Fig. 4. Average truck turn time at yard block 1 ($TT_{1\tau}$) [29].

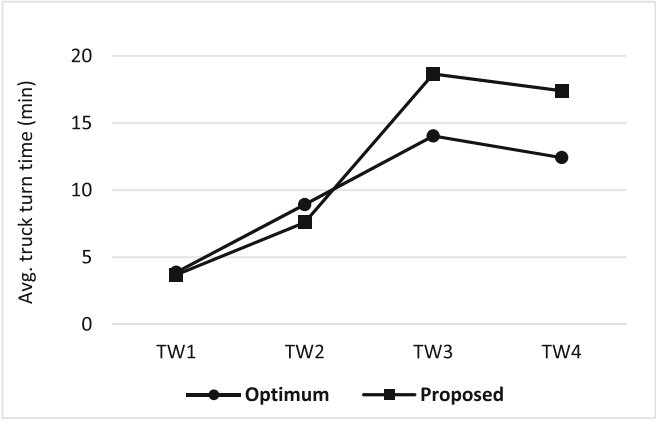

Fig. 5. Average truck turn time at yard block 2 ($TT_{2\tau}$) [29].

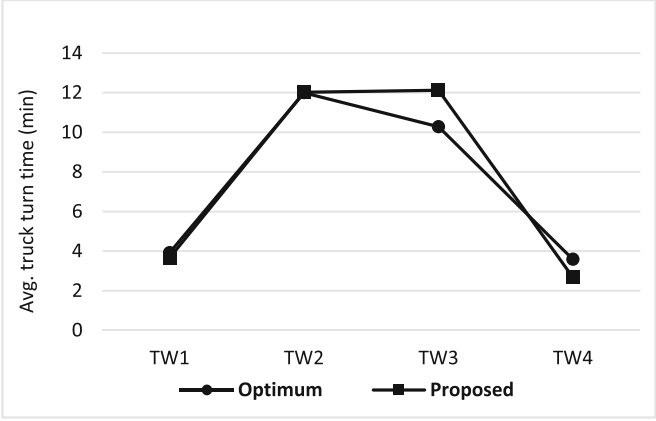

Fig. 6. Average truck turn time at yard block 3 ($TT_{3\tau}$) [29].

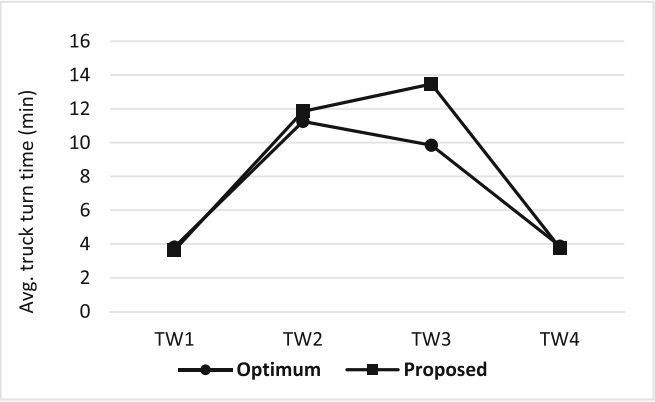

Fig. 7. Average truck turn time at yard block 4 ($TT_{4\tau}$) [29].

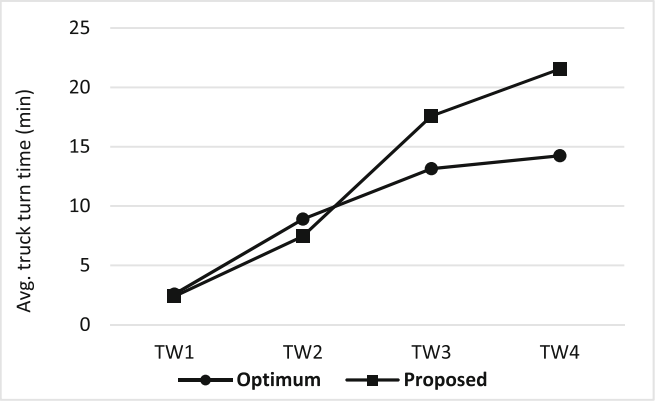

Fig. 8. Average truck turn time at yard block 5 ($TT_{5\tau}$) [29].

It is noticed that the number of proposed tasks within some task groups increased after solution because some task groups are decomposed to two or three tasks. However, this reduces the turn time cost for the external trucks, some trucking companies may be inconvenient due to shifting their preferable arrival times. For the CT, distributing the arrival appointments over the terminal working hours is good to avoid congestion in certain times windows. From another side, reducing congestion and decreasing waiting time will result in less emissions and less fuel cost as well increased efficiency for the trucking companies. The results show also that the average queue length at gates is reduced by 21% and the average truck turn time is reduced by 22.6% after applying the proposed system.

5.2 The Impact of Using DCTAS on Truck Queue Length at Each Yard Block

Long queue lengths at yard block or internal waiting areas inside the terminal create many congestion problems which in turn affect the yard area performance. In this experiment, the queue length of the external trucks at each yard block is determined for the four time widows. The results are compared to understand the improvements that the DCTAS solution provides for the congestion levels at yard blocks. Results illustrated that the maximum queue lengths at each yard block are significantly reduced (see Fig. 9). At yard block 1, the maximum queue length is noticed to have the largest value, however, all yard blocks have an approximate number of external trucks to be routed to it through the gates. By analyzing this situation, *YB*1 is noticed to receive 10 containers from the seaside rather than other yard blocks. This means that the *YB*1 will be more congested due to the presence of internal trucks that transport containers between the yard and vessel and have the priority to be served first rather than the external trucks. The DCTAS showed great benefit for this conflict between the external trucks and internal trucks service in reducing the congestion at *YB*1. Results also illustrate that about 36%, 33%, 17%, 17% and 27% reduction in the maximum queue length are obtained for *YB*1, *YB*2, *YB*3, *YB*4, and *YB*5 respectively with an average of 26% reduction of the maximum queue length at yard area. As a result, the proposed appointment system can contribute to the reduction of the overall congestion level at the yard area which is considered the central area of and any CT and impacts all terminal operations.

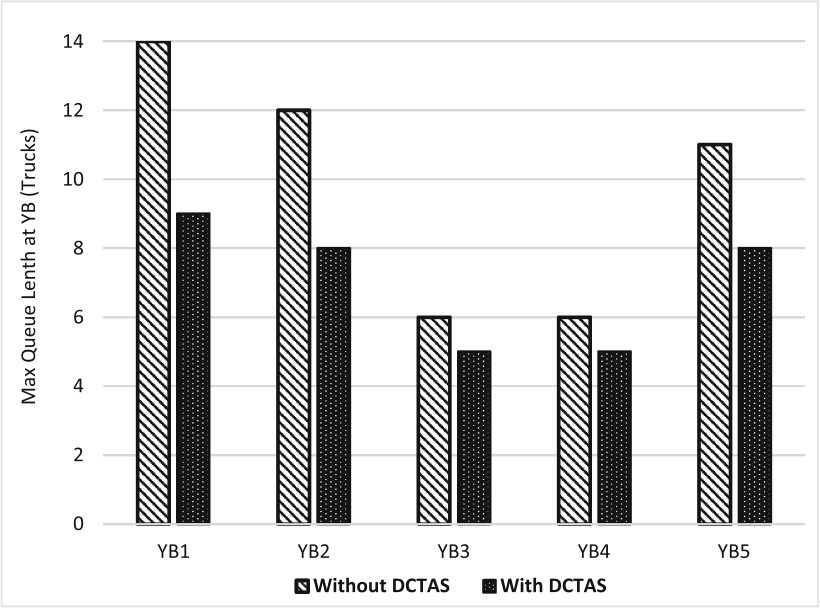

Fig. 9. Impact of DCTAS on truck queue length at each yard block.

5.3 The Impact of Using DCTAS on Waiting Time at Each Yard Block

The waiting time is considered one the most focused objectives in the container terminal. For trucking companies, reducing truck waiting time at the yard area reduces the non-value added time and increases the resources (trucks/drivers) utilization. Consequently, less costs and higher revenues can be achieved by reducing the non-value added fuel consumptions and performing more delivery tasks per day. From the terminal point of view; the less waiting time achieves higher satisfaction for customers, increases the terminal competitiveness, increases the productivity and reduces environmental emissions. The results of solving the instance illustrated that both average and maximum waiting time at yard blocks are reduced (see Figs. 10 and 11). It is also noted that the proposed DCTAS reduced the waiting time in a proportional way with the congestion level. For example, the maximum queue length of 14 and 12 trucks is observed for *YB*1 and *YB*2, and the maximum reduction in waiting time with about 50% for both is also observed for *YB*1 and *YB*2. Therefore, the more the yard blocks are congested the more the DCTAS will resolve the congestion at the yard and shift the arrivals from the congested time windows less congested time windows in such a way that reduces the total truck turn time and inconvenient of trucking companies.

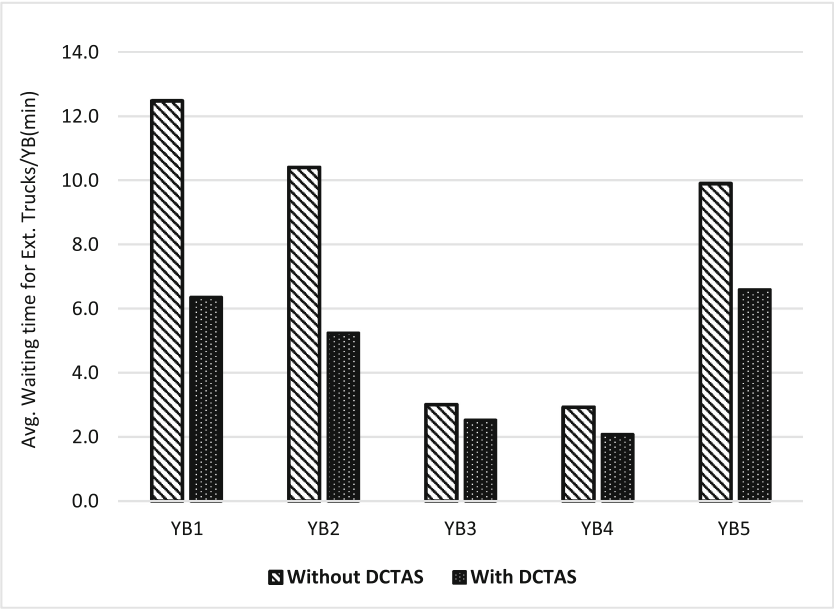

Fig. 10. Impact of using DCTAS on average waiting time at each yard block.

5.4 The Impact of Using DCTAS on Yard Crane Utilization

The experimental results showed that there are no significant difference in the Yard Cranes' (YC) utilizations before and after applying the DCTAS (see Fig. 12). This result is reasonable because the number of external trucks to be served in the solved

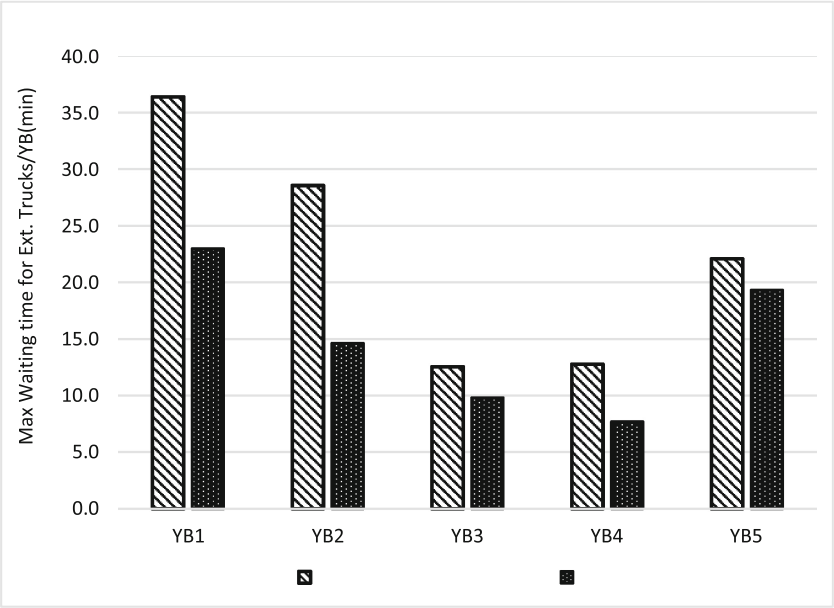

Fig. 11. Impact of using DCTAS on maximum waiting time at each yard block.

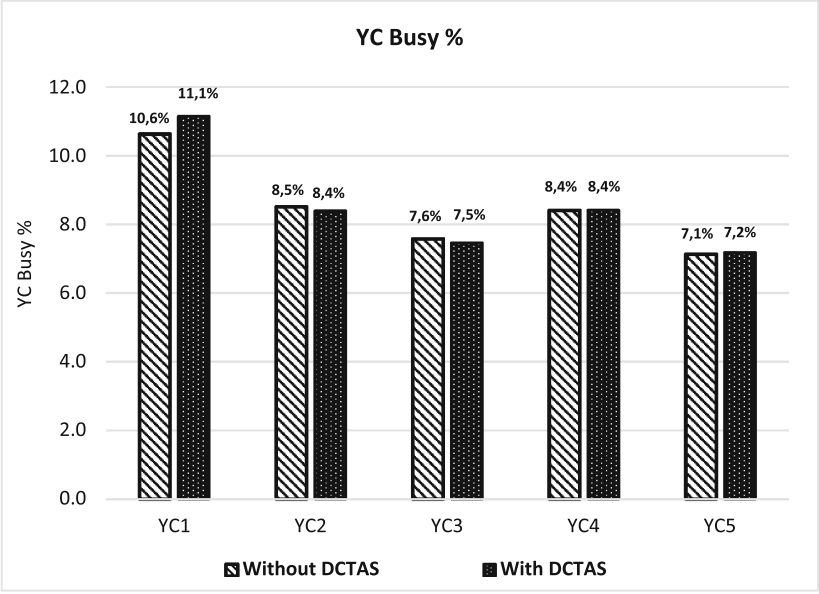

Fig. 12. Impact of using DCTAS on yard crane utilization.

instance per the 4 working hours are not changing, and the crane speeds are fixed. The only change is observed for the schedule of the developed appointments that external trucks shall arrive according to it. Consequently, the service rate is the same before and after using the DCTAS. However, terminal operators can use DCTAS to investigate the idle and busy times of yard cranes in a real-time and use this information to manage the yard operation in more perfectly.

6 Conclusions

This paper studied the effect of using collaborative scheduling of external trucks' appointments on yard performance at container terminal (CTs). A Dynamic Collaborative Truck Appointment system (DCTAS) was developed by integrating a discrete event simulation model for simulating the CT operations with a mixed integer programming model for scheduling the appointments based on the simulation results. The simulation model is used to calculate the average truck turn time which is considered the key performance indicator that the adopted approach relies on. The obtained average turn times for each trucking company's trucks are used to identify the congested times that a trucking company shall avoid sending their trucks within it. Based on this, the mathematical model is solved to obtain the optimum appointments that reduced the inconvenience cost resulting from shifting the arrivals from the preferable arrival times and the congestion cost resulting from the long truck turn times. Some numerical experiments were conducted and the results showed that the proposed DCATS improved the performance measures of yard operations. The DCTAS reduced the truck turn time and waiting time at the yard blocks in such a way that would increase the convenience of trucking companies. Moreover, less congestion levels can be achieved since the queue length at yard blocks were reduced. As a result, the proposed collaborative appointment system achieved many benefits for the trucking companies and the container terminal.

References

1. Bierwirth, C., Meisel, F.: A follow-up survey of berth allocation and quay crane scheduling problems in container terminals. Eur. J. Oper. Res. **244**(3), 675–689 (2010)
2. Karam, A., Eltawil, A.B.: A new method for allocating berths, quay cranes and internal trucks in container terminals. In: 2015 International Conference Logistics Informatics and Service Science, LISS 2015 (2015)
3. Karam, A., Eltawil, A.B.: Functional integration approach for the berth allocation, quay crane assignment and specific quay crane assignment problems. Comput. Ind. Eng. **102**, 1–15 (2016)
4. Gheith, M.S., Eltawil, A.B., Harraz, N.A., Mizuno, S.: An integer programming formulation and solution for the container pre-marshalling problem. In: CIE 2014 - 44th International Conference on Computers and Industrial Engineering and IMSS 2014, pp. 2047–2056 (2014)
5. Gheith, M., Eltawil, A.B., Harraz, N.A.: Solving the container pre-marshalling problem using variable length genetic algorithms. Eng. Optim. **48**(4), 687–705 (2016)

6. Zehendner, E., Feillet, D.: Benefits of a truck appointment system on the service quality of inland transport modes at a multimodal container terminal. Eur. J. Oper. Res. **235**(2), 461–469 (2014)
7. Zhao, W., Goodchild, A.V.: The impact of truck arrival information on container terminal rehandling. Transp. Res. Part E Logist. Transp. Rev. **46**(3), 327–343 (2010)
8. Van Asperen, E., Borgman, B., Dekker, R.: Evaluating impact of truck announcements on container stacking efficiency. Flex. Serv. Manuf. J. **25**(4), 543–556 (2013)
9. Zhao, W., Goodchild, A.V.: Using the truck appointment system to improve yard efficiency in container terminals. Marit. Econ. Logist. **15**, 101–119 (2013)
10. Huynh, N., Walton, C.M.: Robust scheduling of truck arrivals at marine container terminals. J. Transp. Eng. **134**(8), 347–353 (2008)
11. Huynh, N.: Reducing truck turn times at marine terminals with appointment scheduling. Transp. Res. Rec. J. Transp. Res. Board **2100**, 47–57 (2009)
12. Guan, C., (Rachel) Liu, R.: Container terminal gate appointment system optimization. Marit. Econ. Logist. **11**(4), 378–398 (2009)
13. Chen, X., Zhou, X., List, G.F.: Using time-varying tolls to optimize truck arrivals at ports. Transp. Res. Part E Logist. Transp. Rev. **47**(6), 965–982 (2011)
14. Azab, A.E., Eltawil, A.B.: A simulation based study of the effect of truck arrival patterns on truck turn time in container terminals. In: Claus, T., Herrmann, F., Manitz, M., Rose, O. (eds.) ECMS 2016. European Council for Modeling and Simulation (2016). https://doi.org/10.7148/2016-0080
15. Murty, K.G., et al.: Hongkong international terminals gains elastic capacity using a data-intensive decision-support system. Interfaces (Providence) **35**(1), 61–75 (2005)
16. Morais, P., Lord, E.: Terminal appointment system study (2006)
17. Sharif, O., Huynh, N., Vidal, J.M.: Application of El Farol model for managing marine terminal gate congestion. Res. Transp. Econ. **32**(1), 81–89 (2011)
18. Karafa, J.: Simulating gate strategies at intermodal marine container terminals, May 2012
19. Zhang, X., Zeng, Q., Chen, W.: Optimization model for truck appointment in container terminals. Proc. Soc. Behav. Sci. **96**, 1938–1947 (2013)
20. Dekker, R., Van Der Heide, S., Van Asperen, E., Ypsilantis, P.: A chassis exchange terminal to reduce truck congestion at container terminals. Flex. Serv. Manuf. J. **25**(4), 528–542 (2013)
21. Chen, G., Jiang, L.: Managing customer arrivals with time windows: a case of truck arrivals at a congested container terminal. Ann. Oper. Res. **244**, 1–17 (2016)
22. Chen, G., Govindan, K., Golias, M.M.: Reducing truck emissions at container terminals in a low carbon economy: proposal of a queueing-based bi-objective model for optimizing truck arrival pattern. Transp. Res. Part E Logist. Transp. Rev. **55**(X), 3–22 (2013)
23. Schulte, F., González, R.G., Voß, S.: Reducing port-related truck emissions: coordinated truck appointments to reduce empty truck trips. In: International Conference on Computational Logistics, pp. 495–509 (2015)
24. Li, N., Chen, G., Govindan, K., Jin, Z.: Disruption management for truck appointment system at a container terminal: a green initiative. Transp. Res. Part D Transp. Environ. (2015, in press)
25. Namboothiri, R., Erera, A.L.: Planning local container drayage operations given a port access appointment system. Transp. Res. Part E Logist. Transp. Rev. **44**(2), 185–202 (2008)
26. Chen, G., Yang, Z.: Optimizing time windows for managing export container arrivals at Chinese container terminals. Marit. Econ. Logist. **12**(1), 111–126 (2010)
27. Phan, M.H., Kim, K.H.: Negotiating truck arrival times among trucking companies and a container terminal. Transp. Res. Part E Logist. Transp. Rev. **75**, 132–144 (2015)

28. Phan, M., Kim, K.H.: Collaborative truck scheduling and appointments for trucking companies and container terminals. Transp. Res. Part B Methodol. **86**, 37–50 (2016)
29. Azab, A., Karam, A., Eltawil, A.: A dynamic and collaborative truck appointment management system in container terminals. In: Proceedings of the 6th International Conference on Operations Research and Enterprise Systems, ICORES, vol. 1, pp. 85–95 (2017)
30. Azab, A., Mostafa, N., Park, J.: OnTimeCargo: a smart transportation system development in logistics management by a design thinking approach. In: PACIS 2016 Proceedings, 44 (2016)
31. Bierwirth, C., Meisel, F.: A follow-up survey of berth allocation and quay crane scheduling problems in container terminals. Eur. J. Oper. Res. **244**(3), 675–689 (2015)
32. Le-Griffin, H.D., Murphy, M.: Container terminal productivity: experiences at the ports of Los Angeles and Long Beach. In: NUF Conference, pp. 1–21 (2006)

Optimal Repricing Strategies in a Stochastic Infinite Horizon Duopoly

Rainer Schlosser(✉) and Martin Boissier(✉)

Hasso Plattner Institute, University of Potsdam, Potsdam, Germany
{rainer.schlosser,martin.boissier}@hpi.de

Abstract. Due to the rise of e-commerce, an increasing number of markets is characterized by dynamic pricing competition. Many competitors adjust their prices in response to changing market environments caused by other competitors' repricing strategies. In this paper, we study repricing strategies in an infinite horizon duopoly model with stochastic demand. Assuming that the competitor's pricing strategy is known, we derive optimal response strategies that effectively avoid a decline in price. For different pairs of competing strategies, we analyze resulting price trajectories over time and evaluate the firms' associated expected long-term profits. We measure the effect of price reaction frequencies on a strategy's performance. Further, we extend our model to analyze settings with randomized reaction times as well as mixed strategies. Finally, we study mutual optimal reaction strategies. We show that equilibrium strategies can be identified by iterating optimal response strategies. We find that equilibrium strategies are characterized by specific structures which are illustrated by numerical examples.

Keywords: Dynamic pricing · Duopoly competition
Response strategies · Reaction time · Equilibrium strategies

1 Pricing Strategies for Stochastic Demand

Firms offering goods on online marketplaces have to face increasing competition and stochastic demand. One reason for the increasing competition is the rising application of automated repricing algorithms and the resulting shortening of time spans between price updates. The time pressure and stochastic demand make it challenging for firms to determine prices fast and efficiently (often for a large number of products) while ensuring to employ pricing strategies that maximize their own expected profits. But at the same time, online marketplaces also provide numerous advantages. Sellers are now able to observe the market situation at any given point in time and set prices accordingly. Having historical market data at hand also enables sellers to learn the demand over time and better understand the consumers' decision making. More interestingly for the context of this paper, firms can learn the competitors' strategies. Pricing strategies that use that demand knowledge and further competitor strategies will thus be of increasing interest.

G. H. Parlier et al. (Eds.): ICORES 2017, CCIS 884, pp. 129–150, 2018.
https://doi.org/10.1007/978-3-319-94767-9_7

Nevertheless, determining suitable price reactions is a highly challenging task. While fixed price strategies are relatively straightforward to manage, in an increasing number of contexts involving both perishable (e.g., fashion goods, seasonal products, event tickets) as well as durable goods (e.g., books, natural resources, gasoline) automated price adjustment strategies are employed. A typical pattern observed on markets with automated response strategies are cyclic price patterns over time, e.g., Edgeworth cycles as illustrated in Fig. 1. Here, firms compete with each other by undercutting the competitor's price until the lower bound is reached (e.g., when margin nears zero) and one competitor raises the price in order to allow for future profits [1,2].

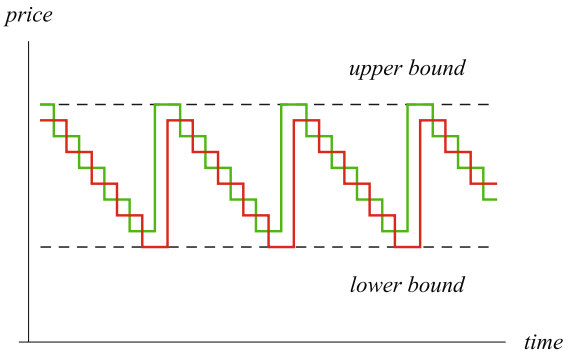

Fig. 1. Exemplary illustration of Edgeworth price cycles in a duopoly. Both firms undercut each other until the green firm reaches his lower bound and adjusts his price to the upper bound. (Color figure online)

In this paper, we present a model for duopoly pricing models in a stochastic dynamic framework in which sales probabilities are allowed to be an arbitrary function of time and competitor prices. The goal is to take into account *(i)* varying (randomized) reaction times, *(ii)* various given competitor strategies, *(iii)* additional passive competitors that use constant prices, and *(iv)* competitors that optimally react.

1.1 Literature Review

The challenge of determining optimal prices for the sale of products is one of the key aspects of revenue management theory. This field of *dynamic pricing* has been discussed in an array of books (e.g., [3–5]). Chen and Chen published a survey giving an excellent overview of recent pricing models under competition [6]. Gallego and Wang consider a continuous time multi-product oligopoly for differentiated perishable goods using optimality conditions to reduce the multi-dimensional dynamic pricing problem to a one-dimensional one [7]. Gallego and Hu analyze structural properties of equilibrium strategies in more general oligopoly models for the sale of perishable products [8], basing the

solution model on a deterministic version of the model. Martínez-de-Albéniz and Talluri consider duopoly and oligopoly pricing models for identical products [9]. They use a general stochastic counting process to model customer demand.

Further related models are studied by Yang and Xia [10] as well as Wu and Wu [11]. Levin et al. [12] and Liu and Zhang [13] analyze dynamic pricing models under competition including strategic customers. Dynamic pricing competition models with limited demand information are analyzed by Adida and Perakis [14], Tsai and Hung [15], and Chung et al. [16] using robust optimization and learning approaches. Many models consider continuous time models with finite horizon and limited inventory. In most existing models, discounting is not included and the demand is assumed to be of a somewhat artificial and stylized form. We consider an infinite horizon model without inventory restrictions (i.e., products can be reproduced or reordered) [17]. Demand is allowed to depend generally on time as well as on the market participants' prices.

Current automated pricing strategies are comparatively simple and aggressive. One example is the often employed strategy of slightly undercutting the price of the cheapest competitor [18]. We do not assume that all market participants act rationally. In order to be able to respond to arbitrary suboptimal pricing strategies we provide applicable solution algorithms that allow computing optimal response strategies.

1.2 Contribution

This paper is an extended version of [17] in which we analyzed optimal price response strategies that are based on anticipated competitor strategies. The model is characterized by a discrete time setting, an infinite horizon, subsequent price reactions, and no inventory considerations.

Compared to [17], in this paper we make the following contributions: First, instead of applying value iteration, we compute optimal strategies by solving the Hamilton-Jacobi-Bellman equation using a non-linear solver. Second, we allow *both* firms to apply optimal price response strategies in order to study iterated mutual strategy adjustments. Third, we identify equilibrium strategies and analyze their characteristics. Fourth, we study how equilibrium strategies are affected by the discount factor.

The remainder of this paper is structured as follows. In Sect. 2, we describe the stochastic dynamic duopoly model with infinite time horizon for durable goods. We allow sales probabilities to depend on competitor prices as well as on time (seasonal effects). The state space is characterized by time and the actual competitors' prices. The stochastic dynamic control problem is expressed in discrete time. In Sect. 3, we consider a duopoly competition. The competitor is assumed to frequently adjust its prices using a predetermined strategy. We assume that the price reactions of competitors as well as their reaction times can be anticipated. We set up a firm's Hamilton-Jacobi-Bellman equation and use recursive methods (value iteration) to approximate the value function. We are able to compute optimal feedback prices as well as expected long-term profits of the two competing firms. Evaluating price paths over time, we are able to

explain specific price cycles. Additionally, the results obtained are generalized to scenarios with randomized reaction times and mixed strategies.

In Sect. 4, optimal response strategies in the presence of active and passive competitors are analyzed. We examine how the duopoly game of two active competitors is affected by additional passive competitors. We show how to compute optimal pricing strategies and to evaluate expected profits. We also discuss how the cyclic price paths of the active competitors are affected by different price levels of passive competitors.

In Sect. 5, we evaluate the expected profits when different strategies are played against each other. We study scenarios in which the competitor also applies optimal response strategies. In Sect. 6, we study mutual optimal reaction strategies. We show that equilibrium strategies can be identified by iterating optimal response strategies. Eventually, the conclusion and managerial recommendations are given in Sect. 7.

2 Model Description

For this work, we consider the situation where a firm wants to sell goods (e.g., groceries, technical devices, gasoline) on a digital marketplace (e.g., Amazon, eBay, Alibaba). We assume that several sellers compete for the same market, i.e., customers are able to compare prices of different competitors at any given point in time.

We assume that the time horizon is infinite. We assume that firms are able to reproduce or reorder products (promise to deliver), and the ordering is decoupled from pricing decisions. If a sale takes place, shipping costs c have to be paid, $c \geq 0$. A sale of one item at price a, $a \geq 0$, leads to a net profit of $a - c$. Discounting is also included in the model. We will use the discount factor δ, $0 < \delta < 1$, for the length of one period.

On the majority of marketplaces, prices cannot be continuously adjusted. Thus, we consider a discrete time model. The sales intensity of our product is denoted by λ. Due to customer choice, the sales intensity will particularly depend on our offer price a and the competitors' prices. We also allow the sales intensity to depend on time, e.g., the time of the day or the week. We assume that the time dependence is periodic and has an integer cycle length of J periods. In our model, the sales intensity λ is a general function of time, our offer price a and the competitors' prices $\boldsymbol{p}$. Given the prices a and $\boldsymbol{p}$ in period t, the jump intensity λ satisfies, $t = 0, 1, 2, ...$, $a \geq 0$, $\boldsymbol{p} \geq \boldsymbol{0}$,

$$\lambda_t(a, \boldsymbol{p}) = \lambda_{t \mod J}(a, \boldsymbol{p}). \tag{1}$$

We assume the sales probabilities (for one period) to be Poisson distributed in our discrete time model. That means the probability to sell exactly i items within one period of time is given by, $t = 0, 1, 2, ...$, $a \geq 0$, $\boldsymbol{p} \geq \boldsymbol{0}$, $i = 0, 1, 2, ...$,

$$P_t(i, a, \boldsymbol{p}) = \frac{\lambda_t(a, \boldsymbol{p})^i}{i!} \cdot e^{-\lambda_t(a, \boldsymbol{p})}. \tag{2}$$

A price a has to be determined for each period t. We call strategies $(a_t)_t$ admissible when they belong to the class of Markovian feedback policies; i.e., pricing decisions $a_t \geq 0$ may depend on time t and the current prices of the competitors. By A we denote the set of admissible prices. A list of variables and parameters is given in the Appendix, cf. Table 4.

By X_t we denote the random number of sales in period t. Depending on the chosen pricing strategy $(a_t)_t$, the random accumulated profit from time/period t on (discounted on time t) amounts to, $t = 0, 1, 2, ...$,

$$G_t := \sum_{s=t}^{\infty} \delta^{s-t} \cdot (a_s - c) \cdot X_s. \tag{3}$$

The objective is determining a non-anticipating (Markovian) pricing strategy that maximizes the expected total profit $E(G_0)$.

In the next sections, we will solve dynamic pricing problems that are related to (1)–(3). Further, we mostly assume a duopoly situation. We assume that the competitor frequently adjusts his/her prices and show how to derive optimal response strategies. We analyze the impact of different reaction times as well as randomized reaction times. We also consider the case in which the competitor plays mixed strategies. In Sect. 4, we compute pricing strategies for duopoly scenarios with additional passive competitors. Eventually, we let the competitor also apply optimized response strategies in Sects. 5 and 6.

3 Duopoly: Optimal Reaction Strategies

Due to the increasing market transparency on e-commerce platforms, sellers can observe and thus anticipate transitions of the market situation. In this section, we examine a duopoly where we compete with a seller that frequently adjusts her prices using a predetermined strategy.

3.1 Fixed Reaction Times

Having information about a competitor's strategy at hand and being able to anticipate it allows us to optimize expected profits. Here, the price responses of competitors as well as their reaction time can be taken into account. In this case, a change of the market situation $\boldsymbol{p}$ can take place within a period. A typical scenario is that a competitor adjusts its price in response to our price with a certain delay. Throughout this section, we assume that the pricing strategy and the reaction time of the competitor is known; i.e., we assume that choosing a price a at time t is followed by a state transition (e.g., a competitor's price reaction) and the current market situation $\boldsymbol{p}$ changes to a subsequent state described by a transition function F, which can depend both on the market situation $\boldsymbol{p}$ as well as price a.

We want to derive optimal price response strategies to a given competitor's strategy. For simplicity, we consider the sale of one type of product in a duopoly

situation. We assume that the state of the system (the market situation) is one-dimensional and simply characterized by the competitor's price p, i.e., we let $\boldsymbol{p} := p$.

In real-life applications, a firm is not able to adjust its prices immediately after the price reaction of the competing firm. Consequently, we assume that in each period the price reaction of the competing firm takes place with a delay of h periods, $h < 1$. Thus, after an interval of size h the competitor adjusts its price from p to $F(a)$, as illustrated in Fig. 2.

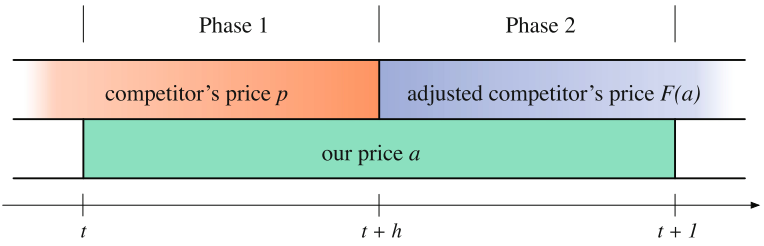

Fig. 2. Duopoly: sequence of price reactions, cf. [17].

In period t, the probability to sell exactly i items during the first interval (Phase 1, cf. Fig. 2) of size h is

$$P_t^{(h)}(i, a, p) := Pois\left(h \cdot \lambda_t(a, p)\right)$$

while for the rest of the period (Phase 2, cf. Fig. 2) the sales probability changes to $P_t^{(1-h)}\left(i, a, F(a)\right) = Pois\left((1-h) \cdot \lambda_t\left(a, F(a)\right)\right)$.

We will use value iteration to approximate the value function which represents the present value of future profits. For a given "large" number T, $T \gg J$, we let $V_T(p) = 0$ for all p, and compute, $t = 0, 1, 2, ..., T-1$, $0 < h < 1$, $p \in A$,

$$V_t(p) = \max_{a \in A} \left\{ \sum_{i_1 \geq 0} P_t^{(h)}(i_1, a, p) \cdot \sum_{i_2 \geq 0} P_{t+h}^{(1-h)}\left(i_2, a, F(a)\right) \right.$$
$$\left. \cdot \left((a-c) \cdot (i_1 + i_2) + \delta \cdot V_{t+1}\left(F(a)\right)\right) \right\}. \tag{4}$$

The associated pricing strategy $a_t^*(p)$, $t = 0, 1, 2, ..., J-1$, $p \in A$, is determined by the arg max of

$$a_t^*(p) = \arg\max_{a \in A} \left\{ \sum_{i_1 \geq 0} P_t^{(h)}(i_1, a, p) \cdot \sum_{i_2 \geq 0} P_{t+h}^{(1-h)}\left(i_2, a, F(a)\right) \right.$$
$$\left. \cdot \left((a-c) \cdot (i_1 + i_2) + \delta \cdot V_{t+1}\left(F(a)\right)\right) \right\}. \tag{5}$$

Given $a_t^*(p)$ is not unique, we choose the largest one.

Remark 1. The recursive solution approach also allows to solve problems with perishable products and finite horizons T. Simply be evaluating Eqs. (4)–(5) for all $t = 0, 1, 2, ..., T-1$.

In order to illustrate the approach, let us consider a numerical example for durable goods. We assume the competitor applies one of the most common strategies: our current price is undercut by ε down to a certain minimum (e.g., the shipping costs c). The sales dynamics of the following example above are based on a large data set from the Amazon marketplace for used books [19].

Definition 1. *By* $P_t^{(h)}(i, a, \boldsymbol{p}) := Pois\left(h \cdot e^{\boldsymbol{x}(a,\boldsymbol{p})'\boldsymbol{\beta}}/(1 + e^{\boldsymbol{x}(a,\boldsymbol{p})'\boldsymbol{\beta}})\right)$ *we define sales probabilities for oligopoly settings which are based on linear combinations of the following five regressors* $\boldsymbol{x} = \boldsymbol{x}(a, \boldsymbol{p})$, $\boldsymbol{p} = (p_1, ..., p_K)$ *with given coefficients* $\boldsymbol{\beta} = (\beta_1, ..., \beta_5)$*:*

(i) constant/intercept

$$x_1(a, \boldsymbol{p}) = 1$$

(ii) rank of price a within the set of competitor prices $\boldsymbol{p}$

$$x_2(a, \boldsymbol{p}) = 1 + |\{k = 1, ..., K \,|p_k < a\}| + 0.5 \cdot |\{k = 1, ..., K \,|p_k = a\}|$$

(iii) price gap between price a and the best competitor price

$$x_3(a, \boldsymbol{p}) = a - \min_{k=1,...,K}\{p_k\}$$

(iv) total number of competitors

$$x_4(a, \boldsymbol{p}) = K$$

(v) average price level

$$x_5(a, \boldsymbol{p}) = (a + \sum\nolimits_k p_k)/(1 + K)$$

Example 1. We assume a duopoly, i.e., $K = 1$ and $\boldsymbol{p} = p$. Let $c = 3$, $\delta = 0.99$, $0 \le h \le 1$, and let $F(a) := \max(a - \varepsilon, c)$, $\varepsilon = 1$, $a \in A := \{1, 2, ..., 100\}$. For the computation of the value function, we let $T := 1000$. We assume the sales probabilities $P_t^{(h)}(\cdot, a, p)$, cf. Definition 1, where $\boldsymbol{\beta} = (-3.89, -0.56, -0.01, 0.07, -0.02)$.

Figures 3(a) and 4(a) illustrate optimal response strategies for different reaction times $h = 0.1$ and $h = 0.9$. The case $h = 0.1$ illustrates a fast reaction time of the competitor; $h = 0.9$ represents a slow reaction of the competitor. In the case of $h = 0.5$, both competing firms react equally fast. In all three cases the optimal response strategies are of similar shape. If the competitor's price is either very low or very large, it is optimal to set the price to a certain moderate level. If the competitor's price is somewhere in between (intermediate range), it

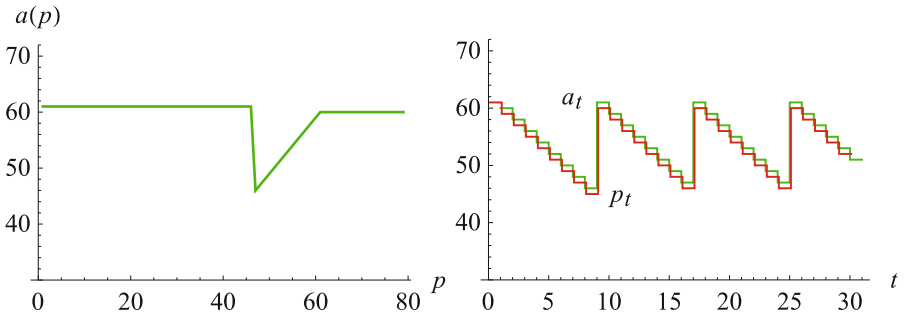

(a) Optimal response strategy. (b) Evaluated price paths.

Fig. 3. Example 1 with $h = 0.1$: optimal response strategy and price paths, cf. [17].

is advisable to undercut that price by one price unit ε. If h is larger, also the intermediate range is larger and the upper price level is increasing.

Employing optimal response strategies can create cyclic price patterns over time, so-called Edgeworth cycles [1,2,18]. The resulting price paths are illustrated in Figs. 3(b) and 4(b). We observe that the cycle length and the amplitude of the price patterns are increasing if the reaction time of the competitor is longer. Note, roughly $h \cdot 100\%$ of the time our firm is offering the lowest price; i.e., the parameter h can also be used to model situations in which one firm is able to adjust its prices more often than another firm [20,21].

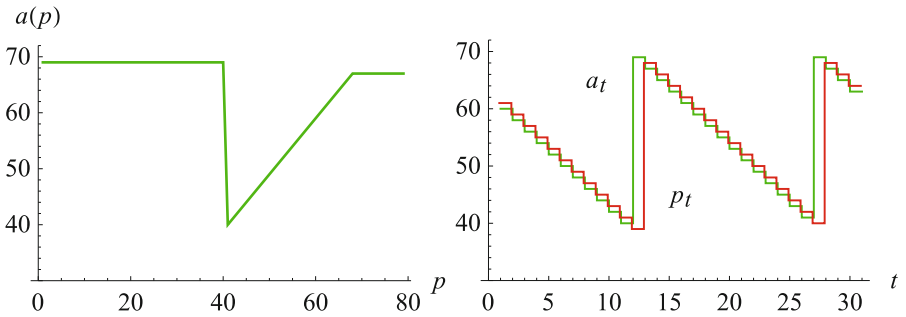

(a) Optimal response strategy. (b) Evaluated price paths.

Fig. 4. Example 1 with $h = 0.9$: optimal response strategy and price paths, cf. [17].

Additionally, we are able to analyze the impact of the reaction time on expected long-term profits of our firm as well as the competitor. We assume that the competitor faces the same sales probabilities and shipping costs. The competitor's expected profits can be recursively evaluated by, cf. (4), $t = 0, 1, 2, ..., T-1$, $0 < h < 1$, $a \in A$, $V^{(c)}_{T+h}(a) = 0$,

$$V_{t+h}^{(c)}(a) = \sum_{i_2 \geq 0} P_{t+h}^{(1-h)}(i_2, F(a), a) \cdot \sum_{i_1 \geq 0} P_{t+1}^{(h)}\left(i_1, F(a), a^*_{t+1 \bmod J}(F(a))\right)$$

$$\cdot \left((F(a) - c) \cdot (i_1 + i_2) + \delta \cdot V_{t+h+1}^{(c)}\left(a^*_{t+1 \bmod J}(F(a))\right)\right). \tag{6}$$

Because of the cyclic price paths, expected future profits $V_0(p)$ and $V_h^{(c)}(a)$ are (almost) independent of the initial states or prices. Figure 5 depicts V as well as the competitor's expected profits $V^{(c)}$ as a function of h. We observe that the expected profit V is linear increasing in the competitor's reaction time; the competitor's profit $V^{(c)}$ is decreasing in h. Note, the impact of h is substantial. The "disadvantage" of the player that stops the undercutting phase can already be compensated in case our reaction time is smaller than 0.46, i.e., if h is larger than 0.54.

3.2 Randomized Reaction Times

Due to the shown significant impact of reaction times firms will try to gain advantage by updating their prices more frequently. In addition, firms might also try to minimize their reaction times by anticipating their competitor's *time* of adjustment. In order not to act predictably, firms will randomize their reaction times.

Our model can be extended to capture the cases in which reaction times are not deterministic. If the distribution of the reaction time of competitors is known, the Hamilton-Jacobi-Bellman (HJB) equation, cf. (4), can be modified. The different reaction scenarios just have to be considered with their corresponding probability. Note, the reaction times of different competitors can be observed over longer time spans.

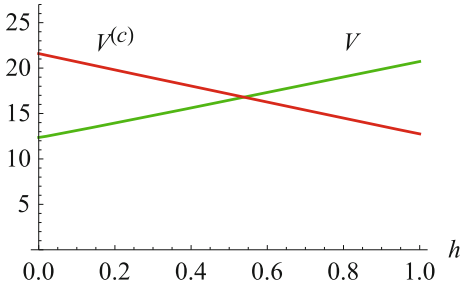

Fig. 5. Expected profit for different reaction times of the competitor (Example 1), cf. [17].

In the following, we consider scenarios with randomized reaction times. We assume that each firm adjusts its price with a certain intensity (e.g., on average once a period of size 1). We model that approach as follows: we assume that at each point in time d, $d = t + \Delta, t + 2\Delta, ..., t + 1$, $0 < \Delta \ll 1$, our firm adjusts

its price with probability q, $0 < q \ll 1$; i.e., on average we adjust our price q/Δ times a period of size 1. Similarly, the competitor adjusts its price with probability $q^{(c)}$, $0 < q^{(c)} \ll 1$. The competitor applies a certain strategy $F(a)$. By a^- we denote our current price at time d, the beginning of the sub-period $(d, d+\Delta)$. With probability $q^{(c)}$, the competitor adjusts its price from p to $F(a^-)$. We adjust the price a^- to price a with probability q. Since q and $q^{(c)}$ are assumed to be "small" we do not consider the case in which both firms adjust their prices at the same time. The related value function is given by, $a^-, p \in A$, $t = 0, \Delta, 2\Delta, ..., T-\Delta$, $\tilde{V}_T(a^-, p) = 0$,

$$\begin{aligned}\tilde{V}_t(a^-, p) = (1 - q - q^{(c)}) \cdot \sum_{i \geq 0} P_t^{(\Delta)}(i, a^-, p) \\ \cdot \Big((a^- - c) \cdot i + \delta^{\Delta} \cdot \tilde{V}_{t+\Delta}(a^-, p) \Big) \\ + q^{(c)} \cdot \sum_{i \geq 0} P_t^{(\Delta)}(i, a^-, F(a^-)) \cdot \Big((a^- - c) \cdot i + \delta^{\Delta} \cdot \tilde{V}_{t+\Delta}(a^-, F(a^-)) \Big) \\ + q \cdot \max_{a \in A} \left\{ \sum_{i \geq 0} P_t^{(\Delta)}(i, a, p) \cdot \Big((a - c) \cdot i + \delta^{\Delta} \cdot \tilde{V}_{t+\Delta}(a, p) \Big) \right\}. \end{aligned} \tag{7}$$

The optimal price $\tilde{a}_t^*(a^-, p)$, $t = 0, \Delta, 2\Delta, ..., J-\Delta$, is determined by the arg max of (7). The competitor's expected profit corresponds to, $t = 0, \Delta, 2\Delta, ..., T-\Delta$, $\tilde{V}_T^{(c)}(a^-, p) = 0$,

$$\begin{aligned}\tilde{V}_t^{(c)}(a^-, p) = (1 - q - q^{(c)}) \cdot \sum_{i \geq 0} P_t^{(\Delta)}(i, p, a^-) \\ \cdot \Big((p - c) \cdot i + \delta^{\Delta} \cdot \tilde{V}_{t+\Delta}^{(c)}(a^-, p) \Big) \\ + q^{(c)} \cdot \sum_{i \geq 0} P_t^{(\Delta)}(i, F(a^-), a^-) \\ \cdot \Big((F(a^-) - c) \cdot i + \delta^{\Delta} \cdot \tilde{V}_{t+\Delta}^{(c)}(a^-, F(a^-)) \Big) \\ + q \cdot \sum_{i \geq 0} P_t^{(\Delta)} \left(i, p, \tilde{a}^*_{t \bmod J}(a^-, p) \right) \\ \cdot \Big((p - c) \cdot i + \delta^{\Delta} \cdot \tilde{V}_{t+\Delta}^{(c)} \left(\tilde{a}^*_{t \bmod J}(a^-, p), p \right) \Big). \end{aligned} \tag{8}$$

Example 2. We assume the duopoly setting of Example 1 and let $c = 3$, $F(a) := \max(a - \varepsilon, c)$, $\varepsilon = 1$, $a \in A := \{1, 2, ..., 100\}$, $\delta = 0.99$, $\Delta = 0.1$. We use $T := 1000$. We consider different reaction probabilities q and $q^{(c)}$.

Table 1. Expected profits $(\tilde{V}, \tilde{V}^{(c)})$ of both firms for different reaction probabilities q, $q^{(c)} = 0.05, 0.1, 0.2$, $\delta = 0.99$, $\Delta = 0.1$; Example 2, cf. [17].

$q^{(c)} \backslash q$	0.05	0.1	0.2
0.05	(16.53, 17.07)	(16.80, 16.81)	(17.01, 16.62)
0.1	(16.26, 17.36)	(16.48, 17.09)	(16.75, 16.84)
0.2	(16.03, 17.59)	(16.22, 17.37)	(16.48, 17.12)

Table 1 contains the expected profits $(\tilde{V}, \tilde{V}^{(c)})$ of the two competing firms for different reaction probabilities. We observe that $\tilde{V}$ is increasing in q and decreasing in $q^{(c)}$. For $\tilde{V}^{(c)}$ it is the other way around. We found that the ratio $q/q^{(c)}$ of the adjustment frequencies is a critical quantity.

The importance of the overall adjustment frequency is alleviated as long as the ratio $q/q^{(c)}$ is the same. Hence, the expected profits of both firms can be approximated by the profits from the model with deterministic reaction time, cf. Sect. 3.1, where $h = q/q^{(c)}$, i.e., the percentage of time our firm has the most recently updated price.

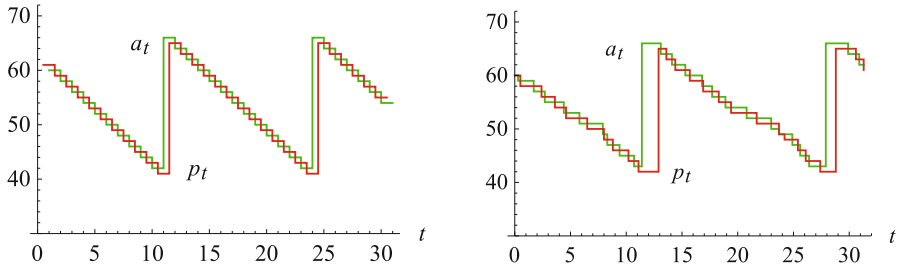

(a) Deterministic reaction times (Example 1 with $h = 0.5$).

(b) Randomized reaction times (Example 2 with $\Delta = 0.1$, $q = q^{(c)} = 0.1$).

Fig. 6. Comparison of evaluated price paths, cf. [17].

Figure 6(b) shows the price paths for the parameter setting of Example 2. Figure 6(a) shows the deterministic case of Example 1 for $h = 0.5$. We observe that overall the price patterns have similar characteristics. However, in the randomized case, the timing of the price reactions is not predictable. While in the deterministic $h = 0.5$ case (cf. Sect. 3.1) we have $\tilde{V} = 16.44$ and $\tilde{V}^{(c)} = 17.13$, in the randomized case ($\Delta = 0.1$, $q = q^{(c)} = 0.1$) the expected profits are $\tilde{V} = 16.48$ and $\tilde{V}^{(c)} = 17.09$. In both models the advantage of the aggressive player is basically the same, but for the model with randomized reaction times the advantage is slightly smaller.

3.3 Mixed Competitors' Strategies

If the competitor's strategy is known, suitable response strategies can be computed. Hence, firms might try to randomize their strategies. In this section, we will analyze scenarios in which competitors play a mixed pricing strategy.

Let us assume that the competitor plays strategy $F_k(a)$, $a \in A$, with probability π_k, $1 \leq k \leq K < \infty$, $\sum_k \pi_k = 1$. Further, we assume deterministic reaction times. We adjust our model, cf. Sect. 3.1, by using a weighted sum of potential price reactions. The Hamilton-Jacobi-Bellman (HJB) equation can be written as, $t = 0, 1, 2, ..., T-1$, $0 < h < 1$, $p \in A$,

$$V_t(p) = \max_{a \in A} \left\{ \sum_{i_1 \geq 0} P_t^{(h)}(i_1, a, p) \cdot \sum_k \pi_k \cdot \sum_{i_2 \geq 0} P_{t+h}^{(1-h)}(i_2, a, F_k(a)) \right.$$

$$\left. \cdot \left((a-c) \cdot (i_1 + i_2) + \delta \cdot V_{t+1}(F_k(a)) \right) \right\}, \tag{9}$$

where $V_T(p) = 0$ for all p. The associated pricing strategy $a_t^*(p)$, $t = 0, 1, 2, ..., J-1$, $0 < h < 1$, $p \in A$, is determined by the arg max of (9). The resulting competitor's expected profits can be computed by (starting from, e.g., $V_{T+h}^{(c)}(a) = 0$), $t = 0, 1, 2, ..., T-1$, $0 < h < 1$, $a \in A$,

$$V_{t+h}^{(c)}(a) = \sum_k \pi_k \cdot \sum_{i_2 \geq 0} P_{t+h}^{(1-h)}(i_2, F_k(a), a)$$

$$\cdot \sum_{i_1 \geq 0} P_{t+1}^{(h)}\left(i_1, F_k(a), a_{t+1 \bmod J}^*(F_k(a))\right)$$

$$\cdot \left((F_k(a) - c) \cdot (i_1 + i_2) + \delta \cdot V_{t+h+1}^{(c)}\left(a_{t+1 \bmod J}^*(F_k(a))\right) \right). \tag{10}$$

Using the models just introduced, we can compute suitable pricing strategies in various competitive markets. As long as the number of competing firms is small, the value function and the optimal prices can be computed. Note, due to the coupled state transitions in general the value function has to be computed for all states in advance. When the number of competitors is large this can cause serious problems since the state space can grow exponentially (curse of dimensionality).

The approach is suitable if the number of competitors is small and their strategies are known. If the number of competitors is large and the strategies are unknown, we recommend using simple but robust strategies [19].

4 Active and Passive Sellers in Competition

In case the pricing strategies and the competitors' reaction times are known, the model can be extended to an oligopoly setting. For each additional competitor the state space of the model has to be extended by one dimension. Note,

only active competitors that frequently adjust their prices should be taken into account. Inactive customers will be treated as external fixed effects.

We assume one active competitor and Z passive competitors. The prices of the passive competitors are denoted by $\boldsymbol{z} = (z_1, ..., z_Z)$, $z_j \geq 0$, $j = 1, ..., Z$, and assumed to be constant over time. The active competitor employs a (non-randomized) strategy $F(a)$ that refers to our price a (not the passive one). The Hamilton-Jacobi-Bellman (HJB) equation can be written as, $t = 0, 1, 2, ..., T-1$, $0 < h < 1$, $p \geq 0$, $V_T(p, \boldsymbol{z}) = 0$ for all $p, \boldsymbol{z}$,

$$V_t(p, \boldsymbol{z}) = \max_{a \in A} \left\{ \sum_{i_1 \geq 0} P_t^{(h)}(i_1, a, p, \boldsymbol{z}) \cdot \sum_{i_2 \geq 0} P_{t+h}^{(1-h)}(i_2, a, F(a), \boldsymbol{z}) \right.$$

$$\left. \cdot \left((a - c) \cdot (i_1 + i_2) + \delta \cdot V_{t+1}(F(a), \boldsymbol{z}) \right) \right\}. \tag{11}$$

The associated pricing strategy amounts to, $t = 0, 1, 2, ..., J-1$, $0 < h < 1$, $p \in A$,

$$a_t^*(p, \boldsymbol{z}) = \arg\max_{a \in A} \left\{ \sum_{i_1 \geq 0} P_t^{(h)}(i_1, a, p, \boldsymbol{z}) \cdot \sum_{i_2 \geq 0} P_{t+h}^{(1-h)}(i_2, a, F(a), \boldsymbol{z}) \right.$$

$$\left. \cdot \left((a - c) \cdot (i_1 + i_2) + \delta \cdot V_{t+1}(F(a), \boldsymbol{z}) \right) \right\}. \tag{12}$$

The competitor's profits can be computed by (using, e.g., $V_{T+h}(a, \boldsymbol{z}) = 0$ for all $a, \boldsymbol{z}$), $t = 0, 1, 2, ..., T-1$, $0 < h < 1$, $a \geq 0$,

$$V_{t+h}^{(c)}(a, \boldsymbol{z}) = \sum_{i_2 \geq 0} P_{t+h}^{(1-h)}(i_2, F(a), a, \boldsymbol{z})$$

$$\cdot \sum_{i_1 \geq 0} P_{t+1}^{(h)}\left(i_1, F(a), a_{t+1 \bmod J}^*(F(a), \boldsymbol{z}), \boldsymbol{z}\right)$$

$$\cdot \left((F(a) - c) \cdot (i_1 + i_2) + \delta \cdot V_{t+h+1}^{(c)}\left(a_{t+1 \bmod J}^*(F(a), \boldsymbol{z}), \boldsymbol{z}\right) \right). \tag{13}$$

It is not necessary to compute the value function for all price combinations of passive competitors in advance. The value function and the associated pricing strategy can be computed separately for specific market situations (e.g., just when they occur). In the following, we consider an example with active and passive competitors.

Example 3. We assume the duopoly setting of Example 1 and let $F(a) := \max(a - \varepsilon, c)$, $\varepsilon = 1$, $c = 3$, $h = 0.5$, $a \in A := \{1, 2, ..., 100\}$, $\delta = 0.99$, and $T = 1000$. Further, we consider an additional passive competitor with a constant price z, $z = 15, 20, 25$.

For the three cases $z = 15$, $z = 20$, and $z = 25$ the results are shown in Figs. 7, 8, and 9. We observe three different characteristics.

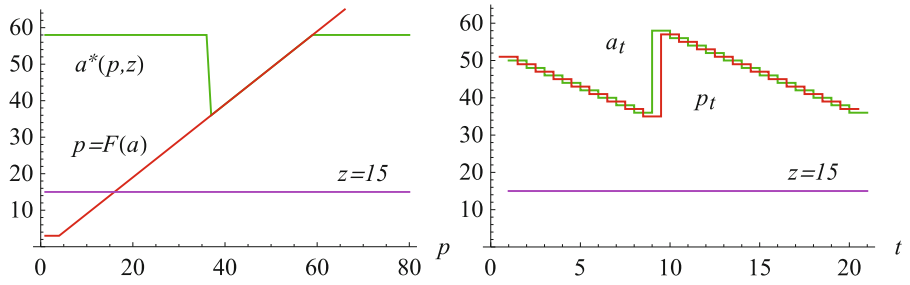

(a) Optimal response strategy. (b) Evaluated price paths.

Fig. 7. Optimal response strategy and evaluated price paths (Example 3; $h = 0.5$, $z = 15$), cf. [17].

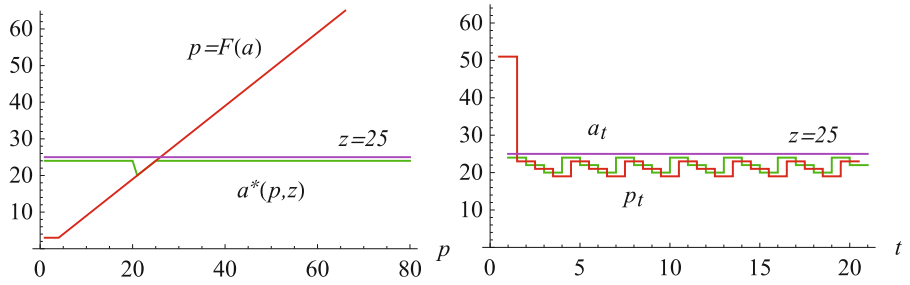

(a) Optimal response strategy. (b) Evaluated price paths.

Fig. 8. Optimal response strategy and evaluated price paths (Example 3; $h = 0.5$, $z = 25$), cf. [17].

If the passive competitor's price is low ($z = 15$) the cyclic price battle between our firm and the aggressive firm takes place at a high price level, see Fig. 7(b). The response strategies of the three firms are illustrated in Fig. 7(a).

In the case that the price of passive firm is sufficiently high ($z = 20$), the cyclic price paths of the two active firms take place below that level. If the constant price is "moderate" ($z = 20$), then a mixture of the characteristics shown in Figs. 7 and 8 is optimal. Note, it is not advisable to place price offers that slightly exceed competitors' prices (see Fig. 9).

5 Duopoly: Iterated Strategy Adjustments

In this section, we generally evaluate the outcome when different strategies are played against each other in a duopoly setting.

5.1 Evaluating Competing Strategies

We assume time homogeneous demand and $h = 0.5$. If firm 1 plays a pure strategy S_1 and firm 2 plays the pure strategy S_2 then the associated expected

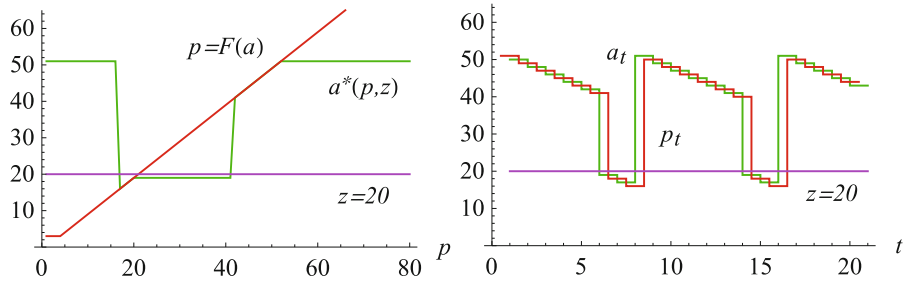

(a) Optimal response strategy. (b) Evaluated price paths.

Fig. 9. Optimal response strategy and evaluated price paths (Example 3; $h = 0.5$, $z = 20$), cf. [17].

profits can be computed by, $t = 0, 1, 2, ..., T-1$, $V_T^{(1)}(p) = V_T^{(2)}(p) = 0$, for all $p \geq 0$,

$$V_t^{(1)}(p) = \sum_{i_1 \geq 0} P^{(h)}\left(i_1, S_1(p), p\right) \cdot \sum_{i_2 \geq 0} P^{(1-h)}\left(i_2, S_1(p), S_2(S_1(p))\right)$$

$$\cdot \Big((S_1(p) - c) \cdot (i_1 + i_2) + \delta \cdot V_{t+1}^{(1)}\left(S_2\left(S_1(p)\right)\right) \Big), \tag{14}$$

$$V_t^{(2)}(p) = \sum_{i_1 \geq 0} P^{(h)}\left(i_1, S_2(p), p\right) \cdot \sum_{i_2 \geq 0} P^{(1-h)}\left(i_2, S_2(p), S_1(S_2(p))\right)$$

$$\cdot \Big((S_2(p) - c) \cdot (i_1 + i_2) + \delta \cdot V_{t+1}^{(2)}\left(S_1\left(S_2(p)\right)\right) \Big). \tag{15}$$

Alternatively, for given strategies S_k, $k = 1, 2$, we can exactly evaluate the associated expected profits $V^{(k)}$ by solving the linear system of equations, $p \in A$, $j, k = 1, 2$, $j \neq k$,

$$V^{(k)}(p) = \sum_{i_1 \geq 0} P^{(\Delta_k)}\left(i_1, S_k(p), p\right) \cdot \sum_{i_2 \geq 0} P^{(\Delta_j)}\left(i_2, S_k(p), S_j(S_k(p))\right)$$

$$\cdot \Big((S_k(p) - c) \cdot (i_1 + i_2) + \delta \cdot V^{(k)}\left(S_j\left(S_k(p)\right)\right) \Big), \tag{16}$$

where $\Delta_k := h$ and $\Delta_j := 1 - h$, $0 < h < 1$. Note, the system (16) has $|A|$ equations and can be solved using standard linear solvers.

5.2 Iterating Optimal Response Strategies

In this subsection we let two firms optimally adjust their strategies in order to identify equilibrium strategies. The approach, cf. (16), cannot only be used to evaluate competing strategies, it can also be applied to exactly compute optimal reaction strategies, cf. (4)–(5), by solving the nonlinear system of equations, $p \in A$, $j, k = 1, 2$, $j \neq k$,

$$V^{(k)}(p) = \max_{a \in A} \left\{ \sum_{i_1 \geq 0} P^{(\Delta_k)}(i_1, a, p) \cdot \sum_{i_2 \geq 0} P^{(\Delta_j)}(i_2, a, S_j(a)) \right.$$
$$\left. \cdot \Big((a - c) \cdot (i_1 + i_2) + \delta \cdot V^{(k)}(S_j(a)) \Big) \right\}. \tag{17}$$

If the number of admissible prices $|A|$ is sufficiently small the system (17) can be solved using standard nonlinear solvers, such as MINOS[1]. The associated pricing strategy $a^{(k)}(p; S_j)$, $p \in A$, $j, k = 1, 2$, $j \neq k$, is given by the arg max of (17). If $a^{(k)}(p)$ is not unique, we choose the largest one. In the following example, we will iterate optimal response strategies.

Example 4. We assume the duopoly setting of Example 1. If not chosen differently, we let $c = 3$, $h = 0.5$, $a \in A := \{1, 2, ..., 100\}$, $\delta = 0.99$. We consider an initial strategy $S^{(0)}(p) := S_U(p) := \max(p - \varepsilon, c)$, $\varepsilon = 1$. Additionally, by $S^{(k)}(p) = S^{(k)}(p; S^{(k-1)})$ we denote the optimal response strategy to strategy $S^{(k-1)}$, $k = 1, 2, ...$, cf. (17).

Considering Example 4, we evaluate the expected profits of the different strategy combinations according to (16). The results are summarized in Table 2. We observe that the aggressive strategy S_U yields good results with the exception when the competitor also plays S_U. The strategy $S^{(1)}$ yields good results in all constellations. Strategy $S^{(2)}$ is excellent when played against $S^{(1)}$ but yields only moderate results in the other cases.

Table 2. Expected profits $V_0^{(1)}(50)$ of firm 1 when its strategy $S^{(k)}$ is played against a strategy $S^{(j)}$, $k, j = 0, 1, 2, ..., 5$, $S^{(0)} := S_U$; Example 4.

$S_1 \backslash S_2$	$S^{(0)}$	$S^{(1)}$	$S^{(2)}$	$S^{(3)}$	$S^{(4)}$	$S^{(5)}$
$S^{(0)}$	2.56	17.14	15.41	12.38	17.24	15.04
$S^{(1)}$	16.19	16.78	12.07	16.06	16.16	12.07
$S^{(2)}$	14.74	20.98	14.74	12.05	17.71	14.54
$S^{(3)}$	11.23	16.84	16.59	12.00	16.84	16.59
$S^{(4)}$	16.19	17.45	15.00	16.11	17.24	12.41
$S^{(5)}$	14.31	20.55	15.26	11.81	20.55	14.81

Our example shows that optimal response strategies have a significant impact on expected profits. They help to gain profits, especially, when aggressive competitors are involved. On the other hand, we learn that it is also important to know a competitor's strategies. In practical applications, a competitor's price reactions can be inferred from market data over time.

[1] MINOS solver: https://www.gams.com/latest/docs/solvers/minos.

6 Equilibrium Strategies

In this section, we want to identify mutual best response strategies. We consider the duopoly setting of Sect. 5. In order to identify equilibrium strategies, we further iterate mutual strategy responses.

We consider the setting of Example 4. Starting with the aggressive strategy S_U we allow the two competing firms to repeatedly adjust their strategies using optimal response strategies. Figure 10 illustrates the different iterated response strategies $S^{(k)}$ for $k = 0, 1, 2, ..., 20$.

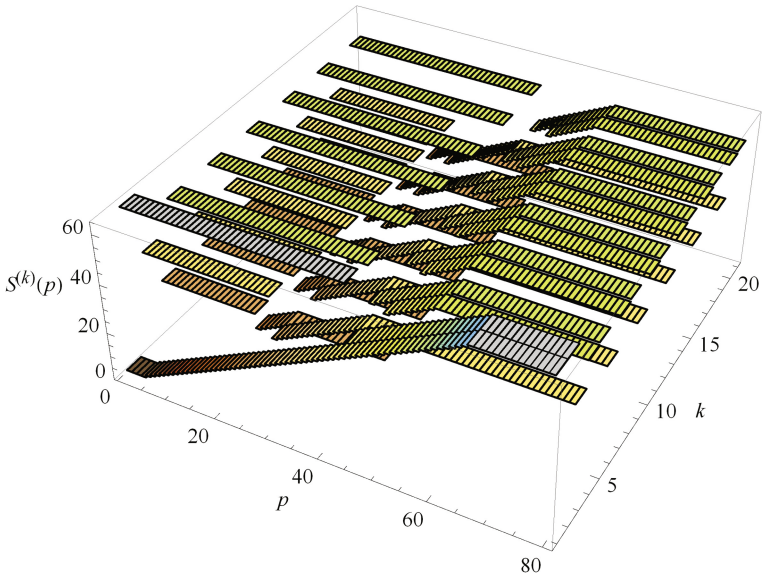

Fig. 10. Iterated response strategies (Example 4; $S^{(0)} := S_U$, $h = 0.5$).

We observe that optimal response strategies do not converge to mutual optimal pure strategies. Instead, we obtain a repeating cyclic sequence of strategy adjustments. The structure of the single response strategies is similar to those shown in Figs. 3 and 4.

However, pure mutual optimal response strategies do exist. We consider Example 4 for a different starting strategy. Figure 11 illustrates iterated response strategies $S^{(k)}$, $k = 0, 1, 2, ..., 20$, for $S^{(0)} := S^{(0)}(p) \equiv 20$.

We observe that after 11 iterations the optimal response strategies converge to a pure equilibrium strategy S^* which is such that no firm has an incentive to deviate. The equilibrium strategy has a characteristic structure which can be described as follows.

Remark 2. If the competitor's price is either below a certain low price p_{min} or a above a certain large price p_{max}, it is optimal to set the price to the upper level p_{max}. If the competitor's price is slightly under that upper price level p_{max} (upper intermediate range), it is best to undercut that price by one price unit ε as long as the competitor's price is above a certain medium price p_{med}. Is the competitor's price below the medium price p_{med} and above p_{min} (lower intermediate range) it is optimal to decrease the price to p_{min}.

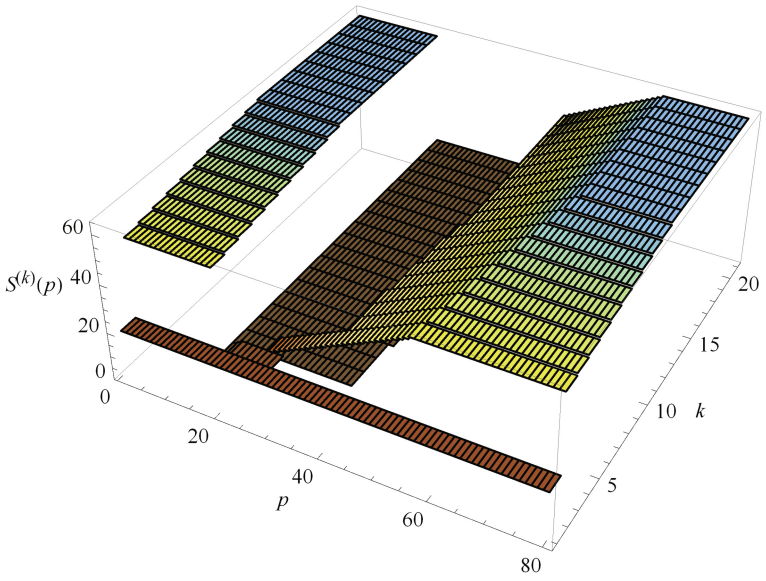

Fig. 11. Iterating equilibrium strategies (Example 4; $S^{(0)} := 20$, $h = 0.5$).

The equilibrium strategy is similar to the type of strategy derived in Sect. 3, see Figs. 3 and 4. The difference is the counterintuitive massive price drop (lower intermediate range) to the minimal price p_{min}.

This phenomenon can be explained as follows. The price drop forces the rational competitor to give in and to raise the price immediately. This way the price range in which the undercutting price battle takes place is shifted to a higher level, which in turn is advantageous for both competitors.

Table 3 illustrates the expected profits of a firm when different iterated response strategies are played against each other, cf. Table 2, for $S^{(0)} := 20$, i.e., the equilibrium case. We observe that profits quickly converge at a moderate level (16.43) compared to those in Table 2.

We varied different parameters of our model, such as the price granularity, the discount factor, and the initial strategy $S^{(0)}$. We found that mainly the initial strategy $S^{(0)}$ is responsible for pure equilibrium strategies to exist. In the context of Example 4 we obtain the same equilibrium, see Fig. 11, as long as $S^{(0)} \geq 18$. For $S^{(0)} < 18$ we obtain response cycles similar to Fig. 10.

Table 3. Expected profits $V_0^{(1)}(50)$ of firm 1 when its strategy $S^{(k)}$ is played against a strategy $S^{(j)}$, $k, j = 0, 1, 2, ..., 5$, $S^{(0)} := 20$; Example 4.

$S_1 \backslash S_2$	$S^{(0)}$	$S^{(1)}$	$S^{(2)}$	$S^{(3)}$	$S^{(4)}$	$S^{(5)}$
$S^{(0)}$	10.74	8.14	8.14	8.14	8.14	8.14
$S^{(1)}$	13.62	15.28	16.13	16.13	16.13	16.13
$S^{(2)}$	12.42	16.19	16.23	16.19	16.19	16.19
$S^{(3)}$	12.42	16.19	16.23	16.25	16.31	16.23
$S^{(4)}$	12.42	16.19	16.23	16.27	16.31	16.27
$S^{(5)}$	12.42	16.17	16.23	16.27	16.31	16.31

Remark 3. If the starting strategy is aggressive, i.e., characterized by low prices we do not obtain a pure strategy equilibrium. If the starting strategy is not aggressive, we usually obtain a pure strategy equilibrium. Furthermore, in case a pure equilibrium strategy exists it is of the structure described above, cf. Remark 2.

At the end of this section, we study how equilibrium strategies are affected by the discount factor. We consider the setting of Example 4. Figure 12 illustrates pure equilibrium strategies for five different discount factors between 0 and 0.99.

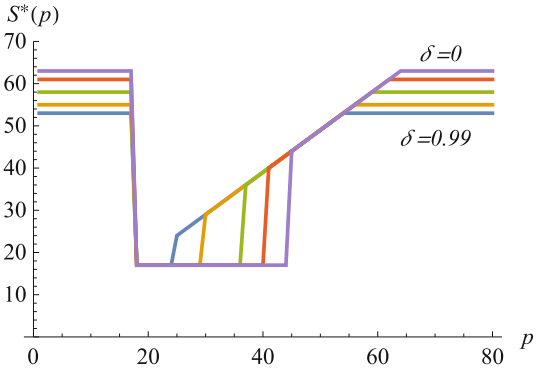

Fig. 12. Equilibrium strategies for different discount factors, $\delta = 0, 0.4, 0.7, 0.85, 0.99$, $h = 0.5$; Example 4.

We observe that for all S^* the mutual optimal response strategies δ is of the structure described above which is characterized by $(p_{min}, p_{med}, p_{max})$. While p_{min} is not affected by δ the thresholds p_{med} and p_{max} increase in δ. The range of the resulting staircase like price trajectories is hardly affected by δ but the level at which the price battle takes place is higher if δ increases.

7 Conclusion

The recent rise of e-commerce and the development of web technologies made it increasingly easy for merchants to observe market situations and automatically adjust their prices. Subsequently, more and more companies employ dynamic pricing strategies. In this paper, we analyze stochastic dynamic infinite horizon duopoly models characterized by active competitors. We set up a dynamic pricing model including discounting and shipping costs. The sales probabilities are allowed to arbitrarily depend on time, our price as well as the competitor's prices. Data-driven estimations of sales intensities under pricing competition can be used to calibrate the model.

Assuming that a competitor's response strategy is known, we show how to compute optimal reaction strategies that take advantage of price anticipations. As expected, it is often optimal to slightly undercut the competitor's price. However, when the price falls below a certain lower bound it is advisable to raise the price to a certain upper bound. Our optimized strategies optimally choose these critical price bounds. Optimized feedback strategies effectively avoid a decline in price. Especially, when competitors play aggressive strategies it is important to react in a reasonable way in order not to lose potential profits.

Furthermore, we analyze reaction times or price adjustments frequencies, respectively. We find that they have a huge impact on expected profits. To be able to adjust prices more often than the competitor does is a competitive advantage. Hence, the ratio of the competitors' prices adjustment frequencies is crucial for the firm's expected profits. Moreover, it can be profitable to strategically time price adjustments. In order not to use predictable reaction time firms should randomize their price adjustments. We show how to derive optimal response strategies when reaction times are randomized.

We also derive optimal response strategies if additional players are involved that employ fixed price strategies. We analyzed how the presence of such additional passive competitors affects the price battle of two active players that frequently adjust their prices. Our technique to compute prices is simple and easy to implement.

Finally, we evaluated expected profits of competing pairs strategies if both players apply optimized price reactions. In order to identify equilibrium strategies, we analyzed iterated strategy adjustments. Mutual strategy responses do not necessarily have to converge as pure strategy equilibria might not exist. However, pure equilibrium strategies can be identified by iterating mutual strategy responses. We found that as long as strategies are not too aggressive optimal strategy adjustments lead to equilibrium strategies. These strategies have a characteristic structure: in a certain price range it is optimal to undercut the competitor's price, otherwise it is optimal to either raise the price or force the competitor to restore the price level by significantly dropping the price.

In future research, we will use market data to estimate competitors' response strategies. We will also extend the model to study the sale of perishable products with inventory restrictions.

Appendix

Table 4. Notation table.

t	Time/Period
X	Random number sold items
G	Random future profits
c	Shipping costs
δ	Discount factor
F	Competitor's reaction strategy
Z	Number of passive competitors
A	Set of admissible prices
V	Value function
$V^{(c)}$	Competitor's value function
a	Offer price
$\boldsymbol{p}$	Competitors' prices
$\boldsymbol{z}$	Competitors' prices (fixed)
K	Number of competitors
λ	Sales intensity
P	Sales probability
$\boldsymbol{\beta}$	Logit coefficients
J	Cycle length
h	Reaction time
q	Reaction probability
$q^{(c)}$	Competitor's reaction probabilities
S	Response strategy

References

1. Maskin, E., Tirole, J.: A theory of dynamic oligopoly, II: price competition, kinked demand curves, and edgeworth cycles. Econometrica **56**, 571–599 (1988)
2. Noel, M.D.: Edgeworth price cycles, cost-based pricing, and sticky pricing in retail gasoline markets. Rev. Econ. Stat. **89**, 324–334 (2007)
3. Phillips, R.L.: Pricing and Revenue Optimization. Stanford University Press (2005)
4. Talluri, K.T., Van Ryzin, G.J.: The Theory and Practice of Revenue Management, vol. 68. Springer, New York (2004)
5. Yeoman, I., McMahon-Beattie, U.: Revenue Management: A Practical Pricing Perspective. Springer, Boston (2011)
6. Chen, M., Chen, Z.L.: Recent developments in dynamic pricing research: multiple products, competition, and limited demand information. Prod. Oper. Manage. **24**, 704–731 (2015)

7. Gallego, G., Wang, R.: Multiproduct price optimization and competition under the nested logit model with product-differentiated price sensitivities. Oper. Res. **62**, 450–461 (2014)
8. Gallego, G., Hu, M.: Dynamic pricing of perishable assets under competition. Manage. Sci. **60**, 1241–1259 (2014)
9. Martínez-de Albéniz, V., Talluri, K.: Dynamic price competition with fixed capacities. Manage. Sci. **57**, 1078–1093 (2011)
10. Yang, J., Xia, Y.: A nonatomic-game approach to dynamic pricing under competition. Prod. Oper. Manage. **22**, 88–103 (2013)
11. Wu, L.L.B., Wu, D.: Dynamic pricing and risk analytics under competition and stochastic reference price effects. IEEE Trans. Industr. Inf. **12**, 1282–1293 (2016)
12. Levin, Y., McGill, J., Nediak, M.: Dynamic pricing in the presence of strategic consumers and oligopolistic competition. Manage. Sci. **55**, 32–46 (2009)
13. Liu, Q., Zhang, D.: Dynamic pricing competition with strategic customers under vertical product differentiation. Manage. Sci. **59**, 84–101 (2013)
14. Adida, E., Perakis, G.: Dynamic pricing and inventory control: uncertainty and competition. Oper. Res. **58**, 289–302 (2010)
15. Tsai, W.H., Hung, S.J.: Dynamic pricing and revenue management process in internet retailing under uncertainty: an integrated real options approach. Omega **37**, 471–481 (2009)
16. Do Chung, B., et al.: Demand learning and dynamic pricing under competition in a state-space framework. IEEE Trans. Eng. Manage. **59**, 240–249 (2012)
17. Schlosser, R., Boissier, M.: Optimal price reaction strategies in the presence of active and passive competitors. In: Proceedings of the 6th International Conference on Operations Research and Enterprise Systems, ICORES, vol. 1, pp. 47–56 (2017)
18. Kephart, J.O., Hanson, J.E., Greenwald, A.: Dynamic pricing by software agents. Comput. Netw. **32**, 731–752 (2000)
19. Schlosser, R., Boissier, M., Schober, A., Uflacker, M.: How to survive dynamic pricing competition in E-commerce. In: Proceedings of the Poster Track of the 10th ACM Conference on Recommender Systems (RecSys 2016) (2016)
20. Boissier, M., Schlosser, R., Podlesny, N., Serth, S., Bornstein, M., Latt, J., Lindemann, J., Selke, J., Uflacker, M.: Data-driven repricing strategies in competitive markets: an interactive simulation platform. In: ACM Conference on Recommender Systems, pp. 355–357 (2017)
21. Serth, S., et al.: An interactive platform to simulate dynamic pricing competition on online marketplaces. In: 21st IEEE International Enterprise Distributed Object Computing Conference, EDOC, pp. 61–66 (2017)

Location-Scheduling Optimization Problem to Design Private Charging Infrastructure for Electric Vehicles

Michal Kohání[1(✉)], Peter Czimmermann[1], Michal Váňa[1]
Matej Cebecauer[2], and Ľuboš Buzna[1,3]

[1] Department of Mathematical Methods and Operations Research, University of Žilina, Univerzitná 8215/1, 01026 Žilina, Slovakia
{michal.kohani,peter.czimmermann,lubos.buzna}@fri.uniza.sk, michal.vana@gmail.com
[2] Department of Transport Science, KTH Royal Institute of Technology, Teknikringen 10, 100 44 Stockholm, Sweden
matej.cebecauer@gmail.com
[3] ERA Chair for Intelligent Transport Systems, University of Žilina, Univerzitná 8215/1, 01026 Žilina, Slovakia

Abstract. We propose optimization model to design a charging infrastructure for a fleet of electric vehicles. Applicable examples include a fleet of vans used in the city logistics, a fleet of taxicabs or a fleet of shared vehicles operating in urban areas. Fleet operator is wishing to replace vehicles equipped with an internal combustion engine with fully electric vehicles. To eliminate interaction with other electric vehicles it is required to design a private network of charging stations that is specifically adjusted to the fleet operation. First, to derive a suitable set of candidate locations from GPS data, we propose a practical procedure where the outcomes can be simply controlled by setting few parameter values. Second, we formulate a mathematical model that combines location and scheduling decisions to ensure that requirements of vehicles can be satisfied. We validate the applicability of our approach by applying it to data characterizing a large taxicab fleet operating in the city of Stockholm. The model assumes that all vehicles posses complete information about all other vehicles. To study the role of available information, we evaluate the resulting designs considering the coordinated charging when vehicle drivers, for example, reveal to each other departure times, and the uncoordinated charging when vehicle drivers know only actual occupation of charging points. Our results indicate that this approach can be used to estimate the minimal requirements to set up the charging infrastructure.

Keywords: Electric vehicles · Charging infrastructure
Urban areas · GPS traces

G. H. Parlier et al. (Eds.): ICORES 2017, CCIS 884, pp. 151–169, 2018.
https://doi.org/10.1007/978-3-319-94767-9_8

1 Introduction

Road transport is one of the major producers of the carbon dioxide (CO_2) which is the main greenhouse gas. Transport produces 20% of total carbon dioxide (CO_2) emissions. While these emissions decreased by 3.3% in 2012, they are still 20.5% higher than in 2011 and it could have been even more if there is no economic crises [1]. Stong influence on the carbon dioxide (CO_2) reduction have the generation of the electric energy as mentioned in [2]. One possibility how to reduce CO_2 emission in densely populated urban areas is to continue the process of electrification of individual and public transport together with the higher penetration of renewable sources of energy. Higher interest in converting large fleets of vehicles serving urban areas into electric can be caused by advances in battery technologies and continuously decreasing prices of electric vehicles over the next years. Although, the purchase of a new electric vehicle is connected with high purchasing cost, this obstacle can be easily compensated by lower operational costs. The expected benefits could be considerable due to the high utilization of such vehicles.

To avoid delays in charging, caused by interaction with other electric vehicles, a choice of a fleet operator can be to built the private charging infrastructure. Planning of charging infrastructure for electric vehicles is rapidly growing topic in the scientific literature over the last years. Researchers has been focusing on creating models to predict the future expansion of electric vehicles [3] as well as models designed to estimate the size of the future demand for charging vehicles [4]. An approach, where GPS traces of vehicles were used to extract the travel behaviour and hence to estimate the expected demand for charging vehicles, was used in [5–7]. Such analysis can provide valuable hints when searching for suitable positions of charging stations. The data driven approach to predict the penetration of EVs in the region of Lisbon and the future refuelling demand was proposed in [8].

Optimization algorithms have been often used to address this problem as well. A city transportation model to verify various locations of charging stations, which were generated by the genetic algorithm, was used in [9]. In [10] a bi-level approach was proposed. It combines the solution of the location problem (considering the capacity of charging stations) on the upper level, where the total costs and waiting time are minimized. To evaluate each design, the simulation approach is used on the lower level. This approach is iterative, i.e., it is repeated until the locations of charging stations do not change. Simulation can be used to estimate the expected number of vehicles successfully charged at each candidate location [11]. In the reference [12] was proposed an approach that allows for analysing the impact of public charging infrastructure deployment on the electric miles travelled. A genetic algorithm is used to find locations of charging stations and it is evaluated by the activity-based assessment method. In [13] authors developed the simulation-optimization approach where the area is divided into regions. The OD-matrix for the regions is known and it is used to estimate the EV flows between them. Linear IP model is used to determine the location

and size of the charging stations subject to the limited budget. Combination of a simulation approach with a genetic algorithm that utilizes GPS traces of vehicles was presented in [14].

Several authors considered a location problem constituting a mixed integer programming problem. For example, in [15] the demand for charging electric vehicles on public parking lots was estimated, based on a traffic survey conducted in the city of Seattle. The suitable location of charging stations was found by minimising the costs and the optimisation problem was solved by the general purpose optimisation solver. A similar methodology was also used for the city of Lyon [16] and the city of Coimbra [17]. When designing a network of charging stations, capacity constraints are typically included in the model [18–20] and apart from minimising costs, the area covered within the driving distance is maximised [4]. Methodologically different approach has been presented in [21]. Here authors considered constraints implied by the daily activity of car users and the capacity of electrical network and the location of charging stations were found by the clustering algorithm. The advantage of this approach is that several types of constraints can be taken into account simultaneously, without significantly affecting the computational complexity of the algorithm.

Special class of models was developed to cover trajectories of vehicles [22–24]. This approach is applicable in the design of the charging infrastructure along a highway network to cover long distance trips. An elegant (and simple) way how to locate charging stations along the paths, not to have larger distance between the neighbouring charging stations than is the maximum distance reachable by the electric vehicles, was proposed by [22]. The approach is based on adding artificial links to the network graph connecting places that fulfil some reachability rules. The model locates the minimum number of refuelling stations along paths to make the path traversal feasible. The approach [25] further extends [22] by considering multi-period case. Extension of this approach that considers multiple paths connecting origins and destinations of trips was proposed in [26] to take into account that vehicles can make short detours to reach a charging station.

Some authors considered this topic in the context of autonomous electric vehicles. An agent based simulation model was proposed in [27]. Model runs in two stages. In the first stage, the fleet size and the charging infrastructure is determined for an area that is characterized by the values of demographic indicators. In the second phase, the model is simulated for long enough time period in order to determine performance characteristics. Similar model presenting extended computational experiments was presented in [28].

Our contribution is the approach that is purely based on optimization where we combine location and scheduling problems and thus we avoid the need to validate the locations and capacity of charging stations by computer simulations. Because the approach is based on historic data it can be used to estimate the minimum design of the system that is sufficient to cope with various scenarios occurring in the past. Obtained results are evaluated by investigating the role of the available information.

This paper extends work presented in conference paper [29]. In order to improve and extend the paper we have introduced several amendments. We improved the description of the mathematical model and eliminated the unnecessary constraints that have not been taken into account in the numerical experiments. We have proposed a procedure to evaluate the role of available information and applied it to selected designs of the infrastructure. At the moment when drivers chose a charging station, they may possess various levels of information. We summarize our findings about the role of available information in the conclusions. We have re-run numerical experiments and we get optimal solutions in all test cases and we have improved the presentation of the results in all tables and figures.

The paper is organized as follow: in Sect. 2 we describe the data requirements and the methodology. In Sect. 3, we describe the data used in the case study and we introduce the results of numerical experiments. To conclude, we summarise our main findings in Sect. 4.

2 Methodology

2.1 Data Requirements

Suggested method requires low-frequency GPS data describing the mobility patterns of individual vehicles that belong to the fleet. Data have been collected for several, typical and sufficiently long-time periods representing relevant scenarios that should be included in the design of the charging network. The collection of low-frequency data is easy in practice as there is no need to use expensive GPS trackers. However, such data are not precise enough to determine the travel distances. Therefore, we need the second dataset - the graph model of the road network consisting of nodes and edges. This data helps estimating the travel distances more precisely.

2.2 Algorithm to Determine a Candidate Set for Charging Station Locations

In this section, we describe the method that we used to identify the set of places where the charging of electric vehicles is possible. Here, we do not wish to affect the actual trajectories that are taken by the vehicle drivers. Thus, the proposed method allows for the evaluation of the percentage of vehicles that could be transformed to electric vehicles without affecting their operation, with the minimal requirements on building the charging infrastructure. Therefore, we use the GPS data to identify the set of suitable candidate locations for the charging stations. Here, we aim to identify the locations where large numbers of vehicles frequently park. To do so, we propose the following two-phase procedure:

- Phase 1: Identify the set of candidate locations for charging stations as locations where many vehicles tend to park for a long time.
- Phase 2: Identify the set of vehicles that can be served by a selected set of candidate locations.

In the phase one, the following parameters are used: As a parking event we identify the time period, when the average speed of a vehicle is below the maximum speed limit V_{max} for at least the time period T_{min}. To ensure that we select a relevant set of candidate locations, we require that each candidate is associated with at least M_{min} parking events taking place in its circular neighbourhood defined by the radius of ρ_{max}. In the first phase, we process one-by-one the GPS traces of all vehicles executing the following steps (for illustration example see Fig. 1):

- Step 1: Identify in the GPS trace the traversals that have the average speed below the speed limit V_{max}.
- Step 2: Identify in the GPS trace the maximum connected sequences of traversals longer than the time period T_{min}.
- Step 3: Identify as a candidate location the last node of each connected sequence if there is no other candidate location within the distance ρ_{max}.

After processing all GPS traces we remove all candidate locations that are associated with less than M_{min} parking events.

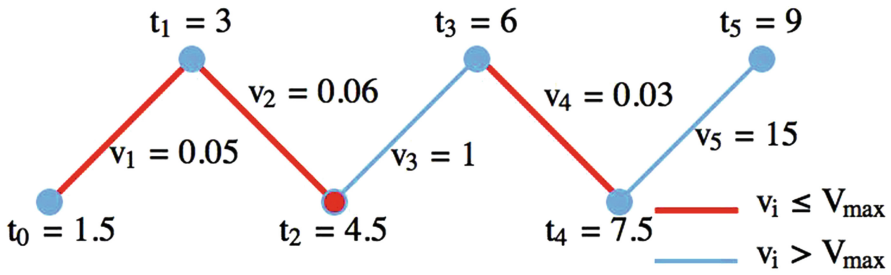

Fig. 1. Diagram illustrating the identification of candidate locations. Nodes represent the GPS position of the vehicle at the time t_i, links are traversals between two GPS positions. Red coloured links represent traversals where the average speed v_i is below the limit V_{max} and the red coloured node t_2 represents the candidate location. Node t_4 is not a candidate location because it does not fulfil the distance condition defined in the Step 3. Time t_i is in minutes, v_i is in meters per second and $V_{max} = 0.1$ m/s.

The second phase of the procedure evaluates the proposed set of candidate locations and identifies the set of vehicles that could be replaced by the electric vehicles. For each vehicle we evaluate its trajectory and we evaluate whether it could be sufficiently recharged during parking events, to cover the travel distances. Here, we consider the unlimited capacity of charging points being located in each candidate location. We assume that the capacity of each vehicle is β (measured in kilometres), i.e., it corresponds to the reachable driving distance. As a vehicle is driven its state of charge is decreasing according to the distance travelled. Charging speed is denoted by s. We record the number of vehicles that cannot be served by a given set of candidate locations. In the mathematical model, we consider only vehicles that can be recharged, otherwise the proposed mathematical model has no feasible solution.

2.3 Mathematical Model

Our goal is to minimize the costs that are required to set up the charging infrastructure, while ensuring that all vehicles identified in Phase 2 are satisfied. The costs are proportional to the number of charging points. Previous studies [11–13] indicated that an important requirement is to consider queueing behaviour of vehicles when they are charging. Hence, we formulate a location optimization problem, considering the scheduling problem to ensure that there exists a feasible schedule how to recharge vehicles.

We suppose that the algorithm from the previous section provides the set I of candidate locations where it is possible to locate the charging infrastructure. We split the time into the set T of non-overlapping time intervals. Then for each vehicle we distinguish two possible states (see Fig. 2). A vehicle is either parking at the candidate location and it is available for charging or it is located somewhere else where it cannot be charged.

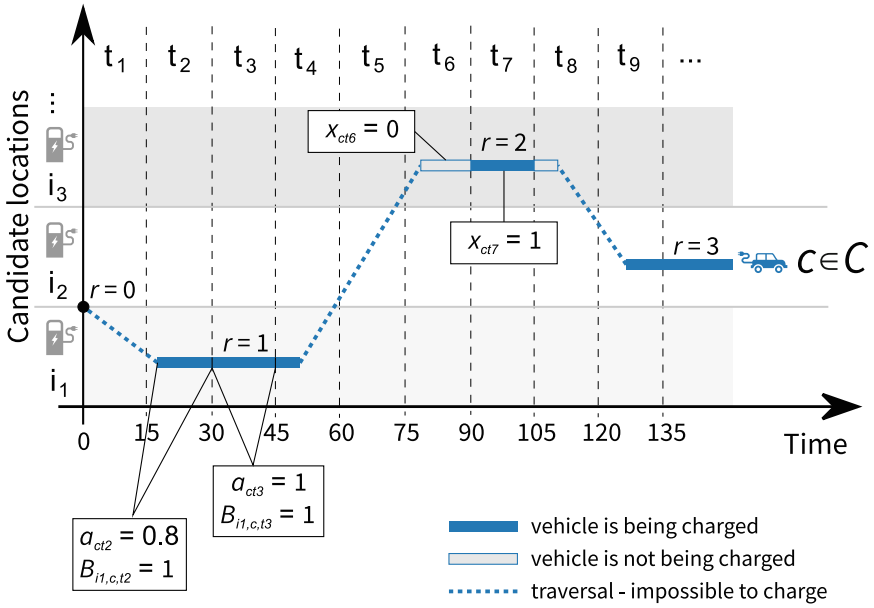

Fig. 2. Diagram illustrating the movement of an individual vehicle between the candidate locations. Vehicle is either parking at the candidate locations (filled or empty rectangles) and can be charged (filled rectangles) or it is located elsewhere and cannot be charged (dashed lines). Selected values of optimisation variables are shown to illustrate the modelling concept.

The fleet is composed of the set C of vehicles and each vehicle is equipped with a battery of capacity β. The capacity β is expressed as the distance in kilometres that the fully charged battery allows a vehicle to drive. This assumption is a

simplification of the model, however it is possible to find models with take into consideration the details of the EV operation, e.g. [30]. From the data we can obtain for each vehicle $c \in C$ an ordered sequence of parking events R_c and we determine the list N_{cr} of all time intervals $t \in T$ that have an overlap with the parking event $r \in R_c$. The fraction of the time interval $t \in T$ when the vehicle $c \in C$ is parking we denote by $a_{ct} \in \langle 0, 1 \rangle$. To simplify the description of the mathematical model we define $B_{itc} \in \{0, 1\}$, where $B_{itc} = 1$ if the vehicle $c \in C$ parks at the location $i \in I$ during the time interval $t \in T$, and $B_{itc} = 0$ otherwise. We use the graph of the road network to extract the information about the real travel distances. Vehicle $c \in C$ drives u_{cr} kilometres while driving from the parking event $r - 1$ to the parking event r. Each vehicle enters into the model with a fictive parking event $r = 0$ of zero duration and ends with a fictive parking event $r = r_c$ of zero duration. Decisions are described by the set of variables:

- $s_i \in Z^+$ for $i \in I$, representing the number of charging points placed at the location $i \in I$,
- $x_{ct} \in \{0, 1\}$ for $c \in C, t \in T$, where $x_{ct} = 1$ when vehicle $c \in C$ is being charged during the time interval $t \in T$ and $x_{ct} = 0$ otherwise, and
- $d_{cr} \geq 0$ for $c \in C, r \in R_c \cup \{0\} \cup \{r_c\}$ corresponds to the distance that the vehicle $c \in C$ at the beginning of the parking event $r \in R_c$ is able to drive.

We use this notation to formulate the location-scheduling problem that is shown in Fig. 3.

In the objective function (1) we minimize the number of located charging points. In each time interval we cannot use more charging points than specified by the set of constraints (2). We set the initial upper limit for the driving distance to $\alpha\beta$, where $\alpha > 0$ is the parameter of the model (see constraints (3)). Constraints (4) ensure that battery capacity is not exceeded and constraints (5) ensure contiguity of charging and discharging of batteries.

Model formulation

$$\text{Minimize} \sum_{i \in I} s_i \tag{1}$$

$$\text{subject to} \sum_{c \in C} B_{itc} x_{ct} \leq s_i \qquad \text{for } i \in I, t \in T \tag{2}$$

$$d_{c0} \leq \alpha\beta \tag{3}$$

$$d_{cr} + \sum_{t \in N_{c,r}} a_{ct} x_{ct} s \leq \beta \qquad \text{for } c \in C, r \in R_c \cup \{r_c\} \tag{4}$$

$$d_{cr} \leq d_{c,r-1} - u_{cr} + \sum_{t \in N_{c,r-1}} a_{ct} x_{ct} s \qquad \text{for } c \in C, r \in R_c \cup \{r_c\} \tag{5}$$

Fig. 3. Mathematical formulation of the location-scheduling optimization problem.

2.4 Evaluation of the Role of Available Information

In the mathematical model, we suppose that complete information about the charging requests of car drivers is available. The reality is, however, often different. We consider two approaches, which work with various levels of information (coordinated charging and uncoordinated charging). We consider the set $\overline{I} \subset I$ of all charging stations that contain at least one charging point (positions of charging points are found by solving the mathematical model). K_i is the set of charging points placed in station $i \in \overline{I}$ (we suppose that $0 \notin K_i$). R is the set of possible charging events (parking events), P is the set of taxicab journeys, and $E = R \cup P$ is the set of all events. The charging speed is denoted by s. If $e \in P$, then $l(e)$ is the driving distance. Vehicle associated with event $e \in E$ is denoted as $c(e)$. The start time and the end time of the event $e \in E$ are denoted by $b(e)$ and $z(e)$, respectively. The level of the battery of vehicle $c \in C$ is d_c. Parameter characterizing the maximum acceptable distance of a vehicle at the time of charging event from the charging station we denote ρ_{max}. T_k is the end time of the last charging event at the charging point $k \in K_i$ (for $i \in \overline{I}$). Evaluation procedure follows these steps:

Step 1: (Initialization)
For $c \in C$, set $d_c = \beta/2$. Initialize the value $k_{max} = 0$. Order events in E ascendingly with respect to the $b(e)$. Set $T_k = 0$ for $k \in K_i$ and $i \in \overline{I}$.
Step 2: (Event list processing)
For each $e \in E$ do:

If $e \in R$, then order the set $\overline{I}$ in descending order according to the number of charging points $k \in K_i$ that are free in time $b(e)$.
For $i \in \overline{I}$ do:

If distance of vehicle $c(e)$ at time $b(e)$ from station i is less than ρ_{max}, then process the charging event following either **coordinated or uncoordinated strategy**.

If $e \in P$, then set $d_{c(e)} = d_{c(e)} - l(e)$.

Step 3: (Evaluation)
Set $c \in C$ as feasible, if $d_c \geq 0$ all the time during the run of the algorithm.

Strategy of coordinated charging (Strategy 1): Identify the set $K_{full} = \{k \in K_i | (z(e) - max\{b(e), T_k\})s \geq \beta - d_{c(e)}\}$ of charging points where $c(e)$ can be fully charged.
If $K_{full} \neq \emptyset$:
Choose $k \in K_{full}$ and set
$T_k = b(e) + (\beta - d_{c(e)})/s$ and $d_{c(e)} = \beta$,
else:
Find $k_{max} \in argmax((z(e) - max\{b(e), T_k\})s)$, where $k \in K_i$.
If $k_{max} \neq 0$:
If $z(e) - max\{b(e), T_{k_{max}}\} > 0$:

Set $d_{c(e)} = d_{c(e)} + (z(e) - max\{b(e), T_{k_{max}}\})s$.
Set $T_{k_{max}} = z(e)$, $k_{max} = 0$ and continue with the step 2, and process the next event.

Strategy of uncoordinated charging (Strategy 2): Find $k \in K_i$ such that $T_k \leq b(e)$.
If $k \neq 0$:
Set $d_{c(e)} = max\{d_{c(e)} + (z(e) - b(e))s, \beta\}$. Set $T_k = z(e)$, $k = 0$ and continue with the step 2, and process the next event.

In Step 1, we initialize the values of some variables and order the elements of the set E. In Step 2, we process all events from the ordered set E. If e is a parking event, we choose a location $i \in \overline{I}$ considering the number of free charging points and the distance of the vehicle $c(e)$ from the location i. Charging stations and charging points are assigned to the vehicle $c(e)$ by either coordinated or uncoordinated charging strategy. If e is a journey, then the level of the battery of vehicle $c(e)$ is decreased by the value of the driving distance $l(e)$. In Step 3, we set the vehicle c as feasible, if the state of the battery remains all the time nonnegative.

Strategy of coordinated charging assumes that drivers posses information about charging points and know when the charging stations that are occupied will be freed, thus, drivers can selected those charging points where the batteries can be charged to the maximum capacity. Moreover, drivers are assumed to be cooperative, i.e., they unplug the vehicle when the charging is terminated.

When applying the strategy of uncoordinated charging, drivers choose the charging station $i \in \overline{I}$ with the largest number of free charging points at the time $b(e)$. The level of the battery of vehicle $c(e)$ is updated and the charging point is freed when the vehicle starts next journey.

3 Numerical Experiments

3.1 Data

In the case study we consider a fleet of more than 1,500 taxicabs operating in the area of great Stockholm, in Sweden. Each vehicle reported on average every 90 s its id, GPS position, time-stamp and information whether it is hired or not. In total, there is 8,989,143 probe data records, covering four selected weeks (see Fig. 4) representing different scenarios: Week 1 is a typical spring week with 1542 taxicabs. Week 2 represents typical summer week with 1526 taxicabs. Week 3 is the Christmas week with 1491 taxicabs and Week 4, with 1550 taxicabs, is a special week when the major disruption of the public transport occurred due to many failed railway connections.

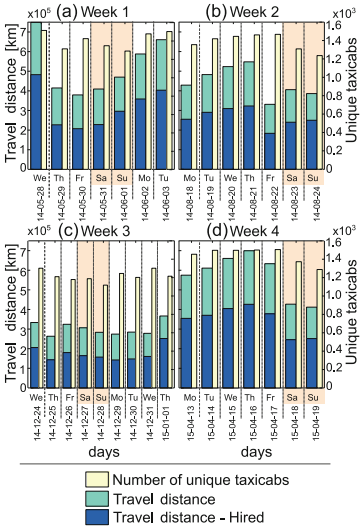

Fig. 4. The travel distance, the travel distance when the taxicabs are hired and the number of unique taxicabs for individual weekdays in Weeks 1–4. Figure is reproduced from the reference [29].

As the reporting frequency of probe data is relatively low, to be able to measure the travel distances more accurately, probes coordinates's are map-matched onto the road network and path is inferred, using the methodology proposed in [31]. The road network is used to estimate the travel distances. In the digital model of the road network each link is attributed a number of parameters, including the length, presence of a traffic signal, road class, speed limit and etc. Graph of the road network, used in the case study, consists of 231,839 links. To visualise the origin-destination flows of passenger trips between selected zones, we produced circular plots shown in the Fig. 5. In Fig. 5(a) are displayed relative values of origin-destination flows among the selected communes, covering both airports and extended Stockholm inner city. The majority of taxi trips is made inside the Stockholm commune, therefore, we created Fig. 5(b) considering only selected zones of the Stockholm's city centre.

3.2 Numerical Results: Mathematical Model

To test the proposed approach, we performed numerical experiments with the following values of parameters: the driving range of all vehicles was set to $\beta = 300$ km and the initial fraction of the driving range $\alpha = 0.5$. The charging speed was set to $s = 5$ km/min, the maximum speed limit for vehicles to be considered as parked $V_{max} = 0.1$ m/s and the associated time limit $T_{min} = 15$ min. In the mathematical model we discretize the time in steps of 15 min. Numerical experiments were performed on the computer equipped with CPU Intel (R) Core i7-5500U CPU with two 3 GHz cores and with 8 GB RAM. Mathematical model was solved using IP-solver

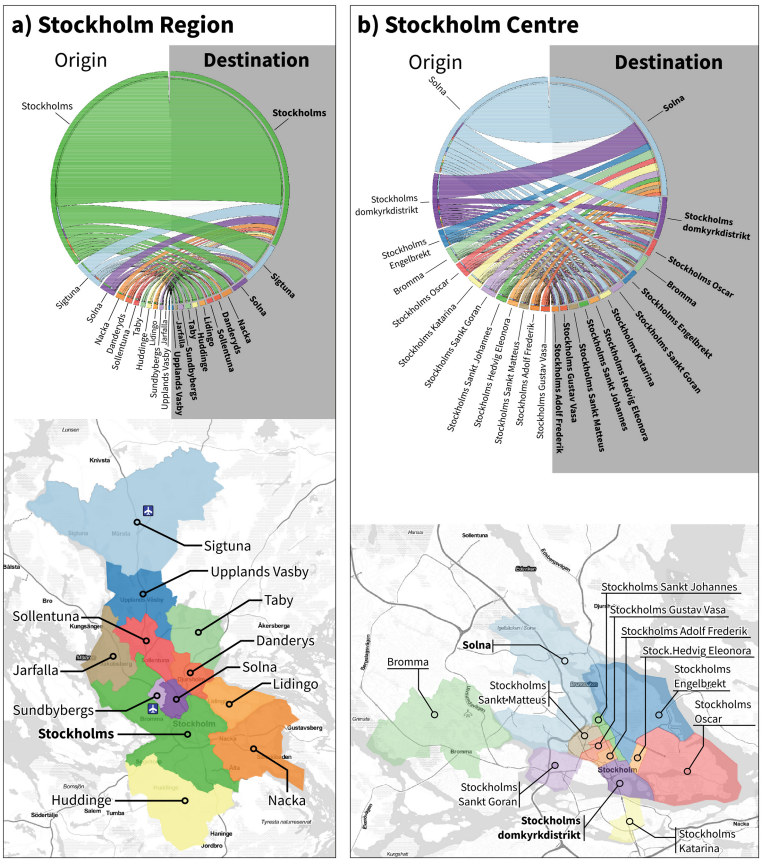

Fig. 5. Relative values of the origin-destination flows for selected zones (Weeks 1–4). Thickness of bands represents the proportion of taxicab trips that are in the data flagged as hired and start in the origin zone and terminate in the destination zone. (a) Selected administrative communes cover the area of extended Stockholm inner city till Arlanda Airport on the north-west that corresponds to the geographical area covered by the data. Most of the trips have both origin and destination in the city centre. (b) More detailed view at trips having both origin and destination in the city centre.

FICO Xpress IVE 7.3. Results of numerical experiments are shown in Tables 1, 2, 3 and 4. To explore various situations in scenarios, we selected the following values of input parameters: $\rho_{max} \in \{100, 500, 1000\}$ meters and $M_{min} \in \{100, 150, 800\}$ parking events. In tables we report the following output values: Column labelled as $|I|$ is the cardinality of the set of candidate locations identified in the Phase 1. The number of taxicabs that can be served by the set of candidate locations, determined in the Phase 2, is shown in the column denoted as $Cars$. Results of the optimisation process are summarized in the following columns: $Stations$ represents the number of located charging stations, CP_{total} is the total number of charging points and

CP_{max} represents the maximal number of charging points located in one charging station. Column $Time$ contains computational time in seconds. Running time of a single experiment was unlimited and for all tested instances we found the optimal solution. These results extend those presented in [29]. All numerical experiments were re-run without any limitation on computation time and all presented solutions are optimal. Heuristic methods to solve this type of problems can be found in [32].

Table 1. Results of numerical experiments for the scenario Week 1 - a typical spring week (1542 taxicabs).

ρ_{max}	M_{min}	$Cars$	$\mid I \mid$	$Stations$	CP_{total}	CP_{max}	$Time[s]$
100	800	609	3	3	14	9	1.88
	150	1186	27	27	37	6	3682.50
	100	1287	44	44	54	6	22.10
500	800	1102	5	5	20	10	46.05
	150	1442	46	40	44	5	4235.23
	100	1475	77	51	53	3	6987.36
1000	800	1347	6	6	17	5	13789.59
	150	1499	51	39	42	3	6532.00
	100	1510	70	48	50	2	27896.50

Table 2. Results of numerical experiments for the scenario Week 2 - a typical summer week (1526 taxicabs).

ρ_{max}	M_{min}	$Cars$	$\mid I \mid$	$Stations$	CP_{total}	CP_{max}	$Time[s]$
100	800	785	4	4	17	9	2.83
	150	1292	30	30	35	4	16.64
	100	1363	46	44	49	4	27.67
500	800	1188	5	5	17	7	8963.32
	150	1477	46	36	38	2	218.37
	100	1498	73	45	46	2	72563.65
1000	800	1409	8	8	19	5	6598.20
	150	1506	50	38	58	3	7896.50
	100	1513	69	46	59	2	36523.36

To verify the proposed approach, we visualised in Fig. 6 the resulting locations of charging stations for the scenario Week 1 and the parameter value $M_{min} = 150$ of parking events and two different values of parameter $\rho_{max} = \{100, 800\}$ in meters. From the map it is obvious that the charging stations are located at

Table 3. Results of numerical experiments for the scenario Week 3 - the Christmas week (1491 taxicabs).

ρ_{max}	M_{min}	$Cars$	$\mid I \mid$	$Stations$	CP_{total}	CP_{max}	$Time[s]$
100	800	449	2	2	4	2	0.34
	150	1019	24	24	27	2	2.84
	100	1094	36	36	37	2	6.83
500	800	843	4	4	5	2	6.17
	150	1324	39	37	39	2	46.86
	100	1359	57	52	53	2	291.05
1000	800	1172	6	6	11	2	27.80
	150	1417	43	38	39	2	547.72
	100	1445	65	47	48	2	898.37

Table 4. Results of numerical experiments for the scenario Week 4 - a special week with the major disruption of the public transport due to many failed railway connections (1550 taxicabs).

ρ_{max}	M_{min}	$Cars$	$\mid I \mid$	$Stations$	CP_{total}	CP_{max}	$Time[s]$
100	800	631	3	3	17	13	7.66
	150	1221	33	33	39	7	2753.50
	100	1325	50	49	53	5	38.21
500	800	1097	5	5	18	10	2632.63
	150	1491	50	40	42	3	3789.50
	100	1515	80	54	56	3	17856.36
1000	800	1408	9	9	21	6	1893.00
	150	1525	29	27	39	7	128.50
	100	1534	74	49	53	2	16589.30

sensible places with the large expected demand for transportation services such as airports, railway stations, ferry terminals and other public spaces located in the city centre. We observe that unless the set $|I|$ is very large, charging points are distributed over all candidate locations. While increasing the willingness of vehicle drivers to make a detour when visiting charging stations (expressed by the value of the parameter ρ_{max}), we observe that the number of vehicles that can be satisfied by the proposed layouts of charging stations is significantly growing. When the number of candidate location is large, we find only occasionally more than one charging point assigned to a charging location. Charging stations with more than one charging point we find to be located at airports or in the cite centre. We found similar results in all scenarios, with slightly smaller number of charging points in Week 3 where also the demand is smaller. The maximum

computational time was in all cases less than one day, what can be considered as a favourable outcome when dealing with strategic decision problems.

3.3 Numerical Results: Evaluation of the Role of Available Information

We used the mathematical model to suggest the layout of the charging infrastructure. The evaluation procedure allows us to simulate the operation of the charging stations in specific cases, when drivers make decisions following an incomplete information. We compare the optimization approach with situations when drivers posses various levels of information at the time when choosing a charging point. The results for Weeks 1–4 can be seen in Table 5.

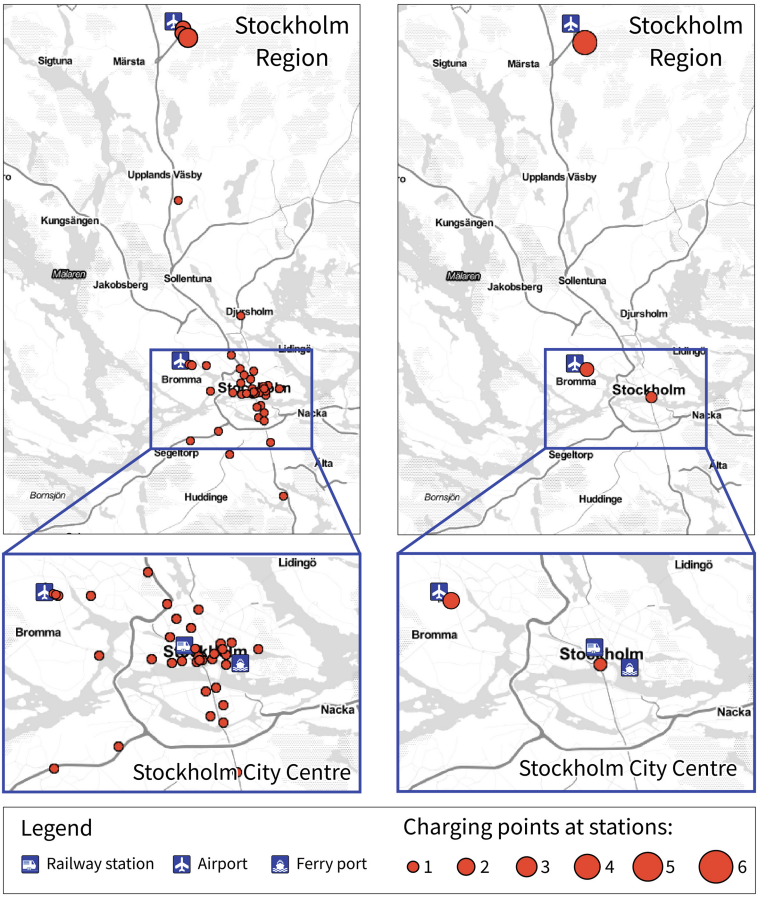

Fig. 6. Locations of charging points obtained for the scenario Week 1 and the values of input parameters $M_{min} = 150$ parking events and two different values of the parameter $\rho_{max} = 100$ m (left panels) and $\rho_{max} = 800$ m (right panels).

Columns ρ_{max} and M_{min} show the values of input parameters: ρ_{max} is the maximum acceptable distance between the parking position of a vehicle and a charging station to make charging possible, M_{min} is the minimum number of parking events that has to be assigned to a location to become eligible as a candidate for a charging station. In the remaining columns we report the number of vehicles, which is the outcome of Phase 2 (the same number of vehicles is also satisfied by the optimisation model); the number of vehicles that are satisfied by the coordinated charging (Strategy 1); and the number of vehicles that can be satisfied when applying uncoordinated charging (Strategy 2).

In Table 5, we observe a large difference in the numbers of feasible vehicles in columns Model and Strategy 1. This difference is caused by the different level of utilized information. In the mathematical model, all information about the future parking events of vehicles is available and it gets utilized. Furthermore, charging decisions are made for each time interval separately. Thus, a vehicle can interrupt the charging and allow other cars to charge and later continue with charging again. In Strategy 1, drivers start charging immediately when initiating the parking event. Drivers posses the information, about the actual

Table 5. Numbers of feasible vehicles obtained when solving the mathematical model (Model) and applying the evaluation procedure with the strategy of coordinated charging (Strategy 1) and the strategy of uncoordinated charging (Strategy 2).

Week 1 (1542 vehicles)					Week 2 (1526 vehicles)				
ρ_{max}	M_{min}	Model	Strategy 1	Strategy 2	ρ_{max}	M_{min}	Model	Strategy 1	Strategy 2
100	800	609	401	363	100	800	785	473	431
	150	1186	652	536		150	1292	623	599
	100	1287	689	586		100	1363	689	604
500	800	1102	592	589	500	800	1188	596	542
	150	1442	653	603		150	1477	699	687
	100	1475	709	695		100	1498	728	685
1000	800	1347	739	692	1000	800	1409	712	596
	150	1499	785	701		150	1506	748	632
	100	1510	793	706		100	1513	783	692
Week 3 (1491 vehicles)					Week 4 (1550 vehicles)				
ρ_{max}	M_{min}	Model	Strategy 1	Strategy 2	ρ_{max}	M_{min}	Model	Strategy 1	Strategy 2
100	800	449	189	163	100	800	631	369	347
	150	1019	436	398		150	1221	631	598
	100	1094	454	412		100	1325	678	642
500	800	843	385	316	500	800	1097	523	521
	150	1324	541	496		150	1491	687	589
	100	1359	559	498		100	1515	703	602
1000	800	1172	536	478	1000	800	1408	688	584
	150	1417	557	492		150	1525	726	632
	100	1445	589	499		100	1534	726	636

occupation of charging points and know the times when charging points are freed. This information is used to maximize the charged energy. Moreover, drivers are cooperative and they unplug the vehicle when it is fully charged. The only available information in Strategy 2 is the actual occupation of charging points at the time when drivers choose a charging point. As before, drivers start charging immediately when initiating the parking event. However, now drivers are careless and unplug their vehicles only when leaving for the next trip.

Systematically we find the difference between the numbers of feasible vehicles in columns Strategy 1 and Strategy 2 to be smaller than between the column Model and the columns Strategies 1 and 2. Thus, our results indicate the high importance of available information when assigning vehicles to charging points. Large benefit brings prioritization of vehicles, i.e., delaying the charging of some vehicles or interrupting charging and continuing it later again. Benefits of knowing when other drivers finish charging their vehicles and unplugging of vehicles when a vehicle is fully charged are not negligible, but not so pronounced.

4 Conclusions

In this contribution we present a method to deploy the charging infrastructure that is adapted to a fleet of electric vehicles operating in large urban areas. We assume that the operation of the fleet is described by the GPS traces that characterize the actual travel patterns of individual vehicles. In the first phase, we used a practical procedure to derive from GPS data a suitable set of candidate locations for charging stations, where the outcomes can be controlled by setting a few parameter values only. In the second phase, vehicles that can be served by the set of candidate locations are selected. Combining the location decisions together with the scheduling decisions we formulated the optimisation model. The model ensures that for a given minimal design there exists a time schedule that allows for satisfying requirements of all vehicles selected in the second phase. The limits of the proposed approach were tested by applying it to the real-world data that characterize the driving behaviour of a large taxicab fleet operating in the region of Stockholm. From numerical experiments we derived the following main conclusions:

- Our results indicate that this approach can be used to estimate the minimal requirements to set up the charging infrastructure. The proposed method is able to handle relatively large instances of problems independently on the scenario. All problems were solved on a personal computer in less than one day.
- Charging points are typically located at parking lots in the vicinity of airports, railways stations and other public spaces, which seem to be natural locations for them. Results show intuitive locations for charging stations and it seems to be better to use less complicated approach, however we weanted to include also capacity constraints for charging stations into the model what was allowed under the scheduling approach in the model.

- When comparing the results across selected scenarios we find similar numbers of located stations in Weeks 1, 2 and 4 and slightly smaller number of charging points in Week 3, which is the most quiet week.
- We did not limit the number of charging stations by adding a special constraint to the mathematical model. Hence, the number of charging stations was limited only by the set of candidate locations $|I|$. From the solutions we can see that if $|I|$ is large enough, the optimization model has the tendency to select the large set of charging stations with only few charging points more frequently than locating only few charging stations with many charging points. Such design can be also favourable for the electricity network as the stations will not load the network largely at few locations, but the load is spatially more distributed.
- Numerical experiments focused on the evaluation of the role of available information, when drivers choose a charging point, revealed that available information and cooperative behaviour of drivers have significant impact on the number of vehicles that the charging infrastructure is able to serve. Thus, our results suggest that methods being able to estimate well the future demand (e.g., time when vehicle drivers will free a charging point, arrival times of vehicles to the charging stations) and tools and technologies that can support organisation of the charging process together with incentive schemes facilitating cooperation between users have a potential to increase utilization and thus can lower investments into the charging infrastructure.

Acknowledgements. This work was supported by the research grants VEGA 1/0463/16 "Economically efficient charging infrastructure deployment for electric vehicles in smart cities and communities", APVV-15-0179 "Reliability of emergency systems on infrastructure with uncertain functionality of critical elements", TRENoP Strategic Research Area, and it was facilitated by the FP 7 project ERAdiate [621386] "Enhancing Research and innovation dimensions of the University of Žilina in Intelligent Transport Systems".

References

1. Europen Commision: Road transport: Reducing CO_2 emissions from vehicles (2015). http://ec.europa.eu/clima/policies/transport/vehicles/
2. Munoz-Villamizar, A., Montoya-Torres, J.R., Faulinc, J.: Impact of the use of electric vehicles in collaborative urban transport networks: a case study. Transp. Res. Part D Trans. Environ. **50**, 40–54 (2017)
3. Sears, J., Glitman, K., Roberts, D.: Forecasting demand of public electric vehicle charging infrastructure. In: 2014 IEEE Conference on Technologies for Sustainability (SusTech), pp. 250–254 (2014)
4. Yi, Z., Bauer, P.H.: Spatio-temporal energy demand models for electric vehicles. In: 2014 IEEE Vehicle Power and Propulsion Conference (VPPC), pp. 1–6 (2014)
5. Gennaro, M.D., Paffumi, E., Martini, G., Scholz, H.: A pilot study to address the travel behaviour and the usability of electric vehicles in two Italian provinces. Case Stud. Transp. Policy **2**, 116–141 (2014)

6. Paffumi, E., Gennaro, M.D., Martini, G., Scholz, H.: Assessment of the potential of electric vehicles and charging strategies to meet urban mobility requirements. Transportmetrica A Transp. Sci. **11**, 22–60 (2015)
7. Gennaro, M.D., Paffumi, E., Martini, G.: Customer-driven design of the recharge infrastructure and Vehicle-to-Grid in urban areas: a large-scale application for electric vehicles deployment. Energy **82**, 294–311 (2015)
8. Frade, I., Riberio, A., Goncalves, G., Antunes, A.: Optimal location of charging stations for electric vehicles in a neighborhood in Lisbon, Portugal. Transp. Res. Rec. J. Transp. Res. Board **2252**, 91–98 (2011)
9. Dickerman, L., Harrison, J.: A new car, a new grid. IEEE Power Energy Mag. **8**, 55–61 (2010)
10. Jung, J., Chow, J.Y., Jayakrishnan, R., Park, J.Y.: Stochastic dynamic itinerary interception refueling location problem with queue delay for electric taxi charging stations. Transp. Res. Part C Emerg. Technol. **40**, 123–142 (2014)
11. Sweda, T., Klabjan, D.: An agent-based decision support system for electric vehicle charging infrastructure deployment. In: 2011 IEEE Vehicle Power and Propulsion Conference, pp. 1–5 (2011)
12. Dong, J., Liu, C., Lin, Z.: Charging infrastructure planning for promoting battery electric vehicles: an activity-based approach using multiday travel data. Transp. Res. Part C Emerg. Technol. **38**, 44–55 (2014)
13. Xi, X., Sioshansi, R., Marano, V.: Simulation-optimization model for location of a public electric vehicle charging infrastructure. Transp. Res. Part D Transp. Environ. **22**, 60–69 (2013)
14. Tu, W., Li, Q., Fang, Z., Shaw, S.l., Zhou, B., Chang, X.: Optimizing the locations of electric taxi charging stations: a spatial-temporal demand coverage approach. Transp. Res. Part C Emerg. Technol. **65**, 172–189 (2015)
15. Chen, T., Kockelman, K., Khan, M.: Locating electric vehicle charging stations. Transp. Res. Rec. J. Transp. Res. Board **2385**, 28–36 (2013)
16. Baouche, F., Billot, R., Trigui, R., Faouzi, N.E.E.: Efficient allocation of electric vehicles charging stations: optimization model and application to a dense urban network. IEEE Intell. Transp. Syst. Mag. **6**, 33–43 (2014)
17. Cavadas, J., Correia, G., Gouveia, J.: Electric vehicles charging network planning. In: de Sousa, J.F., Rossi, R. (eds.) Computer-based Modelling and Optimization in Transportation. AISC, vol. 262, pp. 85–100. Springer, Cham (2014). https://doi.org/10.1007/978-3-319-04630-3_7
18. Nie, Y.M., Ghamami, M.: A corridor-centric approach to planning electric vehicle charging infrastructure. Transp. Res. Part B Methodol. **57**, 172–190 (2013)
19. Lam, A.Y.S., Leung, Y.W., Chu, X.: Electric vehicle charging station placement: formulation, complexity, and solutions. IEEE Trans. Smart Grid **5**, 2846–2856 (2014)
20. Ghamami, M., Nie, Y.M., Zockaie, A.: Planning charging infrastructure for plug-in electric vehicles in city centers. Int. J. Sustain. Transp. **10**, 343–353 (2016)
21. Momtazpour, M., Butler, P., Hossain, M.S., Bozchalui, M.C., Ramakrishnan, N., Sharma, R.: Coordinated clustering algorithms to support charging infrastructure design for electric vehicles. In: Proceedings of the ACM SIGKDD International Workshop on Urban Computing, UrbComp 2012, New York, NY, USA, pp. 126–133. ACM (2012)
22. MirHassani, S.A., Ebrazi, R.: A flexible reformulation of the refueling station location problem. Transp. Sci. **47**, 617–628 (2013)

23. Cruz-Zambrano, M., Corchero, C., Igualada-Gonzalez, L., Bernardo, V.: Optimal location of fast charging stations in Barcelona: a flow-capturing approach. In: 2013 10th International Conference on the European Energy Market (EEM), pp. 1–6 (2013)
24. Capar, I., Kuby, M., Leon, V.J., Tsai, Y.J.: An arc cover-path-cover formulation and strategic analysis of alternative-fuel station locations. Euro. J. Oper. Res. **227**, 142–151 (2013)
25. Chung, S.H., Kwon, C.: Multi-period planning for electric car charging station locations: a case of korean expressways. Euro. J. Oper. Res. **242**, 677–687 (2015)
26. Yıldız, B., Arslan, O., Karaşan, O.E.: A branch and price approach for routing and refueling station location model. Euro. J. Oper. Res. **248**, 815–826 (2016)
27. Chen, T.D., Kockelman, K.M., Hanna, J.P.: Proceedings of the 95th Annual Meeting of the Transportation Research Board (2016), and under review for publication in Transportation Research Part A (2015). With Donna Chen and Josiah Hanna. Transportation Research Part A (2015)
28. Fagnant, D.J., Kockelman, K.M.: The travel and environmental implications of shared autonomous vehicles, using agent-based model scenarios. Transp. Res. Part C Emerg. Technol. **40**, 1–13 (2014)
29. Kohání, M., Czimmermann, P., Váňa, M., Cebecauer, M., Buzna, L.: Designing charging infrastructure for a fleet of electric vehicles operating in large urban areas. In: Proceedings of the 6th International Conference on Operations Research and Enterprise Systems, ICORES, vol. 1, pp. 360–368 (2017)
30. Chau, C.-K., Elbassioni, K., Tseng, Ch.-M.: Fuel minimization of plug-in hybrid electric vehicles by optimizing drive mode selection. In: Proceedings of e-Energy 2016, pp. 13:1–13:11 (2016)
31. Rahmani, M., Koutsopoulos, H.N.: Path inference from sparse floating car data for urban networks. Transp. Res. Part C Emerg. Technol. **30**, 41–54 (2013)
32. Czimmermann, P., Buzna, L., Kohani, M.: Network flows as a tool for solving location-scheduling problem to optimize charging infrastructure for electric vehicles. In: Proceedings of APLIMAT 2018, pp. 280–289 (2018)

Approximate Dominance for Many-Objective Genetic Programming

Ayman Elkasaby(✉), Akram Salah, and Ehab Elfeky

Faculty of Computers and Information, Cairo University, Cairo, Egypt
ayman.kasaby@gmail.com,
{akram.salah,e.elfeky}@fci-cu.edu.eg

Abstract. In recent years, many-objective optimization has become a popular research topic, after it was noted that algorithms that excelled in solving problems with two objectives were not suitable for problems with more than three objectives. In these more difficult problems, selection pressure towards the Pareto front deteriorates, leading to most solutions becoming non-dominated to each other, which makes selection very difficult. To overcome this, approximate measures, for example epsilon-dominance, relax the competition criteria between solutions and make it easier to eliminate worse solutions that would otherwise be non-dominated. In this paper, epsilon dominance is combined with genetic programming to solve a many-objective optimization problem for the first time. Results show that this combination is promising.

Keywords: Genetic programming · Multiobjective optimization
Epsilon · Dominance · Evolutionary algorithms

1 Introduction

Evolutionary algorithms are efficient in solving specific optimization problems with a limited number (~ 2) of objectives, but it was noted that their accuracy worsens and they become increasingly slower when more objectives need to be optimized simultaneously. This led to a different set of problems, called many-objective optimization problems, which usually have a large number of objectives (more than 3). There is much demand for good algorithms for these problems, partly because most real life (especially industrial) problems are considered to have many conflicting objectives. The complexity and large costs of solving them are also additional reasons for the demand making it an active area of research.

To show the complexity of many-objective optimization problems, let's consider the simplest 2-objective problem [1]. For each point in the space of solutions, 4 regions can be defined as follows.

1. Region 'S' that contains solutions that are better than the point in question.
2. Region 'I' that contains solutions that are worse than the point in question.
3. Two regions where solutions are incomparable to each other at that point.

In order to generalize for many-objective problems, for a k-objective problem, there is a region 'S' with better solutions, a region 'I' with worse solutions, and $2^k - 2$

G. H. Parlier et al. (Eds.): ICORES 2017, CCIS 884, pp. 170–185, 2018.
https://doi.org/10.1007/978-3-319-94767-9_9

regions containing incomparable solutions. Additionally, assuming no bias towards any region, the probability of a solution falling into any of these regions is proportional to the volume of this region divided by the volume of the entire solution set. As the number of objectives increases, the number of regions increases, and the probability that a solution will fall into region 'S' is reduced significantly.

Many-objective optimization problems with a large number of objectives have a large number of regions with incomparable solutions, which means that, although they are apparently similar to problems with fewer objectives, they can't be solved efficiently using the same methods used for fewer objectives. They are computationally more intensive, and visualizing their solutions becomes harder as more objectives are added. To avoid the complexity of solving these problems exactly, some approximate measures are used to obtain good-enough results of the problem. Epsilon dominance, notated as ϵ-dominance from now on, is one of these approximate measures [2].

Solutions for many-objective optimization problems are usually not optimal solutions; they are good-enough solutions. This is due to the time restrictions imposed. Also, these solutions have to guarantee a degree of diversity within the solutions, to give various options for each objective to the decision maker.

In this paper, genetic programming, a flexible and powerful type of evolutionary algorithms that can generate programs that solve problems, is used in order to solve optimization problems approximately using ϵ-dominance. This method, called ϵ-GP, was first introduced in an earlier paper [3]. In the following sections, ϵ-GP is explained in more detail and then used to solve an optimization problem with 4 objectives (many-objective) instead of the 2-objective (multi-objective) problem used in the aforementioned paper. Genetic programming was also combined with two other popular algorithms to compare their performance with that of ϵ-GP. Genetic programming, up to our knowledge, has not been used before to solve many-objective optimization problems with an *approximate* measure. However, genetic programming has been recently used to solve many-objective optimization problems *without* approximate measures [4].

The paper is structured as follows. Section 2 starts the paper by giving an outline of related work in the field of evolutionary algorithms. Afterwards, in Sect. 3, some background information is given about optimization and ϵ-dominance. ϵ-GP is introduced in Sect. 4, while Sect. 5 deals with the experimentation and the method's results. Finally, Sect. 6 concludes the paper and lays down future work.

2 Related Work

Evolutionary algorithms (EAs) historically have been very successful in solving multi-objective optimization problems with fewer number of objectives. The need was clear though for better algorithms for problems with more objectives after Khare et al. [5] showed that 3 popular EAs (NSGA-II [6], SPEA2 [7], and PESA [8]) clearly had vulnerability in solving problems with more objectives.

According to a survey done by [9], which tracked the number of publications, until 2007, in correlation with the number of objectives in the problem that need to be optimized, problems with 2 objectives were usually considered to be the main research target, with 3- and 4-objective problems trailing. Problems with more than 4 objectives

had very few publications, and problems with more than 10 objectives were practically nonexistent in the literature.

However, in the last decade, the number of papers tackling many-objective optimization problems increased, as shown in Table 1 [10], which shows the number of papers in major conferences and journals tackling problems with at least 4 objectives.

Table 1. Number of papers focusing on many-objective optimization. (Source [3]).

Year	2007	2008	2009	2010	2011	2012	2013
CEC	17	11	13	14	9	15	16
GECCO	3	3	8	6	8	4	19
EMO	9	–	8	–	9	–	13
PPSN	–	6	–	7	–	2	–
TEC	3	2	4	4	3	3	4
ECJ	2	1	5	1	1	2	1
AIJ	0	0	0	0	1	0	2
Total	34	23	38	32	31	26	54

Many-objective optimization algorithms, created in the last decade, introduced different ideas to overcome the obstacles of problems with more objectives. Some recent popular algorithms for many-objective optimization include Nondominated Sorting Genetic Algorithm III (NSGA-III) [11], which is the latest iteration of the popular NSGA algorithm; Multi-Objective Evolutionary Algorithm based on Decomposition (MOEA/D) [12]; IBEA, the Indicator-Based Evolutionary Algorithm [13]; and Two_Arch2 [14], which uses two different storage archives: one for diversity and another for convergence.

3 Optimization

Solving optimization problems is done by choosing a best element, or elements, from the set of feasible alternatives. The solution is to maximize or minimize the value of the objective function(s) mentioned in the problem statement, by varying the input values that are fed into the objective function and choosing the best values. Many of these problems however exist in a setting that can't be expressed using a single function, as different objectives are usually not measured using the same metrics [3].

A multi-objective optimization problem is thus defined as simultaneously optimizing

$$F(x) = min(f_1(x), \ldots, f_k(x)), \quad subject\ to\ x \in \overline{X} \tag{1}$$

by changing n decision variables, subject to some constraints that define the universe $\overline{X}$.

In other words, a multi-objective optimization solution optimizes the components of a scalar $F(x)$ where x is an n-dimensional decision variable vector $x = (x_1, \ldots, x_n)$ from some universe $\overline{X}$. Thus, the problem consists of k objectives reflected in the k objective functions, a number of constraints on the objective functions reflected on the feasible set of decision vectors $\overline{X}$, and n decision variables. For an optimization problem to become a many-objective optimization problem, k has to ≥ 4.

In the case of optimizing multiple objectives, it may be impossible to find a single solution that optimizes all of the objectives at the same time. This gives rise to the definition of nondominated solutions (also called Pareto-optimal solutions). One solution dominates another if it is strictly better than the other in at least one objective, and not worse than the other in any objective. A solution is nondominated in some set of alternatives if no other alternative in the set dominates it. Visualizing the set of all the Pareto-optimal objective vectors gives what we call the Pareto front. Since these solutions are nondominated, no one solution exists that can be said to be better than the other; all of them are presented to the decision maker as a set of solutions called the Pareto set.

The primary goal of a multi-objective optimizer is to present nondominated solutions, while maintaining the following properties.

- A true Pareto set: the optimizer should present solutions that are as near to the 'true' Pareto front as possible.
- Diverse solutions: the optimizer should present a diverse set. However, diversity isn't an objective in the traditional sense, because it applies more to populations visited during search, not final solutions.
- Few solutions: the optimizer shouldn't overwhelm the decision maker with too many solutions to choose from; it should select the best few.

In the literature, previous work on multi-objective optimization rarely presented optimizers that present solutions that conform to all three properties [15].

3.1 ϵ-Dominance

Elitist EA optimizers (most multi-objective optimization algorithms introduced in the last two decades are elitist) usually sacrifice either returning diverse solutions or better solutions, or risk becoming very slow. Diversity preservation always looks toward empty regions that can have different solutions, and algorithms focusing solely on better solutions using dominance comparisons leave distribution unsolved and can fall into local minima. Algorithms insisting on both diversity and convergence to the Pareto front face Pareto sets of substantial sizes, need huge computation time rendering them unpractical, and are forced to present a large number of solutions to the decision maker which makes them useless until further analysis.

The concept of ϵ-dominance, introduced by Laumanns et al. [2], tries to solve the aforementioned problems by introducing solutions that are good enough, diverse, and few in number. ϵ-dominance approximates domination in the Pareto set by relaxing the strict regular definitions of dominance. ϵ-dominance divides the solution space into hyperboxes of size ϵ, and allows only one solution in each hyperbox. Typically,

this solution is the one dominating other solutions in this hyperbox. If multiple solutions are nondominated to each other, the solution closest to the lower-left side is chosen (in a minimization problem), which means that an individual can ϵ-dominate other individuals that would've been regularly incomparable to it. Domination is then checked between the representative solutions in each hyperbox, and the resulting nondominated hyperboxes are considered to be the best results of the run. The division of the solution space into hyperboxes is shown in Fig. 1.

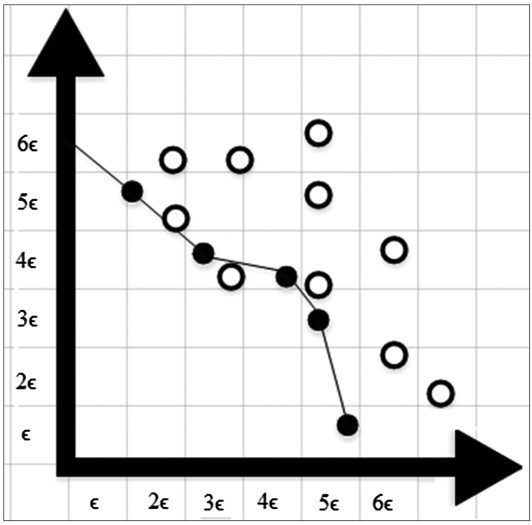

Fig. 1. The division of hyperboxes in ϵ-dominance. The dark circles are the ϵ-nondominated solutions in each hyperbox.

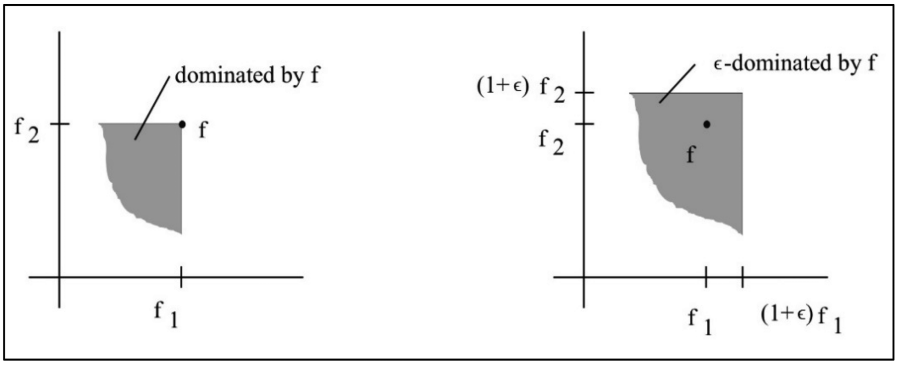

Fig. 2. The difference between (a) regular dominance. (b) ϵ-dominance. (Source [3]).

In Fig. 2 [2], a visual comparison between ϵ-dominance and regular dominance is shown. It makes the differences between regular and epsilon dominance clear. Regular dominance is shown to have very specific and strict rules for defining dominance between two points, while ϵ-dominance relaxes dominance definitions by dividing the solution space into hyperboxes. This results in less competition between points, which makes it quicker, although it could sometimes be less accurate if the value of ϵ is inappropriate or if the decision maker seeks more variable solutions.

3.2 More Objectives

When a problem has more than 3 objectives, it is usually considered a many-objective optimization problem, as opposed to a multi-objective optimization problem (3 or less objectives). Industrial problems usually have many objectives and are the main target of many-objective optimization. Some difficulties of solving problems with more objectives are:

1. Visualization of a Pareto-optimal frontier that is more than three-dimensional is difficult.
2. If the dimensionality of the objective space increases, the dimensionality of the Pareto front increases, and also there will be a greater proportion of nondominated solutions in the population as explained previously.
3. Due to (2), an exponential number of points will be needed to represent the Pareto-optimal front. If N points are needed to represent a one-dimensional Pareto-optimal front, and there exist M objectives, then $O(N^M)$ points will be needed to represent an M-dimensional Pareto-optimal front.
4. Stagnation of the search process due to the larger number of incomparable solutions.
5. Large computational cost.

The first point of difficulty, visualization of the Pareto-optimal frontier, has been handled by some proposed techniques in the literature by mapping objective vectors into a lower dimensional space [16]. On the other hand, the second and third points of difficulty can be tackled by adding preference information into the solving algorithms. Preference information is added so that the algorithms can focus on finding solutions from specific, more-desired regions of the Pareto front [17].

Our work in this paper tries to circumvent the drawbacks of the 2nd, 3rd, 4th points by changing the definition of dominance to an approximate one, tolerating a bigger number of nondominated solutions and a higher-dimensional Pareto front. Lastly, the constant improvement of computing power in the real world has lessened, to a degree, the impact of the large computational cost needed for visualization and finding solutions.

4 Our Proposed Method (ϵ-GP)

Our algorithm, ϵ-GP, uses strongly-typed genetic programming [18], which is based on genetic programming (GP). GP is a subset of evolutionary algorithms that represents solutions as programs [19]. This representation differentiates genetic algorithms from genetic programming. Each solution (program) is judged based on its ability to solve the problem, using a mathematical function called a fitness function. Each program is represented using a decision tree. Two basic genetic programs (decision tree) that resemble the equations $6 + ((x + 4) * (3 + 2))$ and $x - 20$ are shown in Fig. 3. GP evolves a population of programs by selecting some candidates that score high on the fitness function and using variation operators on them (mutation, crossover, and reproduction). New populations are created from these outputs until a specific termination criterion is met.

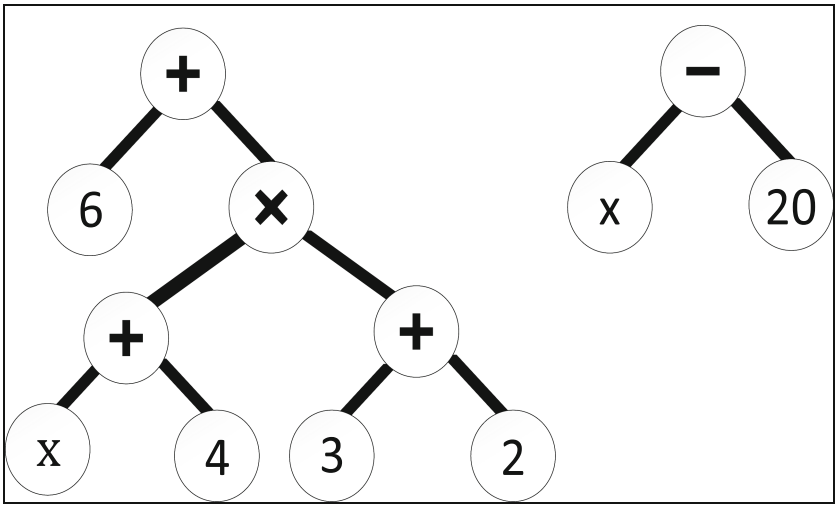

Fig. 3. Two decision trees, used in genetic programming.

The pseudocode of ϵ-GP is shown in Fig. 4. It consists of the following components.

1. Representation: individuals are represented as decision trees using terminals and nonterminals. Strong typing doesn't restrict variables, constants, arguments for functions, and values returned from functions to be of the same data type. The data types need to be specified beforehand though. Additionally, to ensure consistency, the root node of the tree must return a value of the type specified by the problem definition and each nonroot node has to return a value of the type required by its parent node as an argument.
2. Fitness function: this function scores how well the solutions in the population match expected results.

```
for i := 1 to number_of_runs do
  generation := 0
  initialize pop[generation] //population
  check_dominance()
  insert ϵ-nondominated solutions into arxiv
  while (generation < max_generations) do
    check_dominance();select ϵ-nondominated solutions
    for j := 1 to pop_size do
      probability := random(0,1)
      if (probability >= prob_crossover) then
        select individual from pop based on fitness
        j := j+1
        if (probability >= 1 - prob_mutation) then
          mutate individual
        else
          reproduce (copy) individual
        end
        insert individual into pop[generation+1]
      else
        select 2 individuals from pop and arxiv
        perform crossover between both individuals
        insert result into pop[generation+1]
      end
      if (new individual ≺ϵ individuals in arxiv) then
        replace individual in arxiv with new
individual
        remove any newly ϵ-dominated solutions in
arxiv
      end
    end
    generation := generation+1
  end
  result[i] := archive
  run := run+1
end
present result[] to decision maker
```

Fig. 4. Pseudocode of ϵ-GP.

3. Initialization: there are two main methods to initialize populations: full and grow. Koza [19] recommended using a ramped half-and-half approach, combining the two methods equally. The full method requires all paths from the root to any leaf to have the same length. The grow method doesn't have this requirement. Using the method in Fig. 5, each tree is generated recursively. All return values and arguments ensure consistency and are forced to match the types specified when stating the problem.

```
Input: max_depth := 5, generate_method := random(0,1)
generate_tree(max_depth, generate_method)
begin
 if (max_depth == 1) then
   tree_root := randomly chosen terminal
 else if (generate_method > 0.5) then   //full method
   tree_root := randomly chosen nonterminal
   foreach argument of nonterminal run
   generate_tree(max_depth - 1, generate_method)
 else
   node_type = random(0,1)  //terminal or nonterminal
   if (node_type > 0.5) then
     tree_root := randomly chosen terminal
   else
     tree_root := randomly chosen nonterminal
     foreach argument of nonterminal run
     generate_tree(max_depth - 1, generate_method)
   end
 end
end
```

Fig. 5. Initialization of trees using ramped half and half.

To generate trees of different sizes and shapes, the maximum tree depth is varied between 2 and max_depth.

4. Selection: the selection of individuals in the population to undergo crossover or mutation is achieved using a mixture of tournament selection and hyperbox-based ϵ-dominance. First, the solution space is divided into hyperboxes of size ϵ (shown in Fig. 1), computed by the algorithm in Fig. 6, and from each hyperbox a number of solutions are randomly selected, and from these solutions the ϵ-nondominated solutions are chosen for genetic operations (crossover or mutation) according to the algorithm outlined in Fig. 4. The use of tournament selection along with hyperboxes is aimed to ensure diversity between solutions, representing areas in the solution space that otherwise wouldn't be represented.
5. Genetic operators: crossover and mutation are the genetic operators used.
   a. Crossover starts by choosing two parents for reproduction. A crossover point is selected from the first parent randomly, followed by finding a set of all nodes that can satisfy constraints on return values and values of arguments from the first crossover point. A second parent is then selected from this set; otherwise, if no such set exists, either the parent is returned or nothing. Crossover is always performed between a solution from the current generation population and a solution from the archive. This guarantees both elitism and diversity
   b. Mutation works by randomly selecting a point and replacing it with a new subtree generated by the algorithm outlined in Fig. 5. If generation of a subtree with valid data types is impossible, mutation returns the parent or nothing.

6. Parameters: these include maximum tree depth, maximum initial tree depth, max mutation tree depth, population size, and termination criteria.

```
Input: solution x,y; hyperboxes of size ϵ
check_dominance(x,y,ϵ)
begin
  box(x) := x/ϵ   box(y) := y/ϵ
  if (box(x) ≺ box(y)) then
    x ≺ y                //x dominates y
  else if (box(x) ≺ box(y)) then
    y ≺ x                //y dominates x
  else
    check for regular dominance between x and y
    pick nondominated (or closer to corner) solution
  end
end
```

Fig. 6. Checking for ϵ-dominance between two solutions.

Additionally, the performance of ϵ-GP, and of any ϵ-dominance-based EA, depends on the value of ϵ, which is either user defined or computed from the number of solutions required. Bigger ϵ values mean less competition between solutions, as one solution ϵ-dominates a bigger area of other solutions. Although the value of ϵ doesn't have to be constant for each objective, we make it constant across all objectives in our method for ease of use.

ϵ-GP incorporates elitism by having two different storage locations for solutions:

- An archive that ensures elitism by keeping the best solutions so far and removing solutions iff other better solutions are found.
- A population that stores the current generation; this current generation can have worse solutions than a previous generation after crossover and mutation are finished. This encourages diversity and keeps us from falling into local minima if, after some generations, the worse solution's offspring turn out to be more optimal solutions.
- Offspring from crossover are embedded into the archive if the criteria of acceptance (to ϵ-dominate another solution) are met. They are automatically inserted into the next generation population as well.

5 Experimentation

To measure the performance of our algorithm, it was tested on a popular genetic programming problem: the ant trail problem, with two of its variants: the Santa Fe Trail problem and the more difficult Los Altos Trail problem [19]. The study used the MOEA Framework [20]. The set of terminals and nonterminals used for both ant trail problems can be found at Table 2.

Table 2. Terminals and nonterminals in the ant trail problem.

Terminals	Nonterminals
TurnLeft()	If-Else-then
TurnRight()	Sequence (two subtrees to run in sequence)
MoveForward()	Default logic (*and*, *or*, *not*, $=$? $>$, $<$, $\leq$, $\geq$)
IsFoodAhead()	Arithmetic ($+$, $-$, $\times$, $\div$, %, ^, $\sqrt{}$, log x)
Mathematical constants ($-1, 0, 1, etc.$)	Trigonometric functions (sin$x$, cos$x$, tan$x$)
π	$-ve$ sign
	e^x

NSGA-II [6] and IBEA [13] are both combined with GP to test our proposed method against them. This was achieved by adding the solution representation and evolutionary operators of GP to it. They will be, respectively, referred to from now on as NSGA-GP and IBEA-GP. Our algorithm was used with values of ϵ of 0.1 and 0.01.

We solved each test problem 30 times with different random seeds. In all runs, no more than 250,000 evaluations were allowed to be made. We used a crossover probability rate of 0.9, with a point mutation rate at 0.01. Population size was set to 1024. The maximum number of moves an ant can take is 500, and the number of generations per run is 50.

Table 3. IGD results.

IGD		NSGA-GP	IBEA-GP	$\epsilon = 0.1$	$\epsilon = 0.01$
Santa Fe	*Min*	0.03514	0.16	**0.009359**	0.015
	Median	0.074297	0.19498	**0.0246738**	0.027
	Max	0.164658	0.3372	**0.065229**	0.1055
Los Altos	*Min*	0.0227	0.189	**0.01116**	0.019
	Median	0.1617	0.236	0.0484	**0.04338**
	Max	0.20629	0.42	0.11746	**0.11356**

There are four objectives in our version of the problem. The first is to minimize the number of moves the ant takes as much as possible. The second is to maximize the number of captured pieces of food. The third objective is to minimize the amount of turns an ant takes, making it more efficient. This means that an ant that moves in a

straight line is better than one that turns multiple times. The last objective is to maximize the weight; each food piece has a fixed weight, so we maximize weight by encouraging collecting higher-weight food pieces.

The ant can be visualized as a robot in a room, trying to collect all the inventory it can find, with moves and turns consuming power that we try to minimize. The inventory in the room are of different weights as well, with larger weights preferred.

To investigate performance, we choose the Inverted Generational Distance (IGD) [21] as the main performance measure. IGD measures how far away the result is from the Pareto optimal set. If IGD equals zero, that would mean that the result lies on the Pareto front and covers all of it. This means that a smaller IGD value is better.

In Table 3, the values of the IGD metric are shown for NSGA-GP, IBEA-GP, and our algorithm, ϵ-GP, with values of ϵ of 0.1 and 0.01. The results shown are over all 30 runs, and the best results for each metric are shown in bold. They show that our algorithm, ϵ-GP, has better performance with lower IGD values. ϵ-GP overall reaches Pareto sets that are closer to the Pareto front than either of the other algorithms.

In both the Santa Fe and Los Altos problems, the minimum, maximum, and median IGD values are significantly better for our algorithm using both ϵ values of 0.1 and 0.01. In fact, the median IGD value is an order of magnitude better for ϵ-GP with $\epsilon = 0.01$ than both NSGA-GP and IBEA-GP in the more difficult Los Altos problem.

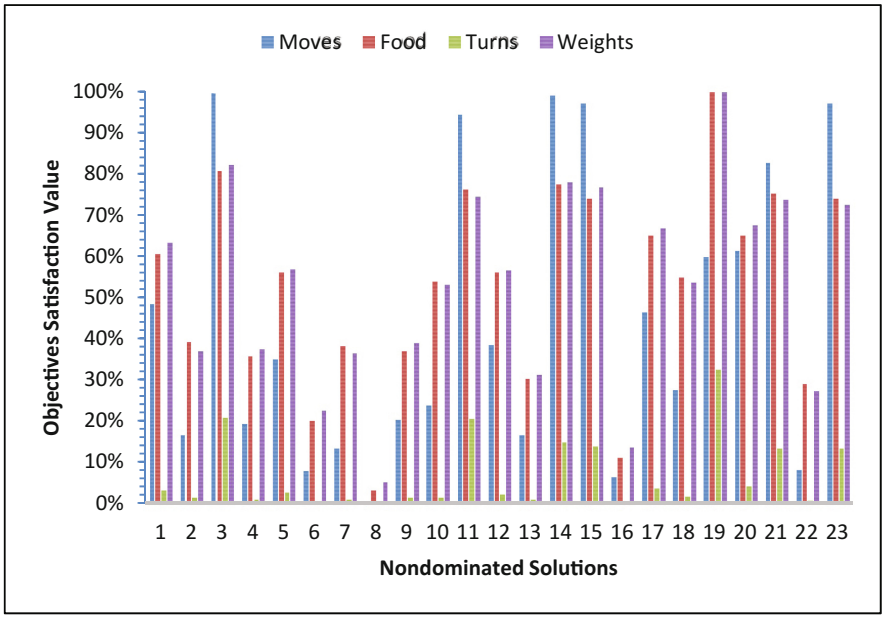

Fig. 7. The set of nondominated solutions resulting from a run of ϵ-GP with $\epsilon = 0.01$.

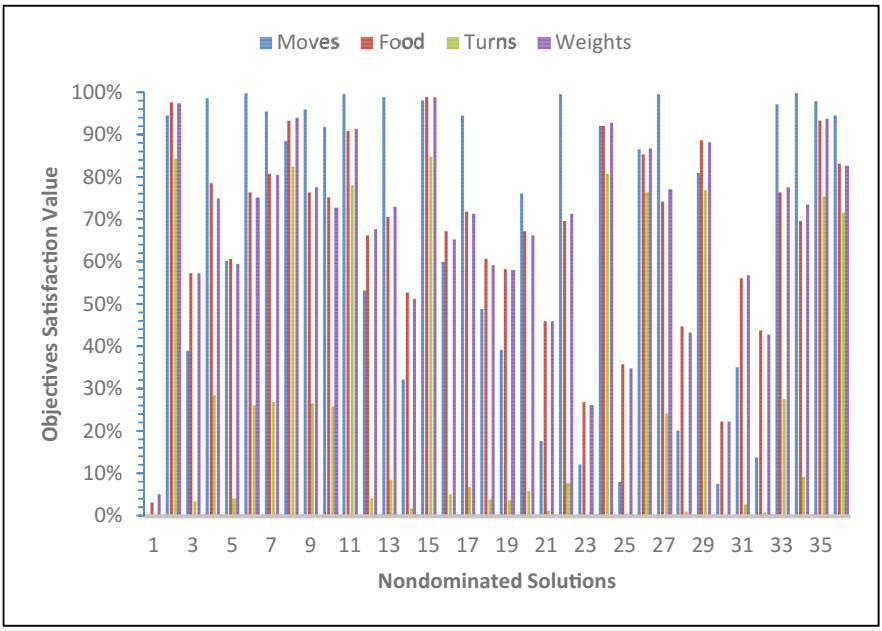

Fig. 8. The set of nondominated solutions resulting from a run of ϵ-GP with $\epsilon = 0.1$.

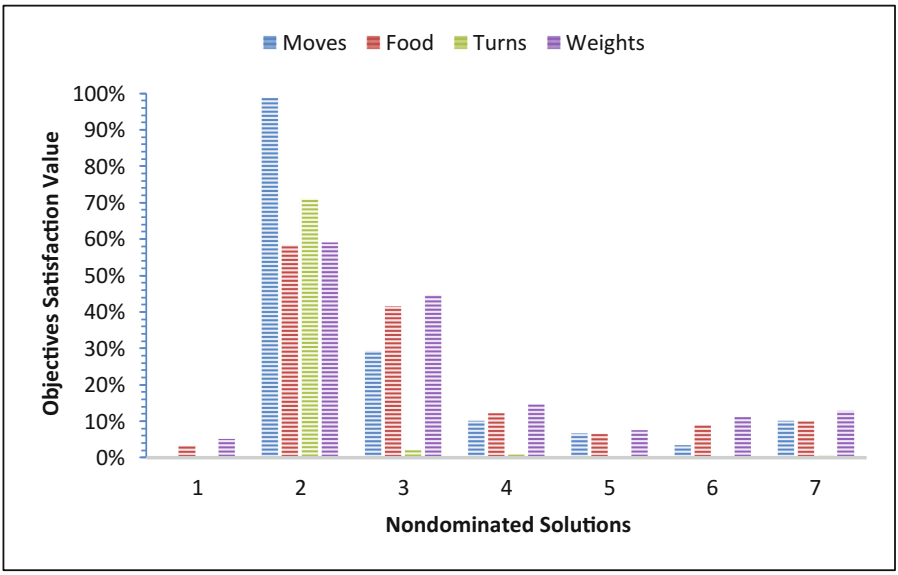

Fig. 9. The set of nondominated solutions resulting from a run of NSGA-GP.

In Figs. 7, 8 and 9, the nondominated resulting front for the Santa Fe Trail problem from a representative run for ϵ-GP, with ϵ values of 0.1 and 0.01, and NSGA-GP are presented, to show the edge our algorithm presents with regards to presenting diverse and accurate solutions. It is clear from comparing the abovementioned figures that ϵ-GP presents more diverse Pareto sets, both in number and in values in comparison to NSGA-GP. IBEA-GP wasn't presented in a figure as it only presents one (and rarely two) solution each run, which isn't optimal for decision makers that seek diverse trade-off solutions. However, the solution it presents is usually of acceptable quality, optimizing all objectives as much as possible.

An additional advantage of ϵ-GP is its quick runtime. The runtime of IBEA-GP in comparison is an order of magnitude slower than ϵ-GP, which is a huge drawback. IBEA-GP usually took an average of $\sim$13 min for each run, versus an average runtime of less than 30 s for ϵ-GP with either ϵ values. NSGA-GP keeps its relatively quick runtime in our runs. It averaged $\sim$38 s per run. The above runtimes are for the Santa Fe trail problem.

On the other hand, for the Los Altos trail, the runtimes of IBEA-GP and NSGA-GP were similar, while for ϵ-GP it increased to about $\sim$37 s per run, which is still significantly better than IBEA-GP and equal to NSGA-GP.

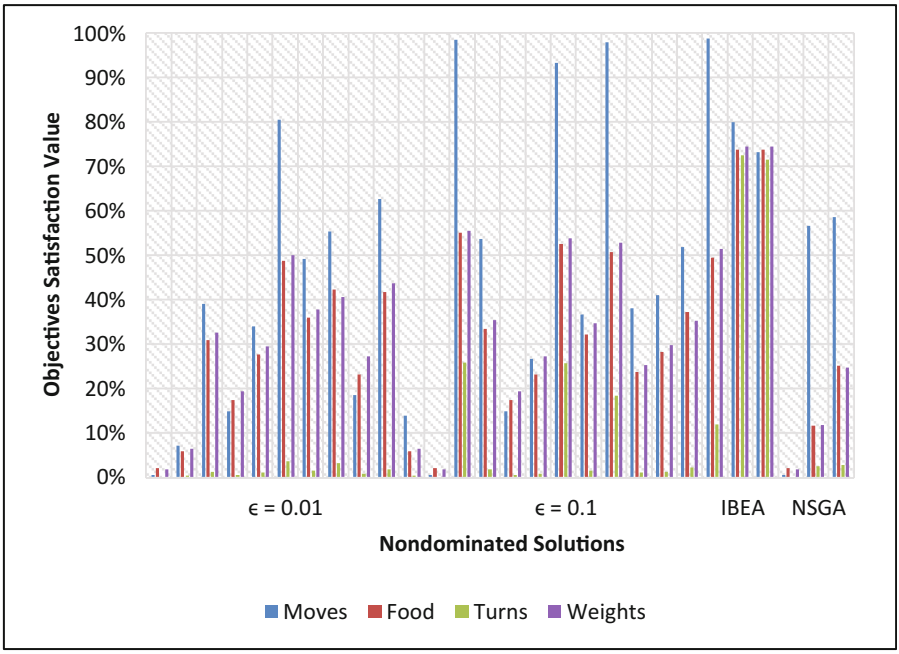

Fig. 10. The set of nondominated solutions for the Los Altos problem from all algorithms.

In Fig. 10, the Pareto set of each algorithm is shown for a sample run. NSGA-GP results in the last three solutions, IBEA-GP in the two solutions preceding those, while ϵ-GP is responsible for the rest of the solutions. The first 10 solutions are for an ϵ value of 0.01, while the following 13 solutions are for an ϵ value of 0.1. Once again, the resulting Pareto set is better in both diversity and convergence for ϵ-GP than either of the other algorithms, which serves its purpose of delivering a diverse set of trade-off solutions for a decision maker. IBEA-GP results in only two solutions in its run, although they score well in all objectives. NSGA-GP results in three weak solutions, especially for the objectives to be maximized.

6 Conclusions and Future Work

The results show that ϵ-GP is a promising algorithm that can simultaneously optimize more than one objective, with the algorithm guaranteeing competitive results in all objectives. The results are a good starting point as genetic programming, up to our knowledge, has never been used to solve a many-objective optimization problem alongside an approximate measure.

As problems increase in difficulty, the tolerance of a high ϵ value starts to decrease and problems can take longer times to find high-quality solutions and can face a possibility of falling into local minima due to the discarding of many solutions. Therefore, choosing the value of ϵ is very important.

Furthermore, future work includes the following:

- since the value of ϵ is important for the method to produce significant results, a prioritized variable ϵ value for each objective can make the method better, which calls for an algorithm that can dynamically choose different ϵ values for the objectives to optimize better;
- dominance can be changed to mean that a solution dominates another if it is better in *more* objectives, even if it is *worse* in other objectives [22]. This can possibly speed up the process of getting a Pareto set by dramatically decreasing the competition between solutions, resulting in the acceptance of good-enough solutions that were discarded previously that could've been useful to the decision maker;
- A more detailed study with more test-set problems is needed to further prove that ϵ-GP is an efficient many-objective optimizer.

References

1. Giagkiozis, I., Fleming, P.J.: Methods for multi-objective optimization: an analysis. Inf. Sci. **293**, 338–350 (2015)
2. Laumanns, M., Thiele, L., Deb, K., Zitzler, E.: Combining convergence and diversity in evolutionary multiobjective optimization. Evol. Comput. **10**(3), 263–283 (2002)
3. Elkasaby, A., Salah, A., Elfeky, E.: Multiobjective optimization using genetic programming: reducing selection pressure by approximate dominance. In: Proceedings of the 6th International Conference on Operations Research and Enterprise Systems, Porto (2017)

4. Masood, A., Mei, Y., Chen, G., Zhang, M.: Many-objective genetic programming for job-shop scheduling. In: 2016 IEEE Congress on Evolutionary Computation (CEC), Vancouver (2016)
5. Khare, V., Yao, X., Deb, K.: Performance scaling of multi-objective evolutionary algorithms. In: Fonseca, C.M., Fleming, P.J., Zitzler, E., Thiele, L., Deb, K. (eds.) EMO 2003. LNCS, vol. 2632, pp. 376–390. Springer, Heidelberg (2003). https://doi.org/10.1007/3-540-36970-8_27
6. Deb, K., Pratap, A., Agarwal, S., Meyarivan, T.: A fast and elitist multiobjective genetic algorithm: NSGA-II. Evol. Comput. **6**(2), 182–197 (2002)
7. Zitzler, E., Laumanns, M., Thiele, L.: SPEA2: improving the strength pareto evolutionary algorithm. In: Computer Engineering and Networks Laboratory (TIK), Swiss Federal Institute of Technology (ETH) Zurich, Zurich (2001)
8. Corne, D.W., Knowles, J.D., Oates, M.J.: The pareto envelope-based selection algorithm for multiobjective optimization. In: Schoenauer, M., Deb, K., Rudolph, G., Yao, X., Lutton, E., Merelo, J.J., Schwefel, H.-P. (eds.) PPSN 2000. LNCS, vol. 1917, pp. 839–848. Springer, Heidelberg (2000). https://doi.org/10.1007/3-540-45356-3_82
9. Coello, C.A.C., Lamont, G.B., Veldhuizen, D.A.V.: Evolutionary Algorithms for Solving Multi-objective Problems, 2nd edn. Springer, New York (2007). https://doi.org/10.1007/978-0-387-36797-2
10. Li, B., Li, J., Tang, K., Yao, X.: Many-objective evolutionary algorithms: a survey. ACM Comput. Surv. **48**(1), 13 (2015)
11. Deb, K., Jain, H.: An evolutionary many-objective optimization algorithm using reference-point-based nondominated sorting approach, part I: solving problems with box constraints. Evol. Comput. **18**(4), 577–601 (2013)
12. Zhang, Q., Li, H.: MOEA/D: a multiobjective evolutionary algorithm based on decomposition. IEEE Trans. Evol. Comput. **11**(6), 712–731 (2007)
13. Zitzler, E., Künzli, S.: Indicator-based selection in multiobjective search. In: Yao, X., et al. (eds.) PPSN 2004. LNCS, vol. 3242, pp. 832–842. Springer, Heidelberg (2004). https://doi.org/10.1007/978-3-540-30217-9_84
14. Wang, H., Jiao, L., Yao, X.: Two_Arch2: an improved two-archive algorithm for many-objective optimization. IEEE Trans. Evol. Comput. **19**(4), 524–541 (2015)
15. Bandyopadhyay, S., Chakraborty, R., Maulik, U.: Priority-based ϵ dominance: a new measure in multiobjective optimization. Inf. Sci. **305**, 97–109 (2015)
16. Yu, Y., Ma, H., Zhang, M.: F-MOGP: a novel many-objective evolutionary approach to QoS-aware data intensive web service composition. In: Proceedings of 2015 IEEE Congress on Evolutionary Computation (CEC 2015), Sendai (2015)
17. Cheng, R., Jin, Y., Olhofer, M., Sendhoff, B.: A reference vector guided evolutionary algorithm for many-objective optimization. IEEE Trans. Evol. Comput. **20**(5), 773–791 (2016)
18. Montana, D.J.: Strongly typed genetic programming. Evol. Comput. **3**(2), 199–230 (1995)
19. Koza, J.R.: Genetic Programming: On the Programming of Computers by Means of Natural Selection, 1st edn. A Bradford Book, London (1992)
20. Hadka, D.: MOEA Framework - A Free and Open Source Java Framework for Multiobjective Optimization. Version 2.8 (2015). http://www.moeaframework.org/
21. Zhang, Q., Zhou, A., Zhao, S., Suganthan, P.N., Liu, W., Tiwari, S.: Multiobjective optimization test instances for the CEC 2009 special session and competition. University of Essex, Nanyang Technological University (2009)
22. Farina, M., Amato, P.: A fuzzy definition of "optimality" for many-criteria optimization problems. Syst. Man Cybern. **34**(3), 315–326 (2004)

Allocation Strategies Based on Possibilistic Rewards for the Multi-armed Bandit Problem: A Numerical Study and Regret Analysis

Miguel Martín, Antonio Jiménez-Martín(✉), and Alfonso Mateos

Decision Analysis and Statistics Group, Universidad Politécnica de Madrid, Campus de Montegancedo S/N, Boadilla del Monte, Spain
miguel.martin@alumnos.upm.es, {antonio.jimenez,alfonso.mateos}@upm.es

Abstract. In this paper, we propose a novel allocation strategy based on possibilistic rewards for the multi-armed bandit problem. First, we use possibilistic reward distributions to model the uncertainty about the expected rewards from the arms, derived from a set of infinite confidence intervals nested around the expected value. They are then converted into probability distributions using a *pignistic probability transformation*. Finally, a simulation experiment is carried out to find out the one with the highest expected reward, which is then pulled. A parametric probability transformation of the proposed is then introduced together with a dynamic optimization. A numerical study proves that the proposed method outperforms other policies in the literature in five scenarios accounting for Bernoulli, Poisson and exponential distributions for the rewards. The regret analysis of the proposed methods suggests a logarithmic asymptotic convergence for the original possibilistic reward method, whereas a polynomial regret could be associated with the parametric extension and the dynamic optimization.

1 Introduction

The *multi-armed bandit problem* has been at great depth studied in statistics [8], becoming fundamental in different areas of economics, statistics or artificial intelligence, such as reinforcement learning [26] and evolutionary programming [18].

The name *bandit* comes from imagining a gambler playing with K slot machines. The gambler can pull the arm of any of the machines, which produces a reward payoff. Since the reward distributions are initially unknown, the gambler must use exploratory actions to learn the utility of the individual arms. However, exploration has to be controlled since excessive exploration may lead to unnecessary losses. Thus, the gambler must carefully balance *exploration* and *exploitation*.

G. H. Parlier et al. (Eds.): ICORES 2017, CCIS 884, pp. 186–209, 2018.
https://doi.org/10.1007/978-3-319-94767-9_10

In its most basic formulation, a K-armed bandit problem is defined by random variables $X_{i,n}$ for $1 \leq i \leq K$ and $n \geq 1$, where each i is the index of an arm of a bandit. Successive plays of arm i yield rewards $X_{i,1}, X_{i,2}, ...$ which are independent and identically distributed according to an unknown law with unknown expectation μ_i. Independence also holds for rewards across arms; i.e., $X_{i,s}$ and $X_{j,t}$ are independent (and usually not identically distributed) for each $1 \leq i < j \leq K$ and each $s, t \geq 1$.

A gambler learning the distributions of the arms' rewards can use all past information to decide about his next action. An *allocation strategy*, A is then an algorithm that chooses the next arm to play based on the sequence of previous plays and obtained rewards.

The goal is to maximize the sum of the rewards received, or equivalently, to minimize the regret, which is defined as the loss compared to the total reward that can be achieved given full knowledge of the problem. The *regret* of A after n plays can be computed as

$$\mu^* n - \sum_{i=1}^{K} \mu_i E[n_i], \quad \text{where} \quad \mu^* = \max_{1 \leq i \leq K} \{\mu_i\}, \tag{1}$$

where $E[\cdot]$ denotes expectation and n_i be the number of times arm i has been played by A during the first n plays.

In this paper, we describe two allocation strategies, the *possibilistic reward* (PR) method and a dynamic extension (DPR), in which the uncertainty about the arm expected rewards are first modelled by means of possibilistic reward distributions. Then, a *pignistic probability transformation* from decision theory and transferable belief model is used to convert these possibilistic functions into probability distributions following the *insufficient reason principle*. Finally, a simulation experiment is carried out by sampling from each arm according to the corresponding probability distribution to identify the arm with the higher expected reward and play that arm.

This paper is an extension of [24], where the *possibilistic reward* method and its extensions were introduced together with a numerical study. However, a regret analysis was not carried out. This regret analysis constitutes the main contribution of this paper.

The paper is structured as follows. In Sect. 2 we briefly review the allocation strategies in the literature. In Sect. 3, we describe the possibilistic reward method and its dynamic extension. A numeric study is carried out in Sect. 4 to compare the performance of the proposed policies against the best ones in the literature on the basis of five scenarios for reward distributions. Section 5 reports a regret analysis for the proposed policies. Finally, some conclusions are provided in Sect. 6.

2 Allocation Strategy Review

As pointed out in [14], two families of bandit settings can be distinguished. In the first, the distribution of X_{it} is assumed to belong to a family of probability distributions $\{p_\theta, \theta \in \Theta_i\}$, whereas in the second, the rewards are only assumed to be bounded (say, between 0 and 1), and policies rely directly on the estimates of the expected rewards for each arm.

Almost all the policies or allocation strategies in the literature focus on the first family and they can be separated, as cited in [20], in two distinct approaches: the frequentist view and the Bayesian approach, see Fig. 1. In the *frequentist view*, the expected mean rewards corresponding to all arms are considered as unknown deterministic quantities and the aim of the algorithm is to reach the best parameter-dependent performance.

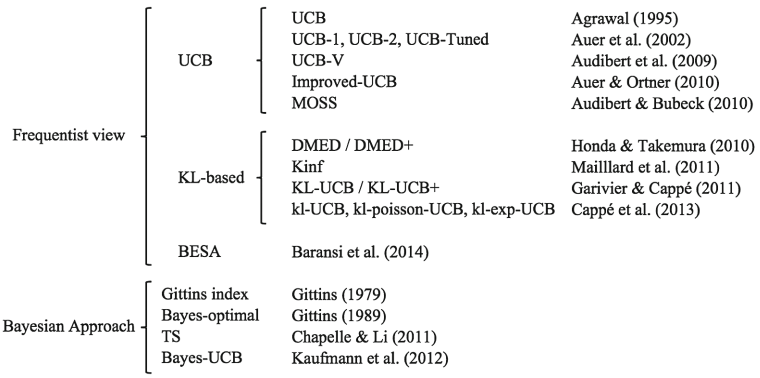

Fig. 1. Review of allocation strategies.

In the *Bayesian approach*, each arm is characterized by a parameter that is endowed with a prior distribution, and the Bayesian performance is then defined as the average performance over all possible problem instances weighted by the prior distribution of the parameters.

2.1 Frequentist View

Lai and Robbins [21] first constructed a theoretical framework for determining optimal policies. For specific families of reward distributions (indexed by a single real parameter), they found that the optimal arm is played exponentially more often than any other arm, at least asymptotically. They also proved that this regret is the best one.

These policies work by associating a quantity called *upper confidence index to each arm*. This index is generally hard to compute. In fact, it relies on the entire sequence of rewards obtained so far from a given arm. Once the index for

each arm has been computed, it is used by the policy as an estimate for the corresponding reward expectation, according to which the arm with the currently highest index is selected for the next round of play. Burnetas and Katehakis [9] proposed an extension to multiparameter or non-parametric models that facilitated the computation of the *upper confidence index*.

Later, [1] introduced a generic class of index policies termed *upper confidence bounds* (UCB), where the index can be expressed as simple function of the total reward obtained so far from the arm. These policies are thus much easier to compute than Lai and Robbins', yet their regret retains the optimal logarithmic behavior.

From then, different policies based on UCB can be found in the literature. First, Auer et al. [4] strengthen previous results by showing simple to implement and computationally efficient policies (UCB1, UCB2 and UCB-Tuned) that achieve logarithmic regret uniformly over time, rather than only asymptotically.

Specifically, policy UCB1 is derived from the index-based policy of [1]. The index of this policy is the sum of two terms. The first term is simply the current average reward, $\bar{x}_i$, whereas the second is related to the size of the one-sided confidence interval for the average reward within which the true expected reward has an overwhelming probability of falling, i.e. we must play arm i that maximizes

$$\bar{x}_i + \sqrt{\frac{2 \ln n}{n_i}}, \tag{2}$$

where n is the current number of rounds of play so far and n_i is the number of times arm i has been played so far.

In UCB2, the plays are divided in epochs. In each new epoch an arm i is picked and then played $\tau(r_i+1)-\tau(r_i)$ times, where τ is an exponential function and r_i is the number of epochs played by that arm so far. The machine picked in each new epoch is the one maximizing $\bar{x}_i + a_{n,r_i}$, where

$$a_{n,r_i} = \sqrt{\frac{(1+\alpha)\ln(en/\tau(r_i))}{2\tau(r_i)}}, \tag{3}$$

$\tau(r_i) = \lfloor (1+\alpha)^{r_i} \rfloor$ and α is a parameter.

In the same paper, UCB1 was extended for the case of normally distributed rewards, which achieves logarithmic regret uniformly over n without knowing means and variances of the reward distributions. A different higher bound for the expected regret after any number n of rounds of play was derived for the above policies. Finally, UCB1-Tuned was proposed to more finely tune the expected regret bound for UCB1.

The empirical behavior of the above policies was compared with the so-called ϵ_n-greedy rule [26] on Bernoulli reward distributions with different parameters. They conclude that an optimally tuned ϵ_n-greedy rule almost always performs best. However, UCB1-Tuned performs comparably, and UCB2 performs similarly to, but always slightly worse than UCB1-Tuned.

Later, Audibert et al. [3] proposed the UCB-V policy, which is also based on upper confidence bounds but taking into account the variance of the different arms. It uses an empirical version of the Bernstein bound to obtain refined upper confidence bounds. They proved that the regret concentrates only at a polynomial rate in UCB-V and that it outperformed UCB1.

In [5] the UCB method of Auer et al. [4] was modified, leading to the improved-UCB method. An improved bound on the regret with respect to the optimal reward was also given. UCB confidence intervals are shorter than for the original method, in particular for arms with high estimated rewards. Besides, arms that perform badly are eliminated.

An improved UCB1 algorithm, termed *minimax optimal strategy in the stochastic case* (MOSS), was proposed by Audibert and Bubeck [2], which achieved the distribution-free optimal rate while still having a distribution-dependent rate logarithmic in the number of plays. The key idea was to reduce the exploration of sufficiently pulled arms, using

$$\bar{x}_i + \sqrt{\frac{\max\{\log(\frac{n}{Kn_i}), 0\}}{n_i}}, \tag{4}$$

instead of Eq. (2).

Thus, an arm that has been pulled more than n/K times has an index equal to the empirical mean of the rewards obtained from the arm. However, when it has been pulled close to n/K times, the logarithmic term is much smaller than reducing the exploration of this already much pulled arm.

Another class of policies under the frequentist perspective are the Kullback-Leibler (KL)-based algorithms, including DMED, K_{inf}, KL-UCB and kl-UCB.

The *deterministic minimum empirical divergence* (DMED) policy was proposed by Honda and Takemura [19] motivated by a Bayesian viewpoint for the problem (although a Bayesian framework is not used for theoretical analyses). This algorithm, which maintains a list of arms that are close enough to the best one (and which thus must be played), is inspired by large deviations ideas and relies on the availability of the rate function associated to the reward distribution. Note that DMED is also referred to as DMED+ in the literature.

In [23], the K_{inf}-based algorithm was analyzed by Maillard et al. It is inspired by the ones studied in [9,21], taking also into account the full empirical distribution of the observed rewards. The analysis accounted for Bernoulli distributions over the arms and less explicit but finite-time bounds were obtained in the case of finitely supported distributions (whose supports do not need to be known in advance). These results improve on DMED, since finite-time bounds (implying their asymptotic results) are obtained, UCB1, UCB1-Tuned, and UCB-V. Note that DMED considers non-parametric distributions on [0,1] with the optimal bound, whereas Maillard et al. [23] derives the finite-time bound for finite-parametric models.

Later, the KL-UCB algorithm and its variant KL-UCB+ were introduced by Garivier and Cappé [14]. KL-UCB satisfied a uniformly better regret bound than UCB and its variants for arbitrary bounded rewards, whereas it reached the lower

bound of Lai and Robbins when Bernoulli rewards are considered. Besides, simple adaptations of the KL-UCB algorithm were also optimal for rewards generated from exponential families of distributions. Furthermore, a large-scale numerical study comparing KL-UCB with UCB, MOSS, UCB-Tuned, UCB-V, DMED was performed, showing that KL-UCB was remarkably efficient and stable, including for short time horizons.

New algorithms were proposed by Cappé et al. [10] based on upper confidence bounds of the arm rewards computed using different divergence functions. The kl-UCB uses the Kullback-Leibler divergence; whereas the kl-poisson-UCB and the kl-exp-UCB account for families of Poisson and Exponential distributions, respectively. A unified finite-time analysis of the regret of these algorithms shows that they asymptotically match the lower bounds of Lai and Robbins, and Burnetas and Katehakis. Moreover, they provide significant improvements over the state-of-the-art when used with general bounded rewards.

The *best empirical sampled average* (BESA) algorithm was proposed by Baransi et al. [6]. It is not based on the computation of an empirical confidence bounds, nor can it be classified as a KL-based algorithm. BESA is fully non-parametric. As shown in [6], BESA outperforms TS (a Bayesian approach introduced in the next section) and KL-UCB in several scenarios with different types of reward distributions. Moreover, BESA stands out for its flexibility, since the same implementation can be used for any type of reward distributions, whereas TS or KL-UCB implementations differ according to the distribution under consideration.

Note that although they have been tested for different distributions regarding arm rewards, UCB methods and some of their variants, together with BESA, only need the rewards to be bounded in an interval.

2.2 Bayesian Approach

Stochastic bandit problems have been analyzed from a Bayesian perspective, i.e. the parameter is drawn from a prior distribution instead of considering a deterministic unknown quantity. The Bayesian performance is then defined as the average performance over all possible problem instances weighted by the prior on the parameters.

The origin of this perspective is in the work by Gittins [15]. Gittins' index based policies are a family of Bayesian-optimal policies based on indices that fully characterize each arm given the current history of the game, and at each time step the arm with the highest index will be pulled. However, Gittins indices were limited to a specific set of distributions and with high associated computational costs.

Later, Gittins proposed the Bayes-optimal approach [16] that directly maximizes expected cumulative rewards with respect to a given prior distribution.

A lesser known family of algorithms to solve bandit problems is the so-called *probability matching* or *Thompson sampling* (TS). The idea of TS is to randomly draw each arm according to its probability of being optimal. The algorithm assumes that arm distributions belong to a parametric family of distributions $P = \{p(.|\theta), \theta \in \Theta\}$, where $\Theta \subseteq R$. It starts by putting a prior distribution on

each one of the arm parameters, and a posterior distribution is maintained at each time step according to the rewards observed so far.

In contrast to Gittins' index, TS can often be efficiently implemented. Some empirical results are reported in [11], both for simulated and real-world problems. Despite its simplicity, TS achieved state-of-the-art results, and in some cases significantly outperformed other alternatives, like UCB methods.

However, the results of experiments carried out in [22] suggest that a particular version of the Gittins index strategy is an improvement on existing algorithms with finite-time regret guarantees such as UCB and Thompson sampling.

Finally, Bayes-UCB was proposed by Kaufmann et al. [20] inspired by the Bayesian interpretation of the problem but retaining the simplicity of UCB-like algorithms. It constitutes a unifying framework for several UCB variants addressing different bandit problems (parametric multi-armed bandits, Gaussian bandits with unknown mean and variance, linear bandits). Moreover, its generality makes Bayes-UCB suitable for addressing more challenging models.

3 Possibilistic Reward Method

The allocation strategy we propose accounts for the frequentist view but they cannot be classified as either a UCB method nor a Kullback-Leibler (KL)-based algorithm. The basic idea is as follows: the uncertainty about the arm expected rewards are first modelled by means of possibilistic reward distributions derived from a set of infinite nested confidence intervals around the expected value on the basis of Chernoff-Hoeffding inequality. Then, we follow the *pignistic probability transformation* from decision theory and transferable belief model [25], that establishes that when we have a plausibility function, such as a possibility function, and any further information in order to make a decision, we can convert this function into an probability distribution following the *insufficient reason principle*.

Once we have a probability distribution for the reward in each arm, then a simulation experiment is carried out by sampling from each arm according to their probability distributions to find out the one with the highest expected reward higher. Finally, the picked arm is played and a real reward is output.

We shall first introduce the algorithm for rewards bounded between [0,1] in the real line for simplicity and then, we will extend it for any real interval. The starting point of the method we propose is Chernoff-Hoeffding inequality [17], which provides an upper bound on the probability that the sum of random variables deviates from its expected value, which for [0,1] bounded rewards leads to:

$$
\begin{array}{l}
P\left(\left|\frac{1}{n}\sum_{t=1}^{n} X_t - E[X]\right| > \epsilon\right) \leq 2e^{-2n\epsilon^2} \Rightarrow \\
P\left(\left|\frac{1}{n}\sum_{t=1}^{n} X_t - E[X]\right| \leq \epsilon\right) \geq 1 - 2e^{-2n\epsilon^2} \Rightarrow \\
P\left(E[X] \in \left[\frac{1}{n}\sum_{t=1}^{n} X_t - \epsilon, \frac{1}{n}\sum_{t=1}^{n} X_t + \epsilon\right]\right) \geq 1 - 2e^{-2n\epsilon^2}.
\end{array}
$$

It can be used for building an infinite set of nested confidence intervals, where the confidence level of the expected reward ($E[X]$) in the interval $I = [\frac{1}{n}\sum_{t=1}^{n} X_t - \epsilon, \frac{1}{n}\sum_{t=1}^{n} X_t + \epsilon]$ is $1 - 2e^{-2n\epsilon^2}$.

Note that other inequalities than the Chernoff-Hoeffding inequality could be derived to build an infinite set of nested confidence intervals and possibilistic reward methods with different features. For instance, an alternative Hoeffding's extension of the Chernoff bound or its combination with the Bernstein bound [7] could be considered.

Besides, a fuzzy function representing a possibilistic distribution can be implemented from nested confidence intervals [12]: $\pi(x) = sup\{1 - P(I), x \in I\}$.

Consequently, in our approach for confidence intervals based on Hoeffding inequality, the *sup* of each x will be the bound of minimum interval around the mean $(\frac{1}{n}\sum_{t=1}^{n} X_t)$ where x is included. That is, the interval with $\epsilon = \left|\frac{1}{n}\sum_{t=1}^{n} X_t - x\right|$.

If we consider $\hat{\mu}_n = \frac{1}{n}\sum_{t=1}^{n} X_t$, for simplicity, then we have:

$$\pi(x) = \begin{cases} min\{1, 2e^{-2n_i \times (\hat{\mu}_n - x)^2}\}, & \text{if } 0 \leq x \leq 1 \\ 0, & \text{otherwise} \end{cases}.$$

Note that $\pi(x)$ is truncated in $[0, 1]$ both in the x axis, due to the bounded rewards, and the y axis, since a possibility measure cannot be greater than 1. Figure 2 shows several examples of possibilistic rewards distributions.

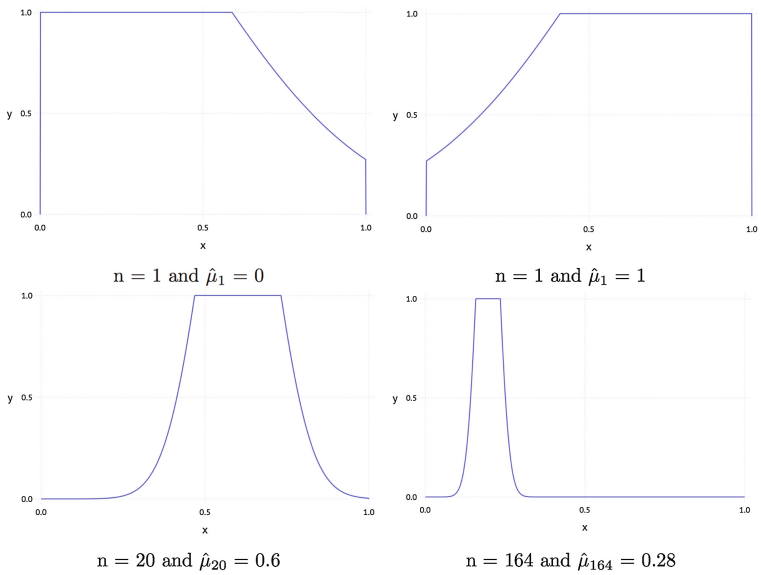

Fig. 2. Possibilistic rewards distributions [24]. (Color figure online)

3.1 A Pignistic Probability Transformation

Once the arm expected rewards are modelled by means of possibilistic functions, next step consists of picking the arm to pull on the basis of that uncertainty. For this, we follow the *pignistic probability transformation* from decision theory and transferable belief model [25], which, in summary, establishes that when we have a plausibility function, such as a possibility function, and any further information in order to make a decision, we can convert this function into an probability distribution following the *insufficient reason principle* [13], or consider equipossible the same thing that equiprobable. In our case, it can be performed by dividing $\pi(x)$ function by $\int_0^1 min\{1, 1 - e^{-2n_i \times (\hat{\mu}_n - x)^2}\}dx$.

However, further information is available in form of restrictions that allow us to model a better approximation of the probability functions. Since a probability density function must be continuous and integrable, we have to smooth the gaps that appear between points close to 0 and 1. Besides, we know that the probability distribution should be a unimodal distribution around the sampling average $\hat{\mu}_n$. Thus, the function must be monotonic strictly increasing in $[0, \hat{\mu}_n)$ and monotonic strictly decreasing in $(\hat{\mu}_n, 1]$. We propose the following approximation to incorporate the above restrictions:

1. $\pi(x)$ is transformed into an intermediate function $\pi_r(x)$ as follows:
   (a) Multiply the not truncated original function, $2e^{-2n_i \times (\hat{\mu}_n - x)^2}$, by $\frac{1}{2}$ in order to reach a maximum value 1.
   (b) Fit the resulting function in order to have $\pi_r(0) = 0$ and $\pi_r(1) = 0$:

$$\Delta_{low} = e^{-2n_i \times (\hat{\mu}_n)^2}, \qquad \Delta_{up} = e^{-2n_i \times (\hat{\mu}_n - 1)^2},$$

$$\pi_r(x) = \begin{cases} \frac{e^{-2n_i \times (\hat{\mu}_n - x)^2} - \Delta_{low}}{1 - \Delta_{low}}, & \text{if } x \leq \hat{\mu}_n \\ \frac{e^{-2n_i \times (\hat{\mu}_n - x)^2} - \Delta_{up}}{1 - \Delta_{up}}, & \text{if } x > \hat{\mu}_n \\ 0, & \text{otherwise} \end{cases}.$$

   Two exceptions have to be considered. When all the rewards of past plays are 0 or 1, then the transformations to reach $\pi_r(0) = 0$ or $\pi_r(1) = 0$ are not applied, respectively.
2. The pignistic transformation is applied to $\pi_r(x)$ by dividing by $\int_0^1 \pi_r(x)dx$, leading to the probability distribution

$$P(x) = \pi_r(x)/C, \quad \text{with } C = \int_0^1 \pi_r(x)dx.$$

Figure 3 shows the application of the pignistic probability transformation to derive a probability distribution (in green) from the $\pi(x)$ functions (in blue) in Fig. 2.

The next step is similar to Thompson sampling (TS) [11]. Once we have built the pignistic probabilities for all the arms, we pick the arm with the highest expected reward. For this, we carry out a simulation experiment by sampling

from each arm according to their probability distributions. Finally, the picked arm is pulled/played and a real reward is output. Then, the possibilistic function corresponding to the picked arm is updated and started again.

Algorithm 1 synthesizes the allocation strategy.

Algorithm 1. PR.

Data: ($T = 20.000$; K = no. of arms; a_i = arm i, $i = \{1, ..., K\}$)

for ($i = 1$ **to** K)
  Build $\pi_i(x)$ for arm a_i with 0 trials;
  Compute $p_i(x)$ from $\pi_i(x)$;
end
Randomly select an arm a_i; $t = 1$;
while $t < T$ **do**
  Play the selected arm a_i and get the reward X_{it};
  Update $\pi_i(x)$ accounting for X_{it};
  for ($i = 1$ **to** K)
    Sample a_i from its $p_i(x)$;
  end
  Pick the arm with the highest expected reward; $t = t + 1$;
end

3.2 Parametric Probability Transformation and Dynamic Optimization

In the previous section, rewards were bound to the interval [0,1] and the most used possibility-probability transformation according to pignistic or maximal entropy methods [25] was implemented. Now, we extend rewards to any real interval $[a, b]$ and interpret the possibility distribution $\pi_r(x)$ as a probability distribution set that encloses any distribution $P(x)$ such as $\forall A = [a, b] \rightarrow \pi_r(x \in A) \leq P(x \in A) \leq 1 - \pi_r(x \notin A)$. Consequently, another distribution enclosed by $\pi_r(x)$ that minimizes the expected regret for any particular reward distribution could be used.

In order to trade off performance and computational cost issues, we were able to modify our previous probabilistic-possibilistic transformation to create a family of probabilities just adding an α parameter as follows:

$$P(x) = \pi_\alpha(x)/C \quad \text{with} \quad C = \int_a^b \pi_\alpha(x)dx$$

and

$$\pi_\alpha(x) = \begin{cases} \frac{e^{-2n_i \times \alpha(\frac{\hat{\mu}_n - x}{b-a})^2} - \Delta_{\alpha_{low}}}{1 - \Delta_{\alpha_{low}}}, & \text{if } x \leq \hat{\mu}_n \\ \frac{e^{-2n_i \times \alpha(\frac{\hat{\mu}_n - x}{b-a})^2} - \Delta_{\alpha_{up}}}{1 - \Delta_{\alpha_{up}}}, & \text{if } x > \hat{\mu}_n \\ 0, & \text{otherwise} \end{cases},$$

where

$$\Delta_{\alpha_{low}} = e^{-2n_i \times \alpha(\frac{\hat{\mu}_n}{b-a})^2}, \Delta_{\alpha_{up}} = e^{-2n_i \times \alpha(\frac{\hat{\mu}_{n-1}}{b-a})^2}, \text{and } \alpha > 1.$$

By adding parameter α, it is possible to adjust the transformation for any particular reward distribution to minimize the expected regret. For this, an optimization process for parameter α will be required. We denote this extension of the PR method as PR-opt.

Alternatively to manually tuning parameter α, we propose modifying the PR algorithm to dynamically tune it while bearing in mind the minimization of the expected regret. Thus, the advantage of the new *dynamic possibilistic reward* (DPR) is that it requires neither previous knowledge nor a simulation of the arm distributions. In fact, the reward distributions are not known in the majority of the cases. Besides, the performance of the DPR against PR and other policies in terms of expected regrets will be analyzed in the next section.

Several experiments have shown that the scale parameter α is correlated with the inverse of the variance of the reward distribution shown by the experiment. As such, analogously to Auer et al. [4], for practical purposes we can fix parameter α as

$$\alpha = 0.5 \times \frac{(b-a)^2}{\tilde{var}}, \tag{5}$$

where $\tilde{var}$ is the sample variance of the rewards seen by the agent and $[a, b]$ the reward interval.

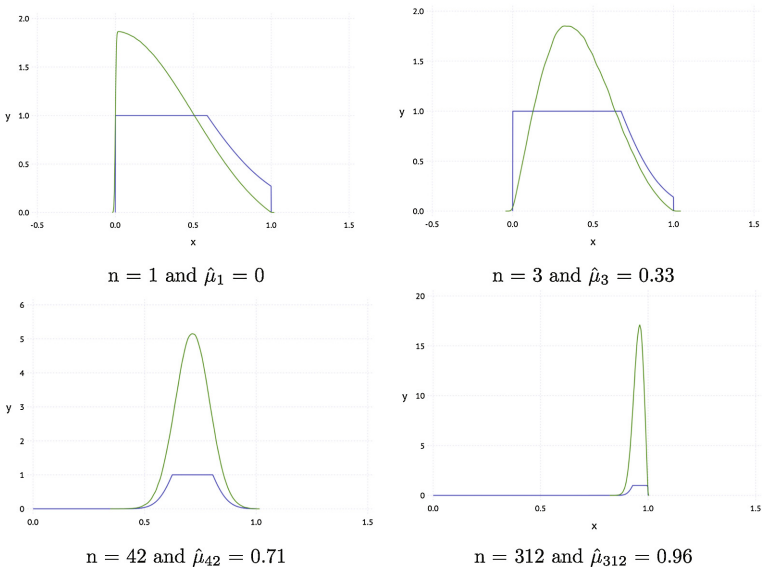

Fig. 3. Pignistic probability transformation examples [24]. (Color figure online)

4 Numerical Study

In this section, we show the results of a numerical study in which we have compared the performance of PR and DPR methods against other allocation strategies in the literature. Specifically, we have chosen KL-UCB, DMED+, BESA, TS and Bayes-UCB, since they are the most recent proposals and they outperform other allocation strategies [6,10,11]. Additionally, we have also considered the UCB1 policy, since it was one of the first proposals in the literature that accounts for the uncertainty about the expected reward.

We have selected five different scenarios for comparison. For this, we have reviewed numerical studies in the literature to find out the most difficult and representative scenarios. An experiment consisting on 50,000 simulations with 20,000 iterations each was carried out in the five scenarios. The Python code available at http://mloss.org/software/view/415 was used for simulations, whereas those policies not implemented in that library have been developed by the authors, including DMED+, BESA, PR and DPR.

4.1 Scenario 1: Bernoulli Distribution and Very Low Expected Rewards

This scenario is a simplification of a real situation in on-line marketing and digital advertising. Specifically, advertising is displayed in banner spaces and in case the customer clicks on the banner then s/he is redirected to the page that offers the product. This is considered a success with a prize of value 1. The success ratios in these campaigns are usually quite low, being about 1%. For this, ten arms will be used with a Bernoulli distribution and the following parameters: [0.1, 0.05, 0.05, 0.05, 0.02, 0.02, 0.02, 0.01, 0.01, 0.01].

First, a simulation is carried out to find out the best value for parameter α to be used in the PR-opt method, see Fig. 4. $\alpha = 8$ is identified as the best value and used for this scenario 1. Note that in DPR, no previous knowledge regarding the scenario is required. Besides, although the best value for parameter α to be used in the PR-opt method is identified for all the scenarios under consideration, we also take into account the PR method with $\alpha = 1$ in all cases.

Now, the 50,000 simulations with 20,000 iterations each are carried out. Figure 5a shows in a logarithmic scale the evolution of the regret for the six best allocation strategies under comparison along the 20,000 iterations corresponding to one simulation (using a logarithmic scale), whereas Fig. 6 shows the multiple violinplot corresponding to regrets throughout the 50,000 simulations.

The first two columns in Table 1 show the mean regrets and standard deviations for the policies. The three with lowest mean regrets are highlighted in bold, corresponding to DPR, PR-opt and BESA, respectively. The variance is similar for all the policies under consideration. It is important to note that although PR-opt slightly outperforms DPR, DPR requires neither previous knowledge nor a simulation regarding the arm distributions, which makes DPR more suitable in a real environment.

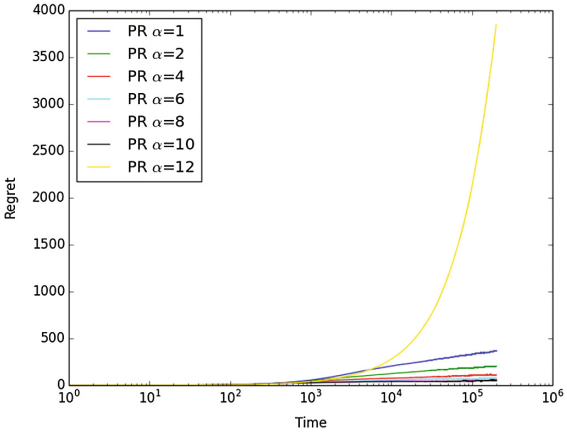

Fig. 4. Selecting parameter α for PR in scenario 1 [24].

Note that in the above multiple violinplot negative regret values are displayed. It could be considered an error at first sight. The explanation is as follows: the optimum expected reward μ^* used to compute regrets is the theoretic value from the distribution, see Eq. (1). For instance, in an arm with Bernoulli distribution with parameter 0.1, μ^* after n plays is $0.1 \times n$. However, in the simulation the number of success if the arm is played n times may be higher than this amount, overall in the first iterations, leading to negative regret values.

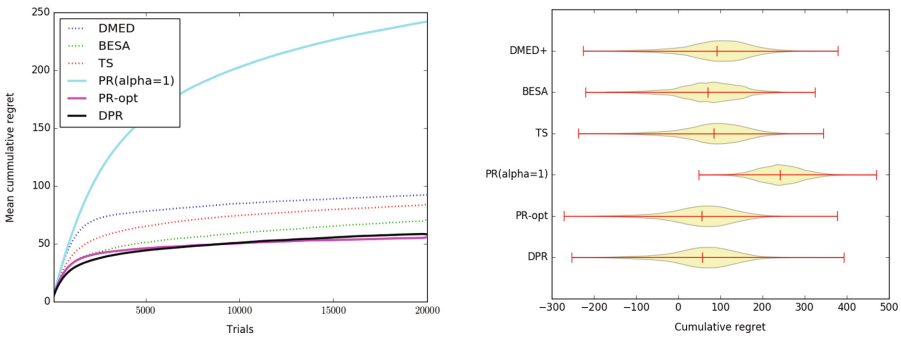

(a) Policies in one simulation **(b)** Multiple violinplot

Fig. 5. Analysis of scenario 1.

4.2 Scenario 2: Bernoulli Distribution and Medium Expected Rewards

In this scenario, we still consider a Bernoulli distribution but now parameters are very similar in the 10 arms and close to 0.5. This leads to the greatest variances in the distributions, where in almost all arms in half of the cases they have a value 1 and 0 in the other half. Thus, it becomes harder for algorithms to reach the optimal solution. Moreover, if an intensive search is not carried out along a sufficient number of iterations, we could easily reach sub-optimal solutions. The parameters for the 10 arms under consideration are: [0.5, 0.45, 0.45, 0.45, 0.45, 0.45, 0.45, 0.45, 0.45, 0.45].

Table 1. Statistics in scenarios 1, 2 and 3 [24].

	Bernoulli (low)		Bernoulli (med)		Bernoulli (G)	
	Mean	σ	Mean	σ	Mean	σ
UCB1	393.7	57.6	490.9	104.9	2029.1	125.9
DMED+	83.1	46.1	356.8	151.5	889.8	313.2
KL-UCB	130.7	47.9	491.5	104.3	1169.6	233.2
KL-UCB+	103.3	46.0	349.7	104.7	879.7	254.5
BESA	**78.1**	53.9	**281.6**	260.9	**768.75**	399.2
TS	91.1	45.6	**284.2**	125.1	-	-
Bayes-UCB	115.1	46.6	366.3	104.5	-	-
PR ($\alpha = 1$)	242.1	53.5	283.3	124.6	1937.6	148.5
PR-opt	**51.1**[a]	49.2	380.5	426.2	**431.0**[a]	383.5
DPR	**63.6**	49.1	**214.6**[a]	185.1	**643.0**	

[a] points out the lowest values in the corresponding columns.

First, a simulation was carried out again to find out the best value for parameter α to be used in the PR-opt method in this scenario and $\alpha = 2$ was selected.

In Fig. 6a the regrets throughout the 50,000 simulations corresponding to the different policies are shown by means of a multiple violinplot.

The three allocation strategies with lowest average regrets, highlighted in bold in the third and fourth columns in Table 1, corresponds to DPR, BESA and TS, respectively. However, DPR outperforms BESA and TS, whose performances are very similar but BESA has a higher variability.

It is noteworthy that PR is the fourth best allocation strategy in this scenario, outperforming Bayes-UCB, KL-UCB, KL-UCB+, DMED+ and UCB1.

4.3 Scenario 3: Bernoulli Distribution and Gaussian Rewards

In this scenario, Bernoulli distributions with very low expected rewards (about 1% success ratios) are again considered but now rewards are not 0 or 1, they are

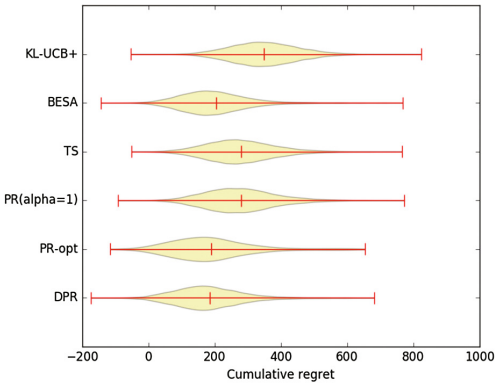

(a) Scenario 2

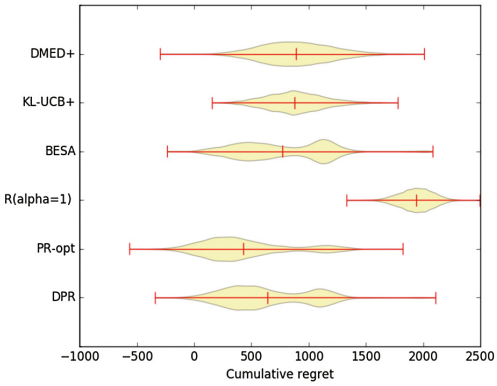

(b) Scenario 3

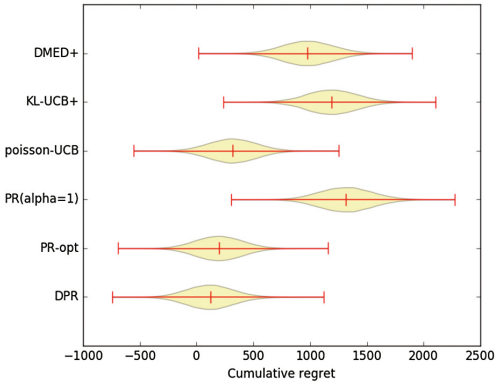

(c) Scenario 4 (Poisson)

Fig. 6. Multiple violinplot in scenarios 2, 3 and 4.

normally distributed. This scenario has never been considered in the literature but we consider it interesting for analysis. We can also face this scenario in online marketing and digital advertising. As in scenario 1, advertising is displayed in banner spaces and in case the customer clicks on the banner then s/he is redirected to the page that offers the product. However, in this new scenario the customer may buy more than one product, the number of which is modeled by a normal distribution.

The success ratios in these campaigns are usually quite low, as in scenario 1, being about 1%. For this, the ten arms will be used with a Bernoulli distribution and the following parameters: [0.1, 0.05, 0.05, 0.05, 0.02, 0.02, 0.02, 0.01, 0.01, 0.01]. Besides, the same $\sigma = 0.5$ is used for the normal distributions, whereas the following means (μ) are considered: [1, 2, 1, 3, 5, 1, 10, 1, 8, 1]. Moreover, all rewards are truncated between 0 and 10. Thus, the expected rewards for the ten arms are [0.1, 0.1, 0.05, 0.15, 0.1, 0.02, 0.2, 0.01, 0.08, 0.01], and the seventh arm is the one with the highest expected reward.

TS and Bayes-UCB policies are not analyzed in this scenario since both cannot be applied. $\alpha = 70$ will be used in the PR-opt method. Figure 6b shows the multiple violinplot for the regrets throughout the 50,000 simulations, whereas the mean regrets and the standard deviations are shown in last two columns of Table 1.

The three policies with lowest mean regrets, highlighted in bold in Table 1, correspond to PR-opt, DPR and BESA, respectively, the three with a similar variability. However, PR-opt outperforms DPR and BESA in this scenario.

4.4 Scenario 4: Truncated Poisson Distribution

A truncated in [0,10] Poisson distribution is used in this scenario. It is useful to model real scenarios where the reward depends on the number of times an event happens or is performed in a time unit, for instance, the number of followers that click on the "like" button during two days since it is uploaded. The values for parameter λ in the Poisson distribution for each arm are: [0.75, 1, 1.25, 1.5, 1.75, 2, 2.25].

The variant kl-poisson-UCB was also considered for analysis, whereas TS and Bayes-UCB will no longer be considered since both cannot be applied in this scenario.

First, the selected value for parameter α to be used in the PR-opt method in this scenario is 12. Figure 6c shows the multiple violinplot for the regrets throughout the 50,000 simulations, whereas the first two columns in Table 2 show the mean regrets and standard deviations.

One should observe the high variability on the regret values in BESA. Figure 7 shows the violinplot corresponding to BESA. As expected, regret values are mainly concentrated around 7 values (0, 5000, 10,000, 15,000, 20,000, 25,000, 30,000), with the highest number of regret values around 0, followed by 5000 and so on. Note that the different of λ values in the 7 arms is 0.25 and $0.25 \times 20,000$ iterations carried out in each simulation is 5000, which matches up with the amount incremented in the 7 points the regrets are concentrated around.

DPR again outperforms the other algorithms on the basis of the mean regrets, including PR-opt, see Table 2. kl-poisson-UCB Poisson is the only policy whose results are close to DPR and PR-opt. However, we should take into account that kl-poisson-UCB is based on the assumption that rewards are known to follow a Poisson distribution and, consequently, takes advantage of that information.

Besides, the variability in DPR is higher than in all the other policies apart from BESA.

Finally, we should also stress that PR outperforms BESA, KL-UCB+, KL-UCB+ and UCB1 in this scenario.

4.5 Scenario 5: Truncated Exponential Distribution

A truncated exponential distribution is selected in this scenario, since it is usually used to compare allocation strategies in the literature. It is used to model continuous rewards, and for scales greater than 1 too. Moreover, it is appropriate to model real situations where the reward depends on the time between two consecutive events, for instance, the time between a recommendation is offered on-line until the customer ends up buying. The values for parameter λ in the exponential distribution for each arm are: [1, 1/2, 1/3, 1/4, 1/5, 1/6].

The variant kl-exp-UCB was incorporated into the analysis in this scenario, whereas TS and Bayes-UCB cannot be applied.

The best value for parameter α for the PR-opt method is 6. Figure 8 shows the multiple violinplot for the regrets throughout the 50,000 simulations. The mean regret and the standard deviations are shown in last two columns of Table 2.

PR-opt and DPR again outperform the other policies, with PDR being very similar to but slightly better than PR-opt in this scenario. Moreover, DPR requires neither previously knowledge nor a simulation of the arm distributions,

Table 2. Statistics in scenarios 4 and 5 [24].

	Truncated poisson		Truncated exponential	
	Mean	σ	Mean	σ
UCB1	2632.65	246.03	1295.79	514.03
DMED+	978.56	225.24	**645.70**	493.8
KL-UCB	1817.4	236.57	1219.98	510.69
kl-poisson-UCB	**314.99**	201.79	-	-
KL-exp-UCB	-	-	786.30	498.16
KL-UCB+	1190.64	225.82	813.45	494.59
BESA	2015.73	3561.5	755.87	2323.22
PR ($\alpha = 1$)	1315	234.4	660.7	492.4
PR-opt	**196.24**	212.45	**580.31**	2182.02
DPR	**153.3**[a]	409.17	**282.83**[a]	814.72

[a] points out the lowest values in the corresponding columns.

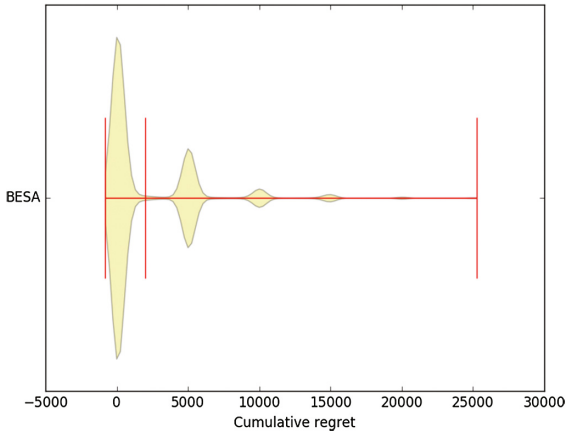

Fig. 7. Violinplot for BESA.

what makes DPR more suitable in a real environment. The best four policies are the same as in scenario 4, with a truncated Poisson, changing the KL-poisson-UCB with KL-exp-UCB.

Finally, we should remark that PR is the fourth best allocation strategy in this scenario, outperforming BESA, Bayes-UCB, KL-UCB+, KL-exp-UCB, KL-UCB and UCB1.

5 Regret Analysis

First, note that the theoretical convergence for the PR, PR-opt and DPR methods has not been demonstrated. In scenarios other than the above, their regrets might behave polynomially since the lower bound proven by Lai and Robbins could be violated [21], thus making the three methods inconsistent.

However, the analyses carried out in this section show that unlike the PR-opt and the DPR methods the PR ($\alpha = 1$) method has a logarithmic asymptotic convergence. The justification is as follows: we start with a scenario with a Bernoulli distribution, where a logarithmic convergence has been demonstrated in the literature for Thompson sampling (TS) with beta priors [1]. The density function for the expected reward for each arm in the PR method is very similar to the beta function used as a density function in Thompson sampling, see Fig. 9. Moreover, the density function for the PR method has a higher variance than for TS, which slightly increases the likelihood of exploring non-optimal arms. By running a wider exploration than TS, we ensure that all the arms have been sufficiently explored, and prevent a potential polynomial regret caused by over exploiting an arm that was not optimal. This argument can be extended to other non-discrete distributions performing the same comparison with TS for general stochastic bandits [1].

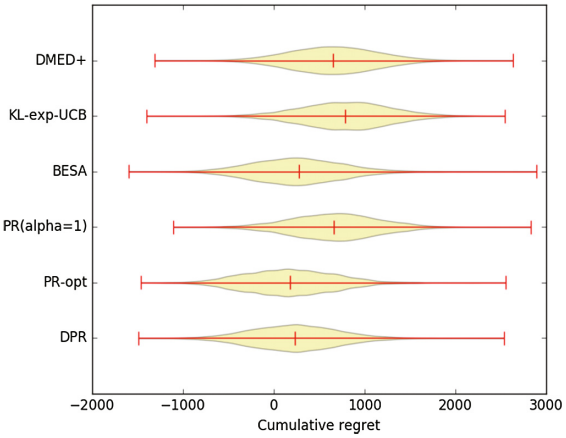

Fig. 8. Multiple violinplot for policies in the fifth scenario.

An analogous reasoning does not apply for the PR-opt method (α different to 1) or the DPR method. In the first case, we must take into account that the value of α can only be set for a specific scenario where the following configurations must be known in advance: the number of arms, the rewards probability, and a difference between the expected awards and the optimal award that is greater than a certain value.

Note, however, that an α value set for a specific scenario can cause the algorithm to have a polynomial convergence as we move away from that scenario. This is mainly due to the fact that density functions with low variance will be produced, and the arms will not be sufficiently explored. The consequence will be a polynomial regret in the worst case.

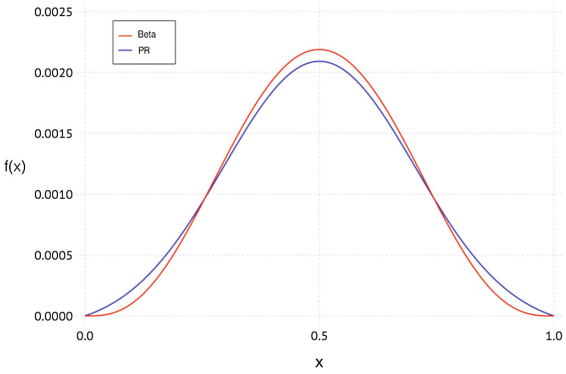

Fig. 9. Density functions for PR and Beta prior.

The same applies with the DPR method when there are initially very low variances, which makes DPR equivalent to PR-opt with an extremely high α.

Like Chapelle and Li [11], we have performed different simulations to experimentally verify the possible violation of the lower bound proven by Lai and Robbins and to check the asymptotic convergence of PR, PR-opt and DPR.

First, we considered a Bernoulli distribution and carried out different simulations with a large number of iterations, where we progressively reduced the distance between the arm reward and the optimal reward, as well as the number of arms.

Figure 10 shows the evolution of the mean cumulative regret on a logarithmic scale during a large number of iterations for a Bernoulli distribution with $k = 100$ and $\alpha = 0.01$. As a logarithmic scale is used, the lower bound proven by Lai and Robbins is a straight line.

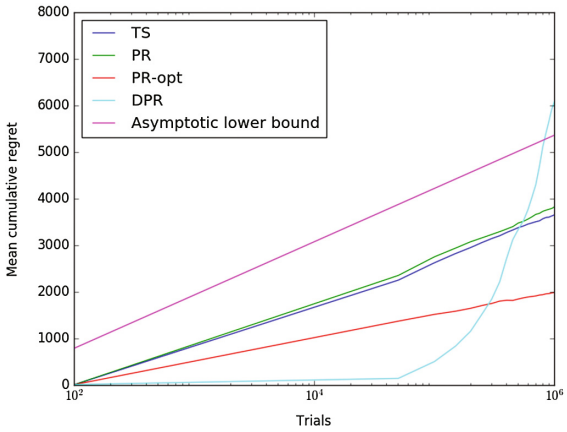

Fig. 10. Regret analysis: Bernoulli $k = 100$ and $\alpha = 0.01$.

This draws attention to the behavior of DPR, whose mean cumulative regret function resembles an exponential function as of a certain number of trials. This implies that this method has a polynomial asymptotic behavior. On the other hand, straight lines are associated with PR, PR-opt and TS and, consequently, there is a logarithmic asymptotic convergence. Note that the logarithmic asymptotic convergence for TS has been demonstrated in the literature.

Besides, we can check whether or not the lower bound proven by Lai and Robbins is violated by comparing the slope of the different straight lines. We can see that the slopes for the straight lines corresponding to TS and PR are parallel to the slope of the lower bound proven by Lai and Robbins as of a certain number of trials. Thus, TS and PR do not violate the lower bound proven by Lai and Robbins. However, the slope for PR-opt is below the lower bound. This implies that PR-opt violates the lower bound proven by Lai and Robbins and,

consequently, is inconsistent. Therefore, its regrets might have a sub-logarithmic or linear asymptotic behaviour in scenarios other than the above.

In a second scenario, we account for a truncated exponential. We consider 100 arms ($k = 100$) where the parameter α is equal to $1/6$ for the best arm and $1/5$ for the others ($\delta \simeq 0.55$); $k = 10$ with the previous α values; $k = 100$ and the parameter α is $1/5.1$ for the best arm and $1/5$ for the others ($\delta \simeq 0.059$); and $k = 100$ with the previous α values.

Figure 11 shows the evolution of the mean cumulative regret on a logarithmic scale during a large number of iterations for $k = 10$ and $\delta \simeq 0.059$. Now, the mean cumulative regret functions for DPR and PR-opt start to resemble an exponential function as of a certain number of trials, implying that this method has a polynomial asymptotic behavior, whereas straight lines are associated with UCB and PR, where there is a logarithmic asymptotic convergence.

Besides, the slopes for the straight lines corresponding to UCB and PR are higher than the slope of the lower bound proven by Lai and Robbins as for a certain number of trials. Thus, UCB and PR do not violate the lower bound proven by Lai and Robbins.

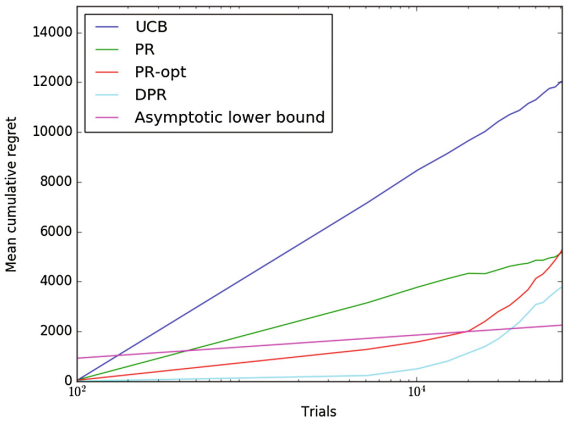

Fig. 11. Regret analysis: exponential $k = 10$ and $\delta \simeq 0.059$.

To conclude, the PR ($\lambda = 1$) method has a logarithmic asymptotic convergence and does not violate the lower bound proven by Lai and Robbins, unlike that the PR-opt the DPR methods.

6 Conclusions

In this paper, we propose a novel allocation strategy, the possibilistic reward method (PR), together with a parametric probability transformation (PR-opt) and a dynamic optimization (DPR).

A numerical study accounting for five complex and representative scenarios suggests that the proposed method outperforms other allocations strategies in the literature. Specifically, we have considered a Bernoulli distribution with very low success probabilities, with success probabilities close to 0.5, and with success probabilities close to 0.5 and Gaussian rewards; a Poisson distribution truncated in [0,10]; and an exponential distribution truncated in [0,10].

In the first three scenarios, in which the Bernoulli distribution is considered, PR-opt or DPR are the policies with the lowest mean regret and with similar variability regarding the other policies. BESA is the only policy with results that are close to DPR and PR-opt, mainly in scenario 1. Besides, DPR and PR-opt clearly outperform the other policies in scenarios 4 and 5, in which a truncated Poisson and exponential are considered, respectively. In both cases, DPR outperforms PR-opt.

However, the experiments performed regarding regret show that the PR ($\alpha = 1$) method has a logarithmic asymptotic convergence and unlike the PR-opt and the DPR methods does not violate the lower bound proven by Lai and Robbins.

In summary, although the PR-opt and DPR methods outperform the other allocation strategies in all five scenarios considered in the numerical analysis, they violate the lower bound proven by Lai and Robbins and their regrets may have a polynomial behavior in other scenarios. Besides, PR ($\alpha = 1$) has good convergence qualities, being the second and third-best allocation strategy in the scenarios accounting for the truncated exponential and Poisson distributions, respectively. Additionally, it performs similarly to TS (the best one) in the scenario accounting for a Bernoulli distribution with medium expected rewards; although performance is worse in scenarios accounting for a Bernoulli distribution with very low expected rewards and with Gaussian rewards, where it only outperforms UCB1.

However, if we only take into account the policies that do not make any assumption about the reward distribution (a very plausible situation in real scenarios where nothing is known about the rewards except the upper and lower bounds) the PR performance is comparable on average in all the scenarios with DMED+, BESA, and KL-UCB+.

We propose as a future research line the use of other inequalities to compute the confidence intervals nested around the expected value when modeling the uncertainty about the expected rewards from the arm by means of possibilistic reward distributions. Specifically, an alternative Hoeffding's inequality could be used, together with its combination with Bernstein inequalities.

Acknowledgment. The paper was supported by the Spanish Ministry of Economy and Competitiveness MTM2014-56949-C3-2-R and MTM2017-86875-C3-3R.

References

1. Agrawal, R.: Regret bounds and minimax policies under partial monitoring. Adv. Appl. Probab. **27**(4), 1054–1078 (1995)
2. Audibert, J.-Y., Bubeck, S.: Sample mean based index policies by O(log n) regret for the multi-armed bandit problem. J. Mach. Learn. Res. **11**, 2785–2836 (2010)
3. Audibert, J.-Y., Munos, R., Szepervári, C.: Exploration-exploitation trade-off using variance estimates in multi-armed bandits. Theor. Comput. Sci. **410**, 1876–1902 (2009)
4. Auer, P., Cesa-Bianchi, N., Fischer, P.: Finite time analysis of the multiarmed bandit problem. Mach. Learn. **47**, 235–256 (2002)
5. Auer, P., Ortner, R.: UCB revisited: improved regret bounds for the stochastic multi-armed bandit problem. Adv. Appl. Math. **61**, 55–65 (2010)
6. Baransi, A., Maillard, O.-A., Mannor, S.: Sub-sampling for multi-armed bandits. In: Calders, T., Esposito, F., Hüllermeier, E., Meo, R. (eds.) ECML PKDD 2014. LNCS (LNAI), vol. 8724, pp. 115–131. Springer, Heidelberg (2014). https://doi.org/10.1007/978-3-662-44848-9_8
7. Bernstein, S.N.: Probability Theory. GTTI, Moscow, Leningrad (1946)
8. Berry, D.A., Fristedt, B.: Bandit Problems: Sequential Allocation of Experiments. Chapman and Hall, London (1985)
9. Burnetas, A.N., Katehakis, M.N.: Optimal adaptive policies for sequential aallocation problems. Adv. Appl. Math. **17**(2), 122–142 (1996)
10. Cappé, O., Garivier, A., Maillard, O., Munos, R., Stoltz, G.: Kullbackleibler upper confidence bounds for optimal sequential allocation. Ann. Stat. **41**, 1516–1541 (2013)
11. Chapelle, O., Li, L.: An empirical evaluation of thompson sampling. In: Advances in Neural Information Processing Systems, pp. 2249–2257 (2001)
12. Dubois, D., Foulloy, L., Mauris, G., Prade, H.: Probability-possibility transformations, triangular fuzzy sets, and probabilistic inequalities. Reliable Comput. **10**, 273–297 (2004)
13. Dupont, P.: Laplace and the indifference principle in the essai philosophique des probabilits. Rendiconti del Seminario Matematico Universit e Politecnico di Torino **36**, 125–137 (1978)
14. Garivier, A., Cappé, O.: The KL-UCB algorithm for bounded stochastic bandits and beyond. Technical report, arXiv preprint arXiv:1102.2490 (2011)
15. Gittins, J.: Bandit processes and dynamic allocation indices. J. R. Stat. Soc. **41**, 148–177 (1979)
16. Gittins, J.: Multi-armed Bandit Allocation Indices. Wiley Interscience Series in Systems and Optimization. John Wiley and Sons Inc., New York (1989)
17. Hoeffding, W.: Probability inequalities for sums of bounded random variables. Adv. Appl. Math. **58**, 13–30 (1963)
18. Holland, J.: Adaptation in Natural and Artificial Systems. MIT Press/Bradford Books, Cambridge (1992)
19. Honda, J., Takemura, A.: An asymptotically optimal bandit algorithm for bounded support models. In: Proceedings of the 24th Annual Conference on Learning Theory, pp. 67–79 (2010)
20. Kaufmann, E., Cappé, O., Garivier, A.: On Bayesian upper confidence bounds for bandit problems. In: International Conference on Artificial Intelligence and Statistics, pp. 592–600 (2012)

21. Lai, T., Robbins, H.: Asymptotically efficient adaptive allocation rules. Adv. Appl. Math. **6**, 4–22 (1985)
22. Lattimore, T.: Regret analysis of the finite-horizon gittins index strategy for multi-armed bandits. J. Mach. Learn. Res. **49**, 1–32 (2016)
23. Maillard, O., Munos, R., Stoltz, G.: Finite time analysis of multi-armed bandits problems with Kullback-Leibler Divergences. In: Proceedings of the 24th Annual Conference on Learning Theory, pp. 497–514 (2011)
24. Martín, M., Jiménez-Martín, A., Mateos, A.: A possibilistic reward method for the multi-armed bandit problem. In: Proceedings of the 6th International Conference on Operations Research and Enterprise Systems, pp. 75–84 (2017)
25. Smets, P.: Data fusion in the transferable belief model. In: Proceedings of the Third International Conference on Information Fusion, pp. 21–33 (2000)
26. Sutton, R.S., Barto, A.G.: Introduction to Reinforcement Learning. MIT Press, Cambridge (1998)

Managing Service Parts for Discontinued Products: An Action Research Approach

Luís Miguel D. F. Ferreira[1(✉)], Amílcar Arantes[2], and Cristóvão Silva[1]

[1] Department of Mechanical Engineering, University of Coimbra, Coimbra, Portugal
{luis.ferreira, cristovao.silva}@dem.uc.pt
[2] CERIS, CESUR, Instituto Superior Técnico, Universidade de Lisboa, Lisboa, Portugal
amilcar.arantes@tecnico.ulisboa.pt

Abstract. The management of service parts inventories in the post- product life cycle is an issue that has often been ignored by companies, resulting in additional problems that may negatively affect their reputation. The main purpose of this research is to develop a methodology to help decision makers manage service part issues in the period following product discontinuation. To this end, an action research case study was carried out in an industrial manufacturer of household appliances, which is bound by legal obligation to provide service parts for its products for a period of 15 years after ceasing production. The work resulted in three deliverables, namely, characterization of the company situation, definition of a procedure to eliminate obsolete stocks, and definition of a procedure to manage active service parts. Implementation of the procedures has made it possible to improve the service levels for service parts and to achieve a 10% decrease in the inventory value of service part components.

Keywords: Service parts · Discontinued products · Empirical study

1 Introduction

For many companies facing increasing competition, customer satisfaction has become a goal of the utmost importance, and one way to keep their customers satisfied is their ability to rapidly repair a product failure. Moreover, while some products, such as consumer electronics, appear to be disposable, for others, including household appliances and automobiles, service parts management has become an increasingly important factor [1].

Service parts are mainly used to replace old parts that are no longer working. They are considered an important area of a company's business. In some sectors, the service parts after-sales business can account for up to 25% of the revenues and 40% to 50% of the profits of manufacturing firms [2, 3]. In a benchmark study covering more than 120 companies from various industries, [4], revealed that business units related to service provided on average 75% higher profitability as compared to the overall business profitability. Managing service parts can, thus, also improve customer loyalty,

G. H. Parlier et al. (Eds.): ICORES 2017, CCIS 884, pp. 210–223, 2018.
https://doi.org/10.1007/978-3-319-94767-9_11

sustainability, and profits. While poor management can be detrimental to business performance and generally hinder attainment of objectives [1].

This situation goes some way to explaining why many companies have shifted their efforts from improving their manufacturing and delivery processes to improving after sales service and customer support [5]. As a result of this shift, companies are required to keep inventories of many of those service parts and, as many of these service parts are expensive, this entails a great sum of money being wrapped up in inventory matters.

Unfortunately, the lack of availability of service parts is frequently recognized as a main source of obsolescence of many products. Furthermore, the levels of competition in the market mean that any stock-out of service parts cannot be tolerated, since this has an adverse impact on the brand and corporate image [6]. Inventory costs related with service parts for current products are much lower than those for service parts for discontinued products. Additionally, after a product has been discontinued, many of the service parts needed in the post-product life cycle are often no longer in production [7].

Accordingly, meticulous management of service parts is imperative because the production lines used for manufacturing those service parts have most likely already been discontinued in advance of the demand for them dropping to zero. In some geographic areas, companies are required by law to provide past model service parts for many years after production has finished. The procurement and inventory management of such service parts is a complex matter due to the intermittent nature of their demand patterns, the high responsiveness needed to minimize the downtime cost for the customer, and the high risk of stock obsolescence [6].

However, service parts cannot be managed using the traditional inventory control methods [8]. Most of the literature focuses on the definition of (re)ordering policies or stock control in situations where demand and delivery can be reliably forecasted. This research looks at the management of service parts for discontinued products – where demand is erratic and hence hard to predict, suppliers of components of the service parts may no longer be available, and spare parts must be provided up to 15 years after ceasing the production of a specific model. Literature on such situations is scarce. Research dealing with after-market support, such as service parts, is a matter that is overlooked and under investigated [9]. This is somewhat concerning, considering the importance of after-sales service [5, 10].

Hence, the main aim of this research is to develop a methodology, through an action research approach, to help decision makers manage service part issues in the period following product discontinuation. We focus on defining procedures which will eliminate obsolete stock, and developing procedures to manage active service parts.

This paper is based on an action research project and, for reasons of confidentiality, more detailed information about the case study company, its position within its industry, and its operations is not presented. The company is referred to herein as AVPT. The outline of the paper is as follows. Section 2 presents a review of the literature. This is followed by sections describing the research method (Sect. 3), the case study company and the approach followed (Sect. 4). The application of the model and some results are described in Sect. 4.4, and conclusions are drawn in Sect. 5.

2 Literature Review

Inventory management of service parts is acknowledged as playing a key role in providing adequate after-sales service [1, 5]. First, demand for service parts is usually unpredictable yet must be filled immediately for practical operational reasons. And second, because a relatively long service period paired with a general trend towards decreasing product life cycles is resulting in a steady increase in the number of products which are no longer produced, but for which service parts must still be available.

During the product life cycle companies can easily manage the production of service parts making use of the existing production facilities. The purchase of components or materials for service parts manufacturing does not pose a problem, as suppliers are aware of the market demand for the product. However, this situation changes completely once the company ceases producing the product, in other words, after the end of the product life cycle. Although there is no longer a demand for the product itself, service parts are still consumed to replace the damaged parts of the products already sold. Service parts management during the length of time between end-of-production (EOP) and end-of-service (EOS) is a challenging task for businesses (see Fig. 1). This period may be defined by a legal requirement, or it may be set voluntarily by the company. In some cases, the company may go beyond the legal limit, as a strategy for improving service levels and improving its image.

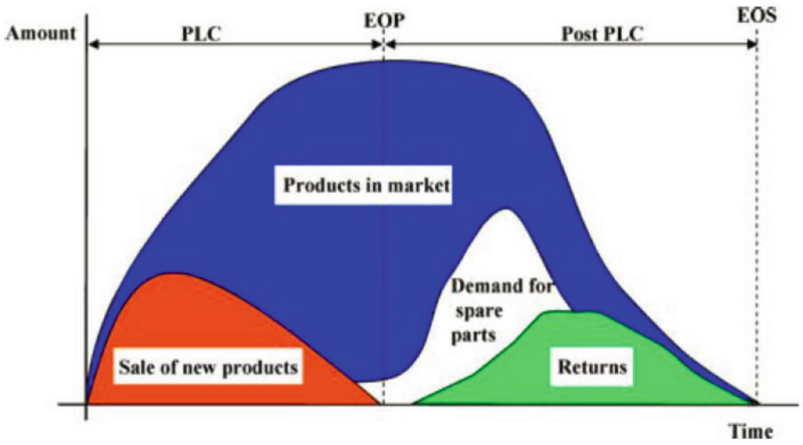

Fig. 1. Demand for new products, spare parts, and product returns (adapted from [11]).

[11] looked at this issue specifically for the automotive electronics industry, arguing that the problem of sourcing the spare parts after product life cycle is more significant and critical for durable products and products with short innovation cycles. In those situations, a high degree of uncertainty in demand for spare parts and in supply of used products with satisfactory recoverability can be identified. The demand for spare parts and supply of returned used products is illustrated in Fig. 1.

According to [11], the following possible sources for and approaches to acquiring spare parts after the end-of-production exist:

- the total demand for spare parts after EOP is forecasted and an extra amount is manufactured together with the last batch in regular production;
- after the end of regular production, the firm continues manufacturing the spare parts;
- the firm may outsource spare parts production to small industrial units;
- the firm may begin remanufacturing its used products. After disassembly of returns, the parts and components may be set aside for remanufacturing, which converts them to "as-good-as-new" products;
- the defective components that have been replaced are simply repaired and stored as spare parts for future use. This option can only be applied in those cases where original spare parts are not required.

Each of these options for sourcing spare parts involves certain benefits and costs.

However, the end of after-sales service may also occur unexpectedly, further complicating the management of service parts. For example, in a situation where the functioning of a machine is dependent on the availability of a specific service part, a stock-out of that part will render the machine obsolete. This means that all the other service parts of that machine will reach the end of the after-sales service period earlier than expected. Another source of uncertainty is given when one service part is replaced by another service part. For example, a company that manufactures mobile computer batteries may bring a new battery to market with extended capacity and at a lower price. Then, when consumers need to replace the battery, they will likely choose the new model over the old model. This source of uncertainty is difficult to predict [6].

There is a considerable body of literature regarding demand forecasting of service parts. Several well-known approaches exist, ranging from relatively simple models, such as Croston's method [12] and the further development thereof [13, 14], to much more sophisticated algorithms, as in the stochastic forecasting model presented by [6]. The latter method considers four key factors in its model for forecasting service parts: product sales, the discard rate of the product, the failure rate of the service part and the replacement probability of the service part.

More recently, [15] presented a pioneering idea for forecasting demand for spare parts that relies upon the demand generation process itself, comparing it favorably with a traditional time-series method. [16] presented two approaches for dealing with the problem of extending maintenance or supply contracts for spare parts of discontinued products: one includes the use of a continuous-time dynamic programme and the other employs a two-stage stochastic algorithm. [17] presented a case study in an automaker that operates in Brazil, considering six years of demand data (10032 spare parts references) and comparing several methods using different forecasting techniques and inventory management policies by simulation. The performance was measured by total costs and realized-fill-rates, and the results of the simulations allowed for the recommendation of best policies to be followed within each spare part category.

Other authors have proposed practical approaches to managing service parts for discontinued products in practice. For example, [18] present a model, which was implemented in an electronic equipment company, to determine the size of a final order

for service parts, with the aim of covering demand until all service obligations have ceased. [19] analyzed the problem of calculating an optimal final order for spare components when, at a certain moment, a company is offered a final chance to order spare parts components for its machines.

However, preceding research has focused primarily on the planning and operational aspects (e.g. the determination of optimal spare parts inventory levels) and has ignored the strategic and organizational issues manufacturing companies must resolve in order to manage their spare parts business successfully during the post product life cycle. Indeed, a gap between research and practice has been acknowledged by several researchers. For a comprehensive literature review on service parts management and on the gap between research and practice please see [20] These authors argue, for example, that "despite the wealth of literature on the subject, no attention has in practice been paid to proper management and control of service-parts inventory" or that "incremental mathematical inventory research is not likely to enhance practice".

This gap between practice and research may be explained by the mathematical complexity of the proposed methods and their need for data which are often not accessible. One should also note that the acceptance of simple but formalized procedures for the management of service parts during the post product life cycle can help companies achieve considerable benefits, not only by reducing costs but also by improving the company's image [8].

3 Research Method

This paper presents the case of an industrial company which manufactures household appliances. In the past, the procurement and inventory management of service parts during the post product life cycle had been largely neglected by the company. This resulted in several problems already reported in the literature. These include such as stock-outs, rush orders and obsolete stock (stock of service parts for which the service contract has expired). Furthermore, service part production also required components for which the original supplier was no longer available, requiring a time-consuming negotiation process with potential new suppliers.

To mitigate the impact of these complications, the company decided to launch a project to define procedures for the procurement and inventory management of service parts during the post product life cycle. Beyond this, the company's service parts decision makers also intended that the procedures to be implemented should avoid using complex mathematical algorithms that employees would find hard to comprehend as well as models that would need data which would not be readily accessible, or even available, in the company information systems.

The research objectives were to propose procedures, effectively implement them within the manufacturing company, and then to provide evidence on their effectiveness. This study was carried out under the principles of action research, allowing for collaboration between the researchers and the company [21].

Two specific conditions had to be respected for the approach taken to meet the requirement of action research. Firstly, the research objective and project plan were driven by the researcher's agenda rather than by the participating company's

representatives. Second, the primary justification for the project plan was the development of procedures for the management of service parts during the post product life cycle and not the transformation of the individual organization's practices. In any case, the focus of the research is to introduce changes in reality [22]. More recently, [23] wrote on the importance of case studies, highlighting the need to focus on real situations and problems and on the way proposed techniques perform when adopted by managers.

4 The Case Study Company, Proposal of Procedures and Results

This section presents a proposal for procedures for the management of service parts during the post product life cycle and results. The project to define the requested procedures was developed in three phases, which are described in the following subsections: the characterization of the company service parts; the definition of a procedure to eliminate obsolete stocks; and the definition of a procedure to manage service parts.

4.1 Characterization of the Case Study Company

The case study company, AVPT, a manufacturer of household appliances, is obliged by law to provide service parts for models for a period of 15 years after the appliance containing said parts has been discontinued. The procurement process for service parts during the post product life cycle was conducted as follows: when the stock for a specified service part reaches its reorder level, a production order for this service part is scheduled by the logistics department. To manufacture that service part, the necessary components are taken from stock, and these components can also eventually reach the reorder level. If this occurs, an order for the component is placed by the purchasing department. The size of this order is calculated to meet the predicted demand for the next six-month period, based on a simple average of the demand for the component since the time the product became discontinued, adjusted in accordance with the contractual conditions between AVPT and the supplier.

This stage of the project was designed to provide a clear understanding of how many spare parts were exclusively used in the post product life cycle. The AVPT information systems contained information on all the components used in the service parts of discontinued products. However, accessing that information was difficult (for example, data on the time remaining until the end of the service contracts was not available for many of the service parts). That particular information was incomplete because each component could be used in several service parts and each service part may be required for several final products. Moreover, the data was spread over two different information systems (IS 1 and IS 2 in Fig. 2).

Accordingly, a support database was developed to easily access all relevant data about the components of discontinued products. This database was fed with data from both information systems (Fig. 2) and was used to identify all the required information for the procurement process. Using data from the first information system (IS 1), each component (Comp.) was linked to the service parts (SP) in which it is used. The second

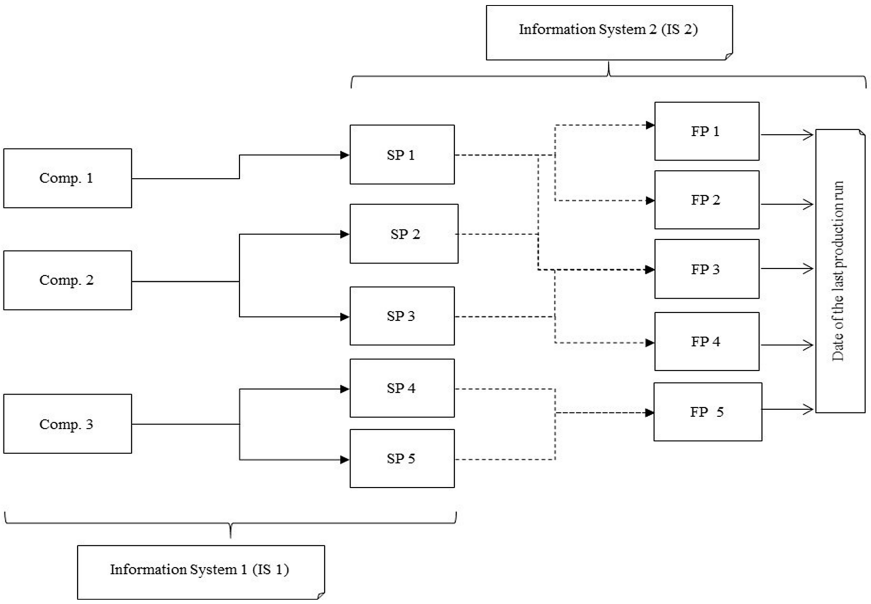

Fig. 2. Data collection from AVPT company information systems (adapted from [24]).

information system (IS 2) shows how each service part was linked to the final products in which they are used, and for each final product (FP) the date of the last production run was recorded. Furthermore, the corresponding supplier of each component was also identified. An illustrative example of the result of this operation is presented in Table 1.

Table 1. Illustrative example of component information.

Component	Time to end service (years)	Stock (units)	Stock (€)	Supplier
C1	8	1680	2825	Sup_1
…	…	…	…	…
C19	1	30	900	Unknown
…	…			
Cn	−1	450	689	Sup_39

The information contained in the database that was developed provided a detailed overview of the discontinued product service parts and their respective components. Some of these characteristics (namely the "Time remaining to end of service") make it possible to divide the service parts and their components into three major groups. For the first group, the company is no longer required to provide support, for the second group, the company is required to provide service up to the 15-year limit, and for the third group, no end-of-service date exists (this accounts for around 50% of the components listed). The complete listing for Table 1 showed that AVPT manages approximately 1300 components, exclusively used in service parts for discontinued products.

These 1300 components are required in some 1800 service parts for discontinued products (there are more service parts than components as each component can be used in various service parts). In turn, these service parts are used in 6530 end products (appliances). The 1300 components make up 14% of the total number managed by AVPT and 9% of the company stock value. Three percent of these components are considered as obsolete stock. Another conclusion that was drawn from the analysis of the database was that roughly 50% of the components has no active supplier assigned.

The lack of an assigned supplier represents a major challenge to the management and procurement of the components, because if a stock-out of one of those components occurred, AVPT would have to start from scratch a negotiation process with a new supplier, meaning long delivery lead times. There are two possible reasons for the lack of an active supplier: the usual component supplier has ceased trading, or a long time has passed since AVPT has placed an order with a supplier and it is neither able nor, perhaps, even willing to supply that component any longer.

4.2 A Procedure to Eliminate Obsolete Stocks

The preceding project phase identified some obsolete stocks. It was then necessary to develop a process to eliminate these stocks. The stock of these components could just be sold as scrap. However, they could still be of value as components for producing service parts for some discontinued products, even though AVPT might no longer have the legal obligation to do so.

In the past, if AVPT received an order for a service part which was no longer active (no longer covered by the post product life cycle period) and for which there was no available stock, the client was informed that AVPT could no longer provide this service part and the stock-out was not considered as a service-level failure by the company. But such situations had a negative impact on the company's reputation. To avoid these kinds of problems a procedure to eliminate obsolete stocks was proposed, as shown in Fig. 3.

Following this procedure, clients are informed which service parts have reached the end-of-service period and that they can place a final order for these service parts. If the stock of components for the end-of-life service parts is sufficient to cover the client's final order, the order is delivered. If the stock of components is not enough to cope with the service part production, an order for the required components is placed. After the final client orders, if some service parts or components still remain in stock, they are then sold as scrap. This procedure is now programmed to be carried out at the beginning of each calendar year for all service parts which have reached their end-of-life date during the previous year.

This procedure allows for obsolete stock to be removed, including both spare parts and the components which they alone use, given the direct link between the two. In addition, the warehouse space allocated to these parts and components becomes available for other items. Finally, and most importantly, this approach ensures customer satisfaction (service level), given that the customer is cautioned in advance of the service part's end of life. Customers are given the chance to place a last order, guaranteeing a fixed quantity and with a lead time of around one month.

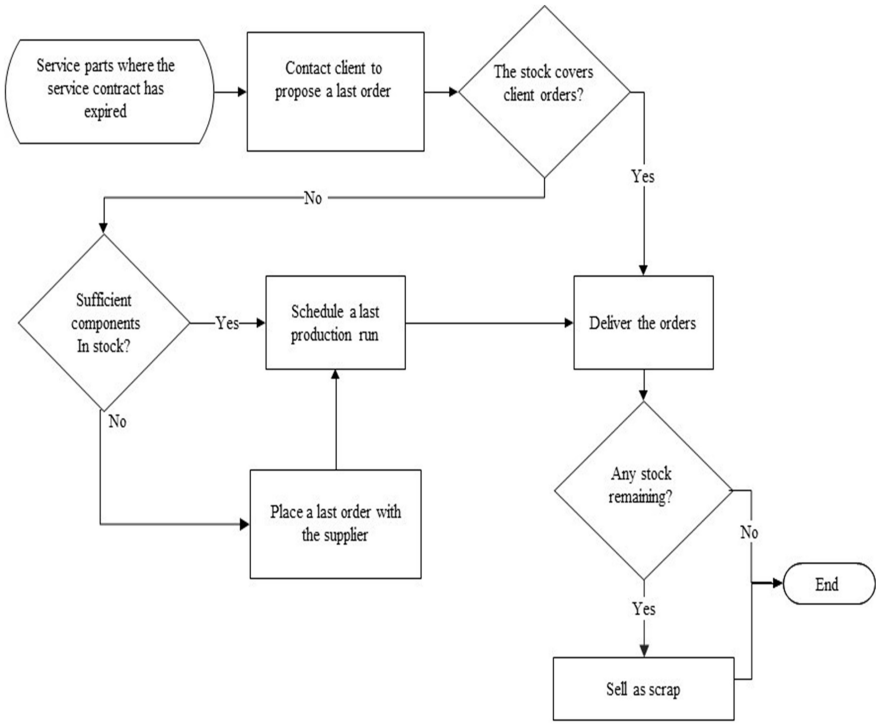

Fig. 3. Flowchart showing the procedure to eliminate obsolete stock (adapted from [24]).

4.3 A Procedure to Manage Active Service Parts

This final phase of the project defined a procedure to improve the management process of active service parts. The main objective in managing service parts is to establish a component ordering procedure which ensures an adequate inventory level. The availability of components for the production of service parts is crucial to AVPT. Long lead times are not acceptable as the end customer is waiting for their household appliance to be repaired.

The process for obtaining the components used to manufacture the service parts for end products which are still currently in production is relatively simple, as it depends on the demand (for service parts). However, in situations where the demand for service parts can be described as intermittent, proper forecasting methods must be used so that inventory levels can be appropriately managed.

In the past, AVPT spare parts decision makers used the average service part demand over the preceding six months to forecast the demand for the following six months, each time the component reorder point was reached. The forecast demand for the following six months would help anticipate the component procurement process and the service part production, thus avoiding long lead times for the final client. In this respect, two distinct situations are possible. Service parts with components for which there are active suppliers, and service parts with components for which there are no

active suppliers. In both cases demand forecasting is important for guaranteeing an effective procurement process and efficient inventory level management. Additionally, in the second case forecasting is also important for helping the procurement department negotiate the right business conditions with potential new suppliers.

At the beginning of the project AVPT spare parts decision makers expressed a number of concerns with respect to the adequacy of the forecasting method currently used. Thus, in order to identify which forecasting methods could be used for managing service parts it was decided to analyze the demand patterns of those service parts (using available data from a seven-year period).

The service parts were classified according to their demand patterns as slow moving, intermittent, erratic and lumpy, in line with the proposal by [25] This classification was made on the basis of the values calculated using inter-demand interval (IDI) and the squared coefficient of variation of the demand sizes (CV^2).

Given that the company expressed the wish to avoid complex algorithms that would be hard for the users to understand, and considering the available data, three demand forecasting models were tested: The Croston Model [12], the SBA model [14] and the simple six-month-average method currently used by the company.

As proposed by these authors, demand for slow moving components should be forecasted using the Croston method, and demand for the others with the SBA model. Using historical data, the accuracy of these models was compared with the result obtained using the simple average-based procedure in place in the company. The comparison of the models centered on the forecasting errors, considering the mean absolute percentage error. Table 2 presents the inter-demand interval (IDI) and the squared coefficient of variation of the demand (CV^2) for three randomly selected service parts.

Table 2. Illustrative example of demand patterns for three randomly selected service parts (adapted from [24]).

	SP. 1	SP. 2	SP. 3
IDI	2.35	1.02	1.94
CV^2	1.25	0.37	2.7

The forecasting errors obtained for each component are presented in Table 3. It is clear that none of the forecasting methods tested outperforms the others in all cases. Thus, it was decided to keep the simple average procedure, already in place in the company. This decision is in accordance with the findings of [25].

Table 3. Illustrative example of the performance of the forecasting models (adapted from [24]).

Service parts	Forecasting model	Mean absolute percentage error
1	SBA ($\alpha = 0.10$)	43%
	Average	42%
2	Croston ($\alpha = 0.17$)	76%
	Average	96%
3	SBA ($\alpha = 0.15$)	202%
	Average	203%

Having identified the proper forecasting model to be used, the support database developed during this project (referred to in the previous section) was used to draw up a list of all the components with no available supplier. For these components, a single average of the past demand (since time 0) was used to estimate their future demand until the end of their service life. This list was sent to the procurement department which was responsible for initiating contacts to find potential suppliers for those components.

The demand estimate based on past demand helped the procurement managers in their negotiations with the selected suppliers. To avoid the same problem in the future (where components have no supplier available), a simple procedure represented in Fig. 4 was implemented in the company.

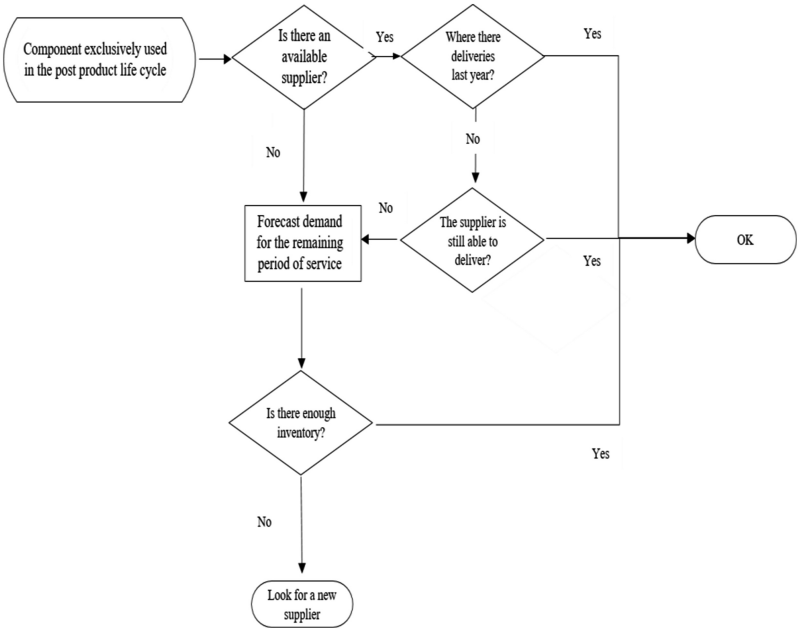

Fig. 4. Procedure to guarantee the availability of suppliers (adapted from [24]).

The database established during this action research project made it possible for a historical record to be created, comprising demand data for all the service parts and respective components. At the beginning of each year, the list of components is checked to identify all components where demand existed last year. For these components, all suppliers are contacted to verify if they are still able to deliver the required component. If not, the procurement department will be required to initiate contacts to find a new supplier.

For the components with available suppliers the procurement process in place in the company will be as follows. Whenever the reorder point is reached, an order that will cover the demand for the next six months will be made, based on the simple average demand over the previous six months.

4.4 Results

This project enabled AVPT to transform the management of spare parts during the post product life cycle. The process is now more efficient and reliable, making it possible to anticipate some of the issues regularly faced. In achieving this objective, several procedures were developed to support the procurement decisions for these spare parts, based on the time period remaining that the company has to assure the availability of spare parts.

The assessment of the different forecasting methods revealed that a simple six-month average could produce acceptable results to define the order quantity for service parts. The procurement and inventory management procedures for service parts described were applied in the company and have been used on an ongoing basis.

The implemented procedures led to a 4% reduction in stock-outs, raising service from a level of 95% to 99%. The improvement was primarily the result of implementation of this set of formal procedures that guarantee the existence of suppliers for any service parts components in the post product life cycle.

Another result of this project was a 10% reduction in the inventory value of service part components. This was mainly achieved through the elimination of obsolete stock, which also helped to improve warehouse efficiency.

5 Conclusions

Management of service parts is generally acknowledged as playing an important role in providing adequate after-sales service. However, it takes on critical importance once the company ceases producing a product. Although there is no longer demand for the product in question, service parts are still consumed through the need to replace the damaged service parts of the products already sold. Service parts management during the length of time between end-of-production and end-of-service is a challenging task for many companies.

Unfortunately, the prior research has focused primarily on the planning and operational aspects (e.g., the determination of optimal spare parts inventory levels) and has ignored the strategic and organizational issues manufacturing companies must resolve in managing their spare parts business successfully during the post product life cycle.

This research demonstrates how an action research project can provide performance improvements in the management of service parts used in the post product life cycle. The simplicity of the procedures proposed was decisive for their acceptance by the service parts decision makers, particularly considering that most of the available methods described in the literature require data which is frequently not readily accessible for companies.

Three well-known forecasting models were tested: the Croston model, the SBA model and a simple six-month average of past demand. It was concluded that no method outperforms the others. Accordingly, it was decided to retain the six-month average of past demand method already in use in the company. The implementation of the procedures has allowed AVPT to improve the service levels for service parts and to achieve a 10% decrease in the inventory value of service part components.

The action research model used in this research project contributed both to achieving practical results and to developing new knowledge. This was achieved through the active involvement of both service parts decision makers and researchers.

We acknowledge that this study has certain limitations, particularly its focus on organizational and information aspects relating to service parts management. A future avenue of research could be to explore the decisions related to the dimensioning of the last order.

References

1. Boone, C., Skipper, J.B., Hazen, B.T.: A framework for investigating the role of big data in service parts management. J. Clean. Prod. **153**(1), 687–691 (2017)
2. Dennis, M.J., Kambil, A.: Service management: building profits after the sales. Supply Chain Manage. Rev. **7**(1), 42–48 (2003)
3. Cohen, M.A., Zheng, Y.S., Wang, Y.: Identifying opportunities for improving Teradyne's service-parts logistics system. Interfaces **29**(4), 1–18 (1999)
4. Glueck, J.J., Koudal, P., Vaessen, W.: The service revolution: manufacturing's missing crown jewel. Research Report. Deloitte Development LLC (2011)
5. Vigoroso, M.W.: Maximizing Profitability with Optimized Service Parts Planning. Aberdeen Group, Boston (2005)
6. Hong, J.S., Koo, H., Lee, C., Ahn, J.: Forecasting service parts demand for a discontinued product. IIE Trans. **40**(7), 640–649 (2008)
7. Inderfurth, K., Mukherjee, K.: Analysis of spare part acquisition in post product life cycle. Otto von Guericke University. FEMM Working Paper 2006/006 (2006)
8. Botter, R., Fortuin, L.: Stocking strategy for service parts: a case study. Int. J. Oper. Prod. Manage. **20**(6), 656–674 (2000)
9. Farris, M.T., Wittman, C.M., Hasty, R.: Aftermarket support and the supply chain. Int. J. Phys. Distrib. Logistics Manage. **35**(1), 6–19 (2005)
10. Pfohl, H.C., Ester, B.: Benchmarking for spare parts logistics. Benchmarking Int. J. **6**(1), 22–39 (1999)
11. Hesselbach, J., Mansour, M., Graf, R.: Reuse of components for the spare parts management in the automotive electronics industry after end-of-production. In: 9th CIRP International Seminar, Erlangen, pp. 191–197 (2002)
12. Croston, J.D.: Forecasting and stock control for intermittent demands. Oper. Res. Q. **23**, 289–303 (1972)
13. Syntetos, A.A., Boylan, J.E.: On the bias of intermittent demand estimates. Int. J. Prod. Econ. **71**(1/3), 457–466 (2001)
14. Syntetos, A.A., Boylan, J.E.: The accuracy of intermittent demand estimates. Int. J. Forecast. **21**, 303–314 (2005)
15. Wang, W., Syntetos, A.A.: Spare parts demand: linking forecasting to equipment maintenance. Transp. Res. Part E Logistics Transp. Rev. **47**(6), 1194–1209 (2011)
16. Leifker, N.W., Jones, P.C., Lowe, T.J.: Determining optimal order amount for end-of-life parts acquisition with possibility of contract extension. Eng. Econ. **59**(4), 259–281 (2014)
17. Rego, J.R., Mesquita, M.A.: Demand forecasting and inventory control: a simulation study on automotive spare parts. Int. J. Prod. Econ. **161**, 1–16 (2015)
18. Teunter, R.H., Fortuin, L.: End-of-life service: a case study. Eur. J. Oper. Res. **107**(1), 19–34 (1998)

19. Teunter, R.H., Haneveld, W.K.: The 'final order' problem. Eur. J. Oper. Res. **107**(1), 35–44 (1998)
20. Bacchetti, A., Saccani, N.: Spare parts classification and demand forecasting for stock control: investigating the gap between research and practice. Omega **40**(6), 722–737 (2012)
21. Middel, R., Coghlan, D., Brennan, L., McNichols, T.: Action research in collaborative improvement. Int. J. Technol. Manage. **33**(1), 67–91 (2006)
22. Baker, T., Jayaraman, V.: Managing information and supplies inventory operations in a manufacturing environment. Part 1: an action research study. Int. J. Prod. Res. **50**(6), 1666–1681 (2012)
23. Childe, S.: Case studies in the management of operations. Prod. Plan. Control **28**(1), 1 (2017)
24. Ferreira, L., Arantes, A., Silva, C.: Discontinued products - an empirical study of service parts management. In: Proceedings of the 6th International Conference on Operations Research and Enterprise Systems, pp. 66–74 (2017)
25. Syntetos, A.A., Boylan, J.E., Croston, J.D.: On the categorization of demand patterns. J. Oper. Res. Soc. **56**, 495–503 (2005)

Optimizing Combination Warranty Policies Using Remanufactured Replacement Products from the Seller and Buyer's Perspectives

Claver Diallo[1,2(✉)], Uday Venkatadri[1,2], Abdelhakim Khatab[1,2], and Sriram Bhakthavatchalam[1,2]

[1] Department of Industrial Engineering, Dalhousie University, 5269 Morris Street, Halifax, NS B4H-4R2, Canada
{claver.diallo,uday.venkatadri,sriram.bhakthavatchalam}@dal.ca
[2] Laboratory of Industrial Engineering, Production and Maintenance (LGIPM), National School of Engineering, Lorraine University, Metz, France
abdelhakim.khatab@univ-lorraine.fr

Abstract. Growing awareness for sustainability and green legislation being implemented worldwide are forcing manufacturers and other organizations to recover and remanufacture used products to extend their lifecycles. These remanufactured products are send back to the marketplace or used in maintenance or used as replacement products to honour warranty offers. This paper presents the development and optimization of two mathematical models to determine the optimal combination rebate warranty policy when remanufactured products are used for replacements from both the seller and buyer's point of view. Several numerical experiments are conducted to derive useful managerial knowledge and consumer guidelines.

Keywords: Warranty policy · Remanufactured products
Seller and buyer perspectives · Reliability optimization

1 Introduction

Sustainable development legislation along with concerns for the environment have forced organizations all over the world to adapt their manufacturing practices and adopt new ways of recovering value from end-of-use or end-of-life products. Remanufacturing processes such as refurbishing and reconditioning are examples of activities that can extend the lifecycles of products. Economical opportunities in remanufacturing have increasingly generated substantial volumes of remanufactured products that are mainly sold to environmentally conscious consumers. Remanufactured parts are also commonly used as spare parts in repair and maintenance of other products. The aim of this paper is to

G. H. Parlier et al. (Eds.): ICORES 2017, CCIS 884, pp. 224–239, 2018.
https://doi.org/10.1007/978-3-319-94767-9_12

investigate the use of remanufactured products as replacement products to honour warranty claims. In the literature these remanufactured products are also sometimes called refurbished or second-hand products.

A product warranty is a contractual agreement offered by the manufacturer or seller to the buyer at the point of sale of a product to establish liability upon failure [3,4,17]. The use of warranties is universal and serves numerous purposes. It assures the consumer or buyer that the seller will rectify all the failures occurring within the warranty period at lower or no cost. For manufacturers, the warranty acts as a promotional tool to increase sales and revenue [3] by inferring the high quality of their products. According to [8,20], American manufacturers spend over 25 billion dollars to service warranty claims which is about 2% of their annual revenue from sales. According to [20], in the 2009 General Motors annual report, the company had a total revenue of $104.2 billion and the future warranty cost on sold cars estimated to be $2.7 billion, about 2.6% of the revenue.

When buying a product, the buyer usually faces the difficult task of deciding between purchasing the warranty or not. And when the decision is to get the warranty, choosing between different characteristics and warranty policies is another challenge. When the warranty period is optional, the consumer has to decide if the warranty is worth the additional cost based on very limited knowledge. This is becoming more and more important, since there is a growing trend among the manufacturers to offer extended term warranties. These involve additional costs with terms that can vary considerably [3,4,25]. Often, at the time of purchase, the consumer has to decide based, on very limited information, whether to opt for an extended warranty or not and to determine the best extended terms for their situation when there are multiple options [3,4]. The average buyer is not capable of conducting a mathematical analysis before making a choice because the consumer neither has the expertise for such an analysis nor the bargaining power to obtain relevant data from the manufacturer or seller. However, consumer bureaus and regulatory agencies can carry out such analyses and inform the general public. Any model developed from the buyer's point of view in this article is then assumed to have been done for a consumer agency on behalf of all consumers and with data obtained by the agency from the manufacturers or from established and recognized independent reviewing bodies such as the Consumer Reports magazine in North America.

There are many different types of warranty policies designed to cover the needs of manufacturers, dealers and consumers. A policy which is based on one factor (usually age) alone is said to be one-dimensional (1-D), on the other hand a two dimensional (2-D) warranty is limited by the first expiry of any of two factors, usually age and a measure of usage of the product. 1-D policies are commonly used for products which are known to last for a fixed time period such as cellphones, computers, and projectors. 2-D warranties apply to products that display wear and tear, degradation with usage. Automobiles, hydraulic and mechanical systems and heavy-duty machinery are examples of products with 2-D warranty policies. Some basic warranty types are the Free replacement (FRW), Pro-rata (PRW), and Rebate warranty.

1. **Free Replacement Warranty (FRW).** The manufacturer agrees to repair/replace a failed item during the warranty period at no charge to the customer. Example: small household appliances, electronics.
2. **Pro-Rata Warranty (PRW).** The customer covers a proportion of the repair cost prorated to the age of the item at failure. Example: Tires.
3. **Rebate Warranty.** The seller agrees to refund some proportion of the sale price to the buyer, if the product fails during the warranty period. The refund amount may be a linear or non-linear function of the failure time. Example: Money Back Guarantee (MBG) for electronic components such as hard drives, computer screens, and high density storage devices.

Basic taxonomies of warranty policies are presented in [3,4]. [20] developed an integrated warranty-maintenance taxonomy based on three categories: product type, warranty policy, and maintenance strategy.

Hybrid (combination) warranties are designed to utilize the desirable characteristics of the pure warranties and downplay some of their drawbacks [3,4]. The combination warranty gives the buyer full protection against full liability for later failures, where the buyer has received nearly the full amount of service that was guaranteed under the warranty. It has a significant promotional value to the seller while at the same time providing adequate control over costs for both buyer and seller. An example for hybrid warranty is seen in the FRW/PRW policy offered on some tires. During the first 2 years of service, the tire is replaced free of charge. Beyond year 2, the replacement price is pro-rated based on years of service from the original purchase date. Some advantages of combination warranties are improved protection towards the product, customer satisfaction, higher ownership lifetime for the buyers and higher sales volume which increases manufacturer profit.

Chari et al. [6] reported that combination warranty was a good type of warranty for remanufactured products as its offers a good protection for both manufacturers and consumers. In their recent paper, Alqahtani and Gupta [1] show how warranty is used as a marketing strategy for remanufactured products. Two main problems faced by the consumers acquiring remanufactured products are their uncertainty and durability due to the lack of past usage and maintenance history [1,20]. In order to reduce the risk and impact of product malfunctioning, sellers usually offer generous warranty policies. A review of warranty models currently available in the literature for remanufactured or second-hand products show that there are very few of them and all deal with the manufacturers perspective [7,10,20,22].

Reliability improvement strategies for second-hand products sold under multiple warranty policies including: failure-free warranty, rebate warranty, and a combination of free replacement and lump sum policies were presented by [19]. The goal of [21] was to find the age of the second-hand product to be used, the warranty period to be offered, and the upgrade level to be performed to maximize the expected profit of the dealer or seller. In [14], the aim was to determine the optimal upgrade level and warranty length to maximize the expected profit for used cars. A joint optimal price and upgrade level model for warranted

second-hand electric drills was proposed by [18]. A mathematical model for a one-dimensional renewing FRW policy with replacements carried out solely with reconditioned components was developed by [5]. A periodic inspection/upgrade model under non-renewing FRW (NFRW) policy with a fixed length of warranty period for a second-hand product is formulated by [13]. It jointly determined the optimal number of inspections required and an optimal improvement level to minimize the expected total warranty cost from the perspective of the dealer during the warranty period. It is apparent from the examples mentioned above that most warranty models for second-hand or remanufactured products are developed from the dealer or buyer's perspective.

The goal of this article is to address this shortcoming by proposing a warranty policy and develop mathematical models from both the manufacturers and consumers perspectives. This paper is an major extension of the following conference paper [2]. The present work is improved and extended to consider remanufactured systems with an initial age. The proposed warranty policy is modified to include a secondary warranty period that is proportional to the primary warranty coverage. Optimality conditions are added by deriving the Hessian matrix of the total expected profit function. New figures and recent relevant references are added.

The remainder of this article is structured as follows. Section 2 details the notation used, presents the warranty policy under consideration and derive two mathematical models for the seller and buyer's points of view. In Sect. 3, both optimization models are solved and two sets of numerical experiments are conducted, and their results are analyzed to derive managerial insights and consumer guidelines. Conclusions are drawn in Sect. 4 and avenues for future research are outlined.

2 Optimal Combination Warranty Models Using Remanufactured Products

For most warranty policies, failed products are repaired or replaced with new components or products. In the context of sustainable manufacturing, remanufactured products may be available and can therefore be re-used as replacements when consumers return failed products [9,23,24]. In doing so, the manufacturers or sellers can lower their costs and consumers can extend their ownership of the products. However, remanufactured products are known to potentially have lower reliability than new ones [7,9], therefore it is important to determine the optimal parameters of the warranty policy to be offered to avoid higher costs to the manufacturer and less than anticipated performance/ownership time for the consumer or buyer. In this article, we will develop two mathematical models for a combination rebate warranty policy using remanufactured products as replacement products.

2.1 Proposed Warranty Policy

Under the proposed warranty policy, a brand new product is sold with a total warranty coverage period of length w. The seller will replace a defective product only once with:

- A new product if the failure occurs before w_1 (Phase 1);
- A remanufactured product if the failure occurs between w_1 and w_2 (Phase 2). The length of the second coverage period is proportional to the first period by a factor k which is a decision variable so that $w_2 = k\, w_1$ with $k \geq 1$. Thus, $w = (1 + k)\ w_1$.

The proposed warranty policy is depicted in Fig. 1. New products have age $u = 0$. Remanufactured (also referred to as refurbished or second-hand) products have age $u > 0$. The policy offered here is equivalent to a rebate warranty where the refund amount is enough to repurchase a new or remanufactured product. Blischke and Murthy [4] provide detailed discussions of common warranty policies.

The Weibull distribution is used as the product failure distribution as is commonly done in reliability theory.

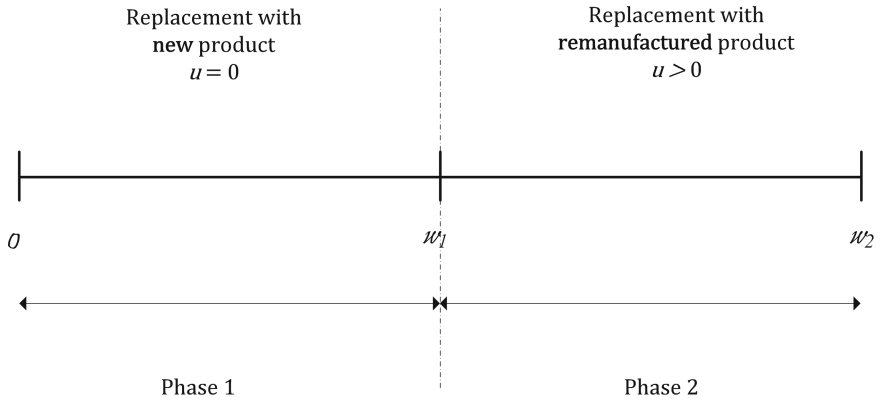

Fig. 1. Proposed warranty policy.

The following notation is used.

Parameters

$C_r(u)$: Cost of replacement by a remanufactured product of age u
C_0: Cost of replacement by a new product
C_w: Warranty cost
a: Price coefficient
b_i: Warranty coefficient
D_0: Demand amplitude factor
D_1: Warranty displacement constant
β, θ: Slope and scale parameters of the Weibull distribution

Decision Variables

p: Unit sale price of the new product
w_1: Length of initial/primary warranty period
k: Multiplier used to determine the length of the secondary warranty period
u: Age of the remanufactured products used as replacements

Functions

$f(t)$: Lifetime probability density function (pdf)
$F(t)$: Cumulative distribution (cdf)
$R(t)$: Reliability function $R(t) = 1 - F(t)$
$\mathcal{P}(p, w_1, k, u)$: Total expected profit for the Seller
$D(p, w_i)$: Total demand
EOT: Expected ownership time
$MTTF$: Expected lifetime of the original new product
$RMTTF$: Expected residual lifetime of the remanufactured products
$EOCR_1$: EOT per cost ratio of the product when warranty is purchased
$EOCR_2$: EOT per cost ratio of the product without warranty

In the following subsections, two mathematical models will be developed for the maximization of the seller's expected profit and the maximization of the buyer's ownership time.

2.2 Model 1: Maximization of Seller's Expected Profit

If the original product fails within w_1, a new product is given to the customer at a cost of C_0 which is incurred by the seller (i.e., the manufacturer in this case). When the original product fails between w_1 and w_2, a remanufactured product of age u is offered to the buyer at a cost of $C_r(u)$ which is incurred by the seller.

$C_r(u)$, the unit cost of a replacement product with age u, is given by Eq. (1) where C_0 is the base price and $\epsilon > 0$, and $\eta > 0$. Parameter ϵ represents the discount rate offered on remanufactured products, and parameter η models the increase in cost due to aging [6].

$$C_r(u) = \frac{C_0}{(1+u)^{\epsilon}} + u^{\eta} \tag{1}$$

A new product will therefore cost

$$C_r(u = 0) = C_0 \tag{2}$$

The cost of remanufactured products initially decrease with age as documented in the literature: remanufactured items cost less than new ones [5,12]. However, this cost for remanufactured products reaches a minimum then increases with age to account for technical, logistics and operational difficulties encountered when trying to collect, sort, disassemble and recondition very old products (availability of parts, obsolescence, corrosion, etc.)

The probability that a product will fail between w_{i-1} and w_i for $i = 1, 2$ is given by:

$$[F(w_i) - F(w_{i-1})] \tag{3}$$

where $w_0 = 0$.

The total expected warranty cost (C_w) is given by the weighted average of the replacement costs in each phase i given in Eq. (4) shown below.

$$C_w = \sum_{i=1}^{2} C_r(u) \times [\text{Prob. failure in phase } i]$$
$$C_w = C_0 \cdot F(w_1) + C_r(u) \cdot (F(w_2) - F(w_1)) \tag{4}$$

Given that the lifetimes of the product follow the Weibull distribution, the cumulative distribution function $F(t)$ is given by

$$F(t) = 1 - e^{-(\frac{x}{\theta})^{\beta}}, \qquad 0 \leq t$$

Then, Eq. (4) can equivalently be re-written as

$$C_w = C_0 \left[\left(1 - e^{-(\frac{w_1}{\theta})^{\beta}}\right) + \left((1+u)^{-\epsilon} + \frac{u^{\eta}}{C_0}\right) \cdot \left(e^{-(\frac{w_1}{\theta})^{\beta}} - e^{-(\frac{w_2}{\theta})^{\beta}}\right) \right] \tag{5}$$

Demand Function. The market demand function $D(p, w_i)$ for the product is modelled as a displaced log-linear function of w_i and p as in [7,11]:

$$D(p, w_i) = D_0 \cdot p^{-a} \cdot \prod_{i-1}^{2} (D_1 + w_i)^{b_i} \tag{6}$$

where $D_0 > 0$, $D_1 \geq 0$, $a > 1$, and $b_i > 0$. Parameter a is the rate of decrease of the demand as the price of the product increases. Parameters b_i are the rate of increase of the sales volume with the increase of the warranty lengths w_i. The factor D_0 is the demand amplitude and D_1 is the warranty displacement constant. These parameters can be estimated from customer surveys and empirical market studies using regression and econometric methods as suggested in [15,16]. Equation (6) models consumers' preference for longer warranty coverage and aversion for high prices.

Total Expected Profit. The seller's total expected profit $\mathcal{P}(p, w_1, k, u)$ is the product of the expected unit profit with the total demand. The expected unit profit is obtained by subtracting the cost of the original product C_0 and the expected warranty cost C_w from the unit sale price p.

$$\mathcal{P}(p, w_1, k, u) = \quad (p - C_0 - C_w) \cdot D(p, w_i) \tag{7}$$

The optimal strategy is solution of the following system of differential equations:

$$\begin{cases} \dfrac{\partial \mathcal{P}(p, w_1, k, u)}{\partial p} = 0, \text{ at } p = p^* \\ \dfrac{\partial \mathcal{P}(p, w_1, k, u)}{\partial w_1} = 0, \text{ at } w_1 = w_1^* \\ \dfrac{\partial \mathcal{P}(p, w_1, k, u)}{\partial k} = 0, \text{ at } k = k^* \\ \dfrac{\partial \mathcal{P}(p, w_1, k, u)}{\partial u} = 0, \text{ at } u = u^* \end{cases} \tag{8}$$

Equation (8) being analytically cumbersome to solve for the Weibull lifetime distribution, a numerical optimization procedure will be used to find the values of the decision variables (p^*, w_1^*, u^*, k^*) which maximize the total expected profit for the seller.

2.3 Model 2: Maximization of Buyers' Expected Ownership Time

This subsection focuses on the consumer or buyer's perspective. The goal is to find an optimal policy that maximizes the expected ownership time per unit of price paid. The warranty policy introduced in Subsect. 2.2 is still under consideration here.
At time of purchase, the consumer has two choices:

- Option 1: Buy the original product with warranty at price p set by the seller and determined using model 1 presented above; or
- Option 2: Buy the original product without warranty at a fraction ρ ($0 \leq \rho \leq 1$) of the price p.

The goal of model 2 is to formulate the Expected Ownership Time per Cost Ratio ($EOCR_i$) for both options ($i = 1, 2$) and compare their behaviour through the analysis of their difference Δ:

$$\Delta = EOCR_1 - EOCR_2. \tag{9}$$

Option 1: Purchase with Warranty

$$EOCR_1 = \frac{EOT_1}{p} \tag{10}$$

A consumer enjoys his original new product from purchase time up to the instant of the first failure which has expected duration $MTTF$. At failure, the consumer gets a replacement product that will have an expected residual lifetime $MTTF$ if the failure occurred in phase 1, otherwise the remanufactured replacement product will have an expected residual lifetime $RMTTF$. The original product fails in phase i with probability $[F(w_i) - F(w_{i-1})]$. Therefore, the expected ownership time for option 1 is given by

$$EOT_1 = MTTF + MTTF \cdot F(w_1) + RMTTF \cdot [F(w_2) - F(w_1)] \tag{11}$$

with

$$RMTTF = \frac{1}{R(u)} \int_u^\infty R(x).dx. \tag{12}$$

Combining Eqs. (10) and (11), gives the expression for $EOCR_1$:

$$EOCR_1 = \frac{MTTF + MTTF \cdot F(w_1) + RMTTF\,[F(w_2) - F(w_1)]}{p} \tag{13}$$

Option 2: Purchase without Warranty

$$EOCR_2 = \frac{EOT_2}{\rho \cdot p}$$
$$EOCR_2 = \frac{MTTF}{\rho \cdot p}$$

where $MTTF$ is the expected lifetime of the original product

$$EOT_2 = MTTF = \theta \cdot \Gamma\left[1 + \left(\frac{1}{\beta}\right)\right].$$

$\Gamma(.)$ is the gamma function. Therefore,

$$EOCR_2 = \frac{\theta \cdot \Gamma\left[1 + \left(\frac{1}{\beta}\right)\right]}{\rho \cdot p}. \tag{14}$$

Finally, Eq. (9) becomes:

$$\Delta = \frac{MTTF}{p}\left[1 + F(w_1) - \frac{1}{\rho} + \frac{RMTTF}{MTTF} \cdot [F(w_2) - F(w_1)]\right]$$
$$\Delta = \frac{MTTF}{p}\left[2 - e^{-(\frac{w_1}{\theta})^\beta} - \frac{1}{\rho} + \frac{RMTTF}{MTTF} \cdot \left[e^{-(\frac{w_1}{\theta})^\beta} - e^{-(\frac{w_2}{\theta})^\beta}\right]\right] \tag{15}$$

The obtained mathematical model is solved for various scenarios in order to derive decision-making guidelines for consumer organizations and bureaus who have the ability to test products, report their findings and influence consumers behaviour.

3 Numerical Results

Two sets of numerical experiments are conducted: one for each of the two models developed in the previous section.

3.1 Numerical Results for Model 1

For illustration purposes and without loss of generality, an example with three decision variables is considered by fixing the length of the first phase of warranty coverage w_1. This is reasonable if there are competitors in the market and the seller matches at minimum their warranty coverage. For the parameter values given below, we solve for the optimal solution (p, u, k) which maximizes the seller's total expected profit: $w_1 = 2; \theta = 25; \beta = 1.2; C_0 = 15; D_0 = 100,000; D_1 = 1; a = 2.9; b_1 = 1.2; b_2 = 0.1; \epsilon = 3.3; \eta = 1.7$.

The optimal strategy obtained is a combination of price $p^* = 25.04$ monetary units (m.u.), an age $u^* = 1.14$ for the remanufactured product to be used as a replacement product, and a factor $k^* = 5.84$ (i.e., $w_2^* = 11.68$). In practice, this would mean that if competitors offer a warranty coverage of 2 trimesters (6 months), then the seller can also match their coverage and add a secondary warranty period with a length of 9.68 trimesters where failed products would be replaced with remanufactured products with age 1.14. The total coverage is then for 11.68 months or about 35 months when the competition would be offering 6 months only. The resulting total expected profit for the seller is 365.6 m.u. These results are also depicted in Fig. 2 which shows a 3D plot of the total expected profit $\mathcal{P}$ as a function of purchase price p and age u for k fixed at its optimal value 5.83. The Hessian $(H(u, p, k))$ and its eigenvalues $(\lambda_1, \lambda_2, \lambda_3)$ are:

$$H(u,p,k) = \begin{bmatrix} -10.91086641 & 5.712003821\ 10^{-8} & -5.275175676\ 10^{-7} \\ 5.712003821\ 10^{-8} & -2.540090311 & 0.5572053122 \\ -5.275175676\ 10^{-7} & 0.5572053122 & -5.749472601 \end{bmatrix}$$

$$\lambda_1 = -10.911, \lambda_2 = -5.843, \lambda_3 = -2.446$$

The Hessian matrix is negative definite because all three eigenvalues are negative. Therefore, the optimal solution found is a local maximum. The 3D-plot shows that it is also a global maximum but it cannot be proven analytically given that Eq. (8) is not tractable.

Figure 3 shows a surface and contour view of the seller's profit. The contour at 345 delimits an area corresponding to a price range of 22 to 29, and an age range of 0.5 to 2.2 for a deviation from the optimal value of about 5.6%. This means that in practice, the seller can use remanufactured products aged between 0.5 and 2.2 to honour the warranty claims without affecting its profit significantly. This is an interesting managerial decision-making guideline as remanufactured products are not always easy to acquire in the quality and quantities needed.

A set of numerical experiments was conducted with model 1 by varying β, the shape parameter of the Weibull distribution. The results are plotted on Figs. 4 and 5. Figure 4 shows a very fast increasing profit function followed by a slowing down after $\beta = 6$. Increasing the shape parameter β increases the reliability of the product so that the warranty cost reduces and thus the profit increases. There is very little return on investment to improve reliability of the products beyond $\beta = 6$. Figure 5 shows that with improving reliability (increasing β), the warranty costs reduce and therefore the model can afford to reduce the unit price which increases profits by stimulating demand. As can also be seen on Fig. 5, the length of the secondary warranty period first decreases as β starts increasing then reaches a minimum around $\beta = 1.5$ after which, it starts to increase. When β is high, the product is very reliable meaning that very few failures will occur during the secondary warranty period. The seller is then able to offer longer warranty coverage. For values of β between 1 and 1.5, the product is not reliable enough that the remanufactured products could fail more often, which causes the model to suggest shorter secondary warranty lengths.

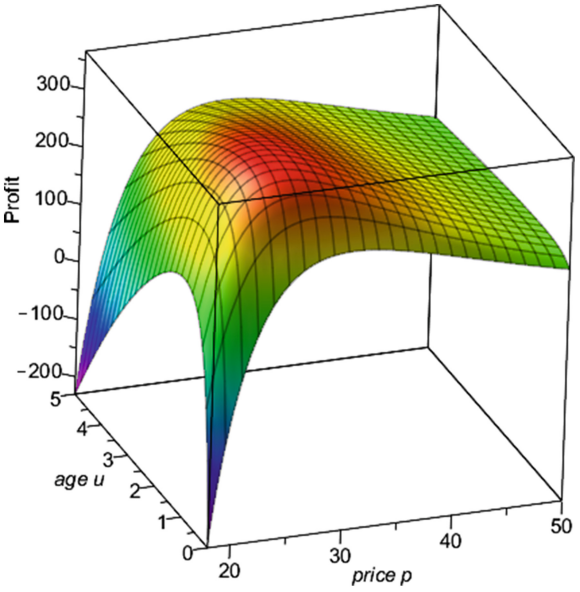

Fig. 2. Seller's total expected profit as a function of price and age when $k^* = 5.84$.

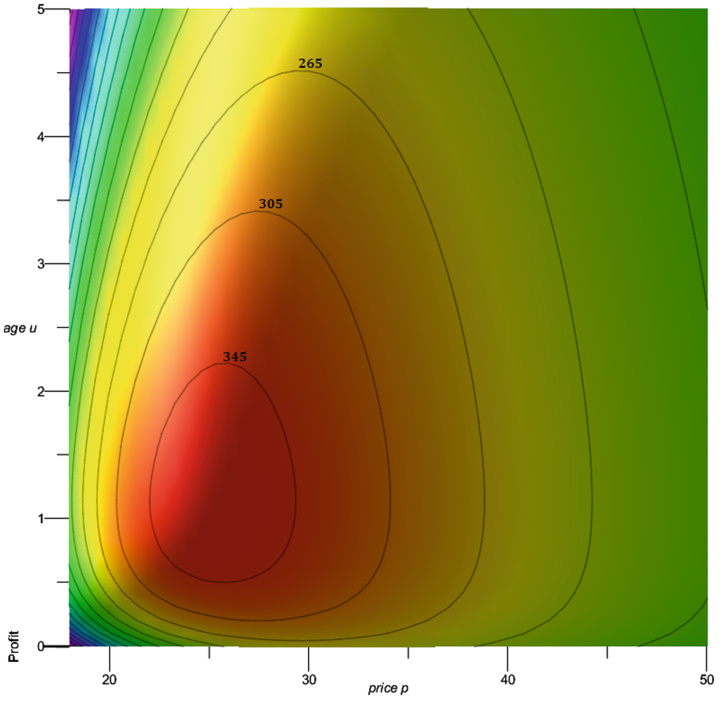

Fig. 3. Surface and contour plot of the seller's total expected profit when $k^* = 5.84$.

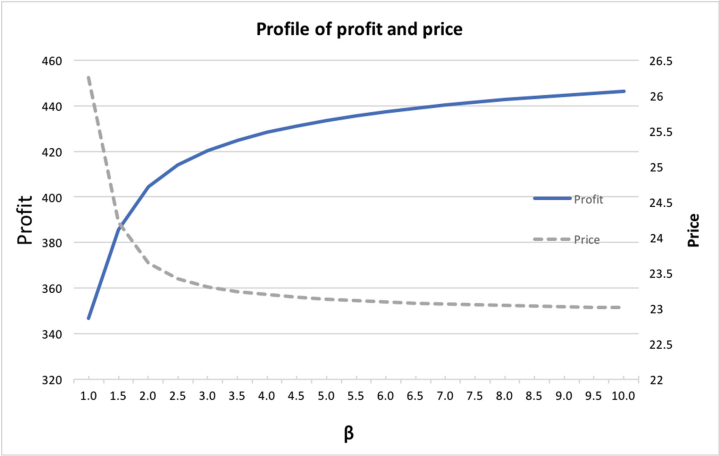

Fig. 4. Profit and price as a function of β.

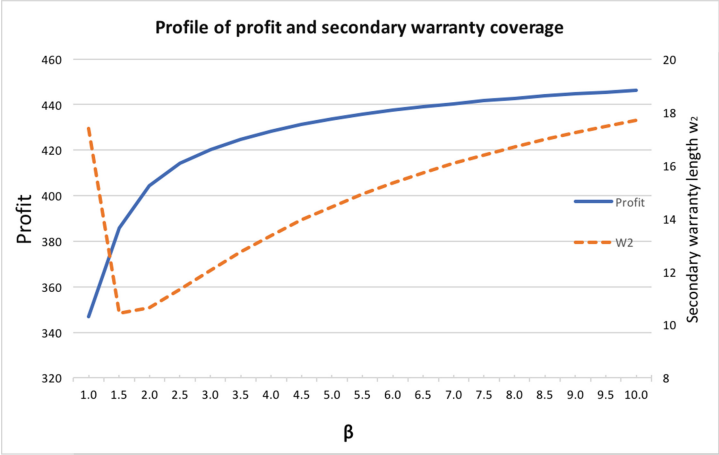

Fig. 5. Profit and price as a function of β.

Figure 6 is obtained by solving the optimization model for various values of k. When $k = 1$, the primary and secondary coverage lengths are equal. As k increases the secondary coverage increase more than the primary coverage. The seller's expected profit increases as k increases from 1 to k^* because more customers are attracted to the product with the increase of the secondary warranty period. After reaching k^*, the profit starts to drop as more failures are experienced during the increasingly long secondary coverage period which increases the warranty cost. Figure 6 displays an operating range ($3 \leq k \leq 5.84$) where the total expected profit is within a 1.5% gap from the optimal total expected profit.

Note that the operating range is not extended beyond k^*, because in practice the seller would never give a longer warranty period for the same profit.

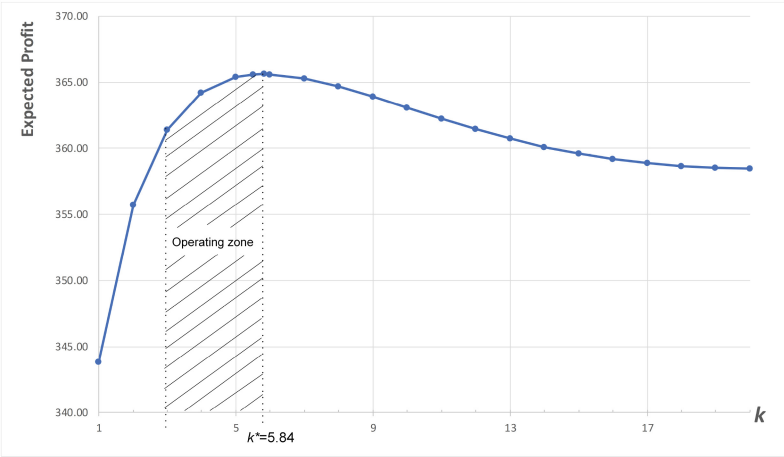

Fig. 6. Seller's expected profit for various values of k.

3.2 Numerical Results for Model 2

In this subsection, numerical experiments are conducted with the goal of deriving recommendations for consumer groups using the mathematical model in Eq. 15.

The first set of experiments is designed to analyze the recommendations made by the model for 6 secondary warranty durations (i.e., 6 values of k) when β changes. Figure 7 depicts the results obtained for the following parameters: $\rho = 0.85, p = 24.42, \theta = 25$, and $w = 2$. The results show two clear zones separated by the horizontal axis. Above the horizontal axis, the difference Δ is positive and means that it is preferable for the buyer to pay a higher price to get the warranty. Below the horizontal axis, the difference Δ is negative and therefore suggests that it is not worthwhile to get the warranty.

The following other observations can be made from the figure:

- The general profile of Δ for any of the 6 policies shows a fast decreasing curve for low values of β and a stabilizing shape for higher values. Δ is higher for $\beta < 1$ because early failures make the purchase of warranty more valuable. Δ stabilizes as β keeps increasing because of the resulting increase in reliability which decreases the likelihood of failure and therefore the purchase of warranty does not add significant value to the consumer. For high values of β (i.e., highly reliable products), all curves dip below the horizontal axis meaning that there is no need to purchase the warranty policy.
- Different warranty policies have different slopes of the same profile.
- As expected, policies with longer secondary warranty policies (higher values of k) are more beneficial to the consumer.

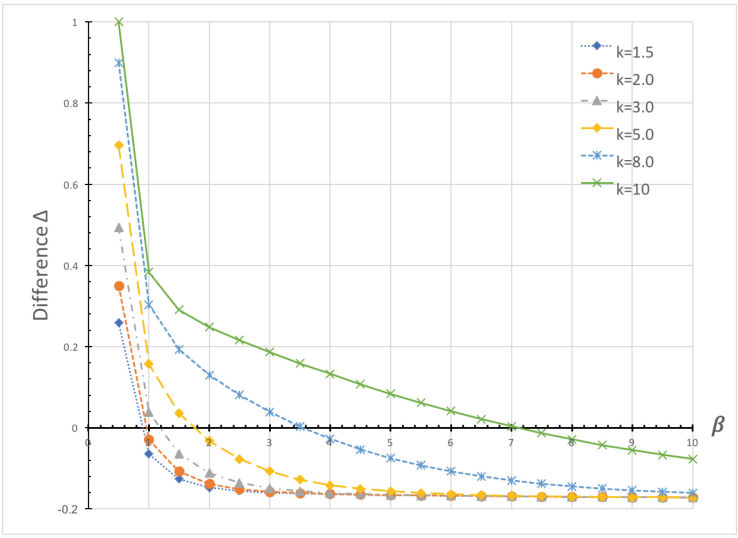

Fig. 7. Values of Δ for various warranty policies as β varies.

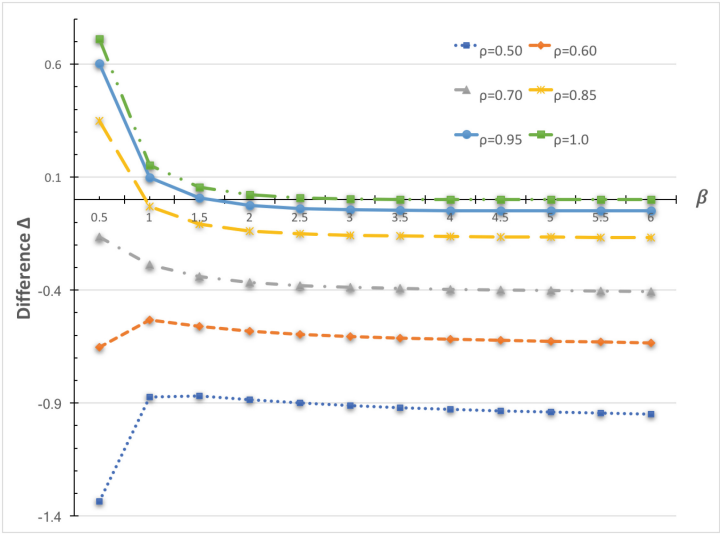

Fig. 8. Values of Δ for various warranty prices.

The second experiment investigates the impact of the warranty discount factor ρ on the decision to purchase the warranty or not. Figure 8 displays the results obtained when varying β for 6 values of ρ. As expected, when ρ decreases the incentive to buy the warranty also diminishes. In general, it is recommended to buy the warranty when β is relatively low and ρ is high.

4 Conclusions

This paper presented the development and optimization of two mathematical models with the aim of determining optimal combination rebate warranty policies when remanufactured products are used for replacements from both the seller and buyer's point of views. The first mathematical model was developed from the sellers' point of view to maximize their total expected profit. The second model dealt with the maximization of the buyer's expected ownership time of the product. The extensive numerical experiments that were conducted have showed that appropriate optimal warranty policy decisions can be reached. Furthermore, it is demonstrated that remanufactured products can efficiently be used to honour warranty claims. Both the manufacturer and consumer groups can use these mathematical models to improve profitability levels and increase ownership durations.

A natural extension of the current models would be to consider other types of combination warranty suitable for remanufactured products such as hybrid pro-rata policies. Another research avenue would be the development of joint imperfect maintenance and warranty policies for remanufactured products.

Acknowledgments.. This work was supported by the Canadian Natural Science and Engineering Council (NSERC) Discovery grants awarded to the first and second authors.

References

1. Alqahtani, A.Y., Gupta, S.M.: Warranty as a marketing strategy for remanufactured products. J. Clean. Prod. **161**, 1294–1307 (2017). ISSN 0959–6526
2. Bhakthavatchalam, S., Diallo, C., Venkatadri, U., Khatab, A.: Optimal combination rebate warranty policy with second-hand products. In: Proceedings of the 6th International Conference on Operations Research and Enterprise Systems (ICORES 2017), pp. 491–498. SCITEPRESS Science and Technology Publications, Lda (2017)
3. Blischke, W.R., Murthy, D.N.P.: Warranty Cost Analysis. Marcel Dekker Inc., New York (1993)
4. Blischke, W.R., Murthy, D.N.P.: Product Warranty Handbook. Marcel Dekker Inc., New York (1996)
5. Chari, N., Diallo, C., Venkatadri, U.: Optimal unlimited free-replacement warranty strategy using reconditioned products. Int. J. Perform. Eng. **9**(2), 191–200 (2013)
6. Chari, N.: Thematic development of recovery, remanufacturing, and support models for sustainable supply chains. Ph.D. thesis, Dalhousie University, Halifax (2015)
7. Chari, N., Diallo, C., Venkatadri, U., Khatab, A.: Modeling and analysis of a warranty policy using new and reconditioned parts. Appl. Stoch. Models Bus. Ind. **32**, 539–553 (2016)
8. Chukova, S., Shafiee, M.: One-dimensional warranty cost analysis for second-hand items: an overview. Int. J. Qual. Reliab. Manage. **30**(3), 239–255 (2013)
9. Diallo, C., Ait-Kadi, D., Venkatadri, U.: Reliability analysis and optimal mixture strategy for a lot composed of new and reconditioned systems. Int. J. Perform. Eng. **10**(6), 557–566 (2014)

10. Diallo, C., Venkatadri, U., Khatab, A., Bhakthavatchalam, S.: State of the art review of quality, reliability and maintenance issues in closed-loop supply chains with remanufacturing. Int. J. Prod. Res. **55**(5), 1277–1296 (2017)
11. Glickman, T.S., Berger, P.D.: Optimal price and protection period decisions for a product under warranty. Manage. Sci. **22**(12), 1381–1390 (1976)
12. Gutowski, T.G., Sahni, S., Boustani, A., Graves, S.C.: Remanufacturing and energy savings. Environ. Sci. Technol. **45**(10), 4540–4547 (2011)
13. Kim, D.K., Lim, J.H., Park, D.H.: Optimal maintenance level for second-hand product with periodic inspection schedule. Appl. Stoch. Models Bus. Ind. **31**(3), 349–359 (2015)
14. Lo, H.-C., Yu, R.-Y.: A study of quality management strategy for reused products. Reliab. Eng. Syst. Saf. **119**, 172–177 (2013)
15. Montgomery, D.B., Urban, G.L.: Management Science in Marketing. Prentice-halls, Englewood (1969)
16. Montgomery, D.C., Peck, E.A., Vining, G.G.: Intorduction to Linear Regression Analysis. Wiley, Hoboken (2012)
17. Murthy, D.N.P., Djamaludin, I.: New product warranty: a literature review. Int. J. Prod. Econ. **3**, 231–260 (2002)
18. Naini, S.G.J., Shafiee, M.: Joint determination of price and upgrade level for a warranted second-hand product. Int. J. Adv. Manuf. Technol. **54**(9–12), 1187–1198 (2011)
19. Saidi-Mehrabad, M., Noorossana, R., Mahmood, S.: Modeling and analysis of effective ways for improving the reliability of second-hand products sold with warranty. Int. J. Adv. Manuf. Technol. **46**(1–4), 253–265 (2010)
20. Shafiee, M., Chukova, S.: Maintenance models in warranty: a literature review. Eur. J. Oper. Res. **229**(3), 561–572 (2013)
21. Shafiee, M., Chukova, S.: Optimal upgrade strategy, warranty policy and sale price for second-hand products. Appl. Stoch. Models Bus. Ind. **29**(2), 157–169 (2013)
22. Su, C., Wang, X.: Optimal upgrade policy for used products sold with two-dimensional warranty. Qual. Reliab. Eng. Int. **32**, 2889–2899 (2016)
23. Yeh, R.H., Chen, G.-C., Chen, M.-Y.: Optimal age-replacement policy for nonrepairable products under renewing free-replacement warranty. IEEE Trans. Reliab. **54**(1), 92–97 (2005)
24. Yeh, R.H., Lo, H.-C., Yu, R.Y.: A study of maintenance policies for second-hand products. Comput. Ind. Eng. **60**(3), 438–444 (2011)
25. Yun, W.Y., Murthy, D.N.P., Jack, N.: Warranty servicing with imperfect repair. Int. J. Prod. Econ. **111**(1), 159–169 (2008)

Applications

Hierarchical Decomposition Approach for Detailed Scheduling of Pipeline Systems with Branches

Hossein Mostafaei[1,2] and Pedro M. Castro[1(✉)]

[1] Centro de Matemática Aplicações Fundamentais e Investigação Operacional, Faculdade de Ciências, Universidade de Lisboa, 1749-016 Lisbon, Portugal
pmcastro@fc.ul.pt
[2] School of Chemical Engineering, Aalto University, Espoo, Finland
h.mostafaei65@gmail.com

Abstract. Scheduling multiproduct pipelines is a complex managerial task with a remarkable impact on the total revenues of the pipeline industry. It consists of sequencing, sizing and timing of injections and removals, to meet product demands on time at minimum cost. Generating the detailed scheduling of pipeline networks can be very challenging, requiring efficient optimization tools to find good feasible solutions. This paper develops a hierarchical decomposition approach for tree-like pipeline systems with two-level branching. Decisions related to the sequence of product injections and the destination for each batch, are made at the higher planning layer, while the lower layer then finds the sequence and timing of product deliveries. Each layer is tackled by a mixed-integer linear programming (MILP) formulation, which neither discretizes the time horizon nor divides a pipeline segment into packs of equal size. Solutions to three case studies present significant reductions in both the operating cost and the computational burden.

Keywords: Optimization · Hierarchical approach · Pipelines · Scheduling MILP

1 Introduction

The petroleum supply chain includes oil exploration, refining and product distribution, with the latter having a major influence on the cost of oil and its derivatives. Of the different means of distributing oil products from refineries to depots, pipelines are the most reliable and cost-effective. They operate without any interruption day and night, and can convey large varieties of petroleum products such as gasoline, gasoil, diesel, jet fuel, kerosene and liquefied petroleum gas (LPG). Products are sequenced back to back, often without any separation in between, resulting into a mixing at the interface of adjacent products. The quantity of interface material is a function of the pipeline profile (pump rate and length of pipeline) and the physicochemical properties of the products. If two products are known to form a vast interface, the pipeline operators must avoid injecting them in immediate succession (forbidden product sequence).

G. H. Parlier et al. (Eds.): ICORES 2017, CCIS 884, pp. 243–266, 2018.
https://doi.org/10.1007/978-3-319-94767-9_13

The main feature of liquid pipelines is that they are always full. Consequently, when a volume of a product is pumped into a pipeline, the same volume is discharged into downstream depots. Pipeline operators must decide how much of each product to inject or discharge in a time interval, to meet demand on time at minimum operating cost. It includes refinery pumping costs, which may vary with products, inventory cost at depots, interface and stoppages cost. The latter accounts for the energy consumed for resuming fluid in idle segments.

In recent years, several authors have introduced optimization tools to solve pipeline scheduling problems. The models satisfy operational constraints related to sequencing, volume balances, flowrate limitations and product distribution, and can rely on discrete- or continuous-time and volume representations. They can be of the mixed-integer linear, or non-linear [1, 2] types. Sometimes, models are part of decomposition algorithms that consider two operational plans: aggregate and detailed. The aggregate plan determines the best sequence of product injections and the destination for each batch, while the detailed plan provides the sequence and timing of batch removals from the pipeline into depots.

To generate a good feasible schedule, discrete-time approaches need to divide the time horizon into several intervals. They can lead to large-scale problems even for short time horizons [3–6]. The major advantage of discrete approaches against their continuous counterparts, is their simplicity. Rejowski and Pinto [3] were the firsts to solve with a discrete-time MILP, the detailed scheduling problem of a straight pipeline, connecting a refinery to multiple depots. In subsequent work [4], they added integer cuts to reduce CPU time by at least 70%.

Cafaro and Cerdá [7] developed the first continuous time MILP model for the aggregate scheduling of pipeline systems with a single refinery and multiple depots. The model was then generalized to tackle the operation of systems with multiple refineries [8], branching lines [9] and even bidirectional flow [10]. Relvas et al. [11] focused on the inventory management of a depot fed by a single-refinery pipeline. All the structures operating with unidirectional flow can be addressed by the continuous-time model developed by Castro [12], which is the first for detailed scheduling of complex pipeline networks.

Cafaro et al. [13] developed a two-level optimization model based on continuous time MILPs for detailed scheduling of a straight pipeline including a refinery and multiple depots, minimizing pump operating and restart/stoppage costs. The model was later generalized [14] to consider simultaneous deliveries to depots. A similar pipeline scheduling problem was studied by Mostafaei and co-workers [15, 16], who developed monolithic MILP continuous-time approaches that achieve better pipeline schedules in terms of cost.

Recent works involving detailed scheduling of multiproduct pipelines have considered pipeline networks with dual purpose stations, acting alternately as input and output node [17, 18]. Both approaches assume that at any time, each pipeline segment can be fed by the adjacent upstream segment or the input node at the segment origin. This assumption was then relaxed by Mostafaei and Castro [19], leading to a substantial reduction on the overall time required to meet demand, i.e., the schedule makespan. In all these approaches, the modeler must properly allocate the initial products to batches, which may include empty lots, and choose the number of batches

to be transported. Otherwise, the resulting mathematical problems will be infeasible or lead to suboptimal solutions. To overcome such usual shortcomings, Castro and Mostafaei [20] recently introduced a product-centric formulation that does not have a priori decisions on batch allocations to products and is capable of rigorously handling forbidden product sequences. Later, Castro [21] extended the model in [20] to account for the optimal operations of all kind of pipeline structures.

In another work, Mostafaei et al. [22] tackled the detailed scheduling of single-level tree-like pipeline networks featuring a unique refinery and multiple depots. The network consists of a set of pipelines with a mainline and several secondary lines branched from the mainline at different sites. Given the product demands, the model finds the optimal sequence of batch injections, batch removals and the size of batches to be transported by each pipeline, all in a single step. However, the optimization model is incapable of finding the detailed schedule of two-level tree-like pipelines, where branches emerging from the mainline can have their own set of lateral branch lines.

This paper presents an MILP optimization framework for the detailed scheduling of complex tree-like pipeline systems. To find the best schedule in a reasonable computational time, the proposed MILP model is decomposed in two, based on the work in [23]. In the upper level, dealing with the aggregate schedule, the optimal sequence of batches is determined, with the aim of meeting product demand at minimum pump and interface costs. The subsequent level, generating the detailed schedule, focuses on finding the optimal sequence of batch removals at depots, to meet demand with the minimum number of ON/OFF pump operations and flow restarts in pipeline segments. The proposed optimization framework is tested by solving three case studies, one of which uses a large scale real-life two level tree-like system from the Iranian products pipeline network.

In contrast to our previous work in [23], the proposed model is capable of considering the operation of two-level tree-like pipelines, rather than single-level pipelines. It strictly tracks the size and the coordinate of new batches and monitors the splitting of product lots and the creation of new interfaces while diverting products to second-level pipelines. This capability allows to precisely handle forbidden product sequences and compute additional costs associated to new interfaces. These are provided by the new constraints (33)–(39), (40), (43)–(44), (47), (51), (55), (58), (63) and described in detail in Subsects. 3.2, 3.3, 3.4, 3.5, 3.6, 3.7 and 3.8.

2 Problem Statement

We deal with a short-term scheduling problem where a unidirectional two-level tree-like pipeline must convey oil derivatives from a single refinery to several distribution centers (depots), as seen in Fig. 1. It consists of a mainline (pipeline $n0$), a few secondary lines (first-level branches) split from the mainline, and lateral branching lines (second-level branches) emerging from the secondary lines. As an example, the network in Fig. 1 has three secondary lines ($n1, n3$ and $n4$) and a lateral branching line ($n2$) emerging from $n1$. A pipeline segment ends with either a depot or a branch point. In Fig. 1, the mainline starts at the refinery and ends at depot D8, featuring a total of 8 segments, $s1_{n0} - s8_{n0}$. The branches involve five segments.

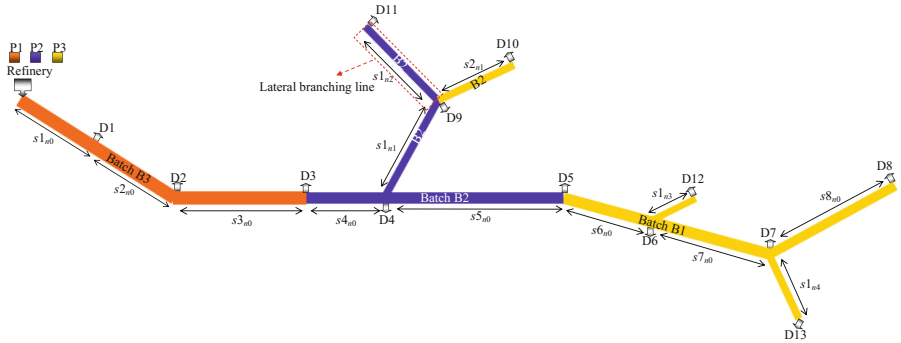

Fig. 1. A two-level tree-like multi-product pipeline.

Batches of petroleum products pumped at the refinery are diverted to the mainline depots and/or reach the secondary and lateral branching lines. The aim is to build an optimization framework to find the optimal sequence of batch input and output operations. The main assumptions are: (A1) each pumping operation involves at most one batch injection in the refinery; (A2) in the detailed level, a pumping operation can at most have one batch input in each active pipeline and active depot, whereas the aggregate plan relaxes such assumption; (A3) the refinery pumping rate must respect the admissible injection rates; (A4) in detailed level, the valves of active depots and segments remain open throughout the pumping operation; in contrast, they may be turned on/off several times in the aggregated plan; (A5) in detailed level, pipeline segments should operate within acceptable flowrate ranges; such restriction cannot be enforced in the aggregated level.

3 Optimization Model

We now present a continuous-time MILP formulation for detailed scheduling of two-level tree-like pipeline systems. Such a MILP model (hereafter referred to as DP) is capable to find the schedule in a single step. It includes the following major sets: (a) pumping runs K, (b) pipelines N, (c) secondary lines on the mainline ($SL \subset N$), (d) lateral branch lines on secondary line $n(LL_n \subset N)$, (e) segments of pipeline n;S_n, (f) depots of pipeline $n(D_n \subset S_n)$, (g) $I = \{i_1, i_2, \ldots, i_{|I|}\}$, batches to be conveyed, with batch i_{j+1} always moving right after batch i_j, (h) $I_n = I_n^{old} \cup I_n^{new}$, batches flowing along pipeline n, with I_n^{old} indicating the batches inside pipeline n at the start, and I_n^{new} denoting the new batches to be transferred, (i) I_n^{batch} batches that can receive material from the origin of pipeline $n(I_n^{batch} \subset I_n)$, (j) I_n^s; batches that can be transferred to depot $s_n(I_n^s \subset I_n)$, and (k) P; oil derivatives. Note that we have $I_n^{batch} = I_n^{new} \cup \{i_{old,n}\}$, where $i_{old,n} \in I_n^{old}$ is an old batch that can receive product from the origin of pipeline n.

The proposed optimization framework is a generalization of our previous model in Mostafaei et al. [22] for the scheduling of single-level tree like pipeline and so we will

focus on the description of the novel constraints in Sects. 3.2, 3.3, 3.4, 3.5, 3.6, 3.7 and 3.8. The list of model entities can be found in Mostafaei et al. [22].

3.1 Common Constraints for Single- and Two-Level Tree-like Pipelines

- Product allocation to batches

$$\sum_{p \in P} y_{i,p} \leq 1, \quad i \in I, \tag{1}$$

$$\sum_{p \in P} y_{i,p} \leq \sum_{p \in P} y_{i-1,p}, \quad i \in I_{n0}^{new}, \tag{2}$$

$$\sum_{p \in P} y_{i,p} \leq \sum_{k \in K} \lambda_{i,k}, \quad i \in I_{n0}^{new}, \tag{3}$$

- Pumping sequence

$$ST_k \geq ST_{k-1} - L_{k-1}, \quad k \in K(k \geq 2), \tag{4}$$

$$ST_1 = stf, \tag{5}$$

$$\sum_{k \in K} L_k \leq h_{\max}. \tag{6}$$

- Location of batches

$$LPV_{i,k,n} = \sum_{\substack{i' \in I_n \\ i' \geq i}} SPV_{i,k,n}, \quad i \in I_n, k \in K, n \in N, \tag{7}$$

$$LPV_{i,k,n} - SPV_{i,k,n} = LPV_{i+1,k,n} \quad i \in I_n, k \in K, n \in N \tag{8}$$

- Injection at refinery

$$\sum_{i \in I_{n0}^{batch}} \lambda_{i,k} \leq 1, \quad k \in K, \tag{9}$$

$$\sum_{i \in I_{n0}^{batch}} \lambda_{i,k} \leq \sum_{i \in I_{n0}^{batch}} \lambda_{i,k-1}, \quad k \in K(k > 2), \tag{10}$$

$$LPV_{i,k-1,n0} - SPV_{i,k-1,n0} \leq PV_{n0}(1 - \lambda_{i,k}), \quad i \in I_{n0}^{batch}, k \in K, \tag{11}$$

$$IPV_{n0}^{\min} \lambda_{i,k} \leq IPV_{i,k,n0} \leq IPV_{n0}^{\max} \lambda_{i,k}, \quad i \in I_{n0}^{batch}, k \in K, \tag{12}$$

$$\sum_{i\in I_{n0}^{batch}} \frac{IPV_{i,k,n0}}{vr_{n0}^{\max}} \le L_k \le \sum_{i\in I_{n0}^{batch}} \frac{IPV_{i,k,n0}}{vr_{n0}^{\min}}, \qquad k \in K, \tag{13}$$

$$\sum_{p\in P} PPV_{i,p,k} = IPV_{i,k,n0,} \qquad i \in I_{n0}^{batch}, k \in K \tag{14}$$

$$\sum_{k\in K} PPV_{i,p,k} \le PPV_{p}^{\max} y_{i,p}, \qquad i \in I_{n0}^{batch}, p \in P. \tag{15}$$

$$\sum_{i\in I_{n0}^{batch}} \sum_{k\in K} PPV_{i,p,k} \le reft_{p}, \qquad p \in P. \tag{16}$$

- Supplying material to output terminals (depots)

$$\sum_{i\in I_{n}^{s}} x_{i,s,k,n} \le 1, \qquad s \in D_n, k \in K, n \in N, \tag{17}$$

$$LPV_{i+1,k,n} \le \tau_{s,n} + (PV_n - \tau_{s,n})(1 - x_{i,s,k,n}), \qquad i \in I_n^s, s \in D_n, k \in K, n \in N, \tag{18}$$

$$LPV_{i,k-1,n} \ge \tau_{s,n} x_{i,s,k,n}, \qquad i \in I_n^s, s \in D_n, k \in K, n \in N, \tag{19}$$

$$DPV_{s,n}^{\min} \le DPV_{i,s,k,n} \le DPV_{s,n}^{\max}, \qquad i \in I_n^s, s \in D_n, k \in K, n \in N, \tag{20}$$

$$\sum_{s'\in D_n}^{s} DPV_{i,s,k,n} \le (\tau_{s',n} - LPV_{i+1,k,n}) + IPV_{i,k,n} + (PV_n - \tau_{s,n})(1 - x_{i,s,k,n}) \quad i \in I_n^s, s \in D_n, k \in K, n \in N, \tag{21}$$

$$\sum_{p\in P} PDPV_{i,p,s,k,n} = DPV_{i,s,k,n,} \qquad i \in I_n^s, s \in D_n, k \in K, n \in N, \tag{22}$$

$$\sum_{k\in K} PDPV_{i,p,s,k,n} \le IPV_{s,n}^{\max} y_{i,p}, \qquad i \in I_n^s, s \in D_n, n \in N, \tag{23}$$

$$\sum_{i\in I_n^s} \sum_{k\in K} PDPV_{i,p,s,k,n} \ge Demand_{p,s,n} - Back_{p,s,n}, \qquad p \in P, s \in D_n, n \in N. \tag{24}$$

- Diverting material from mainline to secondary lines

$$\sum_{i\in I_{n}^{batch}} u_{i,k,n} \le 1, \qquad k \in K, n \in SL, \tag{25}$$

$$LPV_{i+1,k,n0} \le \sigma_n + (PV_n - \sigma_n)(1 - u_{i,k,n}), \qquad i \in I_n^{batch}, k \in K, n \in SL, \tag{26}$$

$$LPV_{i,k-1,n0} \geq \sigma_n u_{i,k,n}, \qquad i \in I_n^{batch}, k \in K, n \in SL, \tag{27}$$

$$IPV_n^{\min} u_{i,k,n} \leq IPV_{i,k,n} \leq IPV_n^{\max} u_{i,k,n}, \qquad i \in I_n^{batch}, k \in K, n \in SL, \tag{28}$$

$$IPV_{i,k,n} \leq (\sigma_n - LPV_{i+1,k,n0}) + IPV_{i,k,n0} + (PV_n - \sigma_n)(1 - u_{i,k,n}), \quad i \in I_n^{batch}, k \in K, n \in SL, \tag{29}$$

New batch $i \in I_n^{new}$ will move ($z_{i,n} = 1$) in secondary line n, if it is transferred from the mainline during the planning horizon ($\sum_{k \in K} u_{i,k,n} \geq 1$). Note that for old non empty batch existence at the secondary line n at time *stf*, we have $z_{i,n} = 0$.

$$z_{i,n} \leq \sum_{k \in K} u_{i,k,n} \leq |K| z_{i,n}, \qquad i \in I_n^{new}, n \in SL. \tag{30}$$

- Constraints on supplying material from a batch to mainline depots and its secondary lines

$$\begin{aligned} &\sum_{s \in D_{n0} | \sigma_n \geq \tau_{s,n0}} DPV_{i,s,k,n0}|_{i \in I_{n0}^s} + \sum_{n' \in SP}^{n} IRV_{i,k,n'}|_{i \in I_{n'}^{batch}} \leq (\sigma_n - LPV_{i+1,k-1,n0}) \\ &+ IPV_{i,k,n0}|_{i \in I_{n0}^{batch}} + PV_{n0}\left(1 - u_{i,k,n}|_{i \in I_n^{batch}}\right) \qquad \forall i \in I_{n0}, k \in K, n \in SL \end{aligned} \tag{31}$$

$$\begin{aligned} &\sum_{s' \in D_{n0}}^{s} DPV_{i,s',k,n0}|_{i \in I_{n0}^s} + \sum_{n \in SL | \sigma_n \leq \tau_{s,n0}} IPV_{i,k,n}|_{i \in I_n^{batch}} \leq (\tau_{s,n0} - LPV_{i+1,k-1,n0}) \\ &+ IPV_{i,k,n0}|_{i \in I_{n0}^{batch}} + PV_{n0}\left(1 - x_{i,s,k,n0}|_{i \in I_{n0}^s}\right) \qquad \forall i \in I_{n0}, k \in K, s \in D_{n0} \end{aligned} \tag{32}$$

3.2 Diverting Material from a Secondary Line to Its Branches

During pumping run k, batch i can be transferred from secondary line n to its branch n' if the following condition holds: $LPV_{i+1,k,n} \leq \mu_{n,n'} \leq LPV_{i,k-1,n}$, where $\mu_{n,n'}$ is the volumetric coordinate of lateral branch line n' located on secondary line n. If $l_{i,k,n,n'} = 1$, then a portion of batch i in secondary line n is transferred to lateral branch line n'. The volume is restricted by $(\mu_{n,n'} - LPV_{i+1,k-1,n})$ plus the material injected to the batch from the secondary line n. All the conditions can be described by the following eqs:

$$\sum_{i \in I_{n'}^{batch}} l_{i,k,n,n'} \leq 1, \qquad k \in K, n \in SL, n' \in LL_n, \tag{33}$$

$$LPV_{i+1,k,n} \leq \mu_{n,n'} + (PV_{n'} - \mu_{n,n'})(1 - l_{i,k,n,n'}), \quad i \in I_{n'}^{batch}, k \in K, n \in SL, n' \in LL_n, \tag{34}$$

$$LPV_{i,k-1,n} \geq \mu_{n,n'} l_{i,k,n,n'}, \qquad i \in I_{n'}^{batch}, k \in K, n \in SL, n' \in LL_n, \tag{35}$$

$$IPV_{n'}^{\min} l_{i,k,n,n'} \leq IPV_{i,k,n'} \leq IPV_{n'}^{\max} l_{i,k,n,n'}, \qquad i \in I_n^{batch}, k \in K, n \in SL, n' \in LL_n \tag{36}$$

$$IPV_{i,k,n} \leq (\mu_{n,n'} - LPV_{i+1,k,n}) + IPV_{i,k,n} + (PV_{n'} - \mu_{n,n'})(1 - l_{i,k,n,n'}), \qquad i \in I_n^{batch}, k \in K, \\ n \in SL, n' \in LL_n, \tag{37}$$

A new batch $i \in I_{n'}^{batch}$ will be transported by the lateral branch line n', split from secondary line n, if binary variable $l_{i,k,n,n'}$ is activated during scheduling horizon.

$$z_{i,n'} \leq \sum_{k \in K} l_{i,k,n,n'} \leq |K| z_{i,n'}, \qquad i \in I_{n'}^{new}, n \in SL, n' \in LL_n. \tag{38}$$

3.3 Constraints on Supplying Material from a Secondary Line to Its Depots and Branches

During pumping run k, the total volume transferred from batch $i \in I_n$ in secondary line n to its depots and branches, can never exceed the volume that is accessible by depots $s \in D_n$ and lateral branch lines $n' \in LL_n$ at time ST_k, plus the total volume injected to the batch $i \in I_n$ from the mainline. We have thus the following eqs:

$$\sum_{s \in D_n | \mu_{n,n'} \geq \tau_{s,n}} DPV_{i,s,k,n}|_{i \in I_n^s} + \sum_{n'' \in LL_n}^{n'} IRV_{i,k,n''}|_{i \in I_{n''}^{batch}} \leq (\mu_{n,n'} - LPV_{i+1,k-1,n}) \\ + IPV_{i,k,n}|_{I_n^{batch}} + PV_n \left(1 - l_{i,k,n,n'}|_{i \in I_{n'}^{batch}}\right) \qquad \forall i \in I_n, k \in K, n \in SL, n' \in LL_n \tag{39}$$

$$\sum_{s' \in D_n}^{s} DPV_{i,s',k,n}|_{i \in I_n^s} + \sum_{n' \in LL_n | \mu_{n,n'} \leq \tau_{s,n}} IPV_{i,k,n'}|_{i \in I_{n'}^{batch}} \leq (\tau_{s,n} - LPV_{i+1,k-1,n}) \\ + IPV_{i,k,n}|_{i \in I_n^{batch}} + PV_n \left(1 - x_{i,s,k,n}|_{i \in I_n^s}\right) \qquad \forall i \in I_n, k \in K, n \in SL, s \in D_n \tag{40}$$

3.4 Interface Material and Forbidden Sequence in the Mainline

Batch $(i+1)_{n0}$ is injected into the mainline right after i_{n0} and consequently there will always be a contamination product at their common boundary which is referred to as interface. If continuous variable $INTF_{i,p,p',n}$ is the interface volume between batch i and its successor in pipeline n conveying products p and p' we have the following eq for batches in the mainline:

$$INFT_{i,p,p',n0} \geq MIX_{p,p',n0}(y_{i+1,p} - y_{i,p'} - 1), \qquad i \in I_n, p, p' \in P. \tag{41}$$

where the model parameter $MIX_{p,p',n}$ is the interface volume between products p and p' inside pipeline n.

For quality reasons, some products should not touch each other inside the pipeline. Since batch i_{n0} is injected into the mainline immediately after batch $(i-1)_{n0}$, we will have Eq. (42) avoiding forbidden sequences between two incompatible products ($Touch_{p,p'} = 0$).

$$y_{i,p} + y_{i-1,p'} \leq 1 + Touch_{p,p'}, \qquad i \in I_{n0}^{new}, p, p' \in P. \tag{42}$$

3.5 Interface Volume and Forbidden Sequence in Split Lines

Unlike the mainline, batch i may have no interface with batch $(i+1)$ in split line n. This is because the batch sequence in a split line may be different to the mainline batch sequence. Batch i_p and $i'_{p'}$ can have an interface in a split line n if: (i) both are diverted to the split line n ($z_{i,n} = z_{i',n} = 1$), (ii) they convey compatible products ($y_{i,p} = y_{i',p'} = 1$ and $Touch_{p,p'} = 1$) and (iii) there are no non-empty batches between them ($\sum_{i'' \geq i'+1}^{i-1} z_{i'',n} = 0$). We have thus the following eq:

$$\begin{aligned} &INFT_{i,p,p',n} \geq MIX_{p,p',n}(y_{i,p} + y_{i',p'} + y_{i,p} + y_{i',p'} \\ &- \sum_{i'' \geq i'+1}^{i-1} z_{i'',n} + Touch_{p,p'} - 4), \quad i, i' \in I_n (i > i'), p, p' \in P, n \neq n0. \end{aligned} \tag{43}$$

Controlling forbidden sequences inside split lines is more difficult than inside the mainline due to the moving of empty batches between two real batches. New batch $i \in I_n^{new}$ should never touch batch $i' \in I_n$ already transferred to split line $n (z_{i',n} = 1)$ if: (i) they convey two incompatible products ($y_{i,p} = y_{i',p'} = 1$ and $Touch_{p,p'} = 0$) and (ii) there are no non-empty batches between them. All the conditions can be described by Eq. (44).

$$\begin{aligned} &z_{i,n} + z_{i',n'} \leq \sum_{i'' \geq i'+1}^{i-1} z_{i'',n} - y_{i,p} - y_{i',p'} + Touch_{p,p'} + 3 \quad i \in I_n^{new}, \\ &i' \in I_n (i' < i), p, p' \in P, n \neq n0. \end{aligned} \tag{44}$$

3.6 Size of Batch i in Pipelines

At the end of pumping run k, the size of batch i in pipeline n can be computed from its size at time $ST_k(SPV_{i,k-1,n})$ by adding the material entered from the origin of pipeline n and subtracting the amount of material transferred to its depots and its split lines, as imposed by Eqs. (45), (46) and (47).

$$\begin{aligned} &SPV_{i,k,n0} = SPV_{i,k,n0} + IPV_{i,k,n0}|_{i \in I_{n0}^{bach}} - \sum_{s \in D_{n0}} DPV_{i,s,k,n}|_{i \in I_n^s} \\ &- \sum_{n \in SL} IPV_{i,k,n}|_{i \in I_n^{bach}}, \quad i \in I_n, k \in K \end{aligned} \tag{45}$$

$$SPV_{i,k,n} = SPV_{i,k,n} + IPV_{i,k,n}|_{i\in I_n^{bach}} - \sum_{s\in D_n} DPV_{i,s,k,n}|_{i\in I_n^s} - \sum_{n'\in LL_n} IPV_{i,k,n'}|_{i\in I_{n'}^{bach}}, \quad i \in I_n, k \in K, n \in N \tag{46}$$

$$SPV_{i,k,n} = SPV_{i,k,n} + IPV_{i,k,n}|_{i\in I_n^{bach}} - \sum_{s\in D_n} DPV_{i,s,k,n}|_{i\in I_n^s}, \quad i \in I_n, k \in K, n \neq n0, n \notin SL \tag{47}$$

3.7 Mass Balance

One of the main aspects of pipelines is that they must always remain full with products, as imposed by Eq. (48).

$$\sum_{i\in I_n} SPV_{i,k,n} = PV_n, \quad k \in K, n \in N. \tag{48}$$

Equations (49)–(51) state that the total volume entering a pipeline is equal to the volume transferred to its depots and branching lines.

$$\sum_{i\in I_{n0}^{batch}} IPV_{i,k,n0} = \sum_{i\in I_{n0}^s} \sum_{s\in D_{n0}} DPV_{i,s,k,n0} + \sum_{n\in SL} \sum_{i\in I_n^{batch}} IPV_{i,k,n}, \quad k \in K, \tag{49}$$

$$\sum_{i\in I_n^{batch}} IPV_{i,k,n} = \sum_{i\in I_n^s} \sum_{s\in D_n} DPV_{i,s,k,n0} + \sum_{n'\in LL_n} \sum_{i\in I_{n'}^{batch}} IPV_{i,k,n'}, \quad k \in K, n \in SL, \tag{50}$$

$$\sum_{i\in I_n^{batch}} IPV_{i,k,n} = \sum_{i\in I_n^s} \sum_{s\in D_n} DPV_{i,s,k,n}, \quad k \in K, n \neq n0, n \notin SL \tag{51}$$

3.8 Flowrate Bounds and Activated and Stopped Volumes

Binary variable $v_{s,k,n}$ is 1 if some material moves in segment s_n (segment s of pipeline n) through pumping run k, otherwise $v_{s,k,n} = 0$ and the segment is idle. Since the pipeline network features a unique refinery, segment $(s-1)_n$ will be active if segment s_n is active, as imposed by Eq. (52). The first segment of a pipeline n is active if some material is injected from the origin of that segment, and vice versa, as expressed by Eqs. (53)–(55). On the other hand, depot s_n will be idle if segment s_n is idle, as imposed by Eq. (56).

$$v_{s,k,n} \leq v_{s-1,k,n}, \quad s \in S_n, k \in K, n \in N, \tag{52}$$

$$v_{s,k,n0} = \sum_{i\in I_{n0}^{batch}} \lambda_{i,k}, \quad s = first(S_{n0}), k \in K, \tag{53}$$

$$v_{s,k,n} = \sum_{i \in I_n^{batch}} u_{i,k,n}, \quad s = first(S_n), k \in K, n \in SL, \tag{54}$$

$$v_{s,k,n} = \sum_{i \in I_{n'}^{batch}} l_{i,k,n,n'}, \quad s = first(S_{n'}), k \in K, n \in SL, n' \in LL_n, \tag{55}$$

$$\sum_{i \in I_n^s} x_{i,s,k,n} \leq v_{s,k,n}, \quad s \in S_n, k \in K, n \in N, \tag{56}$$

Through pumping run k, split line $n(n \neq n0)$ will not receive any material if the segment that this line emerges from is idle, as imposed by Eqs. (57)–(58).

$$\sum_{i \in I_n^{batch}} u_{i,k,n} \leq v_{s,k,n0}, \quad s \in \{s \in S_{n0}, \rho_{s,n0} = \sigma_n\}, k \in K, n \in SL, \tag{57}$$

$$\sum_{i \in I_{n'}^{batch}} l_{i,k,n,n'} \leq v_{s,k,n}, \quad s \in \{s \in S_n, \rho_{s,n} = \mu_{n,n'}\}, k \in K, n \in SL, n' \in LL_n \tag{58}$$

where $\rho_{s,n}$ is the volume of pipeline n between its origin and the end of segment s_n.

The main goal of this paper is to find the best sequence of batch removals at the depots by restarting segments as few times as possible. To avoid unnecessary flow restarts and stoppages, the model incorporates two continuous variables $ACV_{s,k,n}$ and $STV_{s,k,n}$ to detect the activated and stopped volume of segment s_n during pumping run k. If the flow resumes in segment s_n ($v_{s,k-1,n} = 0$ and $v_{s,k,n} = 1$), $ACV_{s,k,n}$ will be equal to $SEG_{s,n}$, the volume of segment s_n. In the stoppage case, segment s_n is idle during run k, but active in run $k-1$. We have thus the following eqs:

$$ACV_{s,k,n} \geq SEG_{s,n}(v_{s,k,n} - v_{s,k-1,n}), \quad s \in S_n, k \in K, n \in N, \tag{59}$$

$$STV_{s,k,n} \geq SEG_{s,n}(v_{s,k-1,n} - v_{s,k,n}), \quad s \in S_n, k \in K, n \in N. \tag{60}$$

The liquids in active segments should flow in feasible rate $[v_{s,n}^{\min}, v_{s,n}^{\max}]$, which is restricted by Eqs. (61)–(63).

$$\begin{aligned} vs_{s,n0}^{\min} L_k - IPV_{n0}^{\max}(1 - v_{s,k,n0}) \leq \sum_{s' \in D_{n0} | s' \geq s} \sum_{i \in I_{no}^{s'}} DPV_{i,s',k,n} \\ + \sum_{n \in SL | \sigma_n \geq \rho_{s,n0}} \sum_{i \in I_n^{batch}} IPV_{i,k,n} \leq vs_{s,n0}^{\max} L_k, \quad s \in S_{n0}, k \in K, \end{aligned} \tag{61}$$

$$\begin{aligned} vs_{s,n}^{\min} L_k - IPV_n^{\max}(1 - v_{s,k,n}) \leq \sum_{s' \in D_n | s' \geq s} \sum_{i \in I_{no}^{s'}} DPV_{i,s',k,n} \\ + \sum_{n' \in LL_n | \mu_{n,n'} \geq \rho_{s,n}} \sum_{i \in I_{n'}^{batch}} IPV_{i,k,n'} \leq vs_{s,n}^{\max} L_k, \quad s \in S_n, k \in K, n \in SL \end{aligned} \tag{62}$$

$$vs_{s,n}^{\min} L_k - IPV_n^{\max}(1 - v_{s,k,n}) \leq \sum_{\substack{s' \in D_n \\ s' \geq s}} \sum_{i \in I_{no}^{s'}} DPV_{i,s',k,n} \leq vs_{s,n}^{\max} L_k, \qquad s \in S_n, k \in K, n \in N/\{n0 \cup SL\} \tag{63}$$

3.9 Objective Function

The objective function is to minimize operating charges including pumping, interface, backorder, flow restarts and ON/OFF pump switching costs.

$$\min z^{\mathrm{DP}} = \sum_{k \in K} \sum_{p \in P} \sum_{i \in I_{n0}^{batch}} CP_p PPV_{i,p,k} + \sum_{n \in N} \sum_{p \in P} \sum_{p' \in P} \sum_{i \in I_n} CIF_{p,p'} INTF_{i,p,p',n} +$$
$$\sum_{n \in N} \sum_{s \in D_n} \sum_{p \in P} CB_{p,s,n} Back_{p,s,n} + \sum_{n \in N} \sum_{s \in S_n} \sum_{k \in K} CA \times ACV_{s,n,k} + CS \times STV_{s,n,k} + \sum_{k \in K} \sum_{i \in I_{n0}^{batch}} CF \times \lambda_{i,k}$$

where the parameter CP_p is the cost of pumping a unit volume of product p from the refinery, the coefficient $CIF_{p,p'}$ stands for the cost of reprocessing of a unit interface material between products p and p', the coefficient $CB_{p,s,n}$ stands for the cost of backorder for a unit of product p at depot s_n, the parameter CF stands for the fixed cost to fulfill a pumping operation and the coefficients CA and CS are the unit flow restart and stoppage costs in each pipeline segment, respectively.

4 MILP Model for Generating an Aggregate Plan (AP)

By slightly changing some constraints of DP, we can obtain an aggregate scheduling model (hereafter referred to as AP). Per assumption (A2), Eqs. (17), (25) and (33) should not be considered in model AP. In addition, Eqs. (18)–(19), (26)–(27) and (34)–(35) enforce feeding an active depot and branch line with a single batch per pumping run. To relax these, the new Eqs. (18')–(19'), (26')–(27') and (34')–(35') are considered instead. Such equations still allow to meet product demand at the minimum number of pumping operations and consequently to reduce the CPU time.

$$LPV_{i+1,k-1,n} \leq \tau_{s,n} + (PV_n - \tau_{s,n})(1 - x_{i,s,k,n}), \qquad i \in I_n^s, s \in D_n, k \in K, n \in N, \tag{18'}$$

$$LPV_{i,k,n} \geq \tau_{s,n} x_{i,s,k,n}, \qquad i \in I_n^s, s \in D_n, k \in K, n \in N, \tag{19'}$$

$$LPV_{i+1,k-1,n} \leq \sigma_n + (PV_n - \sigma_n)(1 - u_{i,k,n}), \qquad i \in I_n^{batch}, k \in K, n \in SL, \tag{26'}$$

$$LPV_{i,k,n} \geq \sigma_n u_{i,k,n}, \qquad i \in I_n^{batch}, k \in K, n \in SL, \tag{27'}$$

$$LPV_{i+1,k-1,n} \leq \mu_{n,n'} + (PV_{n'} - \mu_{n,n'})(1 - l_{i,k,n,n'}), \qquad i \in I_{n'}^{batch}, k \in K, n \in SL, n' \in LL_n, \tag{34'}$$

$$LPV_{i,k,n} \geq \mu_{n,n'} l_{i,k,n,n'}, \qquad i \in I_{n'}^{batch}, k \in K, n \in SL, n' \in LL_n, \tag{35'}$$

On the other hand, aggregated plans do not need to account for flow rate limitations and be concerned with the minimum number of flow resumes. Therefore, Eqs. (52)–(63) should not be considered in AP.

We have the following optimization framework for the AP:

$$\min z^{\mathrm{AP}} = \sum_{k\in K}\sum_{p\in P}\sum_{i\in I_{n0}^{batch}} CP_p PPV_{i,p,k} + \sum_{n\in N}\sum_{p\in P}\sum_{p'\in P}\sum_{i\in I_n} CIF_{p,p'} INTF_{i,p,p',n} + \sum_{n\in N}\sum_{s\in D_n}\sum_{p\in P} CB_{p,s,n} Back_{p,s,n}$$

s.t. Eqs. (1)–(16), (18')–(19'), (21)–(24), (26')–(27') + (29)–(33) + (34')–(35'), (37)–(52)

5 Hierarchic Approach for Generating a Detailed Schedule

The scheduling problem will become intractable if all decisions related to the pipeline input and output operations are taken in a single step, even for relatively short time horizons. To find the best detailed schedule in a reasonable time, we first solve model AP to find the optimal batch sequence in each pipeline. The resulting solution helps us to identify the exact elements of sets $I_n, I_n^{new}, I_n^{batch}$ and I_n^s, and consequently reduce the variables and constraints domain. Then, after fixing the binary variables $y_{i,p}$ and $z_{i,n}$, and removing the interface and forbidden sequencing constraints, we solve model DP to meet demand with the minimum number of pumping operations and flow resumes/stoppages. The proposed decomposition procedure will hereafter be called DSM and is depicted in Fig. 2. The objective function of DSM is given below:

$$\min z^{\mathrm{DSM}} = \sum_{n\in N}\sum_{s\in D_n}\sum_{p\in P} CB_{p,s,n} Back_{p,s,n} + \sum_{n\in N}\sum_{s\in S_n}\sum_{k\in K} CA \times ACV_{s,n,k} + CS \times STV_{s,n,k} + \sum_{k\in K}\sum_{i\in I_{n0}^{batch}} CF \times \lambda_{i,k}$$

Remark 1: Since in DSM all elements of set I_n^s should be sent to depot s_n, we can add constraint $\sum_k x_{i,s,k,n} \geq 1$. While it may lead to no solution for a low number of pumping runs, it speeds up the branch-and-bound procedure.

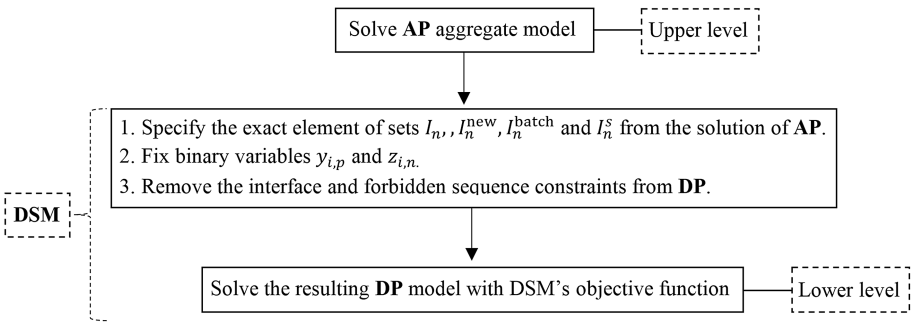

Fig. 2. Proposed DSM framework.

Remark 2: Due to the same batch sequencing, the interface cost will be the same in the AP and DSM approaches. To obtain the same pumping cost, the inventory of product p in DSM will be equal to its injected volume into the mainline in AP i.e., $refit_p^{\mathrm{DSM}} = \sum_{i,k} PPV_{i,p,k}^{\mathrm{AP}}$, where $PPV_{i,p,k}^{\mathrm{AP}}$ is the size of batch i containing product p injected into the mainline during pumping run k in the aggregated plan.

6 Optimal Number of Pumping Runs

To solve both AP and DSM models, we should first guess the number of pumping operations for each step. Like previous continuous-time approaches, we use an iterative procedure to find the optimal number of pumping operations $|K|$ to be performed. Since all pumping operations may not involve the maximum volume ($IPV_{n0}^{\max}$), the lower bound on the number of pumping operations of model AP can be:

$$\left\lceil \sum_{p,s,n} \frac{Demand_{p,s,n}}{IPV_{n0}^{\max}} \right\rceil \leq |K|^{\mathrm{AP}}$$

Unlike in AP, depots and branching lines in DSM should receive material from a single batch during the execution of a pumping operation and so the number of pumping operations in DSM ($|K|^{\mathrm{DSM}}$) will be greater than or equal to $|K|_{\mathrm{opt}}^{\mathrm{AP}}$; the optimal number of pumping runs of the aggregate plan. On the other hand since in the lower level model two binary variables $y_{i,p}$ and $z_{i,n}$ are fixed, and due to Eqs. (3), (31) and (39), $|K|^{\mathrm{DSM}}$ should be at least as large as $\max\{|I_n^{new}|^{\mathrm{DSM}}; n \in N\}$. Besides, due to Remark 1, $|K|^{\mathrm{DSM}}$ should be greater or equal to $\max\{|I_n^s|^{\mathrm{DSM}}; n \in N, s \in S_n\}$. Thus;

$$\begin{aligned} |K|_{\mathrm{opt}}^{\mathrm{AP}} &\leq |K|^{\mathrm{DSM}}, \\ \mathrm{m} = \max\{|I_n^{new}|^{\mathrm{DSM}}; n \in N\} &\leq |K|^{\mathrm{DSM}}, \\ \mathrm{g} = \max\{|I_n^s|^{\mathrm{DSM}}; n \in N, s \in S_n\} &\leq |K|^{\mathrm{DSM}}, \end{aligned}$$

and so, the initial number of pumping operations for DSM can be described by the following expression:

$$\max\{\mathrm{m}, \mathrm{g}, |K|_{\mathrm{opt}}^{\mathrm{AP}}\} \leq |K|^{\mathrm{DSM}}.$$

We start solving both AP and DSM models by setting $|K|$ equal to the lower bounds, and then, following a single increment in $|K|$, keep solving them until the objective function stops improving, if all demand is satisfied.

7 Previous Two-Level Approaches

Cafaro and co-workers [13, 14] were the firsts to develop a two-level approach for the detailed scheduling of straight pipeline systems. In their approach (hereafter CC), after finding the product sequences with minimum pumping and interface costs, they fix the aggregate batch sizes, the starting and completion times of each pumping operation in AP, and solve the second stage to generate a detailed schedule. In fact, the start and end of pumping operations for a batch injection in the lower level must exactly comply with the start and end times specified for that batch injection in the upper level model. To this end, each product delivery in the lower level model should be accomplished in the same time interval of the upper level model. Since the solution quality for the detailed scheduling problem depends on the sequence of product deliveries, the CC algorithm does not usually find cost-effective transportation plans.

8 Computational Results

Three examples are solved to illustrate the capabilities of the new continuous-time formulation for the short-term scheduling of tree-like pipeline systems, two of them involving an industrial case study. All MILP problems were solved on an Intel (R) Core (TM) i7-6700 K (4 GHz) CPU with 16 GB of RAM running Windows 10 (64-bit) using GAMS/CPLEX 12.6 in parallel deterministic mode (using up to 8 threads) as the solver. A relative optimality tolerance of 10^{-9} has been adopted as the stopping criterion.

8.1 Example 1

This example deals with a small network to illustrate the selection of the elements in sets $I_n, I_n^{\text{new}}, I_n^{\text{batch}}$ and I_n^{s}, for both the aggregated and detailed schedules. The pipeline network consists of a refinery, a mainline, a secondary line emerging from the mainline at point 3000 m^3, a lateral branch line splitting from the secondary line at point 1000 m^3 and 4 depots. The first line of Fig. 3 shows the pipeline network, initial product composition, and old-batch to product assignments. The refinery pumping rate can vary between 20 and 100 m^3/h and the minimum flowrate in pipeline segments is 20 m^3/h.

Table 1. Data for Example 1.

	ref_p	CP_p	Demand($10 \times m^3$)				$CIF_{p,p'}$ (10^2\$)/$MIX_{p,p'}$ (m^3)			
P	(m^3)	(\$/m^3)	N1	N2	N3	N4	P1	P2	P3	P4
P1	4000	8	–	100	–	–	0	24/1	25/1	20/1
P2	4000	7	–	–	100	200	24/1	0	30/1	X
P3	4000	8	–	100	–	–	25/1	30/1	0	26/1
P4	4000	5	200	100	–	–	20/1	X	26/1	0

Table 1 lists the initial product inventories in the refinery, product demands for the next 4 days ($h_{max} = 96$ h) and pumping and interface costs. Note that product sequences with an X are forbidden (e.g., product P2 cannot immediately follow product P4). The maximum volume input per operation in each pipeline is 4000 m^3 for a minimum of 1000 m^3. The same values hold for the minimum and maximum batch size diverted to depots. Moreover, $CB_p = 200$ \$/m^3, $CA_n = 1$ \$/m^3, $CS_n = 0$ and $CF = 100$ \$/run.

At time $stf = 0$, the mainline contains three old batches ($I_{n0}^{old} = \{B2,B3,B4\}$), the secondary line has two old batches, B1 and B2, and the lateral branch line is filled with B2. Let us assume $I_{n0}^{new} = \{B5\}$, meaning that batch B5 will be injected into the mainline as a new batch. Note that size of old batch B4 in the mainline can be increased by pumping additional product (P4) from the refinery and so $I_{n0}^{batch} = I_{n0}^{new} \cup \{B4\} = \{B4,B5\}$. Five batches should thus be transported by the pipeline network within the next 4 days ($I = \{B1,\ldots,B5\}$). Before solving AP, we don't exactly know which batches will move in each pipeline and therefore we need to consider all possible combinations.

Secondary line $n1$ is initially filled with old batches B1 and B2 and can receive products from new batches B3, B4 and B5 during the scheduling horizon. Thus, $I_{n1}^{new} = \{B3,B4,B5\}$. No old batch in the secondary line can receive product from the mainline and so $I_{n1}^{batch} = I_{n1}^{new} \cup \emptyset = \{B3,B4,B5\}$. Old batch B2 in the lateral branch line can receive product from the secondary line and so $I_{n2}^{batch} = I_{n2}^{new} \cup \{B2\} = \{B3,B4,B5\} \cup \{B2\} = \{B2,\ldots,B5\}$. Depot $s1$(D1) can only receive product from batch B4 and from new batch B5 that is injected into the pipeline in the future and so $I_{n0}^{s1=D1} = \{B4,B5\}$. Similarly $I_{n0}^{s3=D4} = \{B2,\ldots,B5\}$, $I_{n1}^{s2=D2} = \{B1,\ldots,B5\}$, and $I_{n2}^{s1=D3} = \{B2,\ldots,B5\}$. Finally, we will have $I_{n0} = I_{n0}^{old} \cup I_{n0}^{new} = \{B2,\ldots,B5\}$, $I_{n1} = \{B1,\ldots,B5\}$ and $I_{n2} = \{B2,\ldots,B5\}$.

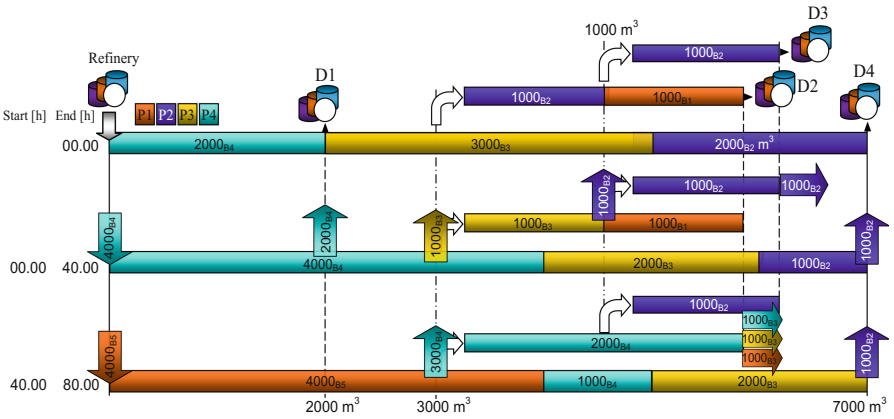

Fig. 3. Optimal aggregate schedule for Example 1.

We start solving model AP with the lower bound $|K|^{\mathrm{AP}} = \left\lceil \sum_{p,s,n} \frac{Demand_{p,s,n}}{IPV_{n0}^{\max}} \right\rceil = \left\lceil \frac{8000}{4000} \right\rceil = 2$. The optimal solution satisfies all product demands and is worth \$67600. To confirm that this is the global optimal solution, the problem is also solved for $|K|_{\mathrm{AP}} = 3$, but no improvement is observed (see Table 2). In fact, the third pumping run is a dummy operation ($\sum_i \lambda_{i,k3} = 0$) and so $|K|_{\mathrm{opt}}^{\mathrm{AP}} = 2$. The optimal schedule from model AP is depicted in Fig. 3.

Table 2. Computational results for Example 1.

Case	$\|K\|$	CPU (s)	C.var	B.var	Eqs	Backorder (%)	Obj. Fun (\$)
AP	2	0.16	504	84	1022	0	67600
AP	3	0.24	626	110	1271	0	67600
DSM	3	0.01	248	110	669	12.5	210300
DSM	4	0.11	317	136	849	12.5	210300
DSM	5	0.13	386	162	1029	0.0	10500
DSM	6	0.22	445	188	1209	0.0	10500

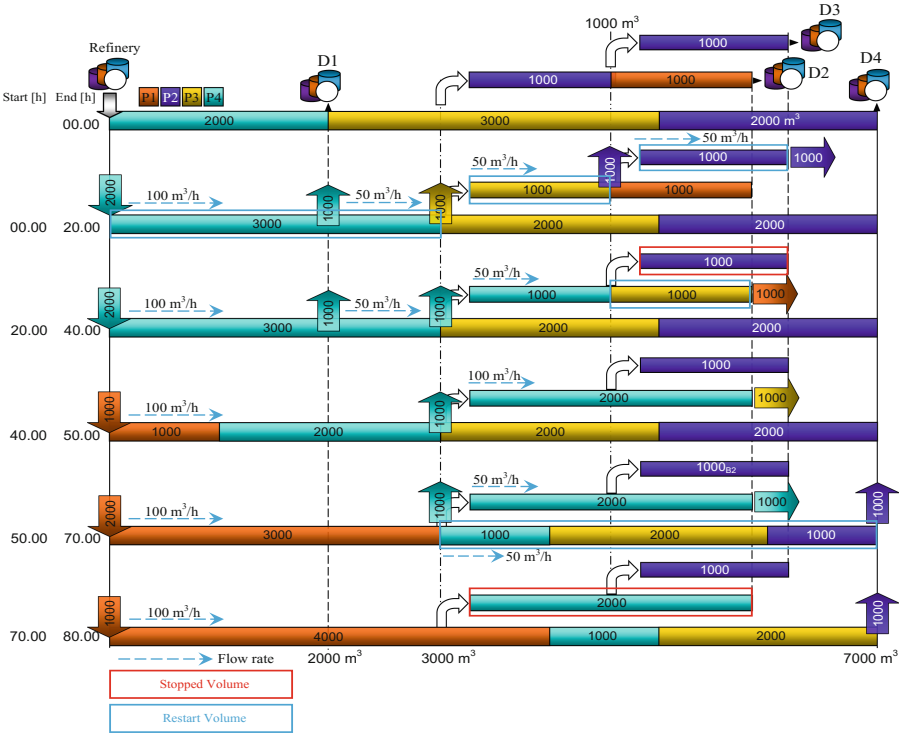

Fig. 4. Optimal schedule of Example 1 using DSM.

To solve DSM, the initial number of pumping operations should be accounted by using the equations introduced in Sect. 6. By doing so, we have $|K|^{DSM} \geq 3$. By setting $|K|^{DSM} = 3$ and 4, the resulting problems present the same solution of \$210300, from which \$200000 correspond to backorders. For $|K|^{DSM} = 5$ and 6 demand is fully satisfied and the value of the objective function is the same (see Table 2). The optimal detailed schedule using model DSM is depicted in Fig. 4.

To show the advantages of the proposed DSM approach, Table 3 gives the results for Example 1 using CC and the monolithic model (DP) presented in Sect. 3. From the table, the CC approach contains 6 pumping runs i.e., one more pumping operation with respect to our DSM approach. Furthermore, a larger volume should be restarted. For example, the third segment of the mainline should be restarted two times, one in the second pumping run and another in the last operation (specified in blue rectangle in Fig. 5). Besides, the same segment stops from time 40.00 h to 50.00 h (specified in red rectangle in Fig. 5). However, in our proposed two level approach, there is only one flow restart in the mainline segment (blue rectangle in Fig. 4) and no flow stoppage. Compared with the single level DP approach, the proposed DSM approach finds the same solution in less time, requiring a smaller model size.

Table 3. Comparison of solutions obtained by DSM, CC and DP for Example 1.

	$\|K\|$	CPU	C.var	B.var	Eqs	Obj. Fun	Total
		(s)				(\$)	cost(\$)
CC	6	0.01	461	146	1209	15600	83200[a]
DP	5	0.89	894	198	1932	78100	78100
DSM	5	0.13	386	162	1029	78100	78100[a]

[a] Total cost for DSM and CC is the optimal cost obtained from AP plus the cost obtained by DSM objective function

8.2 Example 2

Example 2 is taken from Mostafaei et al. [22] and deals with the detailed scheduling of a tree-like pipeline with two first-level branch lines. The first secondary line leaves the mainline at point 3000 m^3 and conveys products to depots D3 and D4. The second secondary line emerges at point 15000 m^3 of the mainline and transports products to depot D5. The pipeline structure and its initial batch profile are given in the first line of Fig. 6. The product injection rate at the refinery should be kept between 300 and 800 m^3/h. Other data for this example, together with the aggregate transportation plan, can be found in [22].

To solve DSM, we adopt $|K|^{DSM} = |K|^{AP}_{opt} = 10$, but the solution presents unsatisfied demands at the optimum. Backorders are also not avoided for $|K|^{DSM} = 11$ and 12. By setting $|K|^{DSM} = 13$, an optimal solution of \$15680 is obtained, which cannot be improved for $|K|^{DSM} = 14$ (see Table 4). Figure 6 shows the optimal detailed schedule for Example 2 using DSM.

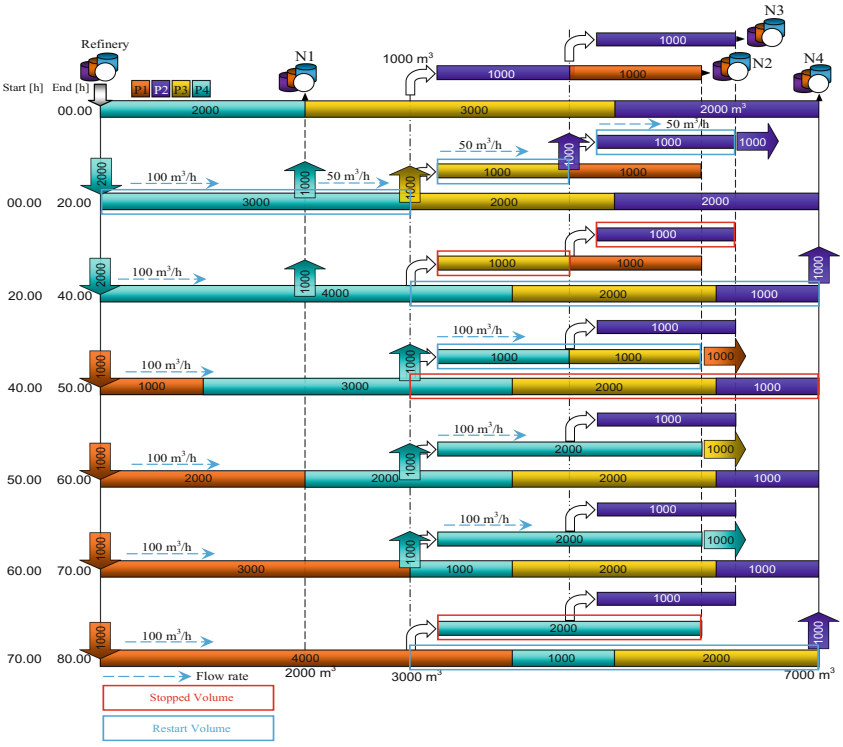

Fig. 5. Optimal schedule of Example 1 using CC.

Table 4. Model size and computational requirements of Example 2 for DSM.

Case	$\|K\|$	CPU (s)	C.var	B.var	eqs	Backorder (%)	Obj. Fun ($)
AP	10	22.14	2850	546	5387	0	817800
DSM	10	4.85	1942	467	3669	3.65	760560
DSM	11	18.38	2128	509	4008	1.38	306800
DSM	12	32.17	2314	551	4347	0.19	55680
DSM	13	48.34	2500	593	4686	0	15680
DSM	14	97.29	2668	635	5025	0	15680

To show that the proposed decomposition approach DSM is more efficient and flexible, we solve Example 2 using the single level model (DP) [22] and CC. Table 5 compares the solutions obtained. DP and DSM generate the same optimal solution, but DSM finds the optimum seven times faster. CC requires a few more pumping operations (22 vs. 13 for DSM) to meet demand for a 3.8% higher cost.

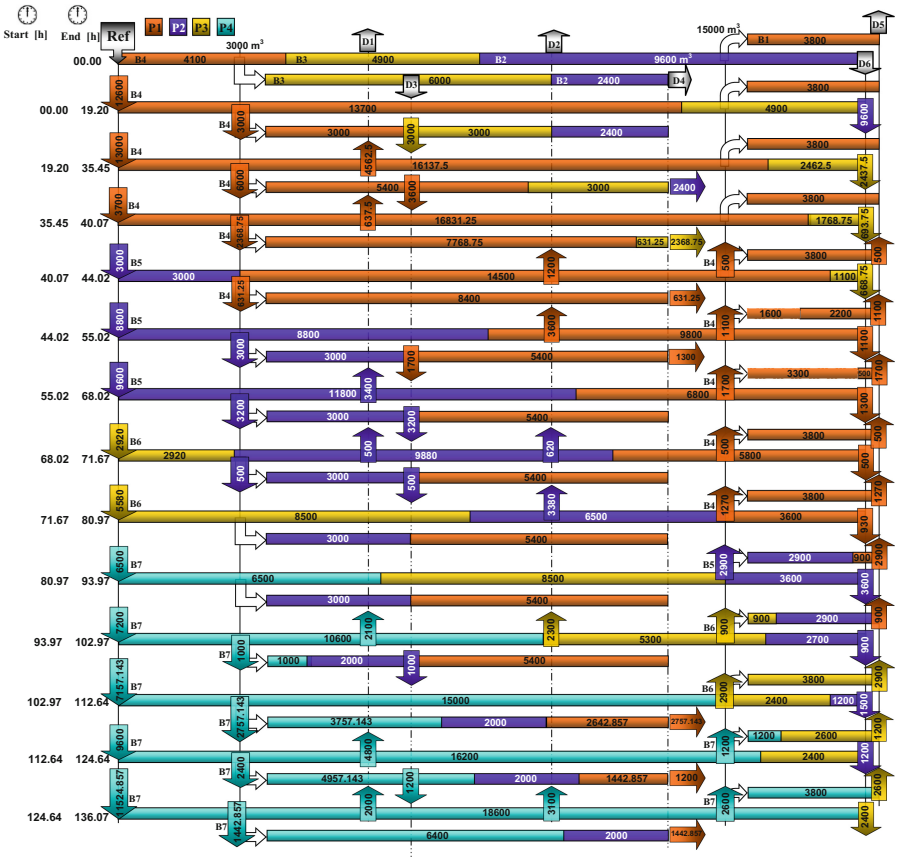

Fig. 6. Optimal detailed schedule of Example 2 using DSM.

Table 5. Comparison of solutions obtained by DSM, CC and DP for Example 2.

	DP [22]	CC	DSM
No of pumping runs	12	22	13
No of binary variables	782	1381	593
No of continuous variables	3714	6281	2500
No of constraints	5864	9090	4686
CPU time (s)	348.21	200.56	48.34
Total cost ($)	833480	865160	833480

8.3 Example 3

Example 3 is a large-scale case study involving a portion of the Iranian pipeline system. The trunk line in Fig. 1 starts at Tondgooyan refinery in Tehran using feedstock from the Ahvaz, Maroon and Shadegan oil fields and ends at Mashhad, the second most

populous city in Iran. The mainline capacity is reduced from 27840 to 22800 m^3/day after the output facility located at Shahrood (depot D4). The first secondary line leaves the mainline at point 87200 m^3 carrying products to three depots D9, D10 and D11. It contains a lateral branch line starting from depot D9 to depot D11, located at Gorgan. The second secondary line emerges at point 153800 m^3 of the mainline and transports products to Khayyam combined cycle power plant (depot D12). The last secondary line branches from the mainline at point 166100 m^3 and carries products to Torbat-e Heydarieh city (depot D13). The pump rate in the refinery should be set between 600 and 1160 m^3/h and the time horizon has a length of 240 h (10-day). Unit restart cost is 0.1 \$/m^3, for all segments, each pumping run has a fixed cost of \$2000, and backorder has a unit cost of 10 \$/m^3. Other data for this example are listed from Tables 6, 7 and 8.

Table 6. Flow rate range in pipeline segment of Example 3.

	Pipeline section						
	Ref–D4	D4–D8	D4–D9	D9–D10	D9–D11	D6–D12	D7–D13
Flow rate (m^3/h)	600–1160	600–850	120–410	50–410	50–410	80–00	100–350

Table 7. Product demands at depots of Example 3.

	Demand ($10 \times m^3$)												
P	D1	D2	D3	D4	D5	D6	D7	D8	D9	D10	D11	D12	D13
P1	289	817	0	430	623	407	–	2837	100	380	185	–	–
P2	–	500	870	680	1060	1882	1451	2140	195	370	800	–	690
P3	350	400	480	890	500	10	1245	2126	370	580	–	137	890

Table 8. Product inventory at refinery and interface cost of Example 3.

	Inventory (m^3)	Interface volume (m^3)/cost (\$)		
	Refinery	P1	P2	P3
P1	24810	–	60/100	X
P2	93366	60/100	–	50/100
P3	128674	X	50/100	–

The optimal aggregated plan for example 3 with 4 pumping runs is depicted in Fig. 7 and was found in just 1.93 s of CPU. The pipeline optimal schedule involves the injection of four product batches $P1_{24810}$, $P2_{35025}$, $P3_{128674}$ and $P2_{58341}$ into the mainline, with subscripts indicating the injection sizes in m^3. To generate a detailed schedule, DSM needs at least 8 pumping operations, which cannot fully meet product demands. By setting the number of pumping runs to 9, DSM finds a solution worth \$40042.8, which is not improved by $|K| = 10$. The model statistics and computational results of Example 3 are all listed in Table 9.

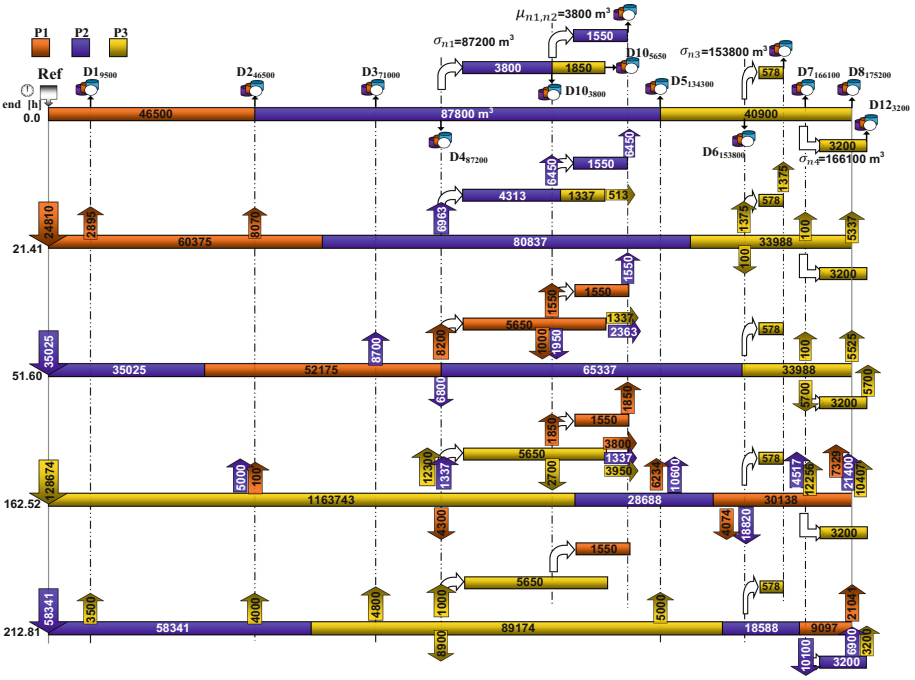

Fig. 7. Optimal aggregate schedule of Example 3 using AP.

Table 9. Model statistics and computational results of Example 3.

Case	$\|K\|$	CPU (s)	C.var	B.var	eqs	Backorder (%)	Makespan[a] (h)	Obj. Fun ($)
AP	4	1.93	1853	458	4360	0	212.82	60000
DSM	5	0.01	1193	497	3006	–	–	Infeasible
DSM	6	0.04	1405	588	3544	–	–	Infeasible
DSM	7	0.81	1621	679	4082	–	–	Infeasible
DSM	8	1.92	1837	770	4620	9.93	213.57	283361.6
DSM	9	31.01	2053	861	5158	0.0	215.37	40042.8
DSM	10	212.7	2269	952	5696	0	215.37	40042.8

[a] For indication only (not part of objective function)

9 Conclusions

This paper has presented an optimization algorithm for detailed scheduling of two-level tree-like pipeline networks featuring a unique refinery and multiple depots. Such pipelines consist of a mainline, first-level branches split from the mainline, and second-level branches emerging from the first-level lines. The algorithm consists of a two-level approach, featuring closely related continuous-time mixed-integer linear programming models in each level. Decisions related to the sequence of product injections and the

destination for each batch are made at the higher planning level, while the lower level then finds the sequence and timing of product deliveries. Through the solution of three example problems, two of them involving real-world case studies, we show that the proposed algorithm is more flexible than previous hierarchic approaches and is able to solve large-scale problems in quite reasonable time. Future work will involve generalizing the proposed method for multi-level tree pipeline networks.

Acknowledgments. Financial support from Fundação para a Ciência e Tecnologia through projects IF/00781/2013 and UID/MAT/04561/2013.

References

1. Rejowski, R., Pinto, J.M.: A novel continuous time representation for the scheduling of pipeline systems with pumping yield rate constraints. Comput. Chem. Eng. **32**, 1042–1066 (2008)
2. Zhang, H., Liang, Y., Liao, Q., Wu, M., Yan, X.: A hybrid computational approach for detailed scheduling of products in a pipeline with multiple pump stations. Energy **119**, 612–628 (2017)
3. Rejowski, R., Pinto, J.M.: Scheduling of a multiproduct pipeline system. Comput. Chem. Eng. **27**, 1229–1246 (2003)
4. Rejowski, R., Pinto, J.M.: Efficient MILP formulations and valid cuts for multiproduct pipeline scheduling. Comput. Chem. Eng. **28**, 1511–1528 (2004)
5. Magatão, L., Arruda, L.V.R., Neves, F.A.: A mixed integer programming approach for scheduling commodities in a pipeline. Comput. Chem. Eng. **28**, 171–185 (2004)
6. Herrán, A., de la Cruz, J.M., de Andrés, B.: Mathematical model for planning transportation of multiple petroleum products in a multi-pipeline system. Comput. Chem. Eng. **34**, 401–413 (2010)
7. Cafaro, D.C., Cerdá, J.: Optimal scheduling of multiproduct pipeline systems using a non-discrete MILP formulation. Comput. Chem. Eng. **28**, 2053–2068 (2004)
8. Cafaro, D.C., Cerdá, J.: Operational scheduling of refined products pipeline networks with simultaneous batch injections. Comput. Chem. Eng. **34**, 1687–1704 (2010)
9. Cafaro, D.C., Cerdá, J.: A rigorous mathematical formulation for the scheduling of tree-structure pipeline networks. Ind. Eng. Chem. Res. **50**, 5064–5085 (2012)
10. Cafaro, D.C., Cerdá, J.: Rigorous formulation for the scheduling of reversible-flow multiproduct pipelines. Comput. Chem. Eng. **61**, 59–76 (2014)
11. Relvas, S., Matos, H.M., Barbosa-Póvoa, A., Fialho, J., Pinheiro, A.S.: Pipeline scheduling and inventory management of a multiproduct distribution oil system. Ind. Eng. Chem. Res. **45**, 7841–7855 (2006)
12. Castro, P.M.: Optimal scheduling of pipeline systems with a resource-task network continuous-time formulation. Ind. Eng. Chem. Res. **49**, 11491–11505 (2010)
13. Cafaro, V.G., Cafaro, D.C., Mendéz, C.A., Cerdá, J.: Detailed scheduling of operations in single-source refined products pipelines. Ind. Eng. Chem. Res. **50**, 6240–6259 (2011)
14. Cafaro, V.G., Cafaro, D.C., Mendéz, C.A., Cerdá, J.: Detailed scheduling of single- source pipelines with simultaneous deliveries to multiple offtake stations. Ind. Eng. Chem. Res. **51**, 6145–6165 (2012)
15. Mostafaei, H., Ghaffari-Hadigheh, A.R.: A general modeling framework for the long-term scheduling of multiproduct pipelines with delivery constraints. Ind. Eng. Chem. Res. **53**, 7029–7042 (2014)

16. Ghaffari-Hadigheh, A.R., Mostafaei, H.: On the scheduling of real world multiproduct pipeline with simultaneous delivery. Optim. Eng. **16**, 571–604 (2015)
17. Cafaro, V.G., Cafaro, D.C., Mendéz, C.A., Cerdá, J.: Optimization model for the detailed scheduling of multi-source pipelines. Comput. Chem. Eng. **88**, 395–409 (2015)
18. Mostafaei, H., Castro, P.M., Ghaffari-Hadigheh, A.R.: Short-term scheduling of multiple source pipelines with simultaneous injections and deliveries. Comput. Oper. Res. **73**, 27–42 (2016)
19. Mostafaei, H., Castro, P.M.: Continuous-time scheduling formulation for straight pipeline. AIChE J. **62**, 1923–1936 (2017)
20. Castro, P.M., Mostafaei, H.: Product-centric continuous-time formulation for pipeline scheduling. Comput. Chem. Eng. **104**, 283–295 (2017)
21. Castro, P.M.: Optimal scheduling of multiproduct pipelines in networks with reversible flow. Ind. Eng. Chem. Res. **56**, 9638–9656 (2017)
22. Mostafaei, H., Castro, P.M., Ghaffari-Hadigheh, A.: A novel monolithic MILP framework for lot-sizing and scheduling of multiproduct tree-like pipeline networks. Ind. Eng. Chem. Res. **54**, 9202–9221 (2015)
23. Mostafaei, H., Castro, P.M.: Two-level approach for scheduling multiproduct oil distribution systems. ICORES **1**, 150–159 (2017). https://doi.org/10.5220/0006196501500159

On the Impact of Considering Power Losses in Offshore Wind Farm Cable Routing

Martina Fischetti[1,2(✉)] and David Pisinger[2]

[1] Vattenfall BA Wind, Kolding, Denmark
[2] Operations Research, DTU Management Engineering, Technical University of Denmark, Kongens Lyngby, Denmark
{martfi,dapi}@dtu.dk

Abstract. Wind energy is a field of main importance in the transition away from fossil fuels. In order to achieve this goal, reducing production cost of wind energy is of primary importance, especially for offshore wind parks. In the present paper we illustrate optimization models to achieve this goal for the cable routing problem. In particular we focus on the economical impact of considering power losses in the optimization. The resulting optimization problem considers both minimizing immediate costs (CAPEX) and minimizing costs due to power losses in the park lifetime. Thanks to the close collaboration with a leading energy company, we have been able to conduct different what-if analyses on a set of existing wind parks. Having a fast and reliable tool to optimize cable routing considering or not power losses, we have been able, for the first time, to quantify the impact of these kinds of decisions at design phase. Our results illustrates the importance of considering power losses already at the design phase, as well as the importance of having a sophisticated optimization tool, compared with the traditional manual design.

Keywords: Mixed Integer Linear Programming
Offshore wind parks · Green energy · Cable routing · Cable losses

1 Introduction

Wind power is a leading technology in the transition to green sources of energy. Having a yearly market growth of 15–20%, it is however necessary to face new challenges on a market that is more and more competitive. According to [11] the expenses for electrical infrastructure of a offshore wind farm account for 15–30% of the overall initial costs. Therefore, high-level optimization in this area is a key factor. Cable layout is a problem of great interest in many companies and it is typically solved only manually. Different types of cable layout problems can be addressed: in this paper we study the inter array cable optimization, i.e., the optimal routing to connect offshore turbines and to collect their energy in one or more substations. In particular, we focus on the impact of considering

G. H. Parlier et al. (Eds.): ICORES 2017, CCIS 884, pp. 267–292, 2018.
https://doi.org/10.1007/978-3-319-94767-9_14

power losses already in the design phase. While the energy flows through a cable, indeed, part of it gets lost due to the intrinsic resistance of the cable. An optimized selection of the cable structure and the cable type, can reduce the amount of these losses.

The main scope of the inter-array cable routing is to collect the power production of turbines in offshore substations. To do that, each turbine must be connected to one substation through a loop-free path. The inter-array cable routing optimization problem consists in finding the cable connection that minimizes the associated cost. Since different cables with different costs, capacities and resistances are available on the market, the task is not only to find the turbines to be directly connected, but also to choose appropriate cable types to minimize losses.

Wind park cable routing optimization has obtained considerable attention in the last years. Due to the large number of constraints and the intrinsic complexity of the problem, many studies (i.e. [6,12,16,18]) preferred to use ad-hoc heuristics. Only a few papers used Mixed Integer Linear Programming (MILP), notably [1,2,4,5,7,14,17]. A MILP approach boosted with heuristics (a so-called matheuristic approach) to deal with large-scale wind parks in an acceptable time has been recently proposed in [8]. The present work is based on [8] but focuses more on real applications of the optimization model and on its economical impact. Several variants of the problem have been proposed in the literature. To the best of our knowledge only [4] has considered power loss in cables. However, [4] does not take into account variable cable loads due to fluctuating wind. [1] proposes an Open Vehicle Routing approach for this problem adding the planarity constraints on the fly. In this Open Vehicle Routing version of the problem, only one cable can enter a turbine, even if this is often not the case in the reality. In [1], the possibility of branching cables in the turbines (as we are doing), is mentioned as a future work. However, the substation limits, that could be a major constraint in practical applications, are not considered in [1]. Different approaches for the cable network design are provided in [2]. The suggested approach is a divide-and-conquer heuristic based on the idea of dividing the big circuit problem into smaller circuit ones. They also propose a MILP model, but it cannot deal with more than 11 turbines. In [14] the cable layout problem for onshore cases is studied.

Thanks to the collaboration with a leading energy company it has been possible to build a detailed model including a majority of the constraints arising in practical applications, and to evaluate the savings of optimized layouts on real cases. First, the energy flow is unsplittable (so the flow leaving a turbine must be supported by a single cable) and the flow in each cable cannot exceed its capacity. Secondly, also the substations that collect the energy has some limitations. In particular, each substation has a maximum number of electric connections, i.e., a maximum number of cables that can be connected to it. Moreover, cable crossings should be avoided. Cable crossing is not impossible in principle, but is highly not recommended in practice. Building one cable on top of another is, indeed, more expensive and increases the risk of cable damages. Therefore it is

important for a model to take this planarity constraint into account. We used a Mixed Integer Linear Programming (MILP) approach with ad-hoc heuristics to solve difficult instances of this problem [8]. The resulting optimization tool has been validated by company experts, and is now routinely used by the planners.

The main contribution of the present paper is to analyse how the inter-array cable routing of real-world wind farms can be improved by using modern optimization techniques. A particularly challenging aspect in the cable routing design is to understand if one could limit power losses by optimizing cable routing. As a general rule, cables with less resistance are also more expensive, therefore we would like to make a proper trade-off between investments and cable losses. We formulate the optimization problem with immediate costs (CAPEX) and losses-related costs as two separate goals. The two objectives can be merged into a single objective by proper weighing of the two parts. The weighing factor can be considered fixed or can vary: this makes it possible to perform various what-if analyses to evaluate the impact of different preferences (i.e. weighing factors). This analysis is important in cases where a positive pay-back is demanded within a short time horizon, or where liquidity problems hinder choosing the best long-term solution. We report a study of both approaches on a set of real-world instances.

In our computation of power losses, we show that wind scenarios can be handled efficiently as part of data preprocessing, resulting in a MILP model of tractable size. Tests on a library of real-life instances proved that substantial savings can be achieved.

Our paper is organized as follows: Sect. 2 describes our MILP model, first presenting a basic model and then improving and extending the formulation. In particular, we show how to model power losses, and propose a precomputing strategy that is able to handle this non-linearity efficiently, thus avoiding sophisticated quadratic models that would make our approach impractical. In Sect. 3 we describe how to handle large size instances using a matheuristic approach. Section 4 compares our optimized solutions with an existing cable layout for a real wind farm (Horns Rev 1), showing that millions of euro can be saved. Section 5 is dedicated to various what-if analyses. In particular, Subsect. 5.1 describes the real-world wind farms that we considered in our tests, while Subsect. 5.2 shows the results of our optimization on a testbed of real-world cases, reporting the impact of considering power losses for all the instances. Section 6 is dedicated to different analyses on the weighting factor: Subsect. 6.1 analyses the impact of different return-of-investment requirements on the cable routing costs, while Subsect. 6.2 studies the impact of considering price fluctuations on the market. Some conclusions are finally addressed in Sect. 7.

The present paper is an extended version of the conference paper [9] from the same authors, where both the methodological and the test part have been extended. In particular, in the present paper, we describe some matheuristic techniques that can be used for difficult instances and we present sensitivity analyses on price fluctuations.

2 Mathematical Models

In order for this paper to be self-contained, we start by reviewing the MILP models and algorithms we proposed in [8]; the interested reader is referred to the given paper for details.

2.1 Basic Model

We assume that the location of the turbines has already been defined. We wish to find an optimal cable connection between all turbines and the given substation(s), minimizing the total cable costs. The optimization problem considers that:

- the energy flow leaving a turbine must be supported by a single cable;
- the maximum energy flow (when all the turbines produce their maximum) in each connection cannot exceed the capacity of the installed cable;
- different cables, with different capacities, costs and impedances, can be installed;
- cable crossing should be avoided;
- a given maximum number of cables can be connected to each substation;
- cable losses (dependent on the cable type, the cable length and the current flow through the cable) must be considered.

We will first model the problem without cable losses and then discuss in Subsect. 2.2 how to efficiently express these latter constraints. We model turbine positions as nodes of a complete and loop-free directed graph $G = (V, A)$ and all possible connections between them as directed arcs. Some nodes correspond to the substations that are considered as the roots of the trees, being the only nodes that collect energy. Let P_h be the power production at node h. We distinguish between two different types of node: V_T is the set of turbine nodes, and V_0 is the set of substation nodes. Let T denote the set of different cable types that can be used. Each cable type t has a given capacity k_t and unit cost u_t, representing the cost per meter of the cable (CAPEX). Arc costs can therefore be defined as $c^t_{i,j} = u_t dist(i,j)$ for each arc $(i,j) \in A$ and for each type $t \in T$, where $dist(i,j)$ is the Euclidean distance between turbine i and turbine j. In our model we use the continuous variables $f_{i,j} \geq 0$ for the flow on arc (i,j). The binary variables $x^t_{i,j}$ define cable connections as

$$x^t_{i,j} = \begin{cases} 1 & \text{if arc } (i,j) \text{ with cable type } t \text{ is selected} \\ 0 & \text{otherwise.} \end{cases}$$

Finally, variables $y_{i,j}$ indicate whether turbines i and j are connected (with any type of cable). Note that variables $y_{i,j}$ are related to variables $x^t_{i,j}$ as $\sum_{t\in T} x^t_{i,j} = y_{i,j}$. The overall model can be stated as follows [8]:

$$\min \sum_{i,j\in V} \sum_{t\in T} c^t_{i,j} x^t_{i,j} \tag{1}$$

$$\text{s.t.} \sum_{t\in T} x^t_{i,j} = y_{i,j}, \qquad i,j \in V : j \neq i \tag{2}$$

$$\sum_{i:i\neq h} (f_{h,i} - f_{i,h}) = P_h, \quad h \in V_T \tag{3}$$

$$\sum_{t\in T} k_t x^t_{i,j} \geq f_{i,j}, \qquad i,j \in V : j \neq i \tag{4}$$

$$\sum_{j:j\neq h} y_{h,j} = 1, \qquad h \in V_T \tag{5}$$

$$\sum_{j:j\neq h} y_{h,j} = 0, \qquad h \in V_0 \tag{6}$$

$$\sum_{i\neq h} y_{i,h} \leq C, \qquad h \in V_0 \tag{7}$$

$$x^t_{i,j} \in \{0,1\}, \qquad i,j \in V, t \in T \tag{8}$$

$$y_{i,j} \in \{0,1\}, \qquad i,j \in V \tag{9}$$

$$f_{i,j} \geq 0, \qquad i,j \in V, j \neq i. \tag{10}$$

The objective function (1) minimizes the total cable layout cost. Constraints (2) impose that only one type of cable can be selected for each built arc, and defines the $y_{i,j}$ variables. Constraints (3) are flow conservation constraints: the energy (flow) exiting each node h is equal to the flow entering h plus the power production of that node (except if the node is a substation). Constraints (4) ensure that the flow does not exceed the capacity of the installed cable, while constraints (5) and (6) impose that only one cable can exit a turbine and none can exit the substations (tree structure with root in the substations). Finally, constraints (7) impose the maximum number of cables (C) that can enter each substation.

In order to model no-cross constraints we need a constraint for each pair of crossings arcs, i.e. a very large number of constraints. We have, therefore, decided to generate them on the fly, as also suggested in [1]. In other words, the optimizer considers model (1)–(10) and adds the following new constraints whenever two established connections (i,j) and (h,k) cross

$$y_{i,j} + y_{j,i} + y_{h,k} + y_{k,h} \leq 1. \tag{11}$$

The reader is referred to [8] for stronger versions of those constraints. Using this approach, the number of non-crossing constraints actually added to the model decreases dramatically, making the model faster to solve. As presented, the model is able to deal with small size instances only. In order to produce high quality solutions in an acceptable amount of time also for large-scale instances, a "matheuristic" framework (as the one proposed in [8]) can be used on top of this basic model. We refer to Sect. 3, for more details.

2.2 Cable Losses

In this section we review an extension of the previous model taking cable losses into account (still from [8]). Consider a generic cable of type t under wind scenario s. Power losses increase with the square of the current $g_{i,j}^{t,s}$, according to the formula:

$$3R^t \cdot dist(i,j)(g_{i,j}^t)^2 \tag{12}$$

where R^t is the electrical resistance of the 3-phase cable of type t, in Ω/m. Decision variable $g_{i,j}^{t,s}$ obviously depends on the considered wind scenario. As a consequence, dealing with Eq. (12) directly in the model, would imply dealing with non-linearities over multiple scenarios. Nevertheless, (12) can be simplified if we assume that all the turbines in the park have the same power production under the same wind scenario. This is a fair assumptions since typical parks are constructed by using only one turbine model and wake effect is not usually considered in electrical studies. Under this assumption, the current I_s passing through a generic cable supporting f turbines (say), can be expressed as $g_{i,j}^{t,s} = fI^S$ where I^s is the current produced by a single turbine under scenario s. Accordingly, power loss can be expressed as a function of f, as

$$PLoss^{t,f,s} = 3R^t dist(i,j)(fI^s)^2. \tag{13}$$

The value $f \in 1, \ldots F$ is limited by the capacity of the cables. By introducing the dependency on f in our main binary variables (now $x_{i,j}^{t,f}$) we can re-write our two cost contribution as:

$$min \sum_{i,j \in V} \sum_{t \in T} \sum_{f \in F} \sum_{s \in S} \pi_s PLoss^{t,f,s} x_{i,j}^{t,f} \tag{14}$$

and

$$\min \sum_{i,j \in V} \sum_{t \in T} \sum_{f \in F} c_{i,j}^t x_{i,j}^{t,f}, \tag{15}$$

where π_s is the probability of scenario s. As we have discussed earlier, minimizing losses can imply an increase of the CAPEX cost, therefore the two objective must be properly balanced. In some cases (e.g., when there is no limit on the CAPEX) they can be merged, by using a converting factor for the loss-related term: this is the estimated cost for each MW of production lost over the wind farm lifetime (Net Present Value). This value (denoted K) is an input value, that the designer can set to the desired project-specific value. The merged objective function, now expressed in €, is then:

$$\min \sum_{i,j \in V} \sum_{t \in T} \sum_{f \in F} c_{i,j}^t x_{i,j}^{t,f} + K \sum_{i,j \in V} \sum_{t \in T} \sum_{f \in F} \sum_{s \in S} \pi_s PLoss^{t,f,s} x_{i,j}^{t,f}. \tag{16}$$

The new set of variables $x_{i,j}^{t,f}$ can actually be handled implicitly in a pre-processing phase, without changing the original model (1)–(10), according to the following idea. We consider the basic model (1)–(10) without cable losses on a modified instance where each cable type is replaced by a series of "subcables" with discretized capacity and modified cable cost taking both CAPEX and revenue losses due to cable losses into account.

Nearly all wind farms are designed for only one turbine type, hence the maximum power production P_h of each turbine can be normalized to 1, meaning that we can express the cable capacity as the maximum number of turbines supported. Consider a certain cable type t that can support up to k_t turbines. We replace it by k_t "subcable" types of capacity $f = 1, 2, \ldots, k_t$ whose unit cost is computed by adding both cable/installation unit costs (u_t) and loss costs (denoted as $loss^{t,f}$) considering the current produced by exactly f turbines. Note that such unit costs increase with f, so the optimal solution will always select the subcable type f supporting exactly the number of turbines connected, hence the approach is correct.

The above approach allows us to easily consider multiple wind scenarios without affecting the model size. This is obtained by precomputing the subcable unit costs by just considering a weighted average of the loss unit cost under different wind scenarios (and hence different current productions). To be more specific, we can now precompute the value

$$loss^{t,f} = 3R^t K \sum\nolimits_{s \in S} \pi_s (fI^s)^2, \tag{17}$$

where π_s is the probability of scenario s and I^s is the current produced by a single turbine under wind scenario s. We refer to the next subsection for a more detailed example of how cable costs are pre-processed when considering losses. As said, K is a factor to estimate the value (in €) of a MW loss, and can be computed as $K = k_{euro} \cdot 8760$ where k_{euro} is the NPV for a MW/h production over the park lifetime, and 8760 is the number of hours in a year. Notice that k_{euro} acts as a weighing factor between the two objectives: minimize CAPEX costs versus minimize losses. In practice, this value is site-specific so it is given by the business team of the specific farm. It takes into account the expected cost of energy and the lifetime of the park. In Sect. 6.1 we will sketch a sensitivity analysis on the variation of this parameter, looking in particular at the effect of considering a shorter return of investment for the park. In general, we will consider a unique k_{euro} that does not follow the variations of the spot price: wind parks, indeed, commonly operate at a protected and fixed price for most of their lifetime (at least in Denmark). In Sect. 6.2 we will consider the case of using market prices, i.e. having a different k_{euro} for different wind scenarios. We will analyse the impact of considering price fluctuation on the losses optimized solution on real-world instances.

2.3 Loss Pre-computation

In this section we illustrate the pre-computing strategy proposed in the previous session, using a concrete example from the real wind park Horns Rev 1. The park consists of 80 2 MW turbines and is located about 15 Km from the Danish shore. This park will be used as one of our test cases in Sects. 4 and 5.

Cable sets can differ in cable cross section or in voltage (33 kV or 66 kV generally), which reflects in different capacities and resistances. The set of most adequate cables is selected by the electrical specialists in the company. Of course, different cable types can lead to different optimal layouts, as we will see in Sect. 5.

Let us suppose that we are given a set of two cables: the cheapest one can support 10 2 MW turbines and the most expensive 14 turbines. This set of cables will be indicated as cb05 in Sect. 5. We are provided with the following table, that reports the characteristics of the two cable types (including installation costs).

Table 1. Cable information for cb05 [9].

Cables	Type	No. of 2 MW turb.	Resistance [Ω/km]	Cost [€/m]	Install. cost [€/m]
cb05	1	10	0.13	180	260
	2	14	0.04	360	260

If we want to optimize on CAPEX costs only, we just need to input to the model the capacity of each cable type and its overall cost (cable price plus installation cost). In this case, for example, this would be:

- type 1: supports up to 10 turbines with a unit cost of 440 €/m
- type 2: supports up to 14 turbines with a unit cost of 620 €/m.

Third column of Table 2 shows how the model will compute the unit price (CAPEX only) depending on the number of turbines connected.

Let us now consider losses using the strategy of Subsect. 2.2. As we discussed earlier, the power loss in a cable depends on the current passing through it. Since only a discrete number of turbines can be connected to each cable path, we can express the current as a function of the number f of turbines connected without any loss of precision in the result.

Still referring to Eq. (17), the losses depend also on the wind statistics in the site. We can define a wind scenario (s) as a wind speed and its probability to occur (π_s). At a given wind speed, a given turbine will produce a specific current (I_s).

Wind scenarios can be defined in different ways. In this paper we used both real measurements and scenarios derived from Weibull distributions for the specific sites. For the Horns Rev 1 case we are considering, we had real measurements from the site, i.e., a wind speed sample each 10 min for 10 years. We grouped all these samples in wind-speed bins of 1 m/s, obtaining 25 wind scenarios (from 1 to 25 m/s). The probability of each scenario was obtained looking at the

frequency of the specific wind speed over all the samples. In our tests we decided to bin our data every 1 m/s, following the practice in electrical losses computations. However this should not be considered a limit: since the wind scenarios are handled in the pre-processing phase, the number of scenarios does not affect the size of the final optimization model.

Having computed I_s and π_s according to the scenario definition, power losses can now be calculated. Parameter $k_{euro} = 690$ €/MWh was computed by the company experts for a wind park lifetime of 25 years, while resistance R_t is defined according to Table 1. Using Eq. (17), the cost for power losses $loss^{t,f}$ can be now precomputed. As shown in (16), the cost considered in the objective for each cable connection will need to include the CAPEX costs (u_t) and the contribution from losses ($loss^{t,f}$). Therefore the final input to the optimization tool for Horns Rev 1 with cb05, will be as shown in the fourth column of Table 2.

Table 2. Precomputed cable prices for cable cb05 (including installation costs) for Horns Rev 1. First column indicates the cable type, second column indicates the number of turbines supported f. Third column indicates the CAPEX costs, while fourth column reports prices with also power losses costs included.

Cable type	No. of 2 MW turb. supported	CAPEX cost [€/m]	Cost with losses [€/m]
1	1	440	441.16
	2	440	442.71
	3	440	445.27
	4	440	448.87
	5	440	453.50
	6	440	459.15
	7	440	465.83
	8	440	473.54
	9	440	482.28
	10	440	492.04
2	11	620	639.77
	12	620	643.41
	13	620	647.36
	14	620	651.63

A comparison between the last two columns of Table 2 shows the impact of considering losses on cable prices. While from a installation perspective the cost for each cable type is fixed, it now varies depending on how many turbines are connected. As we will see, this can have a significant impact on the optimal cable routing.

3 Matheuristics

In a practical setting, one would like to find high-quality solutions in short computing time, making it possible to experiment with different settings. This could be useful, for example, for what-if analyses considering different cables from different manufactures, or to evaluate the effect of different design choices (as we will do in Sect. 5). In some difficult cases, model (1)–(10) could require long computing time before producing even the first feasible solution. On the other hand, due to the intrinsic structure of MILP solvers, having a first solution as soon as possible in the branch-and-bound tree could significantly speed up the overall resolution. In [8] we used MILP-based heuristics on a relaxed version of the model to quickly produce first solutions for the MILP solver. The relaxed model and the matheuristics applied on it, are next outlined for the sake of completeness.

3.1 A Relaxed Model

Model (1)–(10) can be relaxed to find feasible solutions faster. This can be obtained by allowing for disconnected solutions, that are penalized by high costs.

To be more specific, we introduce a new variable, $l_h \geq 0$, that indicates the loss at the node h. The cost of a unit loss is fixed to M, a large positive constant greater than all the prices involved in the optimization (we used 10^9). This is to ensure that a connected solution would always have a lower cost compared with a disconnected one.

The relaxed model is then obtained from (1)–(10) by replacing (1) with

$$\min \sum_{i,j \in V} \sum_{t \in T} c^t_{i,j} x^t_{i,j} + \sum_i M l_i \tag{18}$$

and (3) with

$$\sum_{i:i \neq h} (f_{h,i} - f_{i,h}) = P_h - l_h h \in V_S \cup V_T. \tag{19}$$

A MILP solver applied to the relaxed model is typically able to find, in a few seconds, a feasible (possibly disconnected) first solution and to quickly proceed in the tree enumeration to discover better and better ones. Therefore, the relaxed model is used in our experiments.

3.2 Matheuristics Based on the Relaxed Model

As its name suggests, a matheuristic is the hybridization of mathematical programming with metaheuristics. The idea presented in what follows is to use the relaxed model powered up by the use of a metaheuristic. We refer the interested reader to [3,10,13], for a more general treatment of the subject. The basic idea of our matheuristic is to restrict the number of variables in the optimization by temporary fixing some arcs of the best solution found so far, and re-optimize on the remaining arcs. In other words, given a feasible solution y^* of the relaxed

model, we fix to 1 some of the y variables with $y^*_{i,j}$. Note that in our problem, fixing some arcs implies to exclude all the crossings arcs, with a drastic redaction in the dimension of the model. In order to decide which arcs to fix in the solution, we used different heuristic strategies.

Our first matheuristic works as follows: The relaxed model is solved with a short time limit and the best found solution y^* is returned. Afterwards, the arcs selected in this solution (i.e., all those variables having $y^*_{i,j} = 1$) are temporally fixed with a certain probability (e.g. 0.5). The resulting restricted problem is reoptimized on the remaining arcs, and the approach is repeated.

As already observed, every time some arcs are heuristically fixed on input, in a preprocessing phase we can forbid all possible crossing arcs (i.e. we can set to zero all the variables related to them). This is very important for the success of our heuristic, as the restricted problems become much easier due to the fixing.

Our second matheuristic uses a similar approach, but with a more problem-related strategy to choose the fixing probability. Instead of having a fixed probability to select arcs, the probability is now related with the distance to the substation(s): the arcs closer to the substation(s) are fixed with a higher probability. The distance of an arc (i, j) to the substation(s) is defined as

$$DIST_{i,j} = max\{min_{h \in V_0} dist(i,h), min_{h \in V_0} dist(j,h)\}.$$

Distances are normalized with respect to the longest distance in the specific test instance ($DIST_{MAX}$) and the fixing probability is computed as $1 - DIST_{i,j}/DIST_{MAX}$. In this way the arcs closer to the substation have an higher probability to be fixed and the optimization tends to focus on the more far away arcs.

The third matheuristic is specific for wind farms with only one substation. Analysing the solutions, indeed, the layout appears divided in sectors: the final layout looks as a collection of "irregular rays" connected to the substation. Our third matheuristic is therefore randomly decomposing the problem in sectors, fixing the arcs outside the sector and re-optimizing inside. To be more specific, all the nodes are ordered according to their angle with the substation. A turbine (that we will call "the seed") is randomly selected and the sector is defined by picking the next μ turbines in the ordered sequence (e.g. $\mu = 30\%$ of the total number of turbines). The arcs connecting turbines outside this sector are fixed while any arc (i, j) where i or j is in the sector, is reoptimized. The already discussed pre-processing is applied on the fix arcs and the optimization is re-run. If the new solution is improved, we select a new seed close to the previous one (i.e. in the ordered vector we pick a node in the interval [current seed -2, current seed $+2$], according to a normal distribution), while, if the solution is not improved, the new seed is the 5^{th} turbine after the current seed. Figure 1 illustrates this last heuristic. Turbines are represented as black dots, while the substation is the red square. Different cable types are represented by arcs of different colours. Some turbines are connected to other turbines or to the substation with different types of cables (in blue and green). The first plot in Fig. 1 shows the first (disconnected) solution obtained using a MILP solver on the relaxed model with a few-second timelimit. A sector is defined on this solution (in pink in the picture).

The variables y referring to arcs outside this sector are fixed to 1. This means that these connections are fixed in the next iteration (cable types are instead not fixed, meaning that the colour of the connection in the plot can vary). The restricted MILP model (with fixed variables) is passed again to the MILP solver with a short timelimit. The second plot in Fig. 1 shows the new solution we got from the solver. The arcs outside the sector are kept in the new solution, even if the type of cable changed, while the arcs inside the sector are not reselected in the new solution. By repeating this framework many times, the solutions quickly improve exploring different neighbourhoods.

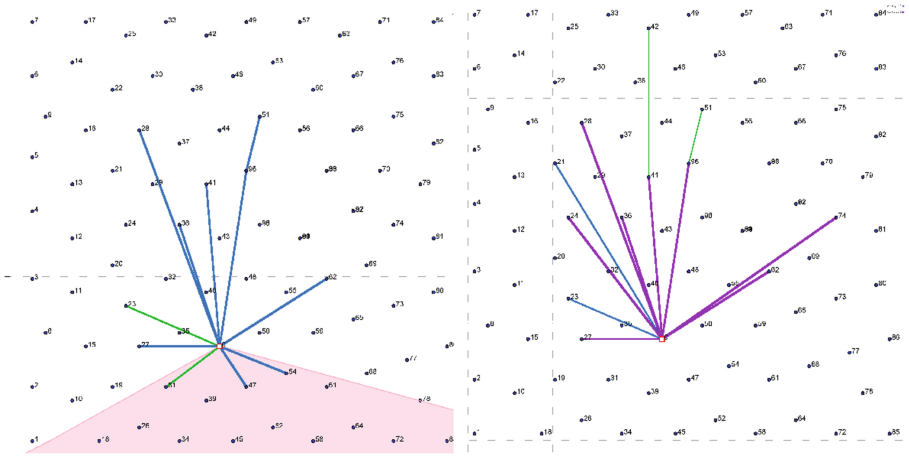

Fig. 1. Two consecutive iterations of the Sector matheuristic: after a short timelimit we receive a first disconnected solution from the solver (left plot). We define a sector (in pink) and we fix all the connections outside the sector (setting the corresponding y variables at 1). We pass the new (restricted) problem to the solver, that returns the solution on the second plot (right plot). We iterate the process obtaining still better solutions to warm start the MILP solver. (Color figure online)

All three matheuristics are used in our tests, repeating them 5 times before starting the final MILP-solver run (without any fixing). We refer to [8] for a computational analysis on the impact of using matheuristics techniques on the wind farm cable routing problem.

4 Comparison with an Existing Layout

We report in this section a comparison between our optimized solutions (considering and not considering losses) and the existing cable routing for Horns Rev 1, a real-world offshore park located in Denmark. Figure 2 shows the actual design for Horns Rev 1 (from [15]).

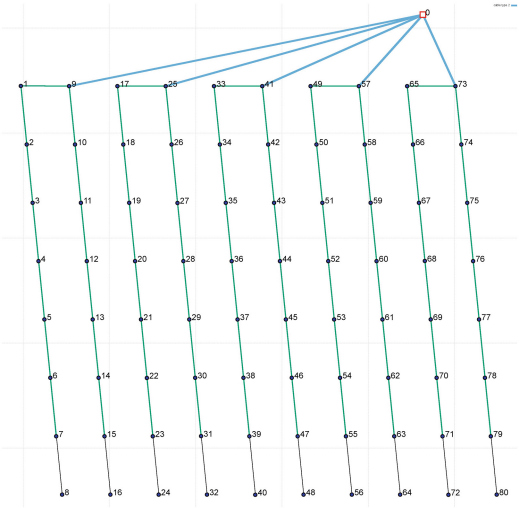

Fig. 2. Existing cable routing for Horns Rev 1 [9]. (Color figure online)

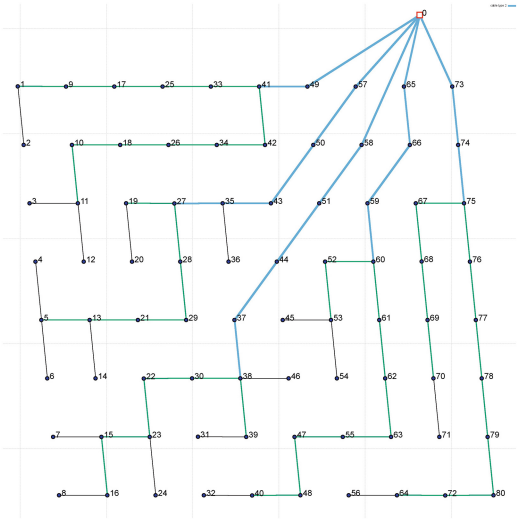

Fig. 3. Optimized layout for Horns Rev 1 (CAPEX costs only): this layout is more than 1.5 M€ more profitable than the existing one [9]. (Color figure online)

Three different types of cables are used: the thinnest cable supports one turbine only, the medium supports 8 turbines, and the thickest 16. We estimated the costs and resistances of these cables based on the cable cross section. The estimated prices are 85 €/m, 125 €/m and 240 €/m, respectively, plus an estimated 260 €/m

for installation costs (independent of the cable type). We ran our CAPEX optimization with the above prices obtaining the layout in Fig. 3. The optimized layout is significantly different from the existing one. Looking at immediate costs, the optimized layout is more than 1.5 M€ less expensive. As already said, this layout is optimized only on immediate costs, nevertheless if we estimate its value in 25 years (considering losses) it is still more profitable than the existing one (by about 1.6 M€).

By optimizing cable losses, one can further increase the value in the long term. Figure 4 shows the optimized solution considering losses (thus optimizing the value of the cable route in its lifetime). Compared with the existing layout (Fig. 2), this new layout is about 1.7 M€ (NPV) more profitable in 25 years, and still around 1.5 M€ cheaper at construction time.

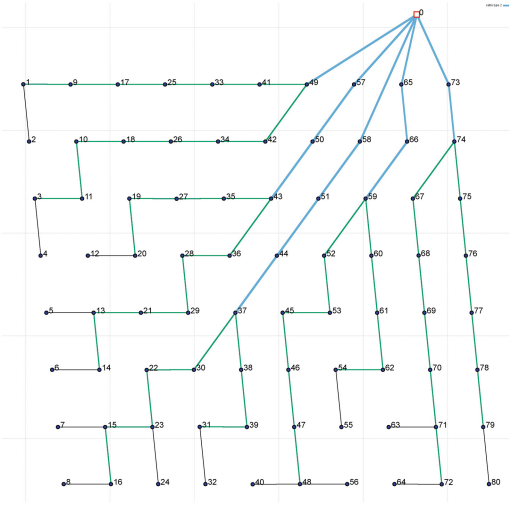

Fig. 4. Optimized layout for Horns Rev 1 (considering losses): in the wind park lifetime this layout is estimated to be more than 1.7 M€ more profitable than the existing one [9]. (Color figure online)

Table 3 summarizes the savings of the two optimized layouts compared with the existing one, both from an immediate cost perspective and from a long-term perspective; all values are expressed in k€.

The test shows that more than one million Euros can be saved using our optimization methods on real parks. In the next section we want to focus on the other big advantage of using automatic optimization tools: the possibility of performing a number of what-if analyses. To the best of our knowledge, this is the first detailed study on the impact of different design choices on the cable routing itself and on its impact on immediate costs (CAPEX) and long term costs.

Table 3. Savings of optimized solutions compared with the existing cable routing for Horns Rev 1 [9].

Opt mode	Savings [k€]	
	Immediate	In 25 years
CAPEX	1544	1605
Lifetime	1511	1687

5 Impact of Considering Power Losses on Real Instances

We performed a number of what-if analyses on different real-world wind farms. In particular, we were interest in evaluating the impact of considering power losses in the design phase. We will next compare solutions optimized only for CAPEX costs, with solutions optimized looking at the whole lifetime of the park. We will then study the usage of different types of cable (with different resistances) in both cases, and the long-term savings compared with the possibly higher investments costs.

5.1 Test Instances

We tested our model on the real-world instances proposed in [8]. They consider five different real wind farms in operation in United Kingdom and Denmark, and one new wind farm under construction. These parks are Horns Rev 1, Kentish Flats, Ormonde, Dan Tysk, Thanet and Horns Rev 3.

This dataset includes old and new parks, with different power ratings and different number of turbines installed, and therefore represents a good benchmark for our tests. Each park has one substation with its own maximum number of connections (C).

In details:

- Horns Rev 1 has 80 turbines Vestas 80-2 MW and $C = 10$.
- Kentish Flats has 30 turbines Vestas 90-3 MW. It is a near-shore wind farm, so it is connected to the onshore electrical grid without any offshore substation. Nevertheless, only one export cable is connected to the shore, therefore the starting point of the export cable is treated as a substation. We set $C = \infty$ as there is no physical substation limitation in this case.
- Ormonde has 30 Senvion 5 MW and $C = 4$.
- DanTysk has 80 Siemens 3.6 MW and $C = 10$.
- Thanet has 100 Vestas 90-3 MW and $C = 10$.
- Horns Rev 3 has 50 Vestas 164-8 MW and $C = 12$ (this is a preliminary layout for this park).

The dataset also includes different sets of cables, indicated as cb01, cb02, cb03, cb04 and cb05.

The cost of the cables considering power losses has been precomputed following the strategy described in Subsect. 2.2. We computed the cable-loss prices using real data (for Horns Rev 1 and 3, Ormonde and DanTysk) and estimates based on Weibull distributions (Kantish Flats and Thanet).

Each combination of site (i.e., wind farm) and feasible cable set represents an instance in the testbed.

5.2 Impact of Considering Power Losses

The aim of this subsection is to analyse how cable routing changes when cable losses are taken into account. We used the real-world instances presented in the previous subsection to perform our tests. We ran our optimization tool with a time-limit of 10 h (on an Intel Xeon CPU X5550 at 2.67 GHz, using Cplex 12.6 as MILP solver) in order to have high quality solutions (for small instances, these are in fact proven optimal solutions).

In all our instances, thicker cables are more expensive and have lower resistance. This means that if the designer of the cable routing aims only at minimizing the initial costs (CAPEX), then he/she would go for the cheapest cables satisfying the load, thus increasing the power losses. On the contrary, focusing only on minimizing the losses, one would go for the most expensive cables, thus increasing the initial costs. Using the methods explained in Sect. 2.2, we aim at finding the optimal balance between the two objectives, looking at the overall costs in the life time of the park.

As it can be seen from Table 4, the amount of savings varies from instance to instance, depending on the prices, on the restrictions of the specific wind farm, and on the structure of the layout.

It should be noticed that the layout optimized on the wind/farm lifetime always provides some savings in the long term, but the amount highly varies from case to case. In Fig. 5 the case of Horns Rev 3 with cable set cb04 is shown.[1] As expected, the usage of thicker cables (green in the figure) increases in the loss-optimized layout.

In this case the loss-optimized layout is 41 k€ more expensive at construction time (with respect to the CAPEX optimized layout). Nevertheless, in 25 years, this amount is paid back and 172 k€ are additionally saved.

We now try to investigate how the optimizer is restructuring the layout in order to achieve savings in the long run. As already noticed, every wind farm is different, so one cannot define a rule of thumb to design a good cable routing. Nevertheless, observing our layouts, we noticed a different proportion in the usage of the cable types (black and green in the figures). In particular, all the CAPEX solutions minimize the use of the expensive cables: looking only at the immediate costs, it is always preferable to go for the cheapest cable when possible, even creating longer connections. When optimizing considering losses, instead, cables with less resistance become more appealing, even if they are

[1] This is a preliminary layout from Vattenfall, not necessarily reflecting the final layout.

Table 4. Increase in the initial investment and long term savings for our test instances (Net Present Value). The first two columns denote the wind farm and possible cable types. The next column shows how much the investment is increased in the layout taking cable losses into account. In all test cases this amount is paid back in 25 years, and the additional savings by using the lifetime-optimized cable layout are shown in the last column [9].

Wind farm	Cable set	Increase in initial investment [k€]	Net savings in 25y [k€]
Horns Rev 1	cb01	1	23
	cb02	24	60
	cb05	103	56
Kentish Flats	cb01	2	3
	cb02	1	4
	cb04	19	8
	cb05	5	1
Ormonde	cb03	9	0
	cb04	19	16
DanTysk	cb01	115	21
Thanet	cb04	15	92
	cb05	1	19
Horns Rev 3	cb04	42	172
	cb05	682	208

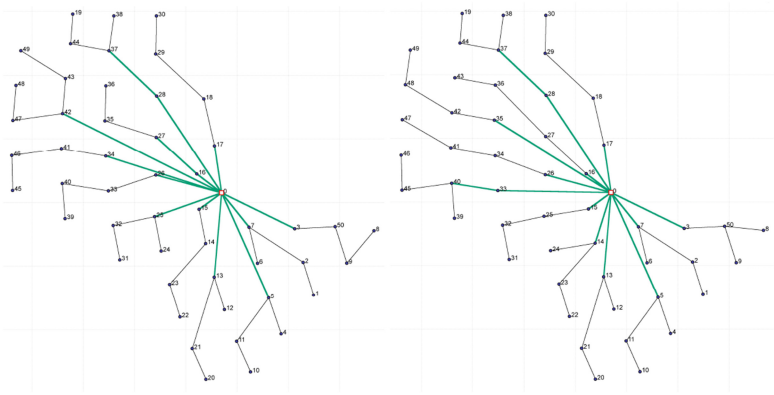

Fig. 5. Optimized cable routing for Horns Rev 3, using cable set cb04. The experts imposed the additional constraint that cable type 2 can support 5 turbines only twice. The top layout is optimized only on CAPEX, the second considers power losses as well [9]. (Color figure online)

more expensive. In the Horns Rev 1 instance, for example, going from CAPEX optimized to lifetime-optimized the usage of type 1 cables decreases (from 55.5% of the total length to 40.3%) and the usage of type 2 cables increases (from 44.5 to 59.7%).

In Table 5 we report the cable usage (percentage of the total cable length) for all our test-bed solutions.

Table 5. Analysis on the usage of different types of cables when optimizing considering or not losses. The last three columns report the usage of the different cable types as percentage of the total cable length of that layout [9].

ID	Wind farm	Cable set	Opt mode	% length		
				Type 1	Type 2	Type 3
1	Horns Rev 1	cb01	CAPEX	55.1	40.1	4.8
2			Lifetime	53.6	41.7	4.7
3		cb02	CAPEX	57.4	42.6	
4			Lifetime	44.1	55.9	
5		cb05	CAPEX	100.0	0.0	
6			Lifetime	87.7	12.3	
7	Kentish Flats	cb01	CAPEX	66.4	33.6	0.0
8			Lifetime	66.1	33.9	0.0
9		cb02	CAPEX	66.4	33.6	
10			Lifetime	60.8	39.2	
12		cb04	CAPEX	90.1	9.9	
13			Lifetime	90.1	9.9	
14		cb05	CAPEX	95.6	4.4	
15			Lifetime	95.6	4.4	
16	Ormonde	cb03	CAPEX	69.6	30.4	
17			Lifetime	76.7	23.3	
18		cb04	CAPEX	66.9	33.1	
19			Lifetime	67.4	32.6	
20	DanTysk	cb01	CAPEX	39.0	19.4	41.7
21			Lifetime	38.7	22.5	38.8
26	Thanet	cb04	CAPEX	86.3	13.7	
27			Lifetime	82.7	17.3	
28		cb05	CAPEX	71.9	28.1	
29			Lifetime	71.9	28.1	
30	Horns Rev 3	cb04	CAPEX	57.4	42.6	
31			Lifetime	60.7	39.3	
32		cb05	CAPEX	51.8	48.2	
33			Lifetime	52.6	47.4	

All in all, it can be observed from our results on real-world instances that in most cases it is convenient to invest in cables with lower resistance. The cable route and the type of cable selection for each connection is not an obvious choice and an optimization tool is necessary to determine it.

6 Analysis on the Energy Price *k*

In this section we will focus on the value K appearing in Eq. (17). As we have seen, K is the a factor to estimate the value (in €) of a MW of loss, and is computed as $K = k_{euro} \cdot 8760$ where k_{euro} is the NPV for a MW/h production over the park lifetime, and 8760 is the number of hours in a year. Note that K acts as a balancing factor between the immediate costs (CAPEX) and the power losses. In this section we will investigate the impact of this balancing factor on the final layout. In Subsect. 6.1, we will perform a multi-criteria analysis where we consider different values of k_{euro}, supposing that the company requests that the extra investment must be paid off in a limited number of years. Secondly, in Subsect. 6.2, we will evaluate the impact of considering fluctuating prices depending on the wind scenario.

6.1 Sensitivity Tests on the Return of Investment

As discussed in Subsect. 2.2, one has to balance between two opposite objectives: minimizing immediate costs and minimizing revenue losses in the long run. As we have seen in the previous tests, these two objectives are not always aligned since the more expensive cables have lower resistances (so less losses). The balancing factor between the two objectives is k_{euro}, that represents the price of energy (Net Present Value). Setting k_{euro} to zero, for example, means that there is no revenue from selling energy, therefore it does not matter to have losses, but it is instead important only to minimize immediate costs. This corresponds to the case that we called "CAPEX optimized" in the previous tests. On the contrary, setting k_{euro} to a high value, implies that big revenue can be earned selling more energy, so it is very important to minimize losses (whatever initial costs this could imply). The balance between the two objectives, in practice, is set by defining the parameter k_{euro} for the specific project of interest. This is a value known by the designer, and varies from project to project. A realistic value for k_{euro} has been used in the tests of the previous subsection (this value considers weighted average cost of capital (WACC), subsidies for 10 years of operations and estimated market price). Nevertheless, one could be interested in studying how the balance between immediate costs and long term costs varies when varying k_{euro}. As a practical example, one could be interested in optimizing CAPEX and losses at the same time, but being sure to pay off the extra investment in a short time. We considered, in this test, Horns Rev 3 with cable set cb04. For $k_{euro} = 0$ we have our CAPEX solution of Fig. 5 (top), for $k_{euro} = 690$ €/MWh we have our life-time loss-optimized solution of Fig. 5 (bottom). Company experts estimated 690 €/MWh to be a realistic value for the energy earning

Table 6. Bi-objective analysis for Horns Rev 3 with cable set cb04: solutions change when varying parameter k_{euro} [9].

k_{euro}	Immediate cost [k€]	Total lifetime cost [k€]	Revenue loss due to power losses [k€]
0	47283	52663	5379
176	47291	52551	5259
252	47309	52508	5199
321	47325	52490	5165
386	47325	52490	5165
690	47325	52490	5165

over 25 years of operation (expected lifetime of a wind park). We asked them to recompute this value assuming that we want a return of investment in a shorter time. They recomputed it to be $k_{euro} = 176$ for two years, $k_{euro} = 252$ for 3 years, $k_{euro} = 321$ for 4 years, and $k_{euro} = 386$ for 5 years. Setting our balancing factor k_{euro} to these values translates in imposing that extra CAPEX cost will be paid back in 2, 3, 4 or 5 years, respectively. We recomputed the cable costs according to these different values of k_{euro} and re-optimized the layout accordingly. Once the optimized layouts were found, we re-evaluated them with $k_{euro} = 0$ to evaluate their CAPEX costs and $k_{euro} = 690$ to estimate their cost in 25 years. Table 6 shows these figures. For k_{euro} higher than 321 €/MWh the layout is not changing. This means that in the lifetime optimized solution ($k_{euro} = 690$) all the additional CAPEX costs were actually paid back in 4 years of operation. In Fig. 6 we plot the values from Table 6: the value of the different layouts is decomposed into its CAPEX (x axis) and lifetime-cost part (y axis). The first point (marked by "+" on the leftmost extreme) represents the value for the CAPEX optimized solution ($k_{euro} = 0$): it has the lowest immediate cost, but the highest cost on the long run. Proceeding from left to right, the next "+"s represent the solutions optimized over 2, 3, 4 and 5 years respectively. As already mentioned, from the 4th year on, the layout is not changing any more, and is equal to the solution optimized on the park lifetime ($k_{euro} = 690$), therefore all these layouts are represented at the same coordinates in the plot in Fig. 6.

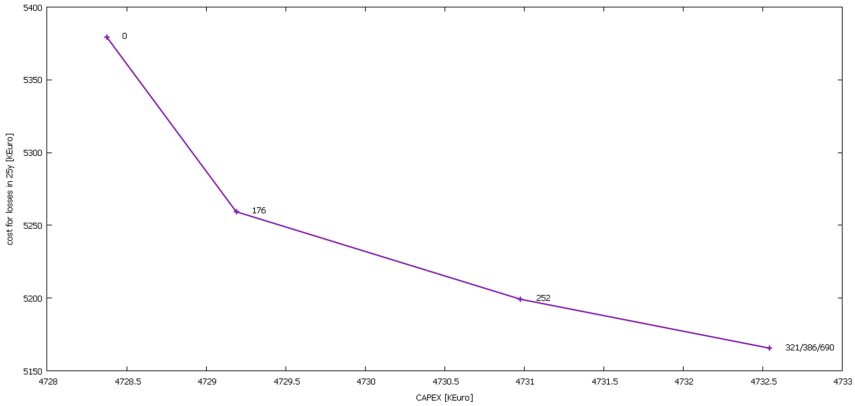

Fig. 6. Bi-objective analysis from Table 6. Each "+" corresponds to a layout optimized for a given value of k_{euro} (specified beside each "+") and its coordinates correspond to its immediate cost (x axis) and costs in 25 years (y axis). The layouts optimized with $k_{euro} = 321$, 386, and 690 are the same [9].

6.2 Considerations on Price Fluctuations

In all our analyses we assumed to have a unique price for energy, independently of the wind scenario. This is in general true, since, at least in Denmark, parks operate with a protected price for about 10 years. Nevertheless, in other countries, this could not be the case, and the price of energy would depend on the market.

In this subsection we suppose not to have a warranted price for wind energy, but to sell energy at the market price. Of course this analysis requires a sufficient amount of data on the spot market price variations. We recorded the Nord Pool prices over the first semester of 2015, sampling the market price every hour together with the wind speed in the park at that time. Figure 7 plots these samples against the wind speed in Horns Rev 1.

It can easily be observed from Fig. 7 that there is a correlation between energy prices and wind: when there is low wind (under 5 m/s) the price tends to be higher, while when the wind is high (over 12–15 m/s) the price drops. This is because of a surplus of MWh production at high wind speeds.

Looking at this analysis, one could then re-consider the power losses figures we have used so far, and investigate the impact of price fluctuations on the cable routing. In order to do so, we had to reformulate the loss cost-related part of the objective function, considering that now the value k_{euro} depends itself on the wind scenario s, and therefore will be indicated as k^s_{euro} in the following. The value $loss^{tf}$ to precompute is now

$$loss^{tf} = 3R^t \sum_{s \in S} \pi_s (fI^s)^2 k^s_{euro}. \tag{20}$$

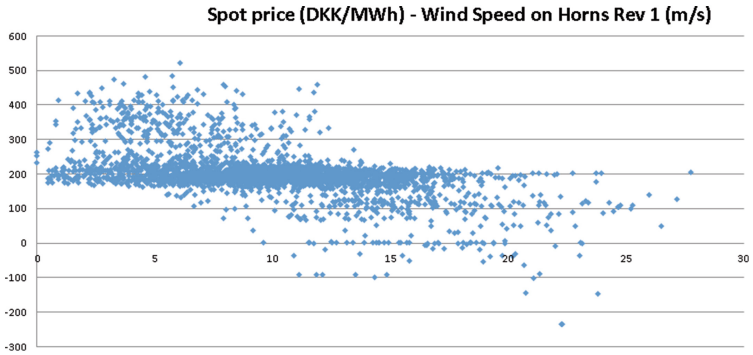

Fig. 7. Spot price (DKK/MWh) on the y-axis vs wind speed (m/s) on the x-axis for HR1. Each dot represents a real-world sample recorded in 2015.

We consider again the Horns Rev 1 case in our test, with the same cable set as in Sect. 4. In order to estimate the impact of considering a k^s_{euro} that varies with scenarios s, we compared with the case of a fixed k_{euro}, equal to the average spot price. In both cases we considered a WACC of 8%. Figure 8 shows the two options: in yellow, the value of k_{euro} that varies over the different wind speeds (x-axis); in red, the value of k_{euro} that is fixed at the average market price (0.22 €/KWh). The value of k_{euro} in the varying case (yellow line) has been computed by a simple interpolation of the registered spot prices (Fig. 7), by computing their average at each wind speed. Note that, in formula (20), the different scenarios s are weighted by their probability π_s: the blue line in Fig. 8 represents the probabilities used in our test case (extracted from samples of real-data from Horns Rev).

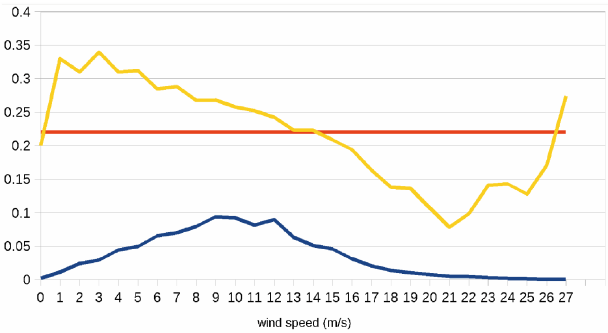

Fig. 8. k_{euro} variations over different wind speeds in the two possible approaches: considering one fixed value equal to the average market price (red line), or explicitly considering the price variations (yellow line). The blue line shows the frequency of the different wind scenarios in the site. (Color figure online)

We computed the cable prices for the two strategies, using the precomputing strategy of Subsect. 2.3 with formula (17) for fixed price, or with formula (20) for fluctuating price. Table 7 shows the result of the precomputation: the first two columns give the details of the cable set (type of cables, and capacities in terms of number of turbines), the third column reports CAPEX prices, the fourth column the prices computed considering losses with a fixed k_{euro}; and the fifth column considering a price of energy that varies over different wind scenarios.

Table 7. Costs for the cables. In the first two columns we indicate the type of cable and its capacity, expressed as number of 2 MW turbines supported. The third column reports the CAPEX costs of the cables, including installation costs. The last columns show the cable prices taking power losses into account: in the fourth column assuming a fixed price of energy (i.e., the average market price), in the fifth column considering a different price of energy for each scenario.

Type	No. of turb.	CAPEX	Avg.	Fluctuating
1	1	345	345.56	345.56
2	2	385	385.85	385.85
	3	385	386.65	386.64
	4	385	387.77	387.76
	5	385	389.21	389.19
	6	385	390.97	390.95
	7	385	393.04	393.02
	8	385	395.44	395.41
3	9	500	509.12	509.09
	10	500	511.21	511.17
	11	500	513.52	513.47
	12	500	516.05	515.99
	13	500	518.80	518.74
	14	500	521.77	521.69
	15	500	524.96	524.87
	16	500	528.37	528.27

As already discussed, until the max capacity of the cable is reached, the CAPEX cost (third column) does not depend on the number of turbines connected – while the costs including losses (fourth-fifth column) do. Comparing the last two columns, it can be noticed that the input cable prices are not very sensitive to the variation of k_{euro}. This is also explained by the fact that the extreme wind speeds, where k_{euro} varies the most, are also the less frequent ones. At the most frequent wind speeds (between 5 and 15 m/s) k_{euro} is closer to its average value (see Fig. 8). If we run the optimization tool on the HR1 case using the losses prices, we obtain the two layouts in Fig. 9. As in our previous

layout plots, different colours indicate different cable types. Referring to Table 7, black lines represent cable type 1, green cable type 2, and blue cable type 3.

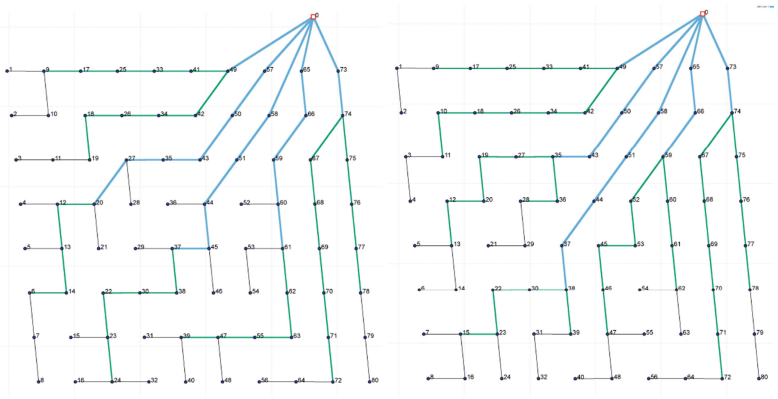

Fig. 9. Layout considering no protected price of energy: the first plot shows the optimized layout considering a fixed price of energy, equal to the average market price. The second plot shows the optimized layout considering price variations over the different wind scenarios. (Color figure online)

Assume that the company decides to use the layout optimized for the average price (first plot in Fig. 9). If we re-evaluate this layout considering fluctuating prices, we can conclude that the company would loose 1400 € (0.006%) in the park lifetime, with respect with the fluctuating-price layout (second plot in Fig. 9). This shows that the impact of considering fluctuating prices is, in this example, very small.

All in all, our results suggests that price fluctuations do not significantly impact the layout. Even if it is less profitable to avoid losses when the price of energy drops, this event is so rare in reality that it does not pay off to consider it in the cable routing optimization.

7 Conclusions

In this paper we used Mixed Integer Linear Programming (MILP) and Matheuristic approaches to optimize inter-array offshore cable routing. The main focus of the paper is to quantify the impact of considering both the immediate cable costs and power losses already at design phase. First, we illustrated how to mathematically model the problem and how to deal with large scale instances using a matheuristic approach. Next, we performed different analyses on real-world instances. To begin with, we compared the optimized solution with an existing cable layout, proving that more than one million Euro can be saved by using adequate optimization tools for the offshore cable routing problem.

Afterwords, we compared optimized solutions under different assumptions to understand and (for the first time) quantify the impact of considering cable losses in real offshore cable routings.

In general, we observed that it is convenient to use cables with less resistance in order to reduce power losses, even if these cables are more expensive at construction time. We used our testbed to evaluate the profitability of the new solutions, both in terms of CAPEX and revenue in the long term. Results show that it is very difficult to define some "rules-of-thumb" for this problem, since usage of cables and savings highly vary from instance to instance. This proves that a proper optimization tool, as the one presented here, is necessary for an optimal design of each layout. Finally, we performed different analyses on the balancing parameter k_{euro}. This corresponds to giving more or less importance to power losses in the objective function, and it is of great importance for designers. In this way, indeed, they can evaluate the return of investment and the impact of their assumptions on the long-term energy price, when designing their cable routing. In particular, we looked at two specific reasons for which the company could consider different energy prices: requirements on the return of investments and fluctuations of the energy price on the market. In the latter case, we extended the original model to consider the dependency of the energy price over the different wind scenarios, using real-world measurements. Our tests showed that it is important to define a value of k_{euro} that well reflects the requirements of the specific project, whereas the layout is not very sensible to small variations of this parameter.

Acknowledgements. This work was supported by Innovation Fund Denmark. The authors would like to thank Jesper Runge Kristoffersen, Kenneth Skaug, Thomas Hjort, Iulian Vranceanu and Mads Rajczyk Skjelmose from Vattenfall BA Wind who helped in defining the cable routing constraints, the cable losses and the price fluctuation analysis.

References

1. Bauer, J., Lysgaard, J.: The offshore wind farm array cable layout problem: a planar open vehicle routing problem. J. Oper. Res. Soc. **66**(3), 360–368 (2015)
2. Berzan, C., Veeramachaneni, K., McDermott, J., Reilly, U.M.O.: Algorithms for cable network design on large-scale wind farms. Technical report. Tufts University (2011)
3. Boschetti, M.A., Maniezzo, V., Roffilli, M., Bolufé Röhler, A.: Matheuristics: optimization, simulation and control. In: Blesa, M.J., Blum, C., Di Gaspero, L., Roli, A., Sampels, M., Schaerf, A. (eds.) HM 2009. LNCS, vol. 5818, pp. 171–177. Springer, Heidelberg (2009). https://doi.org/10.1007/978-3-642-04918-7_13
4. Cerveira, A., De Sousa, A., Pires, E.J.S., Baptista, J.: Optimal cable design of wind farms: the infrastructure and losses cost minimization case. IEEE Trans. Power Syst. **31**(6), 4319–4329 (2016)
5. Dutta, S.: Data mining and graph theory focused solutions to smart grid challenges. Master's thesis, University of Illinois (2012)

6. Dutta, S., Overbye, T.J.: A clustering based wind farm collector system cable layout design. In: Power and Energy Conference at Illinois (PECI), pp. 1–6 (2011)
7. Fagerfjall, P.: Optimizing wind farm layout - more bang for the buck using mixed integer linear programming. Master's thesis, Department of Mathematical Sciences, Chalmers University of Technology and Gothenburg University, Goteborg, Sweden (2010)
8. Fischetti, M., Pisinger, D.: Optimizing wind farm cable routing considering power losses. Eur. J. Oper. Res. **270**(3), 917–930 (2018). https://doi.org/10.1016/j.ejor.2017.07.061. ISSN 0377-2217
9. Fischetti, M., Pisinger, D.: On the impact of using mixed integer programming techniques on real-world offshore wind parks. In: Proceedings of the 6th International Conference on Operations Research and Enterprise Systems (2017)
10. Fischetti, M., Fischetti, M.: Matheuristics, pp. 1–33. Springer, New York (2016). https://doi.org/10.1007/978-3-319-07153-4/14-1. ISBN 978-3-319-07153-4
11. González, J.S., Payán, M.B., Santos, J.M.R., González-Longatt, F.: A review and recent developments in the optimal wind-turbine micro-siting problem. Renew. Sustain. Energ. Rev. **30**, 133–144 (2014)
12. González-Longatt, F.M., Wall, P.: Optimal electric network design for a large offshore wind farm based on a modified genetic algorithm approach. IEEE Syst. J. **6**(1), 164–172 (2012)
13. Hansen, P., Maniezzo, V., Voß, S.: Special issue on mathematical contributions to metaheuristics editorial. J. Heuristics **15**(3), 197–199 (2009)
14. Hertz, A., Marcotte, O., Mdimagh, A., Carreau, M., Welt, F.: Optimizing the design of a wind farm collection network. INFOR **50**(2), 95–104 (2012)
15. Kristoffersen, J.R., Christiansen, P.: Horns rev offshore windfarm: its main controller and remote control system. Wind Eng. **27**(5), 351–359 (2003)
16. Li, D.D., He, C., Fu, Y.: Optimization of internal electric connection system of large offshore wind farm with hybrid genetic and immune algorithm. In: Third International Conference on Electric Utility Deregulation and Restructuring and Power Technologies (DRPT 2008), pp. 2476–2481 (2008)
17. Pillai, A.C., Chick, J., Johanning, L., Khorasanchiand, M., De Laleu, V.: Offshore wind farm electrical cable layout optimization. Eng. Opt. **47**(12), 1689–1708 (2015)
18. Zhao, M., Chen, Z., Blaabjerg, F.: Optimisation of electrical system for offshore wind farms via genetic algorithm. IET Renew. Power Gener. **3**(2), 205–216 (2009)

A Novel Storage Space Allocation Policy for Import Containers

Myriam Gaete[1], Marcela C. González-Araya[2(✉)], Rosa G. González-Ramírez[3], and César Astudillo[4]

[1] Programa de Magíster en Gestión de Operaciones, Facultad de Ingeniería, Universidad de Talca, Camino a Los Niches km 1, Curicó, Chile
mgaete@alumnos.utalca.cl
[2] Department of Industrial Engineering, Faculty of Engineering, Universidad de Talca, Camino a Los Niches km 1, Curicó, Chile
mgonzalez@utalca.cl
[3] Facultad de Ingeniería y Ciencias Aplicadas, Universidad de Los Andes, Mons. Álvaro del Portillo 12.455, Las Condes, Santiago, Chile
rgonzalez@uandes.cl
[4] Departamento de Ciencias de la Computación, Facultad de Ingeniería, Universidad de Talca, Camino a Los Niches km 1, Curicó, Chile
castudillo@utalca.cl

Abstract. In developing countries, such as those in Latin America, inland flows of container terminals present high levels of uncertainty and variability. This situation occurs mainly due to lack of automation procedures, affecting coordination with the hinterlands. In this article, a methodology based on a dwell time segregated container storage policy is proposed. This methodology considers only import containers, due to the difficulty to determine a segregation criterion, which motivated us to use container dwell time information. Dwell times are discretized to determine classes, so that containers of the same class are assigned to close locations at the yard. The architecture of a decision support system to aid the stacking decisions based on this storage policy is proposed. The port of Arica in Chile is considered as a case study, and a discrete-event simulation model is also proposed to estimate potential benefits of this approach. Numerical results for the case study show a good performance, with potential reduction of the rehandles incurred when containers are retrieved from the yard.

Keywords: Container storage policies · Dwell times of containers
Segregation of containers · Classification algorithms

1 Introduction

World container port throughput increased by an estimated 5.1% to 651.1 million TEUs in 2013 and global containerized trade was projected to grow by 5.6% in 2014 [42]. Maritime ports are strategic nodes on the international logistic chain whose current role goes beyond the traditional functions of transferring cargo to a more active participation and promotion of value-added services to the port stakeholders. Ports can be conceptualized from a logistics and supply chain management approach and under

G. H. Parlier et al. (Eds.): ICORES 2017, CCIS 884, pp. 293–316, 2018.
https://doi.org/10.1007/978-3-319-94767-9_15

this vision the traditional port system is extended to an "integrated channel management system" where the port is a key location linking different flows and channels with the port community [6]. In this con-text, efficient cargo handling operations are essential, as new value-added services, as well as better service levels, agility and predictability are demanded by the users of the port. The productivity of a container terminal is related to an efficient use of labor, equipment and land, and is commonly measured as a function of the ship turnaround time, the transfer rate of containers and the dwell times of the cargo at the port [8, 19, 20].

At the port, the yard can serve as a buffer between the arrival and departure of temporarily stored cargo which is later loaded on a ship or dispatched to external carriers. The efficiency of the operations at the yard significantly impact ship turnaround times so adequate container storage space assignment policies and yard equipment planning are needed. In addition, minimizing port dwell times is one of the main objectives from the perspective of the shippers in the port supply chain [29].

Coordination of landside operations at a container terminal is not straightforward in ports in developing countries where there are important challenges in terms of infrastructure development, technology implementation and paper-based documental procedures. Latin American and Caribbean (LAC) ports have seen an important increase in their participation in world foreign trade. This growth has put pressure on the freight distribution systems that need to develop better logistics capabilities [37].

In the article of [23], the problem of defining a container storage space allocation policy for import containers is addressed by considering the case of a container terminal that faces a high level of uncertainty in the dispatching process of import containers. This uncertainty is mainly explained by the lack of coordination mechanisms with the hinterland, a situation that can be very common at ports in emerging countries. In the present chapter, we describe in more detail than [23] the classification algorithms and the evaluation metrics used to select one of them. Also, we include the statistical description of the used database, from which seven factors were considered, including a brief description of them. In addition, we present a comparative analysis of the classification algorithm based on a Pareto-analysis in order to improve the dwell time estimations. Finally, we extend the conclusions derived from the simulation results, and present some recommendations for the Port of Arica that may enhance better container dwell time estimations. For instance, additional information of the type and content of cargo, whether the container is FCL (Full container loaded) or LCL (Less than container loaded), etc.

The assignment of space at the yard for export containers is not considered in this article. The reason is that yard planners of container terminals have general criteria to group export containers into segregations (e.g., vessel, port of destination, weight, etc.), while for import containers is more difficult to determine, as the time in which the containers are retrieved depends on the different consignees of the cargo (importers) and the fulfillment of all the procedures, resulting in more uncertainty, compared to export containers that all will be loaded to a single vessel at the container terminal.

During the dispatching of an import container, it is possible that other containers may be blocking the container and should be removed to be able to reach the required container. These non-value added movements are refereed as "rehandle" or "reshuffle" of containers. Rehandles represent a high cost with no value for the container terminal,

and increase the truck turnaround times of the external trucks at the container terminal, generating congestion and affecting service levels of to the users of the container terminal.

To assign a storage space for the import containers in the yard, a dwell time segregated storage policy is proposed. In this case, segregations of import containers are defined based on dwell time intervals, and containers of the same segregation are assigned to close locations. The aim is to reduce potential container rehandles at the retrieval of containers from their locations at the yard. Hence, containers with the same interval of dwell time located at close positions in the yard, may incur in less number of rehandles. To estimate dwell times of import containers, classification algorithms are employed. This is justified as the results of the estimations are used to define import container groups based on dwell time ranges, so the precise values of the predicted dwell times are not needed. In addition, the design of a decision support system for the assignment of storage space to import containers is proposed with the aim to assist the yard planner with a tool that may be interconnected with the Terminal Operator System (TOS) of the container terminal.

As a case study, the container terminal at the port of Arica in Chile is considered. High levels of uncertainty for import container dispatching as well as long dwell times are observed in the container terminal due to the type of cargo handled; around 70% of the cargo is in-transit from Bolivia. The political agreement between Chile and Bolivia establishes special conditions for the in-transit cargo where no storage fee is charged. The current practice of the yard managers is to assign space to containers in a semi-random fashion where containers are located at the yard considering only the space utilization rules that have been set to avoid unutilized space.

To validate the methodology proposed in a stochastic environment, a discrete-event simulation model was implemented, to determine the potential impacts in terms of rehandles of containers when are retrieved to be dispatched to external transport carriers.

The article is structured as follows: Sect. 2 presents a literature review. Section 3 describes the methodology employed and the proposed dwell time segregated storage policy. Section 4 presents the architecture and components of the decision support system for the storage space assignment of import containers. Section 5 presents the case study as well as the simulation model to estimate the benefits of using the proposed support system to assign storage space to import containers. Conclusions and recommendations for further research are provided in Sect. 6.

2 Literature Review

In this section, we present a literature review and provide some context of the problem addressed in this manuscript. Section 2.1 presents a review of the main contributions in the literature related to dwell time estimation studies, while Sect. 2.2 presents a review on the determinant factors of dwell time.

2.1 Dwell Time Estimation's Contributions in the Literature

Port terminal capacity is defined as the amount of cargo that can be handled by a port per time period [4]. The first contributions related to capacity analysis at the yard of a Container Terminal are presented by [13, 15, 26], where storage capacity at the yard is estimated as a function of container dwell times, the number of stacking containers, and the container storage space available expressed in TEUs (twenty-foot equivalent units), among other factors.

Determining the factors that influence port choice and port competitiveness is another research avenue where cargo dwell times are identified as an explicative variable [14, 33, 40, 44]. [1] identify dwell time as a factor that directly affects operational costs in the ports as it increases inventory levels and uncertainty in the dispatching process. On the other hand, dwell times have also been identified as an element of port competiveness and a factor in port choice related decisions [30].

From a macro-economic perspective, the impact of port delays at Puerto Limón in Costa Rica, over the regional economy in Central America is estimated in [43]. They conclude that reducing port inefficiencies, such as long dwell times of cargo at the ports, may improve the GDP (Gross Domestic Product) of Costa Rica by about 0.5%. [17] employed a gravity model to estimate the impact that each additional day required for dispatching cargo may have on the GDP. The unproductive movements undertaken during quay transfer operations are quantified by [7]. They identify storage density as a factor of unproductive movements during ship loading and unloading operations. This refers to the number of containers stacked in the yard and the ground slots used for storage. Furthermore, their results show that housekeeping moves represent most of the unproductive moves undertaken.

[31] estimates dwell time impact on the capacity of a terminal based on a sensitivity analysis, where he computes the yard storage capacity by employing the model proposed by [11], considering five scenarios with different dwell times and container types. The interaction among the terminal operators and the users of the port (e.g. importers/exporters, freight forwarders) is analyzed by [38] and they conclude that the relationship and collaboration levels could impact container dwell times at the port.

An analysis of dwell times at ports in Sub-Saharan Africa is presented by [36]. Main findings highlight that dwell times are abnormally long, more than 2 weeks, and show an abnormal dispersion which increases the inefficiencies of port operations and, in consequence, total logistic costs. [5] provide an analysis of the causes of these long dwell times from the shipper perspective, discovering the crucial importance of private sector practices and incentives.

[32] analyze the factors that determine container dwell times in a port, employing three data mining algorithms: (i) Naive Bayes Algorithm [28], (ii) Decision Tree C4.5 [34] and (iii) The Hybrid Bayesian decision tree [27]. Estimation results are compared in terms of four indicators: accuracy, the Kappa coefficient, RSME and execution times. In order to evaluate the results they provide a simulation under different scenarios with the results obtained. An important difference with respect to the work presented herein, is that the authors do not use the results to estimate container storage assignment policies. In addition, the data mining algorithms also differ from those proposed in this article.

Another contribution of the work is presented in [23], is the discretization of a continuous variable (dwell time) for its prediction, justified by the fact that the results are employed as criteria to segregate import containers and assign storage space according to this policy. In contrast, [32] do not employ classification algorithms in their approach, which is reasonable as their aim is not to determine storage space policies which is an important difference with respect to the work presented here.

Another contribution of [23] is the simulation proposed model that aims to measure the impact of different storage policies in terms of the number of rehandles incurred when containers are dispatched to external carriers. It is important to point out that in the literature there is no approach proposed in which the input data of a simulation model consists of the results obtained by the classification algorithms for dwell time estimation. In this work, we extend the research of [23], describing in more details the classification algorithms and the evaluation metrics used for selecting a more accurate method.

2.2 Determinant Factors of Dwell Time

The main factors considered in the literature as dwell time determinants are presented in Table 1. The factors are divided into two groups: unique value and nominal value. Factors with a unique value are those that may have a unique value at each port and this

Table 1. Main determinant factors of dwell time (Source: [23]).

Factor	References	Type
Frequency of the sailing schedules of the vessels	[31, 32]	Unique value
Type of container (e.g., empty/full, dry/reefer, etc.), size (20/40 TEUs) and its contents	[31, 32]	Nominal
Modal split of hinterland connections	[31, 32]	Unique value
Port Governance and structure	[31, 32]	Unique value
Location of the Port Terminal and the main products (or logistic chains) that are transferred	[31, 32]	Unique value
Terminal working hours and business days	[31, 32, 38]	Unique value
Shippers and consignee	[32, 38]	Nominal
Inspections and regulatory procedures	[32]	Unique value
Transport corridors	[32]	Nominal
Ocean carriers or Maritime Shipping Company and the demurrage time for the empty containers	[32]	Nominal
Container flow balance (export and import)	[32]	Nominal
Freight Forwarder/Broker and Third Party Logistics Company (3PL)	[32]	Nominal

value does not vary as a function of the cargo transferred at the port (i.e., the frequency on the itineraries, the location of the port terminal, etc.). This type of factor is not considered as the results for predicting dwell time are employed for container space allocation policies and this is influenced by the amount of cargo handled. On the other hand, nominal and numerical factors correspond to factors that vary as a function of the cargo handled, where nominal factors are represented by strings and numerical factors by a number. For instance, a nominal factor is related to the name of the importer or exporter, while the weight of a container is a numerical factor.

3 Methodology Description

The dwell time segregated storage space policy is based on generating segregations of import containers based on dwell time intervals. In this way, containers of the same segregation are those whose dwell time is predicted to be at the same interval. In order to determine the dwell time classes and estimate the potential impact of the proposed storage space policy, the proposed methodology is described in the following Table.

Table 2. General methodology (Source: [23]).

Factor
Input: Data Base of historical information- arrival and departure time of import containers
1. **STAGE 1:** Dwell time prediction by classification algorithms
1.1. Class definition as a function of time intervals to discretize the dwell time numerical variable.
1.2. Application and validation of the classification algorithms based on a predictive model.
1.3. Identification of the interrelation among the dwell time measure units based on a multi-classifier generation.
1.4. Performance evaluation of the classification algorithms.
2. **STAGE 2:** Dwell time segregated storage policy implementation and evaluation
2.1. Segregate containers based on the dwell time classes obtained in Stage 1.
2.2. Run the simulation model for a set of instances, testing the performance in terms of the number of rehandles when containers are retrieved. Compare results with alternative storage policies that may resemble the current practice of the Container Terminal under study.
Output: Policy and impact estimation if dwell-time segregated policy is implemented.

3.1 STAGE 1: Dwell Time Prediction by Classification Algorithms

As observed in Table 2, the first stage consists of applying classification algorithms to predict dwell times. For this, it is necessary to have a database with historical data about the containers' arrival and departure times at the yard. Step 1.1 is related to the class interval definition. We consider that the classes may be measured in three time units: hour, day and week. Table 3 summarizes the classification algorithms evaluated. These algorithms allow to analyze classes with nominal values. Table 4 presents a more detailed description of Step 1.2 of the general methodology.

Depending on the stages of the classification processes, there are diverse types of algorithms. The most commonly used are Naïve Bayes, Lazy Learning and Rules Induction Learning [24]. As indicated in Table 3, the classifiers Naive Bayes are based on the Bayes probability function, while the classifiers Lazy Learning are algorithms that do not require to create a predictive model. On the other hand, the Rules Induction Learning algorithms are classifiers that create a predictive model based on the rules applied to the training set [24]. It is important to highlight that in addition to classification algorithms, in this research we also employ multi-classifiers [41] with the aim to analyze the improvements achieved in the classification results.

For the sample size definition, the formula to be used is provided by [11], in which the size of the population is assumed to be an input data. For the classification model, different classification algorithms can be evaluated according to the specific characteristics of the Container Terminal under study. In addition, Step 1.3 consists of the definition of the multi-classifier to determine the inter-relations among different dwell time measure units. Step 1.4 consists of an evaluation of the results obtained by the different classification algorithms. Four performance metrics are considered: (i) the number of instances classified correctly, (ii) the Kappa coefficient, (iii) the computational time and (iv), the mean squared error in time units [47].

3.2 STAGE 2: Dwell Time Segregated Storage Policy Implementation and Evaluation

A common practice of terminal operators is to assign space to containers at the yard based on segregations. To determine segregations of import containers based on dwell time intervals, the predicted dwell times and intervals found in stage 1 (see Fig. 1) are employed for an instance of the container terminal under study. Then, a real time stacking heuristic for locating the import containers in each dwell time segregation is defined, so that containers of the same segregation may be assigned to close locations with the aim of reducing rehandles when containers are retrieved.

To evaluate the benefits of implementing the policy at the yard, a discrete event simulation model is also proposed, in which the dwell-time storage space policy is implemented to define the location of the import containers at the yard. The dispatching process of the import containers to external carriers is also simulated in order to count the number of rehandles incurred. More details will be provided at Sect. 5 with the case study.

With the aim to define an error index of the predictions obtained with the classification algorithms, several validation methods can be employed. As an example, we

Table 3. Classification algorithms evaluated (based on [23]).

Algorithms	Description	References
K *nearest neighbors* (KNN)	This algorithm is based on a distance measurement. The class of each instance is assigned according to the biggest class of the K nearest neighbors	[12]
Naive Bayes (NB)	This is a family of simple probabilistic classifiers, based on the Bayes conditional probability. To apply this algorithm, it is necessary to guarantee the independence of the attributes	[28]
One Rule (OneR)	The OneR algorithm is a simple classification algorithm that creates a rule for each predictor or attribute in the training data and chose the rule with the smallest total error. In order to create a rule for each attribute, it is necessary to construct a frequency table for each predictor against the target	[25]
Incremental Reduced Error Pruning (IREP) or *Repeated Incremental Pruning to Produce Error Reduction* (RIPPER or JRip)	It is a classifier algorithm based on the construction of decision rules in a greedy fashion (one rule at a time). It integrates pre-prunning and post-prunning into the learning process. The basic idea is each clause is pruned right after it has been generated. In this case, after learning a clause from the growing set, literals are deleted from this clause in a greedy fashion until any further deletion would decrease the accuracy of this clause on the pruning set	[22]
K*	The K* has a similar procedure as the KNN algorithm, but instead distance, it considers the entropy as a measure	[10]
Decision Table (DT)	The DT algorithm is an exact method for the numerical prediction of decision trees. It generates an ordered set of rules If-Then, that have the potential of being more compact and easy to understand than decision trees	[27]
Zero Rule (ZeroR)	This is the simplest classification method. It relies on the target and ignores all predictors. If all the classes are nominals, it predicts the class with more frequency. If classes are numerical, it uses the average value of the class	[47]

Table 4. Classification algorithms based on a predictive model (Source: [23]).

Step 1.2 Classification algorithm application and validation
INPUT: Data base with historical data on the arrival and departure times of import containers 1. Sample size definition 2. Random sample of instances 3. Definition of the classification model 4. Evaluation of the classification model 5. Estimation of the prediction error
Output: Dwell time predictions.

can mention the simple validation, cross-validation, bootstrap and confusion matrixes [41]. These methods are further described.

- Simple validation. It consists on employing a portion of date as the training set, with the aim to construct the model, while the rest of the data is used as the experimentation set.
- Cross validation. It consists on dividing the data into k subsets that are mutually exclusive of approximately the same size [16]. For this validation, training is performed k times, considering as the training set a different subset each time.
- Bootstrap. It involves taking random samples from the data set with re-selection against which to evaluate the model. In this case, a random training set of L instances is created (including re-selection).
- Confusion matrix. The matrix is constructed with a table $M \times M$ where M corresponds to the number of values that takes the class. Each column of the matrix represents the number of predictions of each class, while each row represents the number of instances of the class. This method is used in most of the metrics proposed in the literature to evaluate the performance of a classification algorithm [9, 45, 46].

Table 5 summarizes the main performance metrics used in the literature to evaluate the classification algorithms.

Both the mean squared error as well as the average error for numerical categorical factors correspond to metrics that are commonly employed to measure the performance of regression algorithms. We use these metrics as the class is numerical in our research. Although the values of the dwell time are discretized, these can be transformed to numerical values to measure the error.

Table 5. Main performance metrics of the classification algorithms.

Metric	Description	References
Number of instances correctly classified	Number of correct predictions	[21]
Accuracy	Number of correct predictions divided by the total number of data	[35, 39, 48]
Kappa coefficient	Measure of concordance with respect to the level of randomness of the classification that varies between 1 and −1. A Kappa coefficient of 1 indicates that the model is perfect and a value of zero means that each value of the model is different from the actual value of the class. A negative value of the coefficient indicates that there is no concordance among the observations	[48, 50]
Mean squared error	It measures the average of the squares of the errors or deviations; that is the difference between the estimator and what is estimated	[49, 50]
Precision	Probability that a prediction corresponds to its real value. It is employed when only two possible values can be obtained within a class	[21]
Recall	Proportion of positive cases that were correctly classified. It is employed when only two possible values can be obtained within a class	[21]
C-Statistic	Geometric measure that combines the precision and recall metrics to evaluate the model. It is a measure of goodness or fit for binary outcomes	[50]
Specificity	Capacity of the estimator to correctly identify the negative cases. It is employed when only two possible values can be obtained within a class	[21]
Average error for numerical categorical factors	These metric is employed for numerical categorized factors when the class is measured by a numerical value but it is employed as a nominal value	

4 Decision Support System for the Assignment of Storage Positions to Import Containers

This section details the architecture of a decision support system for the container position assignment at the yard of a Container Terminal. The aim of the system is two-fold. First, we enhance the capabilities of the Terminal Operator System (TOS) by implementing a module which predicts the dwell time based on historical data. Second, we take advantage of that prediction to suggest an explicit storage location for the container under scrutiny.

When an import container is unloaded from the vessel and is transported to the yard, the yard planner examines the container and faces the decision of where to store

it. The yard planner uses the proposed system to estimate the dwell time based on characteristics associated to the container and historical information of other containers stored in the yard. As opposed to expert intuition, this estimation can be used to make an informed decision. If the yard planner desires, the system can suggest a specific storage location for the container.

When a container is assigned to a storage slot at the yard, it is stored until requested by the consignee. There are some cases in which the container may be relocated because it is blocking the access to the yard crane to retrieve another container. These movements are also referred as rehandles. One of the objectives of the yard planner, is to reduce the number of rehandles or relocations of containers, as these are non-value movements that generate additional costs and waiting times.

The storage space at the yard is organized as a three-dimensional matrix ordered in bays, columns and rows (please observe Fig. 1 for a pictorial reference). This abstract representation is convenient for maintaining an internal representation of the current state of the storage space. It is possible to define algorithmic operations for assigning a slot to a container, requesting the coordinates of a container, and analyzing if there are more containers on top of the requested item (i.e., a container), and so on.

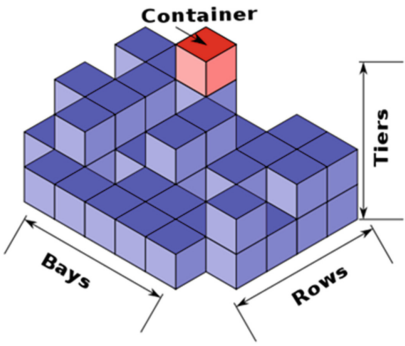

Fig. 1. Baroti index (Source: [23]).

To explain the details of our proposed architecture, we will describe a sequence of temporal events and the relationship with each module of the system. Figure 2 depicts the software architecture for the above-mentioned decision support system. This system is constituted by one main module that is connected to the Terminal Operator System (TOS). The TOS corresponds to a software suite designed to manage the resources of the enterprise and it can be an in-house developed software or a generic commercial product (e.g., Navis N4 TOS).

The whole process begins when the import container arrives to the port. At that moment, the yard planner accesses the graphical user interface (GUI) to identify the container that must be stored (labeled with the number 1 in the Fig. 2). Then, the system connects to the TOS, retrieving statistical information regarding the container such as the name of the consignee, the service or vessel, type of container, weight, etc.

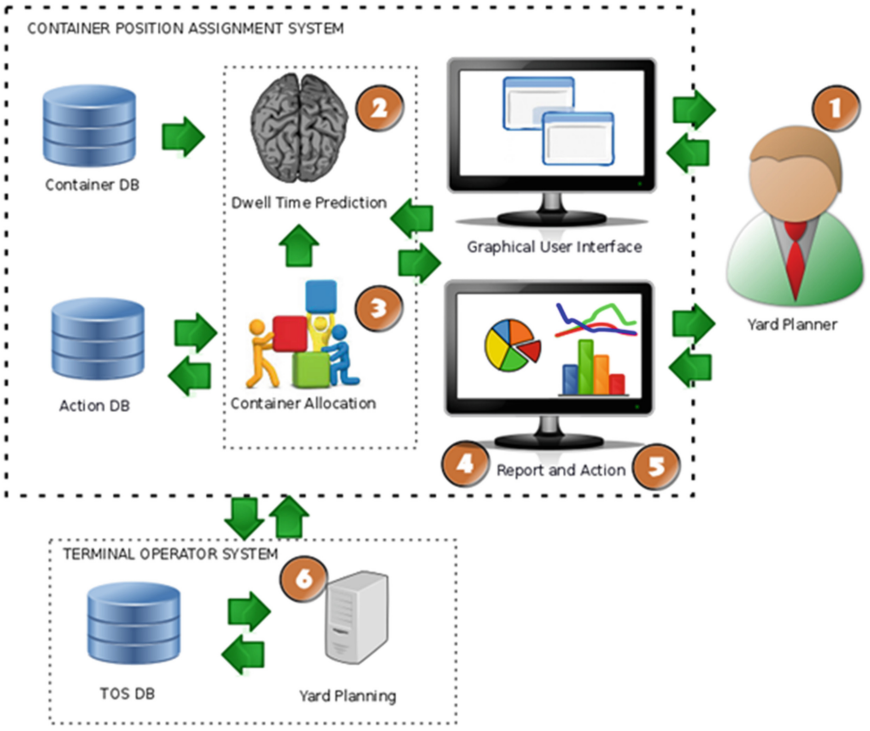

Fig. 2. Container Position Assignment System architecture (Source: [23]).

This information is fed to the predictor and an estimation for the dwell time is obtained (see number 2 in the Fig. 2). This estimation is made based on a mathematical model that use the historical data of containers and dwell time kept in the Container database. The planner use the dwell time estimation to decide where to place the container.

Alternatively, the planner may request to the system a recommendation for the location of the incoming container to the yard. For this matters, the system includes a special module that may suggest to the yard planner, a storage position at the yard (see label 3 in the Fig. 2). The module internally ask for a dwell time prediction, which is used as the input for an internal algorithm that outputs a location. This output location is assumed to be the best option for storing the current container. At this juncture, the general assumption is that two given containers with a similar dwell time must be located in neighboring regions, while two given containers with large difference in their dwell times must be assigned to regions that are far between each other.

Once the dwell time prediction and/or the storage position of each incoming container at the yard have been determined, the system will provide a report to the yard planner with this information. This report may include a graphical representation of the yard, specifying the location in which the current container must be assigned (label 4 in the Fig. 2). Based on this information the yard planner may decide whether to accept to locate the import container in the suggested position. This action (label 5) is recorded in

the Action Database. Here, our idea is that the learning system is generating solutions for the problem and the human expert can validate them as being correct or wrong, knowledge that can be further exploited to refine the learning method of the system.

Finally (label 6), the decision made by the yard planner is communicated to the TOS system, which records the transaction. As a final comment in this matter, we observe that the architecture is not limited for a single user. Rather, more than one yard planner may access the service concurrently, which can be an advantageous feature, as this information for instance, could be provided to the yard crane operators in a mobile device.

5 Case Study: Port of Arica in Chile

The port of Arica, Chile is used in this case study because it presents a high level of uncertainty in the import processes and huge container dwell times. The port of Arica occupies the 43rd position in the Latin American containerized movements ranking provided by UN-ECLAC, and the 6th position in the Chilean port system, with a total of 204,174 TEUs transferred in 2013 [18]. The port consists of a single multi-purpose terminal whose main characteristic is that about 70% of the cargo corresponds to cargo in transit from Bolivia. The port presents special conditions for cargo handling, due to the Political Agreements maintained between Chile and Bolivia, a reason for which the cargo has no storage fee (exports for 60 days and imports up to 365 days). Furthermore, the main hinterland (located in Bolivia) is more than 1000 km away, in contrast with the main Chilean ports, Valparaiso and San Antonio, whose main hinterland (Metropolitan Region of Santiago) is located about 120 km from the ports.

The port of Arica lacks coordination systems such as appointment or booking systems. In addition, most of the procedures are paper-based and performed with no anticipation as in other ports. These foster the uncertainty and variability in port operations, especially for the import processes, resulting in long service times (truck turnaround times) and container rehandles when retrieved to be dispatched to their consignees. Under this situation, the current practice of the yard managers is to assign space to containers in a semi-random fashion, where containers are located at the yard considering only very simple rules that maximize space utilization.

A segregation based policy for storage space assignment of export containers has been an efficient strategy for reducing rehandles incurred when containers are loaded on the ship and is a common strategy at Container Terminals. Segregating export containers is commonly done based on the ship characteristics that are employed when the stowage plan is generated and hence, rehandles are potentially minimized. In contrast, the criteria for segregating import containers is not so straightforwardly determined, especially if high levels of uncertainty are observed.

In this paper a methodology to implement a dwell time segregated policy for assigning space to import containers is proposed. The policy considers segregating containers based on predicted dwell time intervals. To evaluate the different classification and multi-classification algorithms employed, the following metrics have been considered: (i) number of instances correctly classified, (ii) accuracy, (iii) Kappa's

coefficient; (iv) the mean squared error; (v) the mean error in time units" and (vi) the mean error for categorized factors.

A data base with container movements for the years 2011, 2012 and August 2013 is included, with a total of 151,640 import containers. Seven factors were considered: (1) size of the container (20/40), (2) type of container (Dry, Reefer, High Cube, etc.), (3) the status of the container (full or empty), (4) weight, (5) ship where the container is unloaded, (6) consignee or customer, and (7) the cargo's port of origin.

The first four factors correspond to characteristics of the container. The factors are numerical (size of container and weight) and nominal (type, status, ship, port of origin, consignee). The only dual attribute is dwell time, and the nominal variable consignee has the largest number of classes (about 5000 to 7000). It is important to mention that the weight and port of origin are factors not previously employed in the literature (see Table 1).

Unlike the work of [23], the statistical description of the database, considering the three years (2011–2013), is presented in this article. Table 6 shows each confidence interval was computed considering the confidence interval of the average per year. The database was divided into three subsets of data, segregated by year. Seven factors were considered: size, type of container, status of the container, weight, vessel from which the container was unloaded, the corresponding consignee, the port of origin and the dwell time. Each factor is further described.

Table 6. Statistical description of the data.

Factors	Type	Average	Minimum	Maximum	Standard deviation	Number of classes
Size (TEU)	Numerical	30.58 ± 0.59	20.00 ± 0.00	40.00 ± 0.00	9.97 ± 0.04	
Type	Nominal					24 ± 1
Status	Nominal					2 ± 0
Weight (ton)	Numerical	12.97 ± 2.04	0.16 ± 0.11	292.89 ± 6.78	10.65 ± 0.88	
Vessel	Nominal					236 ± 42
Consignee	Nominal					6.613 ± 1.062
Port of Origin	Nominal					329 ± 54
Dwell time (days)	Nominal/Numerical	12.68 ± 2.22	0.33 ± 0.65	885.33 ± 721.54	15.51 ± 1.38	175 ± 11

The first four factors indicated in previous table correspond to characteristics of the container. The size indicates if the container is of 20 or 40 TEUs. The type of container considers if the container is *High Cube*, *Refeer*, *Open Top*, among others. The state of the container indicates if the container is full or empty, while the weight varies according to the cargo of the container. The rest of the factors do not describe characteristics of the container: vessel that transported the container, the consignee of the cargo and the port of origin of the cargo. As observed in previous table, for the numerical attributes, we compute the average, minimum and maximum value and the standard deviation. For the nominal attributes, we estimate the number of different classes. The only dual attribute is the dwell time that is treated as both, nominal and numerical. It is possible to observe in the same table that the attribute "size of the container" has the least standard deviation value with respect to its average value. On the other hand, the attributes "weight" and "dwell time" are the ones that present higher

deviation values. The nominal variables type, state, vessel, port of origin and dwell time have less number of classes than the consignee variable. The port of origin represents the worst case with 329 classes. On the other hand, the consignee has between 5000 to 7000 classes.

Due to the high number of classes that the attributes vessels, consignees and port origin present, we performed a Pareto Analysis with the aim to identify the instances observed in the 80% of the import containers. The Pareto Analysis identified that approximately 9.2% of the consignees represent 80% of the import cargo, which is equivalent to 1,114 consignees. On the other hand, the Pareto Analysis indicated that 27.3% of the vessels transport 80% of the import cargo which corresponds to 39 vessels. Finally, 7.1% of the ports of origin correspond to 80% of the import cargo which are equal to 34 ports.

5.1 Results Obtained with the Classification Algorithms

In this section, we present the results obtained with the classification algorithms. The experiments were performed using both the whole database, and also the data selected based on the Pareto Analysis. This later case was tested for the multi-classifier algorithms in particular. For the classification model, non-supervised classification algorithms were employed as they allow working with known classes (as opposed to supervised algorithms) [2, 3]. This is justified by the fact that classes are known, since they are determined in Step 1.1 (see Table 1). The applied offline algorithms are Naive Bayes, Lazy Learning, and Rules Induction Learning.

Dwell times were measured in days, as this is the commonly used time unit in port Terminals. The year 2011 data was used to generate the model and the 2012 data was used to evaluate it. Data for 2013 was used only for the simulation model described in Sect. 4.2. The algorithms were implemented in JAVA version 1.6.0_25, using the software WEKA (Waikato Environment for Knowledge Analysis) in a personal computer with a processor Intel Core 7, and 8 GB of RAM.

Table 7 summarizes the results found with each algorithm. The classification algorithm that obtained a larger number of correctly classified instances, best accuracy, Kappa's coefficient values and root mean squared error is the K*, and the JRip algorithm obtained the best error values. On the other hand, the K* algorithm had longer computational times (twice as much as JRip).

Table 7. Results obtained with the classification algorithms (Source: [23]).

Algorithms	Number of correctly classified instances	Accuracy	Kappa's coefficient	Mean squared error	Rootmean squared error	Computational time (seconds)	Error (days)
Naive Bayes	3,875.8 ± 188.4	6.77%	0.031 ± 0.002	0.058 ± 0.000	0.069 ± 0.000	34.1 ± 2.9	7.88 ± 0.67
OneR	2,365.9 ± 103.3	4.13%	0.019 ± 0.003	0.058 ± 0.000	0.098 ± 0.000	34.1 ± 3.9	8.51 ± 0.20
ZeroR	2,942.3 ± 167.6	5.14%	0.000 ± 0.000	0.058 ± 0.000	0.068 ± 0.000	62.4 ± 4.9	8.21 ± 0.93
Decision table	3,254.6 ± 256.3	5.68%	0.013 ± 0.005	0.058 ± 0.000	0.068 ± 0.000	**27.4 ± 1.6**	7.12 ± 0.44
K*	**4,116.7 ± 88.1**	**7.19%**	**0.038 ± 0.002**	0.058 ± 0.000	**0.067 ± 0.000**	109.0 ± 3.4	7.42 ± 0.10
KNN, K = 1	3,966.6 ± 135.2	6.93%	0.035 ± 0.002	0.058 ± 0.000	0.070 ± 0.000	31.1 ± 10.5	8.07 ± 0.17
JRip	2,760.6 ± 164.1	4.82%	0.002 ± 0.001	0.058 ± 0.000	0.068 ± 0.000	36.6 ± 4.1	**6.94 ± 0.88**

A multi-classifier algorithm for dwell time predictions was also proposed, and it was trained using the information from the historical data base. Results are presented in Table 8, where it can be observed that the KNN algorithm obtained the larger number of correctly classified instances, accuracy and error values, with a computational time of 40 s.

Table 8. Multi-classifier results (Source: [23]).

Algorithms	N° of correctly classified instances	Accuracy	Computational time (seconds)	Error (days)
Naive Bayes	3,226.9 ± 122.6	5.63%	79.9 ± 1.5	7.47 ± 0.20
OneR	1,309.6 ± 87.9	2.28%	**19.4 ± 0.9**	8.75 ± 0.25
ZeroR	3,216.4 ± 262.9	5.62%	31.1 ± 9.3	7.29 ± 0.41
Decision table	2,992.7 ± 380.5	5.23%	55.2 ± 4.6	7.18 ± 0.42
K*	3,183.5 ± 98.7	5.56%	114.7 ± 1.6	7.63 ± 0.17
KNN, N = 85	**3,608.0 ± 394.8**	**6.30%**	38.7 ± 4.9	**6.92 ± 0.19**
JRip	3,153.1 ± 351.8	5.51%	61.4 ± 8.8	7.27 ± 0.47

As observed in previous tables, the algorithms without the multi-classifier obtained better results in general. On the other hand, the accuracy values are always lower than 10%, which is explained due to the variability of the ship and consignee factors in the data base. For dwell time predictions, the average error is about 7 days, which is high, but under current operations, managers of the port of Arica are not able to estimate container dwell times, hence in the long run, it is expected that this number can be reduced.

In order to reduce the dwell time estimation, we consider only the data that resulted more representative according to the Pareto Analysis for determining data training set. For this reason, the training set considers only the 9.2% of the consignees, 7.1% of the ports of origin and 27.3% of the vessels identified in the analysis as correspond to the most representative. Table 9 presents the results, using the training set obtained from the database of 2011. The training set corresponds to the 2012 data considering 10 replicates. In this analysis, the algorithm with the best performance is the KNN with N = 84, obtaining the highest number of instances correctly classified and the least error measured in days. Therefore, in this chapter we explain in more details the performed analysis carried out in [23] in order to improve dwell time estimations.

From results shown in previous table, it is possible to observe that using the Pareto Analysis data, it is possible to reduce the error to 4.56 days. Results obtained can be used to derive operational rules for different storage policies for containers according to the predictive dwell time values.

Table 9. Comparative analysis of the classification algorithm based on the Pareto-Analysis results. Dwell time measured in days.

Algorithm	Number of instances correctly classified	Accuracy (%)	Computational time (min)	Average error (days)
Naive Bayes	2,062.5 ± 74.2	3.86	91.0 ± 23.0	5.30 ± 0.13
OneR	2,053.0 ± 69.8	3.84	18.4 ± 1.7	5.28 ± 0.12
ZeroR	2,003.3 ± 403.0	3.75	14.2 ± 2.6	5.32 ± 0.42
Decision table	2,065.0 ± 127.5	3.86	14.0 ± 0.3	4.86 ± 0.27
K*	2,094.7 ± 66.0	3.92	75.5 ± 2.3	5.19 ± 0.10
KNN, N = 84	2,402.9 ± 152.2	4.50	46.6 ± 7.2	4.56 ± 0.11
JRip	2,192.2 ± 181.2	4.10	12.5 ± 0.6	4.58 ± 0.19

5.2 Impact Assessment of the Proposed Policy via a Discrete Events Simulation Model

A simulation model of the import processes at the port of Arica is proposed to evaluate the impact of the storage policies in terms of the number of rehandles incurred. For comparison purposes, a storage policy was implemented considering two variants for the stacking strategy of containers without dwell time segregation to resemble the current practice of the port managers.

Table 10 outlines the general procedure for the general stacking strategy implemented based on the dwell time segregations policy, while Table 11 outlines the procedure for the non-segregation storage policy that employs two stacking strategies: Semi-random and Sequential, which are illustrated respectively in Figs. 3 and 4.

Table 10. Segregated stacking strategy (Source: [23]).

Dwell time Segregated Stacking Strategy
INPUT: Dwell time predictions for each container and dwell time classes; Yard layout and inventory
1. Define the segregation of containers based on the dwell time class predictions
2. Assign to each block a segregation of containers. One block can contain either a single or several segregations.
3. Once a container arrives, assign it to the corresponding segregation block.
4. Define the location of the container in the block based on the ***Semi-random*** or ***Sequential*** stacking strategies.
5. If a container arrives and there is no available space in the block corresponding to the segregation, then randomly select a block and repeat step 4
OUTPUT: Container location.

Table 11. Non-segregated stacking strategy (Source: [23]).

Dwell time Non-Segregated Stacking Strategy
INPUT: Yard layout and inventory
1. Randomly select a block with available space.
2. Define the location of the container in the block based on the ***Semi-Random*** or ***Sequential*** stacking strategies.
3. If a container arrives and there is no available space in the predetermined block, then randomly select a block and repeat step 4.
OUTPUT: Container location.

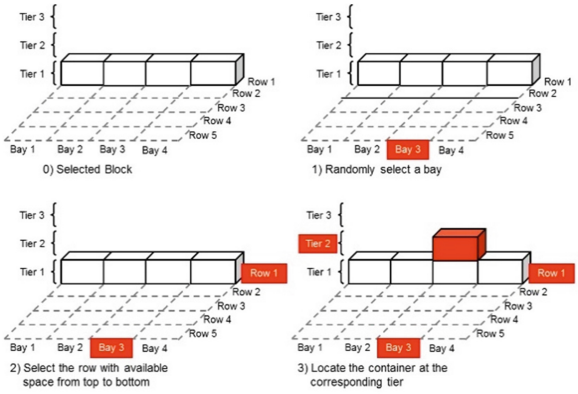

Fig. 3. Semi-random stacking strategy illustration (Source: [23]).

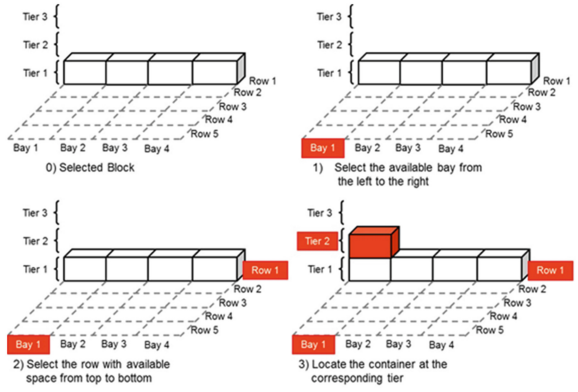

Fig. 4. Sequential stacking strategy illustration (Source: [23]).

The stacking strategies are illustrated respectively in Figs. 3 and 4. The instance implemented considered the movements of containers in the years 2012 and 2013. The yard of the port Terminal consists of 19 blocks for import containers with a total of 4820 TEU slots. To predict the dwell times, the JRip and multi-classifier algorithms were implemented. The real arrival of containers at the port during each year is taken from the data base. For the random stacking strategies, five replicates were run. For the sequential stacking strategies, no replicates were tested given that the solution obtained is the same since the arrival of containers does not change. For the random stacking strategies, standard deviation values were in the range of 140 to 444 rehandles. The simulation model was implemented in the software ExtendSim OR version 9.0 and run in a personal computer with Intel Core 7 and 8 Gb RAM. Table 12 presents the results obtained.

As observed in Table 12, the average number of rehandles incurred for both 2012 and 2013 are always lower for the segregated dwell time policies employing any type of stacking strategy. Furthermore, the gap between the average number of rehandles for the non-segregated and segregated policies is around 13%. Comparing the best stacking strategy in each period for the segregated and non-segregated policies, a 6% and a 37% gap were obtained for the 2012 and 2013 periods respectively.

Table 12. Numerical Results: Rehandles per time period and stacking strategy (Source: [23]).

Storage policy	Stacking strategy	Average per policy (DT vs NS)	Rehandles per period	
			2012	2013
Non-segregated policy (NS)	Non-segregated random stacking strategy	45840.6	48611.8	43083.6
	Non-segregated sequential stacking strategy		48756	42911
Dwell time segregation policy (DT)	Dwell time segregated and random stacking strategy (JRip)	39768.76	45785.8	37423.8
	Dwell time segregated and sequential stacking strategy (JRip)		45343	36531
	Dwell time segregated and random stacking strategy (multi-classifier and KNN, $N = 84$)		46377.4	27909
	Dwell time segregated and sequential stacking strategy (multi-classifier and KNN, $N = 84$)		**45337**	**26986**
GAP (Avg. NS - Avg. DT)/Avg. DT				13.25%
Gap (Best NS - Best DT)/Best DT [2012]				6.74%
Gap (Best NS - Best DT)/Best DT [2013]				37.11%

6 Conclusions and Recommendations for Further Research

Ship turnaround times are an important productivity indicator for a port terminal and efficient container handling is needed during the loading and unloading operations. Among several factors that affect the performance of the ship service, the yard operation efficiency is a key element. In addition, for those terminals in which land is very restricted, the planning and scheduling of resources at the yard (space and equipment) are even more critical.

A common practice among yard managers for storage space assignment consists of defining segregations or groups of containers with common characteristics. Export container segregations depend on the ship loading sequence, which is based on the ship, port of destination, weight, type, empty/full, among other factors. On the other hand, segregating import containers for a port terminal where no hinterland coordination mechanisms exist and where there is a high level of uncertainty results in a difficult task.

In this article a dwell time segregated storage space policy for import containers is proposed as well as the design of a decision support system for the yard planner of a container terminal based on the proposed storage policy. The focus of this article was import containers, due to the difficulty to determine the criteria to segregate import containers, as there is more uncertainty on the dispatching times. Hence, it is very common that an important number of rehandles are incurred when import containers are dispatched to the external transport carriers. For the proposed policy, dwell times of import containers are predicted by classification algorithms, such that containers are segregated based on dwell time classes. Import containers of the same dwell time class, are assigned to close locations at the yard. Using classification methods in this research is justified as we are dealing with a big database and also due to the fact that the dwell time prediction is used to define groups of containers rather than predicting a precise value.

As a case study, we consider the case of the port of Arica in Chile. This port presents special conditions for cargo handling. More than 70% of the cargo transferred by the port of Arica corresponds to transit cargo of Bolivia. Due to the Political Agreements maintained between Chile and Bolivia, there exists a high uncertainty in the dispatching processes of the import containers at the port. To evaluate the potential benefits in the daily operations of the yard, a discrete event simulation model is also implemented. Numerical results of the simulation model show that a dwell time segregated storage policy with a sequential stacking strategy provides a significant reduction in the number of rehandles incurred. Considering the real number of containers handled by the port for a specific instance data set, around to 17% reduction in rehandles is obtained by the proposed policy, compared to the real number of rehandles incurred by the port managers' current practices. In addition, the implementation of the decision support system proposed may provide a valuable tool for the yard planner.

We estimate that implementing the proposed system does not require significant efforts of the port terminal and could lead to more efficient operations at the yard. The current practice of the managers follow a semi-random assignment of containers at the yard, given the limitations of data and uncertainty in the dispatching times of import

containers. Hence, the proposed support system will not change significantly their current operations but in turns, will provide recommendations to the yard planners that they could consider for the assignment of spaces to containers, without replacing the personnel.

We proposed a simulation model with the aim to analyze the impacts of the storage policies for container stacking in the yard. The model developed simulate the stacking process of containers since the moment in which the container is unloaded from the vessel until the moment in which is retrieved to be dispatched to its consignee. When we evaluated the model with the database of the 2012 year, the best policy to stack containers in the yard is the one in which containers are segregated based on the dwell time policy and the sequential policy. This is also consistent with the results obtained using the database of the 2013 year.

In order to improve the dwell time estimations, we recommend that the port of Arica may improve its Terminal Operating System (TOS), to have more precise data as some inconsistencies were found in the records of the database provided by the port. It is also recommendable to register more information, such as the type and value of the cargo transported in the container (content). This information could be also used as an attribute for the dwell time estimation.

As a further research, additional factors that may affect dwell time predictions should be analyzed, such as the content of the container, and whether the container contains cargo that belongs to a single or several importers (Full container loaded, FCL vs Less than container loaded, LCL). The problem addressed in this article is at the tactical decision level. Hence, another research avenue would be to develop real time stacking strategies based on the dwell time segregated policy. Furthermore, impact assessment for different types of yard equipment could be another research project to be developed (reachstackers vs RTG vs straddle-carriers, etc.). In addition, ship turn-around times can be also considered as a performance metric for the different stacking strategies and a sensitivity analysis to determine the most significant factors determining dwell times for the port of Arica could be performed.

References

1. Arvis, J.-F., Raballand, G., Marteau, J.-F.: The cost of being landlocked: logistics costs and supply chain reliability. In: Directions in development trade 55837. The World Bank, Washington DC (2010)
2. Astudillo, C.A., Bardeen, M., Cerpa, N.: Editorial: data mining in electronic commerce - support vs. confidence. J. Theor. Appl. Electr. Commer. Res. **9**(1), I–VIII (2014)
3. Astudillo, C.A., Oommen, B.J.: Topology-oriented self-organizing maps: a survey. Pattern Anal. Appl. **17**(2), 1–26 (2014)
4. Bassan, S.: Evaluating seaport operation and capacity analysis—preliminary methodology. Marit. Pol. Manag. **34**(1), 3–19 (2007)
5. Beuran, M., Mahihenni, M.H., Raballand, G., Refas, S.: The impact of demand on cargo dwell time in ports in SSA. Policy Research Working Paper 6014. The World Bank, Africa Region (2012)
6. Bichou, K., Gray, R.: A logistics and supply chain management approach to port performance measurement. Marit. Pol. Manag. **31**(1), 47–67 (2004)

7. Chen, T., Lin, K., Juang, Y.-C.: Empirical studies on yard operations part 2: quantifying unproductive moves undertaken in quay transfer operations. Marit. Pol. Manag. **27**(2), 19–207 (2000)
8. Chung, K. C.: Port performance indicators. In: Infrastructure Notes: Transportation, Water and Urban Development. Transport No. PS-6. The World Bank (1993)
9. Cios, K.J., Moore, G.W.: Uniqueness of medical data mining. Artif. Intell. Med. **26**, 1–24 (2002)
10. Cleary, J.G., Trigg, L.E.: K*: an instance-based learner using an entropic distance measure. In: Proceedings of the 12th International Conference on Machine Learning, pp. 108–114. Morgan Kaufmann Publishers Inc., Tahoe City, California (1995)
11. Cochran, W.G.: Sampling Techniques. Wiley, New York (1986)
12. Cover, T., Hart, P.: Nearest neighbor pattern classification. IEEE Trans. Inf. Theor. **13**(1), 21–27 (1967)
13. Dally, H.K.: Container Handling and Transport: A Manual for Current Practice. CS Publications, London (1983)
14. De Langen, P.W.: Port competition and selection in contestable hinterlands: The case of Austria. Eur. J. Transp. Infrastruct. Res. **7**(1), 1–14 (2007)
15. Dharmalingam, K.: Design of storage facilities for containers- a case study of Port Louis Habour. Maritius. Ports Harbors **32**(9), 27–31 (1987)
16. Dietterich, T.G.: Machine learning research: four current directions. AI Mag. **18**(4), 97–136 (2000)
17. Djankov, S., Freund, C., Pham, C.S.: Trading on time. In: Policy Research Working Paper 3909. The World Bank, Washington DC (2006)
18. Doerr, O.: Latin American and the Caribbean container port throughput, Ranking 2013. Infrastructure Services Unit. UN-ECLAC, Santiago Chile (2013)
19. Doerr, O., Sánchez, R.: Indicadores de productividad para la industria portuaria: aplicación en América Latina y el Caribe. Serie Recursos naturales e infraestructura, 112. UN-ECLAC, Santiago Chile (2006)
20. Dowd, T.J., Leschine, T.M.: Container terminal productivity: a perspective. Marit. Pol. Manag. **17**(2), 107–112 (1990)
21. Fawcett, T.: ROC graphs with instance-varying costs. Pattern Recogn. Lett. **27**(8), 882–891 (2006)
22. Furnkranz, J., Widmer, G.: Incremental reduced error pruning. In: Proceeding ICML 1994, Proceedings of the Eleventh International Conference on International Conference on Machine Learning, pp. 70–77. Morgan Kaufmann Publishers Inc., New Brunswick (1994)
23. Gaete, G.M., González-Araya, M.C., González-Ramírez, R.G., Astudillo, C.A.: Dwell time-based container positioning decision support system at a port terminal. In: Proceedings of the 6th International Conference on Operations Research and Enterprise Systems (ICORES 2017), pp. 128–139 (2017). https://doi.org/10.5220/0006193001280139. ISBN: 978-989-758-218-9
24. Hall, M., Framk, E., Holmes, G., Pfahringer, B., Reutemann, P., Witten, I.H.: The WEKA data mining software: an update. ACM SIGKDD Explor. Newsl. **11**(1), 10–18 (2009)
25. Holte, R.C.: Very simple classification rules perform well on most commonly used datasets. Mach. Learn. **11**(1), 63–90 (1993)
26. Hoffman, P.: Container facility planning: a case description. In: Port Management Textbook Containerization, Institute of Shipping Economics and Logistics, pp. 353–364 (1985)
27. Kohavi, R.: Scaling up the accuracy of Naive-Bayes classifiers: a decision-tree hybrid. In: Proceedings of the Second International Conference on Knowledge Discovery and Data Mining, pp. 202–207 (1996)

28. Kononenko I.: Comparison of inductive and Naive Bayesian learning approaches to automatic knowledge acquisition. In: Wielinga, B., Boose, J., Gaines, B., Schreiber, G., van Someren, M. (eds.) Current Trends in Knowledge Acquisition. IOS Press, Amsterdam (1990)
29. Lee, T.-W., Park, N.K., Lee, D.-W.: A simulation study for the logistics planning of a container terminal in view of SCM. Marit. Pol. Manag. **30**(3), 243–254 (2003)
30. Magala, M., Sammons, A.: A new approach to port choice modelling. Marit. Econ. Logist. **10**(1–2), 9–34 (2008)
31. Merckx, F.: The issue of dwell time charges to optimize container terminal capacity. In: Proceedings of the International Association of Maritime Economists Annual Conference 2005, Limassol, Cyprus (2005)
32. Moini, N., Bolie, M., Theofanis, S., Laventhal, W.: Estimating the determinant factors of container dwell times at seaports. Marit. Econ. Logist. **14**, 162–177 (2012)
33. Nir, A.-S., Lin, K., Liang, G.-S.: Port choice behaviour: from the perspective of the shipper. Marit. Pol. Manag. **30**(2), 165–173 (2003)
34. Quinlam, J.R.: Induction of decision tree. Mach. Learn. **1**, 81–106 (1986)
35. Paranthaman, J., Victoire, A.: Hybrid techniques for privacy preserving in data mining. Life Sci. J. **10**, 471–475 (2013)
36. Raballand, G., Refas, S., Beuran, M., Isik. G.: Why does cargo spend weeks in Sub-Saharan African ports? Lessons from six countries. In: Directions in Development. The World Bank, Washington DC (2012)
37. Rodrigue, J.P.: The benefits of logistics investments: opportunities for Latin America and the Caribbean. In: Paden, M. (ed.) Technical Notes IDB-TN-395, pp. 1–65. Inter-American Developing Bank, Washington, DC (2012)
38. Rodrigue, J.P., Notteboom, T.: The terminalization of supply chains: reassessing the role of terminals in port/hinterland logistical relationships. Marit. Pol. Manag. **36**(2), 165–183 (2009)
39. Samanta, A., Saha, S.: A new technique involving data mining in protein sequence classification. In: Bhattacharyya, R. et al. (eds.) Computer Science & Information Technology, ACER 2013, pp. 243–254 (2013)
40. Tongzon, J.L., Sawant, L.: Port choice in a competitive environment: from the shipping lines perspective. Appl. Econ. **39**(4), 477–492 (2007)
41. Tuya, J., Ramos, I., Dolado, J.J.: Técnicas cuantitativas para la gestión en la ingeniería del software. NetBiblio, España (2007)
42. UNCTAD 2014: Review of Maritime Transport 2014. United Nations Publications (2014). ISBN: 978-92-1-112878-9
43. USAID: The broad economic impact of port inefficiency: a comparative study of two ports. U.S. Agency for International Development, Reported by Nathan Associates, Washington, DC (2005). http://pdf.usaid.gov/pdf_docs/PNADC612.pdf
44. Veldman, S., Bückmann, E.: A model on container port competition: an application for the West European container hub-ports. Marit. Econ. Logist. **5**(2), 3–22 (2003)
45. Wang, J.H, Deng, P.S., Fan, Y.S., Jaw, L.J., Liu, Y.C.: Virus detection using data mining techniques. In: Proceedings. IEEE 37th Annual 2003 International Carnahan Conference on Security Technology, pp. 71–76 (2003)
46. Weiss, G.M.: Mining with rarity: a unifying framework. ACM SIGKDD Explor. Newsl. **6** (1), 7–19 (2004)
47. Witten, I., Frank, E., Hall, M.A.: Data Mining: Practical Machine Learning Tools and Techniques. Elsevier, Morgan Kaufmann series in data management systems (2011)

48. Wu, F., Zhan, J., Yan, H., Shi, C., Huang, J.: Land cover mapping based on multisource spatial data mining approach for climate simulation: a case study in the farming-pastoral ecotone of North China. In: Advances in Meteorology 2013 Article ID 520803, 12 p. (2013)
49. Xu, T., Tian, J., Murata T.: Research on personalized recommendation in e-commerce service based on data mining. In: Proceedings of the International Multiconference of Engineers and Computer Scientists, IMECS 2013, Hong Kong, vol. I (2013)
50. Yadav, P.K., Jaiswal, K.L., Patel, S.B., Shukla, D.P.: Intelligent heart disease prediction model using classification algorithms. Int. J. Comput. Sci. Mobile Comput. **2**(8), 102–107 (2013)

Author Index